U.S. DEPARTMENT OF THE INTERIOR
U.S. GEOLOGICAL SURVEY

GEOLOGY AND STRUCTURE OF THE PINE RIVER, FLORIDA RIVER, CARBON JUNCTION, AND BASIN CREEK GAS SEEPS, LA PLATA COUNTY, COLORADO

by

James E. Fassett, Steven M. Condon, A. Curtis Huffman, and David J. Taylor

U.S. Geological Survey
P.O. Box 25046, MS 939, Denver Federal Center
Denver, Colorado 80225

Open-File Report 97-59

This report is preliminary and has not been reviewed for conformity with U.S. Geological Survey editorial standards (or with the North America Stratigraphic Code). Any use of trade, product, or firm names is for descriptive purposes only and does not imply endorsement by the U.S. Government.

1997

CONTENTS

CONTENTS—CONTINUED

INTRODUCTION

This study was commissioned by a consortium consisting of the Bureau of Land Management, Durango Office; the Colorado Oil and Gas Conservation Commission; La Plata County; and all of the major gas-producing companies operating in La Plata County, Colorado. The gas-seep study project consisted of four parts; 1) detailed surface mapping of Fruitland Formation coal outcrops in the above listed seep areas, 2) detailed measurement of joint and fracture patterns in the seep areas, 3) detailed coal-bed correlation of Fruitland coals in the subsurface adjacent to the seep areas, and 4) studies of deep-seated seismic patterns in those seep areas where seismic data was available. This report is divided into three chapters labeled 1, 2, and 3. Chapter 1 contains the results of the subsurface coal-bed correlation study, chapter 2 contains the results of the surface geologic mapping and joint measurement study, and chapter 3, contains the results of the deep-seismic study.

A preliminary draft of this report was submitted to the La Plata County Group in September 1996. All of the members of the La Plata Group were given an opportunity to critically review the draft report and their comments were the basis for revising the first draft to create this final version of a geologic report on the major La Plata County gas seeps located north of the Southern Ute Indian Reservation.

Subsurface correlation of Late Cretaceous Fruitland Formation coal beds in the Pine River, Florida River, Carbon Junction, and Basin Creek gas-seep areas, La Plata County, Colorado

By James E. Fassett

INTRODUCTION

The Pine River, Florida River, Carbon Junction, and Basin Creek areas are located in the northern part of the San Juan Basin in La Plata County, Colorado (figure 1-1). These areas are the sites of the major known natural-gas seeps along the Cretaceous Fruitland Formation outcrop in La Plata County (not including the Southern Ute Indian Reservation). Each of the gas seep areas is located in a place where the steeply dipping Hogback Monocline has been breached by a stream cut, therefore, the seeps are in areas that are topographically, relatively low.

The Fruitland Formation is the major coal-bearing rock unit in the San Juan Basin of New Mexico and Colorado. The Fruitland contains in excess of 200 billion tons of coal throughout the basin (Fassett and Hinds, 1971) and crops out around most of the margin of the basin. Fruitland coal is strip mined in three large mines in northwestern New Mexico. Fruitland coal has been mined , mostly underground, in many small workings around the north and northwest rim of the basin; nearly all of those mines are now abandoned. A relatively small Fruitland strip-mining operation in the northeast part of the basin, the Chimney Rock mine, is also now abandoned.

The geology and distribution of Fruitland coal in the San Juan Basin is described in detail in a U.S. Geological Survey Professional Paper (Fassett and Hinds, 1971). That study shows that Fruitland coals are present throughout the subsurface of the basin to a maximum depth of slightly more than 4,000 feet and that the deposition of the coals was closely related to the regression of the Western Interior Seaway as it retreated from the

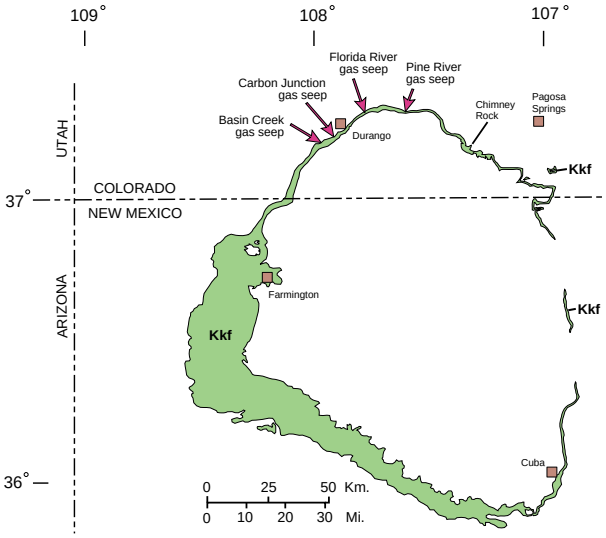

Figure 1-1. Index map showing the locations of the Pine River, Florida River, Carbon Junction, and Basin Creek gas seeps. Kkf is the outcrop of the Fruitland Formation and Kirtland Shale, undivided (from Fassett and Hinds, 1971).

San Juan Basin area in Late Cretaceous time. The study also showed that Fruitland coals formed in a time-transgressive manner; radiometric age dates (Fassett and Steiner, in press) indicate that Fruitland coals in the southwest part of the basin are 3 million years older than coals in the northeast part of the basin. Fruitland coals occur in a complicated, stratigraphically rising, en-echelon geometry across the basin, however it is possible to correlate Fruitland coals using guidelines in the Fassett and Hinds (1971) report.

During the past ten years, the northern San Juan Basin has experienced a gas-drilling boom targeting coal-bed methane in the Fruitland Formation. As a result, thousands of Fruitland

coal-bed wells now produce large volumes of natural gas in this part of the basin. Many wells are located within a mile or two of the margin of the basin where the Fruitland coals crop out. The geophysical logs from these gas wells provide most of the basic data for subsurface correlation of Fruitland coal beds in the La Plata County gas seep areas.

PINE RIVER AREA

Coal-bed correlation

The Pine River gas seep area is located where the Los Pinos river (Pine River) has cut through the Hogback Monocline at the northern margin of the San Juan Basin (figure 1-2). The steeply dipping Hogback Monocline, is formed by the massive, cliff-forming, Pictured Cliffs Sandstone (see chapters 2 and 3 for details of the geologic structure in this area). All of the Fruitland Formation coal-gas wells in the vicinity of the Pine River seeps are shown on figure 1-2. Monitor holes were drilled near the gas seeps in an effort to determine the source of the escaping gas (figures 1-2 and 1-4 through 1-6). Geophysical logs from five of these holes were used to correlate Fruitland coal beds in the Pine River seep area; three of these holes were cored. Examination of core from these holes by the author provided detailed corroboration of the lithologies penetrated in these holes as interpreted from geophysical logs. Two sets of structural and stratigraphic cross sections were constructed to illustrate the correlation of Fruitland coals in the subsurface adjacent to the gas seeps (figures 1-3 and 1-4). The location of the cross sections (A-A' and B-B') are shown on figure 1-2.

Figure 1-3a, a stratigraphic cross section along line A-A' shows the detailed correlation of Fruitland coal beds and major sandstone beds in this area. The line of section is about 4.5 miles long and roughly parallels the outcrop of the rocks shown. This cross section ranges from less than a mile to about 1.5 miles downdip (south) from the outcrop of the Pictured Cliffs in the Pine River area (figure 1-2). The depth from the surface to the base of the Fruitland ranges from 1,260 to nearly 1,700 feet along the line of section. The datum for this section is the top of the lower part of the Pictured Cliffs. Coal beds and non-coal partings within coal beds more than one foot thick are shown on this figure, and on all subsequent cross sections. In order to illustrate these relatively thin beds, it was necessary to construct coal-correlation cross sections with a large element of vertical exaggeration. The geophysical log depths of all of the lithologic units shown on this and the other correlation diagrams in this report are listed in appendix 1-1. Geophysical log depths are shown in 100-foot increments for each drill hole shown on these cross sections as are the total depths of each drill hole. Surface elevations for each drill hole are listed in appendix 1-1.

Three large channel sandstones are present on section A-A'. Sandstone no. 2 is the most continuous and was mapped at this same stratigraphic level at the surface (see geologic map in chapter 2). Sandstone no. 3 was also mapped at the surface. An unnamed sandstone bed is present at the east end of the cross section; this bed apparently does not crop out at the surface west of the Pine River. This cross section shows that the large channel sandstones constrained the geometry of some of the coal beds shown on this cross section by differential compaction of the rocks in this interval. The sandstones clearly compacted less than the coals and other finer-grained lithologies as burial and lithification of these rocks progressed. For example, coals C and D (formed as an essentially horizontal deposit as peat built up in Late Cretaceous coal swamps), owes its present, somewhat twisted form, to differential compaction of it and associated underlying and overlying sedimentary rock layers.

A significant stratigraphic rise in the top of the Pictured Cliffs Sandstone is seen on the east end of the cross section in the Wommer and the Magoon wells (figure 1-3a). Coal bed A splits and thins at the base of the large Pictured Cliffs Sandstone tongue and coal beds of zone B terminate opposite this large sandstone bed. Coals C and D were mapped separately at the surface, west of the Pine River seeps (see chapter 2), but as shown in this cross section, these coals merge eastward in the subsurface. Coal bed E, shown at the west end of the cross section (also mapped at the surface) is discontinuous in the subsurface, but another coal bed is present at about the same level on the eastern end of the section. Two thin coals are present in the uppermost Fruitland in the Magoon well on the east end of the cross section.

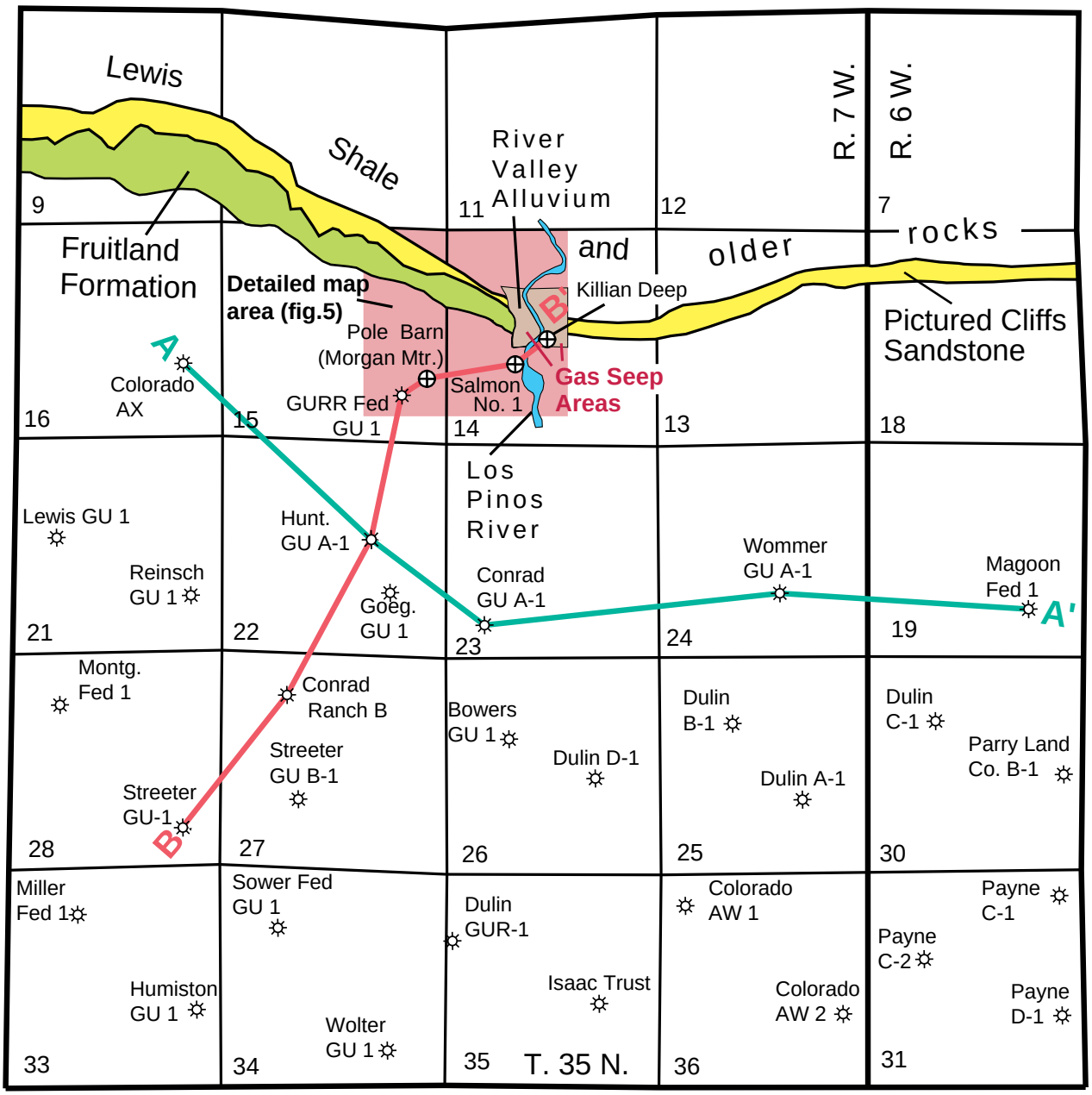

Figure 1-2. Index map of the Pine River gas seep area. Gas seeps are in the river-valley alluvium overlying the Fruitland Formation subcrop in section 14. Producing Fruitland Formation coal-bed methane wells and lines of geologic cross sections A-A' and B-B' are also shown. Figure 1-5 is a large-scale map of the gas seep area. Geology west of Los Pinos river is from plate 5, chapter 2 of this report. Geology east of the river is from Barnes (1953).

Figure 1-3b is a structural cross section along line A-A'. This section was contructed using mean sea level as the datum and has no vertical exaggeration. This cross section shows that the Fruitland Formation is relatively flat in the subsurface along line A-A' .

Stratigraphic cross section B-B' (figure 1-4a), is oriented at right angles to the Fruitland outcrop in the Pine River area (figure 1-2). The Fruitland is about 2,000 feet below the surface at the southwest end of this section. This cross section is approximately 3 miles long and shows the correlation of Fruitland coal beds from deep in the subsurface to near the surface in the vicinity of the Pine River gas seeps (figure 1-2). Vertical exaggeration on this cross section is 34:1. The four deepest

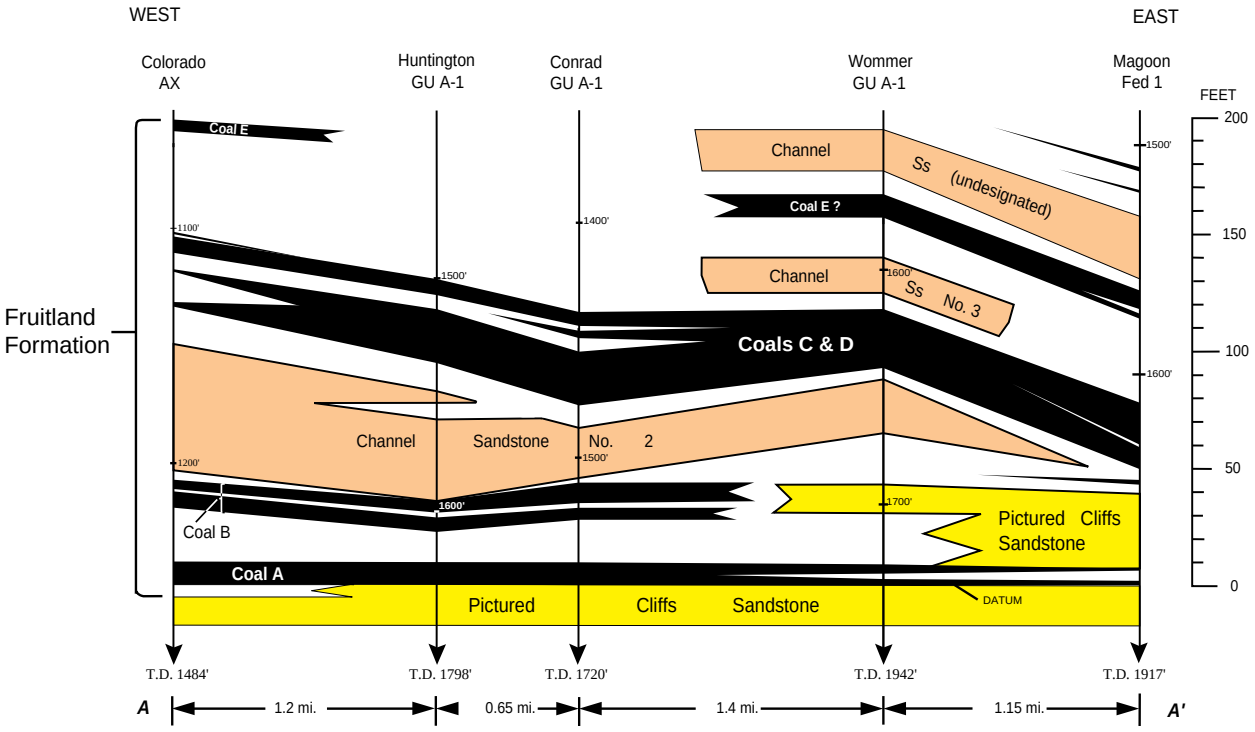

Figure 1-3a. Stratigraphic cross section A-A' showing subsurface coal-bed correlations in the Pine River gas seep area. Coal beds and non-coal partings more than one foot thick are shown. The line of this cross sections is on figure 1-2. Log depths were measured from the Kelly bushing. Vertical exaggeration is 57:1. Tops and bottoms of lithologic units are listed in table 1-1 of appendix 1-1.

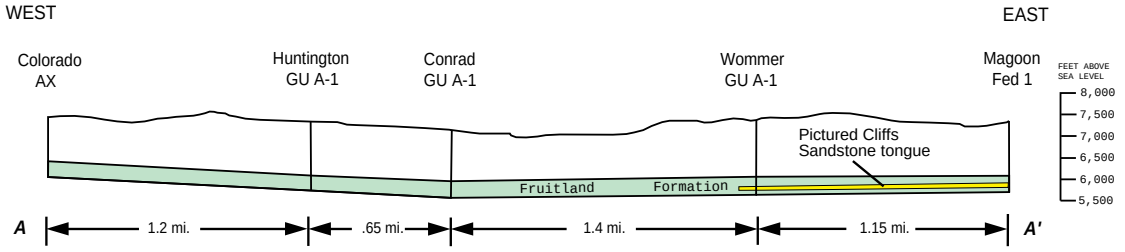

Figure 1-3b. Structural cross section A-A' showing the Fruitland Formation in the subsurface down-dip from the Pine River gas seep area. Line of section is on figure 1-2. There is no vertical exaggeration. Thickness of Pictured Cliffs Sandstone tongue and underlying Fruitland Formation tongue on east end of section is exaggerated about 2.5:1.

holes were drilled as Fruitland coal-bed methane wells and the three near-surface holes, Pole Barn, Salmon No. 1, and Killian Deep, were drilled to provide subsurface information regarding the Pine River gas seeps. Cores from these three shallow holes were examined and described as part of this study.

Coal A, the lowermost Fruitland coal bed, directly overlies the Pictured Cliffs across the entire line of section B-B' (figure 1-4a). At the southwest end of the section in the Streeter well, coal A is 25 feet thick but less than a mile to the northeast, it splits into two thinner coal beds. The upper coal bed pinches out between the Huntington and the GURR wells. The lower part of bed A splits in the Gurr well but maintains its thickness to very near the outcrop in the Salmon No. 1 hole. This basal-Fruitland coal bed thins and becomes

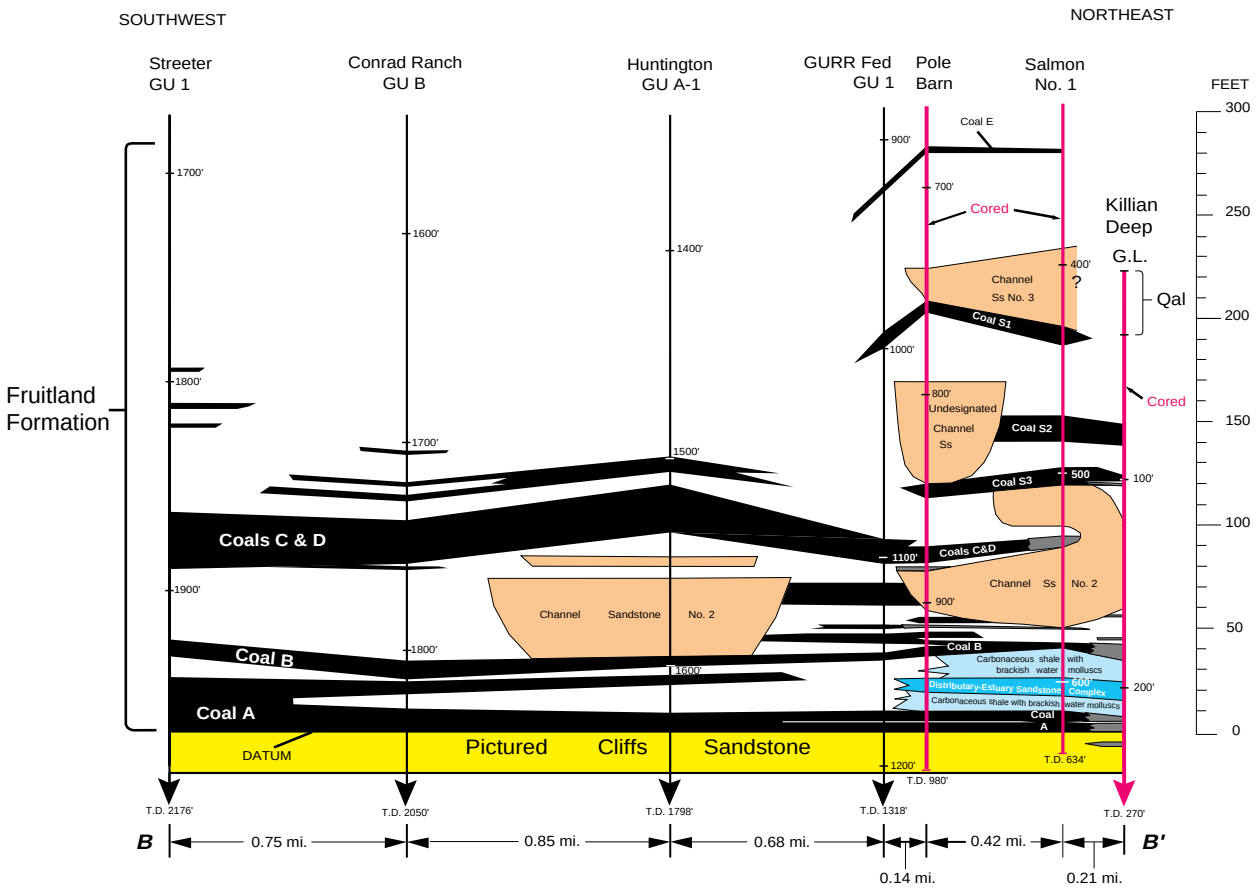

Figure 1-4a. Stratigraphic cross section B-B' showing subsurface coal-bed correlations in the Pine River gas seep area. Vertical exaggeration is 34:1. Coal beds and non-coal partings more than one foot thick are shown. The line of this cross section is on figure 1-2. High-ash coals (density of 1.9 gm/cc) are shown in gray, coals shown in black have a density of 1.75 gm/cc or less). Cores from the GURR Federal, Pole Barn, and Killian Deep drill holes were examined and described to confirm lithologic interpretations based on geophysical logs. Depths to tops and bottoms of lithologic units are listed in table 1-2 of appendix 1-1. Log depths were measured from Kelly bushing.

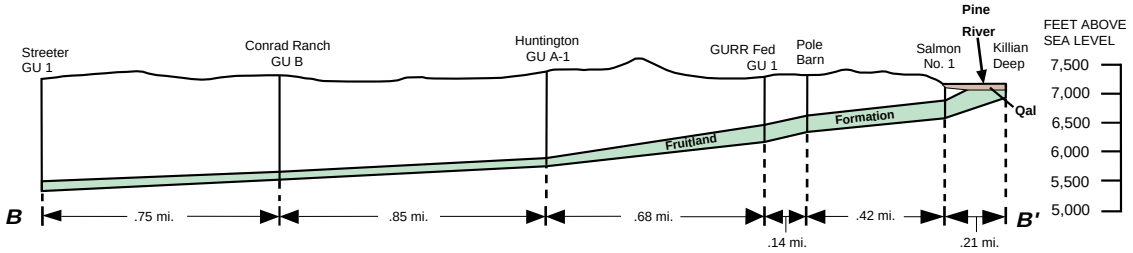

Figure 1-4b. Structural cross section B-B' showing the Fruitland Formation in the subsurface adjacent to the Pine River gas seeps area, no vertical exaggeration. The line of section B-B' is shown on figure 1-2. Thickness of Pine River alluvium (Qal) is exaggerated about 2.5:1.

extremely high ash (density of 1.9 gm/cc) in the Killian Deep hole. Coal bed B generally thins northeastward but maintains its continuity across the entire line of section. This coal bed, however, also becomes very high ash in the Killian Deep drill hole. Coal C and D maintains a thickness of more than 20 feet through the Streeter, Conrad Ranch, and the Huntington wells, but thins to 12 feet

in the GURR well. Northeastward, this bed is thinner and is very high ash in the Salmon hole, pinches out into a sandstone bed, and is absent in the Killian Deep hole. Coal E is a thin, continuous bed in the GURR, Pole Barn, and Killian holes and probably crops out beneath the Pine River alluvium between the Salmon and the Killian holes. Thin, discontinuous coal beds are present above the C and D coal bed in the Streeter, Conrad Ranch, and Huntington wells but none of these coals are continuous into the Pine River gas seep area.

Several discontinuous coal beds in holes adjacent to the seep area (apparently present only in the subsurface) are labeled coal S1 through coal S3 on figure 1-4a. Coal bed S1 might be interpreted as three separate pods of coal in the GURR, Pole Barn, and Killian holes, but it is here portrayed as a continuous coal bed that was draped over the undesignated fluvial sandstone bed in the Pole Barn hole because of differential compaction. This coal bed is apparently not present in the Killian hole but it may have been eroded prior to deposition of the Pine River alluvium (Qal on figure 1-4a). Coal S2 is 13 feet thick in the Salmon No. 1 hole and 11 feet thick in the Killian hole, but abuts against the thick fluvial sandstone bed in the Pole Barn hole. Coal S3 is relatively thick in the Pole Barn and Salmon No. 1 holes, but thins and splits at the Killian hole.

Figure 1-4b is a structural cross section oriented at right angles to the Fruitland outcrop terminating at its northeast end near the Pine River gas seeps. This cross section has no vertical exaggeration. The Pine River gas seeps are coming out of the alluvium (here labeled Qal) between the Killian and the Salmon No. 1 holes (Oldaker, 1996).

Figure 1-5, a larger scale map of the gas seep area, shows the outcrop pattern of the Pictured Cliffs Sandstone and the Fruitland Formation west of the Pine River (from plate 5, chapter 2 of this report) and the alluvium that fills the river's flood plain. The northeast end of cross section B-B' is shown plus the locations of the James No. 1 and Salmon No. 3 drill holes and the line of cross section C-C'. Line of cross section C-B' of figure 1-6 is shown. The subcrop of the Fruitland Formation is shown bounded by dotted lines and a hachure pattern. The upper and lower contacts of the Fruitland subcrop in this area were projected from the four drill holes shown in the alluvium area. The gas seep area (drawn on the basis of data in Oldaker, 1996) is shown as the dark area overlying the upper part of the Fruitland subcrop. Gas seeps have been reported east of the gas-seep area shown here, but those seeps have not been evaluated and no attempt was made to project the gas seep area beyond the documented area.

The trace of the larger scale cross section C-C' is shown through the Salmon No. 1, Salmon No. 3 and the James No. 1 holes. This cross section (upper panel, figure 1-6) is about 0.21 miles long. Cross section C-B' (lower panel, figure 1-6)) is an expanded version of the northeast end of cross section B-B' and is also about 0.21 miles long. These cross sections show the geometry and continuity of the Fruitland coal beds in the seep area itself. The Salmon No. 1 drill hole is common to both cross sections. Down-hole videos were made in the Salmon No. 3, James No. 1, and the Killian Deep holes. These videos were viewed to determine the points at which gas bubbles were entering the drill holes; gas-entry points (as noted by the author) are shown on figure 1-6 with heavy arrows and the capital letter G.

On cross section C-C' (figure 1-6) coals S2 and S3 pinch out short of the Pine River alluvium Fruitland subcrop. Coal S4 is present only in the Salmon No. 3 hole, and coal S5 extends through the Salmon No. 3 and James No. 1 drill holes, and presumably to the subcrop. Coal A is present across the line of section but becomes very high ash in its upper part in the Salmon No. 3 drill hole. The extent of coal S1 updip (north) from the Salmon No. 3 hole is not known. It is interesting to note that coal S2 which is apparently continuous across section C-B' has thinned to a feather edge only about 0.1 mile to the south in the Salmon No. 3 hole. It is also interesting to note that coal B on cross section C-C' is not continuous across this line of section but is missing in the Salmon No. 3 drill hole. Cross section C-B' shows in more detail that coals A and B are very high ash in the Killian Deep hole.

Gas flow through coal beds

The key question regarding the Pine River gas seeps and other gas seeps from Fruitland coal beds

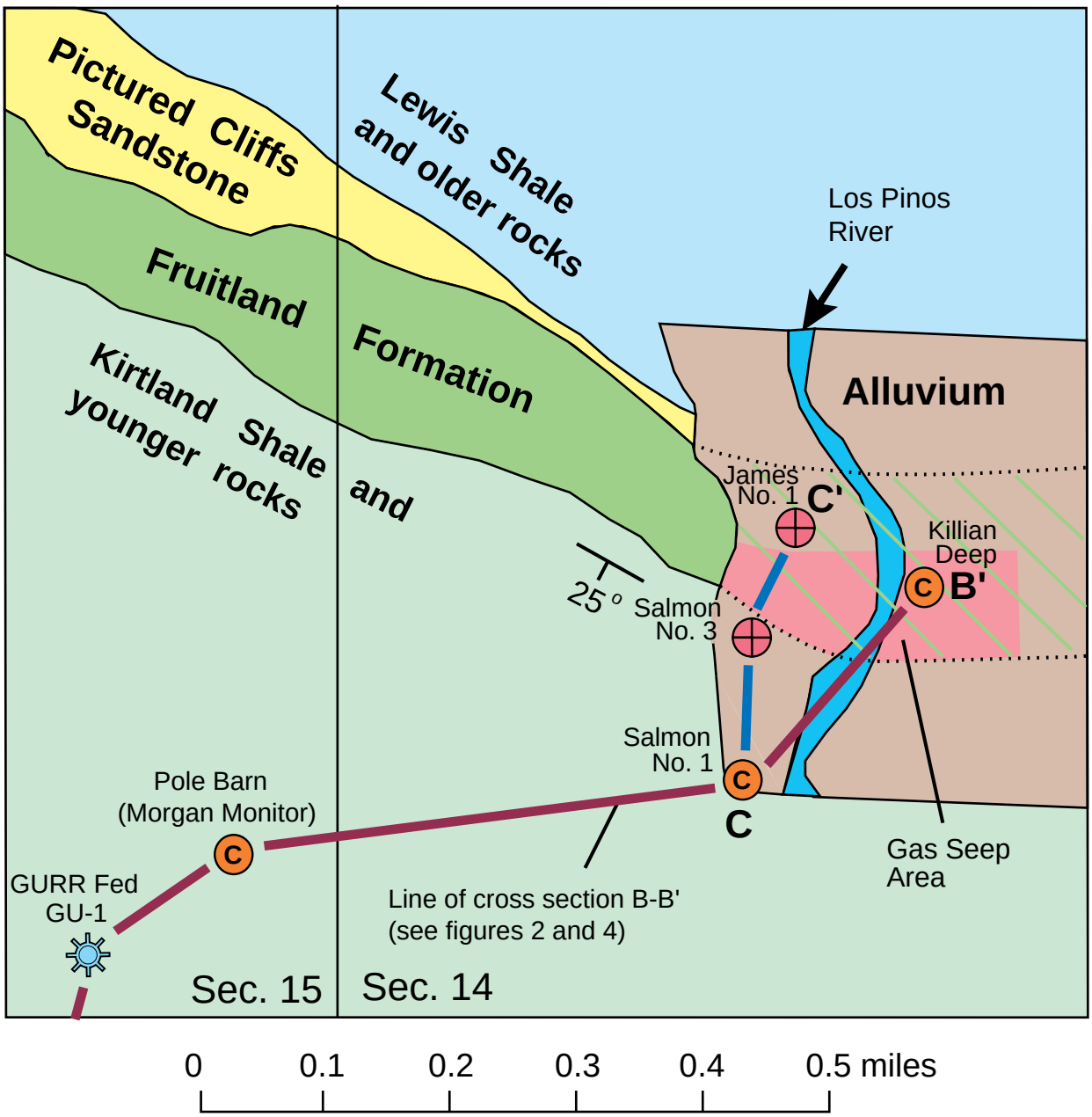

Figure 1-5. Detailed index map of Pine River gas seep area. Geology west of Pine River from plate 5, chapter 2 of this report. Subcrop of Fruitland Formation (hachured area bounded by dotted lines) projected from monitor wells in alluvium area. Gas seep area outline drawn from data in Oldaker (1996). Stratigraphic cross sections C-C' and C-B' are shown on figure 1-6 (section C-B' is the northeast end of section B-B' of figures 1-2 and 1-4). Monitor wells containing the letter C were cored through the Fruitland Formation coal beds and the upper part of the Pictured Cliffs Sandstone.

in the northern San Juan Basin is whether or not the production of water from nearby (down dip, generally southwest) producing coal-bed methane gas wells has liberated adsorbed coal-bed gas and allowed some of this gas to migrate to the surface to emerge as seeps. Figure 1-4a shows that the thicker coals that produce Fruitland gas in the subsurface, notably coal C and D, pinch out before reaching the subcrop in the seep area. Coals A and B do seem to be continuous from the subsurface to the outcrop, however, both of these coals become extremely high ash in the Killian

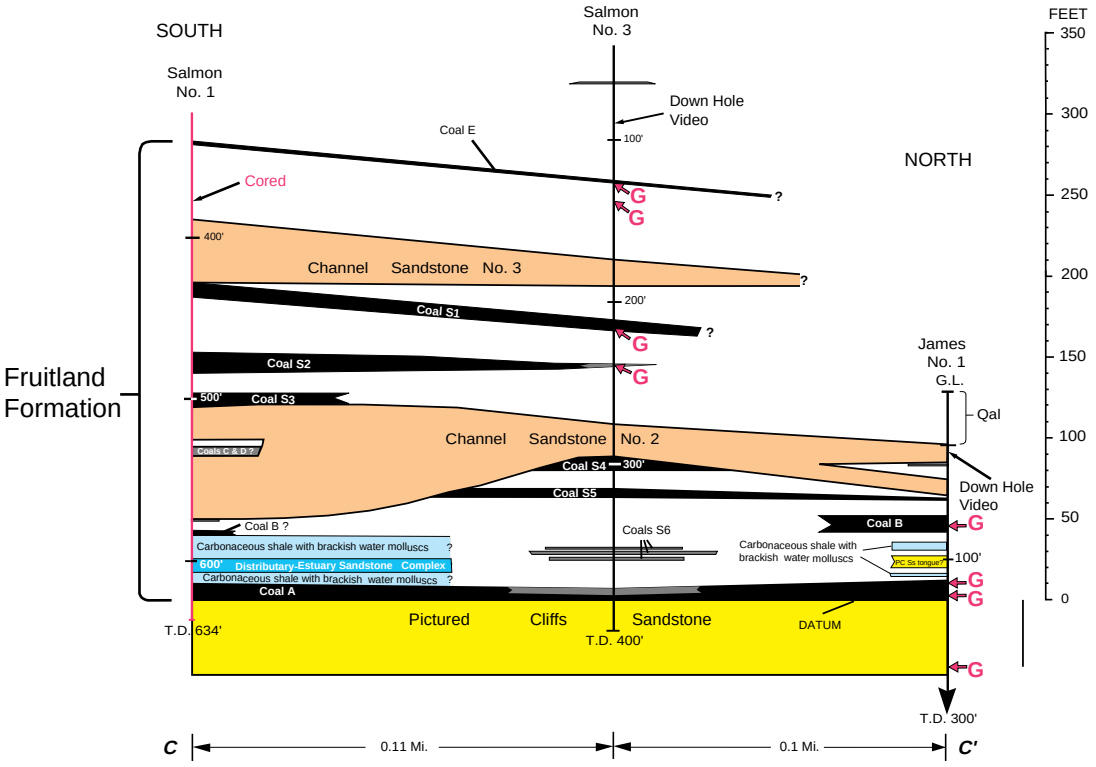
SOUTH
Salmon No. 1
Salmon No. 3
Down Hole Video
Coal E
NORTH
Cored
Channel Sandstone No. 3
Coal S1
Coal S2
Fruitland Formation
Coal S3
Channel Sandstone No. 2
Coals C & D ?
Coal S4
Coal S5
James No. 1 G.L.
Qal
Down Hole Video
Coal B ?
Coals S6
Coal B
Carbonaceous shale with brackish water molluscs
Distributary-Estuary Sandstone Complex
Coal A
Pictured Cliffs Sandstone
DATUM
T.D. 634'
T.D. 400'
T.D. 300'
C
0.11 Mi.
0.1 Mi.
C'
FEET
350
300
250
200
150
100
50
0

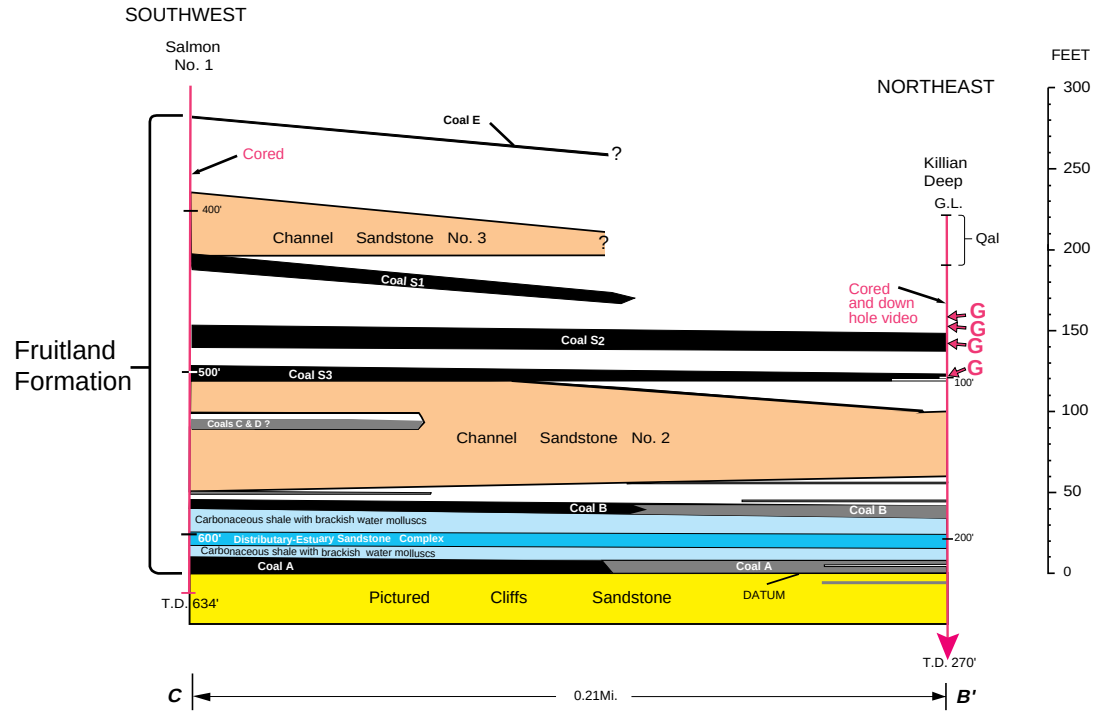
SOUTHWEST
Salmon No. 1
NORTHEAST
Coal E
Cored
Killian Deep G.L.
Qal
Channel Sandstone No. 3
Coal S1
Cored and down hole video
Coal S2
Fruitland Formation
Coal S3
Coals C & D ?
Channel Sandstone No. 2
Coal B
Carbonaceous shale with brackish water molluscs
Distributary-Estuary Sandstone Complex
Coal A
Pictured Cliffs Sandstone
DATUM
T.D. 634'
T.D. 270'
C
0.21Mi.
B'
FEET
300
250
200
150
100
50
0

Figure 6. Geologic cross sections C-C' and C-B' (northeast end of B-B' of figure 1-4a). Lines of sections are on figure 1-5. Vertical exaggeration is 26:1. Lithologic units more than 1 ft thick are shown. Coals shown in black have densities of less than 1.75 gm/cc, coals shown in gray have densities to 1.9 gm/cc. The Salmon No. 1 drill hole is common to both sections. Tops and bottoms of lithologic units and levels of gas bubbles entering hole on down-hole videos are listed in table 1-3 of appendix 1-1. Log depths measured from Kelly bushing. Cores of the Salmon No. 1 and Killian Deep holes were examined to confirm geophysical-log interpretation. Down-hole videos of the Salmon No. 3, Killian Deep, and the James No. 1 holes were viewed to confirm geophysical log interpretations in those holes. These videos also showed gas bubbles entering the drill holes as shown by the arrows and letter G.

hole near where they may subcrop beneath the Pine River alluvium. High-ash coals usually have poorly developed cleat and thus are normally less permeable than low-ash coals. Figure 1-5 shows that the Pine River seeps overlie the upper Fruitland coal beds (coals E, S1, S2, and S3 on figure 1-4a and figure 1-6). Figure 1-4a shows that these upper coal beds are discontinuous and do not extend far into the subsurface and thus have not been major producers of water or gas from commercial gas wells.

Gas-bubble entry points detected on the down-hole videos are shown by heavy arrows and the letter G on cross section C-B' of figure 1-6. Gas emanating from the Killian-hole is entering the hole from noncoal rocks (siltstone beds) above coal S2 and from coals S2 and S3 (cross section C-B', figure 6. No gas whatsoever was entering this drill hole from the lower Fruitland coal beds B or A. It has been argued that the greater water pressure on these deeper coal beds may be preventing the desorption of gas from these coals. However, if these lowermost Fruitland coal beds were serving as conduits for gas moving up from the subsurface, gas liberated by production of coal-bed methane at depth, this gas would be moving through the fractures in these coal beds as free gas (not adsorbed gas) and would be seen bubbling into the Killian hole in the down-hole videos, which is not the case.

Down hole video data from wells on cross section C-C' confirms this interpretation. In the Salmon No. 3 hole, gas is entering the hole only from the higher less continuous coal beds E, S1, and S2 and no gas bubbles are entering the hole from the lower coals S4, S5, S6, and coal A. In the James No. 1 hole, gas bubbles are entering the drill hole from lower Fruitland coal beds A and B; this gas was probably desorbed from these coals due to the presence of the Killian hole which has lowered the pressure on these coal beds. If coal bed A were a conduit for gas from the subsurface, gas would be entering the Salmon No. 3 drill hole from this coal bed and it clearly is not.

FLORIDA RIVER, CARBON JUNCTION, BASIN CREEK AREAS

Cross Section A-A'

Figure 1-7 is a map showing the location of the Florida River, Carbon Junction, and Basin Creek seep areas. The outcrop of the Pictured Cliffs Sandstone is shown as are all of the gas-producing wells within two miles of the Pictured Cliffs outcrop. Lines of cross section A-A', B-B', C-C', and D-D' are shown on figure 1-7. Section A-A' (figure 1-8) is nearly 7 miles long, trends northeast, and parallels the steeply-dipping Pictured Cliffs outcrop on the Hogback Monocline. Depths from the surface to the base of the Fruitland range from less than 2,000 to 2,350 feet along this line of section. The datum for this section is the top of the lower Pictured Cliffs Sandstone (at two levels on this cross section). Section A-A' shows the occurrence and correlation of Fruitland coal beds and the stratigraphic changes in the Pictured Cliffs Sandstone along the line of section. The most striking feature shown on section A-A' is the large stratigraphic rise in the position of the top of the Pictured Cliffs Sandstone in the Federal 4-1 well. The top of the Pictured Cliffs is nearly 100 feet higher in this well than it is at the University 9-2 well less than a mile to the southwest. The large stratigraphic rise in the top of the Pictured Cliffs Sandstone was mapped at the surface in Carbon Junction Canyon (chapter 2 of this report).

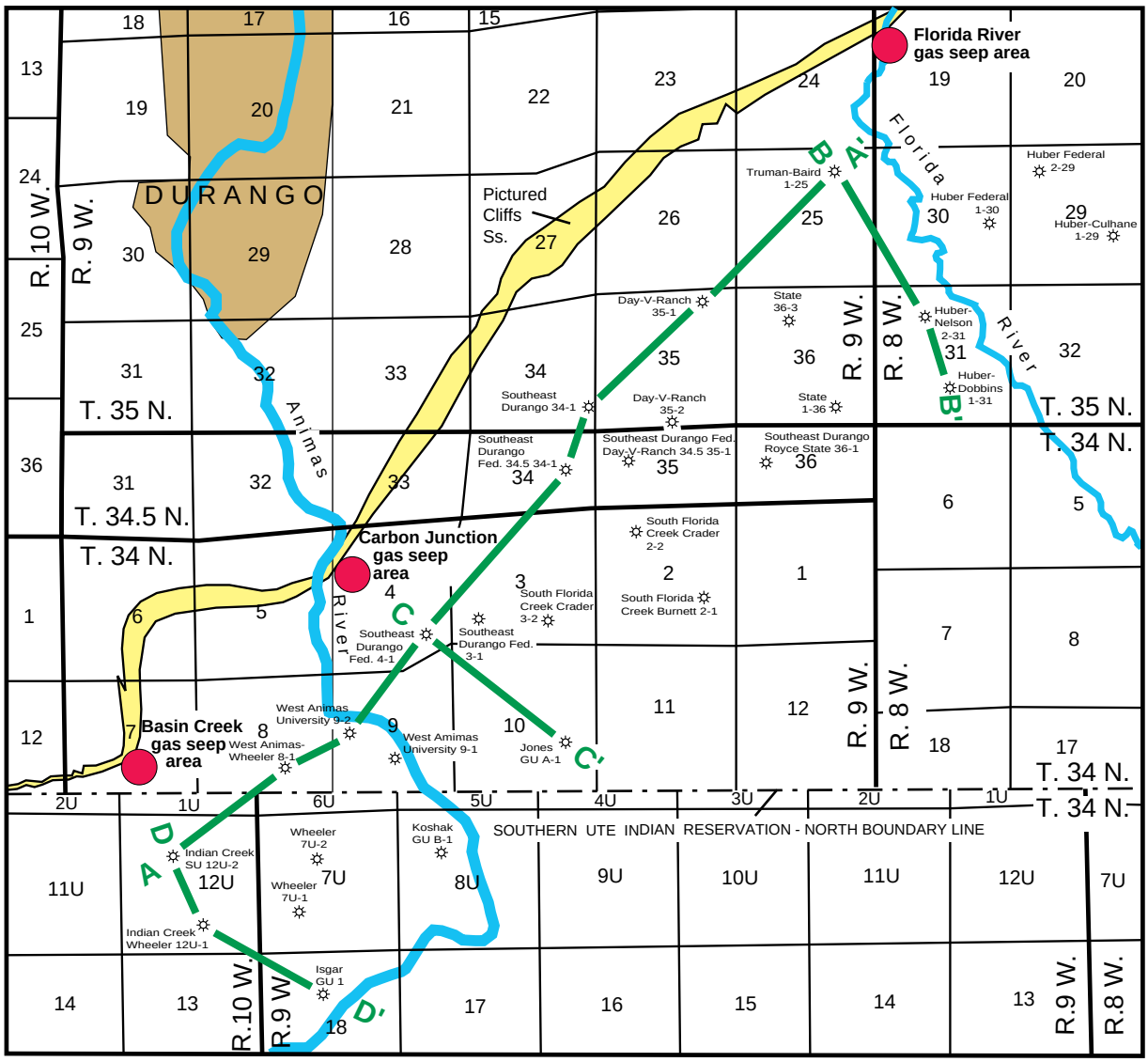

Figure 1-7. Index map of the Florida River, Carbon Junction, and Basin Creek gas seep areas. Gas wells within two miles of the outcropping Pictured Cliffs Sandstone are shown. Lines of cross sections A-A', B-B', C-C', and D-D' show the traces of coal correlation diagrams on figures 1-8, 1-9, 1-10, and 1-11, respectively.

The lack of continuity of the coal beds shown on section A-A' is striking. None of the more than fifty coal beds shown on this cross section are continuous across the entire line of section. The most continuous coal bed on this section is the relatively thin bed lying directly on top of the Pictured Cliffs on the northeast part; this bed extends across most of the line of section but is absent in the Indian Creek and West Animas Wheeler wells at the southwest end. The thick basal Fruitland coal bed present at the southwest end of the section terminates northeastward against the Pictured Cliffs between the West Animas University and the Federal 4-1 wells. The very thick build up of coal in the West Animas University well (a total of 102 feet of coal) is seen to be localized in the vicinity of this well and the West Animas Wheeler well. A very thick coal is present in the Federal 4-1, and Federal 34.5 34-1 wells just above the Pictured Cliffs Sandstone, but this bed thins and pinches out northeastward and is gone at the Truman-Baird well. A slightly higher thick coal is present in the Truman-Baird well, but that bed is not present in the Day-V-Ranch well to the southwest. The only other relatively thick coal is at a depth of about 2,000

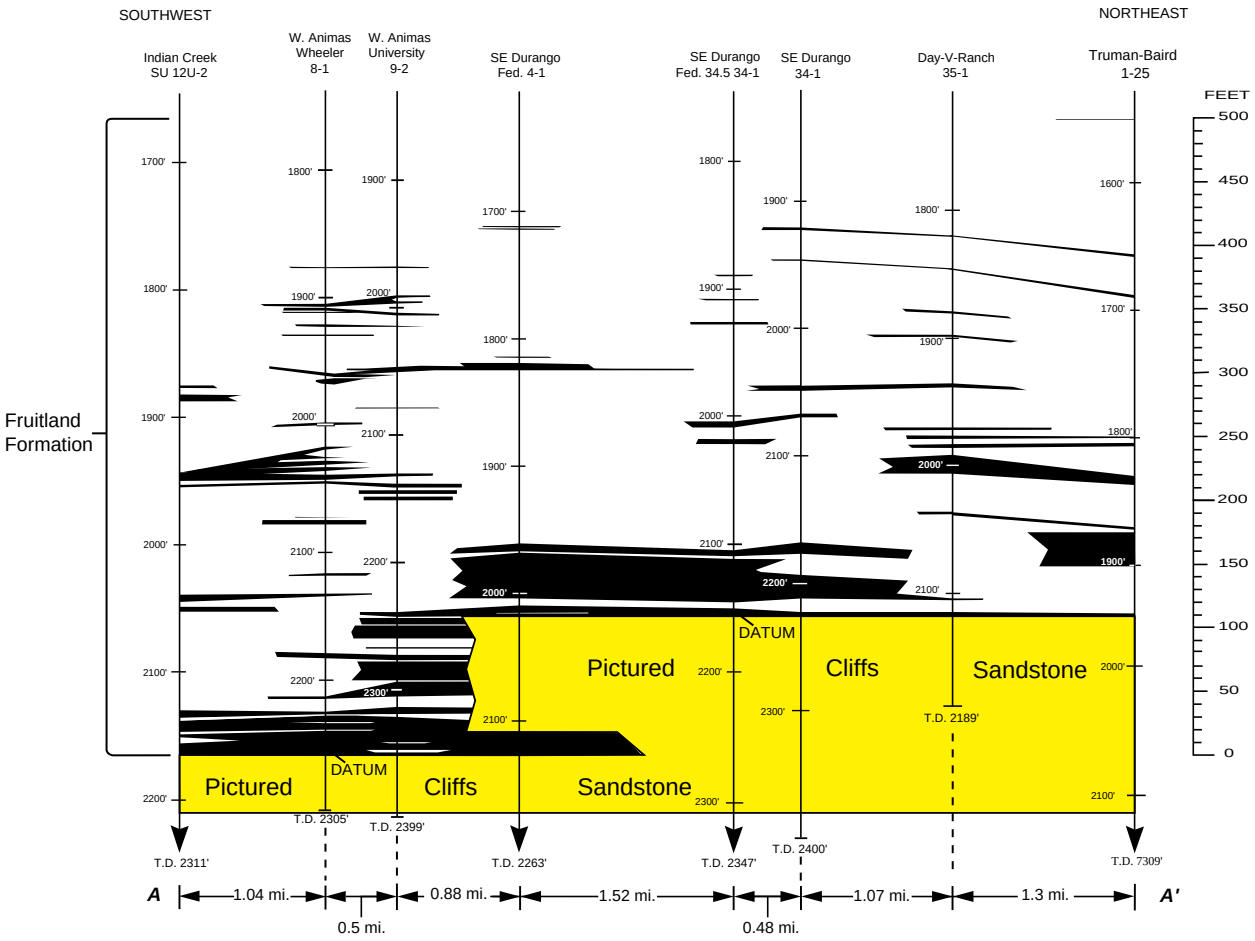

Figure 1-8. Stratigraphic cross section A-A' showing subsurface coal-bed correlations across the Florida River, Carbon Junction, and Basin Creek gas seep areas. Vertical exaggeration is 48:1. Coal beds and non-coal partings more than one foot thick are shown. Trace of cross section on figure 1-7. Tops and bottoms of lithologic units are listed in table 1-4 of appendix 1-1. Log depths measured from Kelly bushing.

feet in the Day-V-Ranch well; this bed thins in the Truman-Baird well and is not present to the southwest. A large number of thinner and more discontinuous coal beds are present throughout the upper part of the Fruitland Formation along this line of section.

Florida River Area

Stratigraphic cross section B-B' (figure 1-9) shows the correlation of Fruitland coals at right angles to the outcrop in the vicinity of the Florida River seep area, the top of the Pictured Cliffs Sandstone is the datum for this section. (This cross section, as well as sections C-C' and D-D', was constructed at the same vertical scale as cross section A-A' to allow for easy comparison of these intersecting cross sections.) This line of section shows relatively good correlation of Fruitland coals; the basal Fruitland coal bed, the two middle coals, and an upper thin coal bed can be correlated across the entire line of section. Coals in the area are relatively thin, with the exception of the thick coal bed in the Truman-Baird well and the thick coal in the Huber-Dobbins well. Surface mapping of Fruitland coals in the vicinity of the Florida River suggests that the coals present in the Truman-Baird well probably extend to the outcrop. However, because the nearest subsurface control point (Truman-Baird well) is a mile away from the Florida gas seep area, continuity of subsurface coals to the outcrop in this area can only be considered speculative, at best.

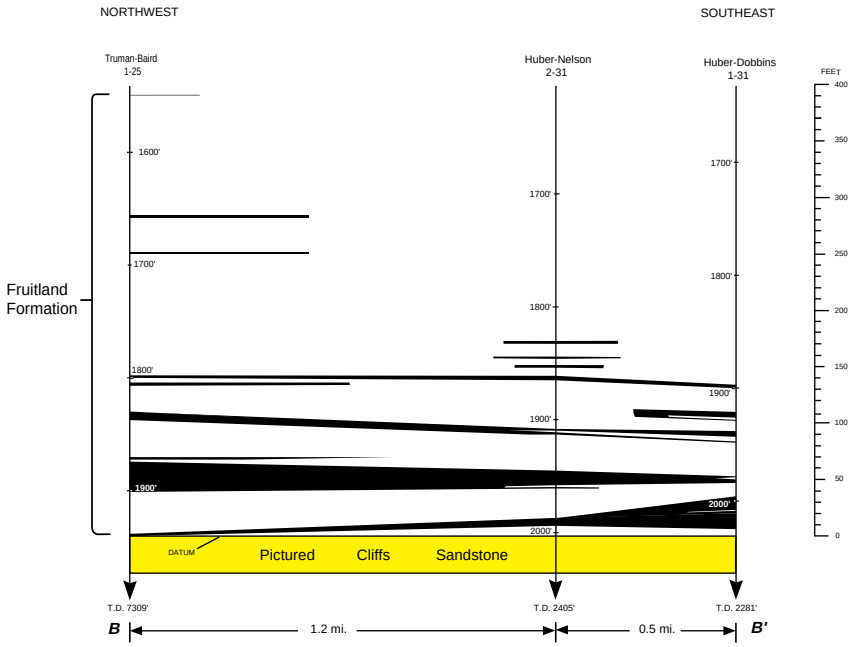

Figure 1-9. Stratigraphic cross section B-B' showing subsurface coal-bed correlations near the Florida River gas seep area. Vertical exaggeration is 17:1. Coal beds and non-coal partings more than one foot thick are shown. Trace of cross section on figure 1-7. Tops and bottoms of lithologic units are listed in table 1-5 of appendix 1-1. Log depths are measured from Kelly bushing.

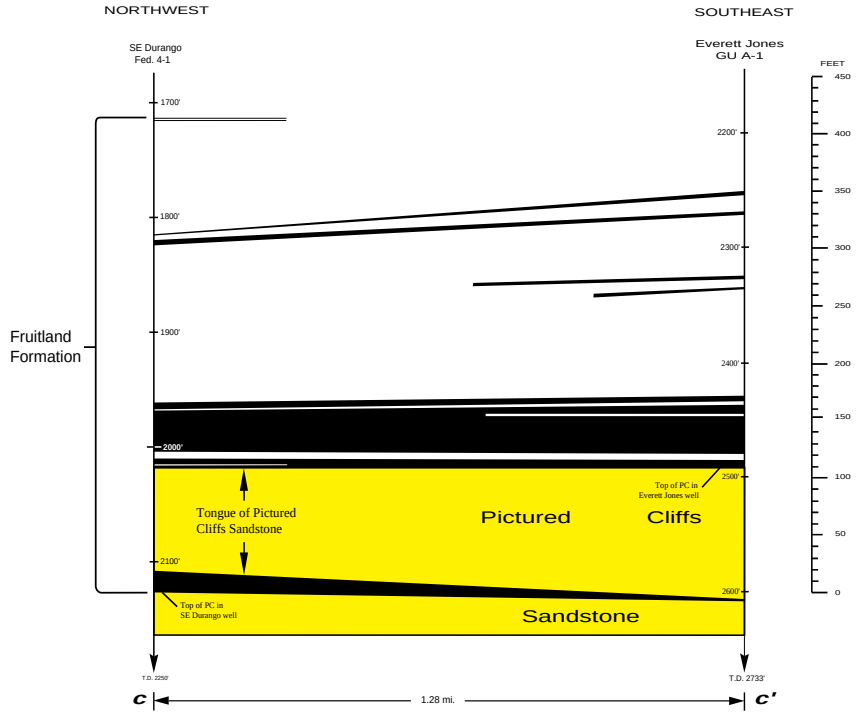

Figure 1-10. Stratigraphic cross section C-C' showing subsurface coal-bed correlations in the Carbon Junction gas seep area. Vertical exaggeration is 13:1. Coal beds and non-coal partings more than one foot thick are shown. The trace of this cross section is shown on figure 1-7. Tops and bottoms of lithologic units are listed in table 1-5 of appendix 1-1. Log depths measured from Kelly bushing. Datum is top of uppermost tongue of Pictured Cliffs Sandstone.

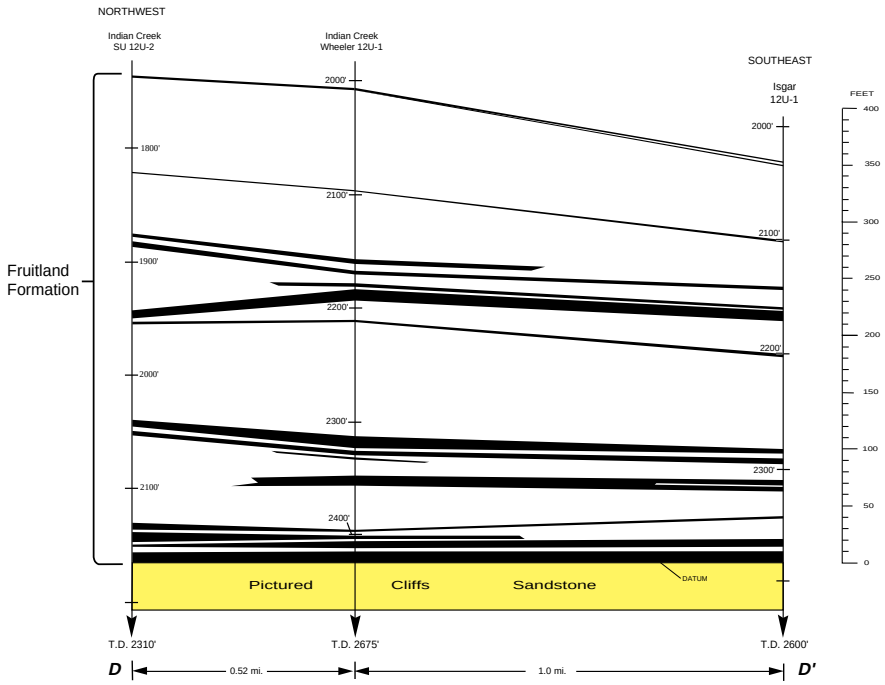

Figure 1-11. Stratigraphic cross section D-D' showing subsurface coal-bed correlations in the Basin Creek gas seep area. Vertical exaggeration is 14:1. Coal beds and non-coal partings more than one foot thick are shown. Line of cross section is on figure 1-7. Tops and bottoms of lithologic units are listed in table 1-6 of appendix 1-1. Log depths measured from Kelly bushing.

Carbon Junction Area

Stratigraphic cross section C-C' (figure 1-10) shows Fruitland coal beds at right angles to the outcrop near the Carbon Junction gas seep area. This two-well cross section shows fairly good continuity of the thick coal bed just above the top of the Pictured Cliffs Sandstone across the line of section, however, this coal bed splits to the southeast. The thinner coal bed lying directly on top of the Pictured Cliffs is also continuous across the line of section. Two thin Fruitland coals extend across both wells in this line of section higher in the Fruitland. The Fruitland coal tongue within the Pictured Cliffs thins to 2-feet thick in the Everett Jones well. At the mouth of Carbon Junction canyon, the thick coal buildup seen at the University 9-2 well on cross section A-A' (figure 1-8) was measured and mapped (see chapter 2), but section C-C' shows that this thick coal zone is not present directly down dip from the Carbon Junction seep area. Because the Federal 4-1 well is only about 0.5 miles from the Carbon Junction gas seep area, and because the thick coals at the outcrop in the gas seep area appear to have the same thickness and geometry in the Federal 4-1 well, there is a high probability that the thick basal Fruitland coal bed is continuous from the subsurface to the outcrop in this area.

Basin Creek Area

Stratigraphic cross section D-D' (figure 1-11) shows the correlation of Fruitland coals in a line of section oriented at right angles to the outcrop. There is excellent correlation of all of the coal zones and most of the coal beds across this line of cross section. Surface mapping at the outcrop near the Basin Creek seep shows thinner and fewer coals than are present in the subsurface, although some of the coal beds shown in the subsurface appear to be present at the outcrop.

REFERENCES CITED

Barnes, Harley, 1953, Geology of the Ignacio area, Ignacio and Pagosa Springs quadrangles, La Plata and Archuleta Counties, Colorado: U.S. Geological Survey Oil and Gas Investigations Map OM-138.

Fassett, J.E., and Hinds, J.S., 1971, Geology and fuel resources of the Fruitland Formation and

Kirtland Shale of the San Juan Basin, New Mexico and Colorado: U.S. Geological Survey Professional Paper 676, 76 p.

Fassett, J.E., and Steiner, M.B., in press, Precise age of C33n-C32r magnetic-polarity reversal, San Juan Basin, New Mexico and Colorado: New Mexico Geological Society 1997 Field Trip Guidebook.

Oldaker, P., 1996, Pilot mitigation program Pine River Ranches, presentation to Colorado Oil and Gas Commission, 3 September, 1996; unpublished report, 20p.

APPENDIX 1-1

Tables 1-1 through 1-6 listing geophysical log depths for lithologic contacts for all drill holes shown on geologic cross sections in this report.

Table 1-1. Geophysical log depths for coal beds in drill holes on Pine River cross section A-A'.

Colorado	Coal	Ss	Above	
AX	Th.	Th.	PC	Notes
0				GL=7467
1053			204	KB=14 ft
1058	5		199	Coal
1101			156	
1102	1		155	Coal
1103			154	
1110	7		147	Coal
1117			140	
1118	1		139	Coal
1131			126	
1133	2		124	Coal
1149			108	
1203		54	54	Sandstone
1207			50	
1211	4		46	Coal
1212			45	
1219	7		38	Coal
1242			15	
1252	10		5	Coal
1257			0	Top PC
1484			-227	T.D.
Total Coal	37			

Wommer	Coal	Ss	Above	
GU A-1	Th.	Th.	PC	Notes
0				GL=7404
1539			195	
1557		18	177	Sandstone
1567			167	KB=12 ft
1577	10		157	Coal
1594			140	
1609		15	125	Sandstone
1616			118	
1641	25		93	Coal
1646			88	
1669		23	65	Sandstone
1691			43	
1703		12	31	Sandstone
1725			9	
1729	4		5	Coal
1731			3	
1734	3		0	Coal
1734			0	Top PC
1942			-208	T.D.
Total Coal	42			

Hunt.	Coal	Ss.	Above	
GU A-1	Th.	Th.	PC	Notes
0				GL=7376
1500			131	KB=12 ft
1507	7		124	Coal
1513			118	
1536	23		95	Coal
1548			83	
1553		5	78	Sandstone
1560			71	
1595		35	36	
1595			36	
1600	5		31	Coal
1602			29	
1608	6		23	Coal
1622			9	
1631	9		0	Coal
1631			0	Top PC
1798			-167	T.D.
Total Coal	50			

Magoon	Coal	Ss.	Above	
Fed 1	Th.	Th.	PC	Notes
0				GL=7382
1508			179	KB=12 ft
1510	2		177	Coal
1518			169	
1519	1		168	Coal
1529			158	
1556		27	131	Sandstone
1561			126	
1569	8		118	Coal
1571			116	
1573	2		114	Coal
1609			78	
1627	18		60	Coal
1628			59	
1637	9		50	Coal
1641			46	
1642	1		45	Coal
1648			39	
1680		32	7	Sandstone
1681	1		6	Coal
1685			2	
1687	2		0	Coal
1687			0	Top PC
1917			-230	T.D.
Total Coal	44			

Conrad	Coal	Ss	Ab	
GU A-1	Th.	Th.		
0				
1437				
1443	6			
1445				
1448	3			
1454				
1477	23			
1483				
1508		25		
1510				
1519	9			
1521				
1526	5			
1544				
1554	10			
1554				
1720				
Total Coal	56			

NOTES: All measurements shown are in feet. Log depths in first column for each drill hole are measured from Kelly bu
PC = Pictured Cliffs Sandstone, T.D. = total depth, GL = ground level.

Killian Deep	Coal Th.	Ss. Th.	Above Kpc	Notes
0			221	GL=7150
31			190	Top bedrk.
73			148	
84	11		137	Coal
98			123	
101	3		120	Coal
102			119	
103	1		118	Hi-ash Coal
121			100	
162		41	59	Sandstone
165			56	
166	1		55	Hi-ash Coal
173			48	
176		3	45	Sandstone
177	1		44	Hi-ash Coal
179			42	
187	8		34	Hi-ash Coal
197			24	CSh, shells
206		9	15	Tongue PC
214			7	CSh, shells
216	2		5	H-ash Coal
217			4	
221	4		0	Hi-ash Coal
221			0	Top P.C.
226		5	-5	Tongue P.C.
228			-7	Tongue Fruit.
270			-49	T.D.
Total C.	31			

Gas bubbles entering hole on video in Killian Deep hole		
Video	Log	Above PC
63-65	61-63	158-160
76-87	73-84	137-148
101-106	98-103	118-123

Hunt. GU A-1	Coal Th.	Ss. Th.	Above PC	Notes
0			1631	GL=7376
1500			131	KB=12 ft
1507	7		124	Coal
1513			118	
1536	23		95	Coal
1548			83	
1553		5	78	Sandstone
1560			71	
1595		35	36	Sandstone
1600	5		31	Coal
1602			29	
1608	6		23	Coal
1622			9	
1631	9		0	Coal
1631			0	Top P.C.
1798			-167	T.D.
Total C.	50			

Salmon No. 1	Coal Th.	Ss. Th.	Above PC	Notes
0			624	GL=7155
342			282	KB=5 ft
344	2		280	Coal
389			235	
428		39	196	Sandstone
437	9		187	Coal
471			153	
484	13		140	Coal
496			128	
505	9		119	Coal
525		20	99	Sandstone
527	2		97	Hi-ash Coal
529			95	
535	6		89	Hi-ash Coal
574		39	50	Sandstone
575	1		49	Hi-ash Coal
581			43	
584	3		40	Coal
598			26	CSh, shells
607		9	17	Tongue P.C.
614			10	CSh, shells
624	10		0	Coal
624			0	Top P.C.
634	45		-10	T.D.
Total C.	53			

Conrad Ranch B	Coal Th.	Above Kpc	Notes
0		1839	GL=7341
1704		135	KB=12ft
1706	2	133	Coal
1719		120	
1721	2	118	Coal
1725		114	
1728	3	111	Coal
1737		102	
1758	21	81	Coal
1759		80	
1761	2	78	Coal
1804		35	
1813	9	26	Coal
1814		25	
1822	8	17	Coal
1827		12	
1839	12	0	Coal
1839		0	Top PC
2050		-211	T.D.
Total C.	59		

Pole Barn	Coal Th.	Ss. Th.	Above PC	Notes
0			962	GL=7244
679			283	KB=4 ft
682	3		280	Coal
737			225	
753		16	209	Sandstone
759	6		203	Coal
776			186	
779		3	183	Sandstone
794			168	
843		49	119	Sandstone
850	7		112	Coal
873			89	
881	8		81	Coal
883			79	
885	2		77	Hi-ash Coal
903		18	59	Sandstone
907			55	
910	3		52	Coal
911			51	
912	1		50	Hi-ash Coal
914			48	
917	3		45	Coal
918			44	
920	2		42	Coal
921			41	
926	5		36	Coal
933			29	
943			19	CSh, shells
951		8	11	Tongue PC
957			5	CSh, shells
958			4	
962	4		0	Coal
962			0	Top P.C.
980			-18	T.D.
Total C.	44			

Streeter Fed. GU 1	Coal Th.	Ss. Th.	Above PC	Notes
0			1968	GL=7330
1794			174	KB=13
1795	1		173	Coal
1813			155	
1814	1		154	Coal
1820			148	
1823	3		145	Coal
1866			102	
1887	21		81	Coal
1928			40	
1934	6		34	Coal
1943			25	
1968	25		0	Coal
1968			0	Top PC
2150			-182	T.D.
Total C.	57			

GURR Fed	Coal Th.	Ss. Th.	A P
0			
822			
824	2		
858			
894		36	
901	7		
906			
918		12	
968			
992		24	
1004	12		
1013			
1024	11		
1025			
1026	1		
1033			
1035	2		
1037			
1042	5		
1043			
1045	2		
1046			
1050	4		
1073			
1079	6		
1080			
1084	4		
1084			
1318			
Total C.	56		

Table 1-2. Geophysical log depths for coal beds in drill holes on Pine River cross section B-B'

NOTES: All measurements shown are in feet. Log depths in first column for each drill hole are measured from Kelly bushing (KB).
PC = Pictured Cliffs Sandstone, T.D. = total depth, GL = ground level, CSh, shells = carbonaceous shale with brackish-water molluscs.
Hi-ash Coal is coal with a density of 1.9 gm/cc on density logs

Table 1-3. Geophysical log depths for coal beds in drill holes on Pine River cross section C-C'

Salmon No. 1	Coal Th.	Ss. Th.	Above Kpc	Notes
0			624	GL=7155
342			282	KB=5 ft
344	2		280	Coal
389			235	
428		39	196	Sandstone
437	9		187	Coal
471			153	
484	13		140	Coal
496			128	
505	9		119	Coal
525		20	99	Sandstone
527	2		97	Hi-ash Coal
529			95	
535	6		89	Hi-ash Coal
574		39	50	Sandstone
575	1		49	Hi-ash Coal
581			43	
584	3		40	Coal
598			26	CSh, shells
607		9	17	Tongue P.C.
614			10	CSh, shells
624	10		0	Coal
624			0	Top P.C.
634	45		-10	T.D.
Total C.	53			

Salmon No. 3	Coal Th.	Ss. Th.	Above Kpc	Notes
0			384	GL=
64			320	
65	1		319	Hi-ash Coal
125			259	
127	2		257	Coal
174			210	
192		18	192	Sandstone
211			173	
217	6		167	Coal
240			144	
241	1		143	Hi-ash Coal
277			107	
294		17	90	Sandstone
304	10		80	Coal
315			69	
321	6		63	Coal
352			32	
353	1		31	Hi-ash Coal
354			30	
356	2		28	Hi-ash Coal
358			26	
359	1		25	Hi-ash Coal
377			7	
381	4		3	Hi-ash Coal
381			3	
384	3		0	Coal
384			0	Top P.C.
400			-16	T.D.
Total C.	37			

Gas bubbles entering hole on down-hole video

Video	Log	
129	127	257
132	130	254
139-140	137-139	245
216	214	170
218	216	168
230	228	156
243	241	143

James No. 1	Coal Th.	Ss. Th.	Above Kpc
0			12
29			9
40		11	8
41			8
42	1		8
49			7
59		10	6
62			6
64	2		6
73			5
83	10		4
98			2
102		4	2
113			1
125	12		
125			
300			-17
Total C.	25		

Gas bubbles entering hole on down-hole video

Video	Log	
79	77	4
115	113	1
120	118	
172	170	-4

NOTES: All measurements shown are in feet. Log depths in first column for each drill hole are measured from Kelly bushing (KB). PC = Pictured Cliffs Sandstone, T.D. = total depth, GL = ground level, CSh, shells = carbonaceous shale with brackish-water molluscs. Hi-ash Coal is coal with a density of 1.9 gm/cc on density logs

Indian Crk.	Coal	Above	
SU-12U-2	Th.	P.C.	Notes
0		2165	GL=6700
1875		290	KB=6
1877	2	288	Coal
1882		283	
1887	5	278	Coal
1943		222	
1950	7	215	Coal
1953		212	
1955	2	210	Coal
2039		126	
2045	6	120	Coal
2049		116	
2053	4	112	Coal
2130		35	
2136	6	29	Coal
2138		27	
2147	9	18	Coal
2149		16	
2151	2	14	Coal
2156		9	
2165	9	0	Coal
2165		0	Top PC
2311		-146	TD
Total Coal	52		

SE Durango	Coal	Above	
34-1	Th.	P.C.	Notes
0		2226	GL=7205
1921		305	KB=14ft
1923	2	303	Coal
1946		280	
1947	1	279	Coal
2045		181	
2049	4	177	Coal
2067		159	
2070	3	156	Coal
2168		58	
2182	14	44	Coal
2195		31	
2212	17	14	Coal
2223		3	
2226	3	0	Coal
2226		0	Top PC
2400		-174	T.D.
Total Coal	44		

W. Animas	Coal	Above	
Wheeler 8-1	Th.	P.C.	Notes
0		2259	GL=6821
1892		367	KB=15
1893	1	366	Coal
1905		354	
1907	2	352	Coal
1908		351	
1910	2	349	Coal
1911		348	
1912	1	347	Coal
1921		338	
1923	2	336	Coal
1929		330	
1930	1	329	Coal
1998		261	
2000	2	259	Coal
2017		242	
2019	2	240	Coal
2025		234	
2026	1	233	Coal
2028		231	
2031	3	228	Coal
2033		226	
2036	3	223	Coal
2039		220	
2043	4	216	Coal
2044		215	
2046	2	213	Coal
2072		187	
2073	1	186	Coal
2074		185	
2078	4	181	Coal
2116		143	
2118	2	141	Coal
2132		127	
2134	2	125	Coal
2156		103	
2162	6	97	Coal
2164		95	
2175	11	84	Coal
2178		81	
2182	4	77	Coal
2213		46	
2215	2	44	Coal
2225		34	
2227	2	32	Coal
2228		31	
2233	5	26	Coal
2234		25	
2239	5	20	Coal
2240		19	
2259	19	0	Coal
2259		0	Top PC
2305		-46	T.D.
Total Coal	89		

W. Animas	Coal	Above	
Univ. 9-2	Th.	P.C.	Notes
0		2351	GL=6720
1968		383	KB=16
1969	1	382	Coal
1990		361	
1992	2	359	Coal
1995		356	
1996	1	355	Coal
2004		347	
2006	2	345	Coal
2014		337	
2015	1	336	Coal
2079		272	
2080	1	271	Coal
2130		221	
2132	2	219	Coal
2138		213	
2141	3	210	Coal
2143		208	
2146	3	205	Coal
2148		203	
2151	3	200	Coal
2239		112	
2242	3	109	Coal
2243		108	
2248	5	103	Coal
2249		102	
2254	5	97	Coal
2256		95	
2257	1	94	Coal
2267		84	
2276	9	75	Coal
2277		74	
2292	15	59	Coal
2293		58	
2305	12	46	Coal
2313		38	
2319	6	32	Coal
2321		30	
2341	20	10	Coal
2342		9	
2347	5	4	Coal
2349		2	
2351	2	0	Coal
2351		0	Top PC
2399		-48	T.D.
Total Coal	102		

SE Durango	Coal	Above	
Fed. 4-1	Th.	P.C.	Notes
0		2127	GL=
1712		415	KB=14ft
1713	1	414	Coal
1714		413	
1715	1	412	Coal
1814		313	
1815	1	312	Coal
1819		308	
1824	5	303	Coal
1961		166	
1967	6	160	Coal
1968		159	
2004	36	123	Coal
2010		117	
2015	5	112	Coal
2016		111	
2018	2	109	Coal
2018		109	
2108		19	
2127	19	0	Coal
2127		0	Top PC
2263		-136	T.D.
Total Coal	76		

Day-V-Ranch	Coal	Above	
35-1	Th.	P.C.	Notes
0		2118	GL=7139
1819		299	KB=13ft
1820	1	298	Coal
1845		273	
1846	1	272	Coal
1880		238	
1881	1	237	Coal
1897		221	
1899	2	219	Coal
1936		182	
1937	1	181	Coal
1969		149	
1974	5	144	Coal
1976		142	
1979	3	139	Coal
1983		135	
1986	3	132	Coal
1991		127	
2006	15	112	Coal
2036		82	
2038	2	80	Coal
2104		14	
2105	1	13	Coal
2115		3	
2118	3	0	Coal
2118		0	Top PC
2189		-71	T.D.
Total Coal	38		

SE Durango	Coal	Above	
Fed 34.5 34-1	Th.	P.C.	
0		2	
1909			
1910	1		
1928			
1929	1		
1946			
1948	2		
2024			
2029	5		
2038			
2042	4		
2125			
2130	5		
2132			
2166	34		
2171			
2177	6		
2177			
2347		-1	
Total Coal	58		

Truman-	Coal	Above	
Baird 1-25	Th.	P.C.	
0		1	
1550			
1551	1		
1656			
1658	2		
1688			
1690	2		
1799			
1800	1		
1804			
1807	3		
1830			
1837	7		
1870			
1872	2		
1874			
1901	27		
1938			
1940	2		
1940			
7309		-53	
Total Coal	47		

NOTES: All measurements shown are in feet. Log depths in first column for each drill hole are measured from Kelly Bushing (KB).
PC = Pictured Cliffs Sandstone, T.D. = total depth, GL = ground level

Table 1-4. Geophysical log depths for coal beds in drill holes in Florida River, Carbon Junction, and Basin Creek areas; cross section A-A'

Table 1-5. Geophysical log depths for coal beds in drill holes on Florida River cross section B-B' and Carbon Junction cross section C-C'.

CROSS SECTION B-B' - - FLORIDA RIVER GAS SEEP AREA											
Truman-	Coal	Above		Huber-	Coal	Above		Huber-	Coal	Above	
Baird 1-25	Th.	P.C.	Notes	Nelson 2-31	Th.	P.C.	Notes	Dobbins 1-31	Th.	P.C.	Notes
0		1940	GL=7323	0		2003	GL=7077	0		2031	GL=7052
1550		390	KB=13ft	1831		172	KB=13.5ft	1897		134	Kb=13ft
1551	1	389	Coal	1832	1	171	Coal	1900	3	131	Coal
1656		284		1844		159		1921		110	
1658	2	282	Coal	1846	2	157	Coal	1926	5	105	Coal
1688		252		1847		156		1928		103	
1690	2	250	Coal	1848	1	155	Coal	1929	1	102	Coal
1799		141		1861		142		1938		93	
1800	1	140	Coal	1865	4	138	Coal	1943	5	88	Coal
1804		136		1908		95		1947		84	
1807	3	133	Coal	1909	1	94	Coal	1948	1	83	Coal
1830		110		1911		92		1978		53	
1837	7	103	Coal	1913	2	90	Coal	1979	1	52	Coal
1870		70		1945		58		1981		50	
1872	2	68	Coal	1958	13	45	Coal	1984	3	47	Coal
1874		66		1960		43		1996		35	
1901	27	39	Coal	1961	1	42	Coal	2008	12	23	Coal
1938		2		1987		16		2010		21	
1940	2	0	Coal	1994	7	9	Coal	2024	14	7	Coal
1940		0	Top Kpc	2003		0	Top PC	2031		0	Top PC
7309		-5369	T.D.	2102		-99		2134		-103	
Total coal	47			2104	2	-101	Coal	2136	2	-105	Coal
				2405		-402	T.D.	2140		-109	
				Total coal	34			2143	3	-112	Coal
								2281		-250	T.D.
								Total coal	50		

CROSS SECTION C-C' - - CARBON JUNCTION GAS SEEP AREA							
SE Durango	Coal	Above		Everett Jones	Coal	Above	
Fed. 4-1	Th.	P.C.	Notes	GU A-1	Th.	P.C.	Notes
0		2127	GL=	0		2492	GL=6876
1712		415	KB=14ft	2250		242	KB=13ft
1713	1	414	Coal	2254	4	238	Coal
1714		413		2268		224	
1715	1	412	Coal	2271	3	221	Coal
1814		313		2324		168	
1815	1	312	Coal	2329	5	163	Coal
1819		308		2334		158	
1824	5	303	Coal	2336	2	156	Coal
1961		166		2429		63	
1967	6	160	Coal	2435	6	57	Coal
1968		159		2437		55	
2004	36	123	Coal	2445	8	47	Coal
2010		117		2447		45	
2015	5	112	Coal	2480	33	12	Coal
2016		111		2485		7	
2018	2	109	Coal	2492	7	0	Coal
2108		19		2492			Top PC
2127	19	0	Coal	2606		-114	
2127		0	Top PC	2608	2	-116	Coal
2250		-123	T.D.	2733		-241	T.D.
Total coal	76			Total Coal	70		

NOTES: All measurements shown are in feet. Log depths in first column for each drill hole are measured from the Kelly bushing (KB). PC = Pictured Cliffs Sandstone, T.D. = total depth, GL = ground level.

Table 1-6. Geophysical log depths for coal beds in drill holes on Basin Creek cross section D-D'.

Indian Crk. SU-12U-2	Coal Th.	Above P.C.	Notes
0		2165	GL
1736		429	KB=6ft
1738	2	427	Coal
1821		344	
1822	1	343	Coal
1875		290	
1878	3	287	Coal
1881		284	
1888	7	277	Coal
1941		224	
1951	10	214	Coal
1952		213	
1956	4	209	Coal
2038		127	
2046	8	119	Coal
2048		117	
2053	5	112	Coal
2129		36	
2136	7	29	Coal
2137		28	
2148	11	17	Coal
2149		16	
2151	2	14	Coal
2152		13	
2165	13	0	Coal
2165		0	Top PC
2310		-145	T.D.
Total Coal	73		

Indian Crk. SU-12U-1	Coal Th.	Above P.C.	Notes
0		2425	GL
1874		551	KB=6ft
1875	1	550	Coal
2007		418	
2009	2	416	Coal
2097		328	
2098	1	327	Coal
2158		267	
2162	4	263	Coal
2168		257	
2171	3	254	Coal
2179		246	
2182	3	243	Coal
2184		241	
2194	10	231	Coal
2211		214	
2213	2	212	Coal
2313		112	
2324	11	101	Coal
2326		99	
2330	4	95	Coal
2332		93	
2334	2	91	Coal
2348		77	
2357	9	68	Coal
2396		29	
2398	2	27	Coal
2401		24	
2404	3	21	Coal
2406		19	
2412	6	13	Coal
2415		10	
2425	10	0	Coal
2425		0	Top PC
2675		-250	T.D.
Total Coal	73		

Isgar GU 1	Coal Th.	Above P.C.	Notes
0		2384	Gl
2031		353	KB=12ft
2032	1	352	Coal
2034		350	
2035	1	349	Coal
2100		284	
2102	2	282	Coal
2141		243	
2144	3	240	Coal
2159		225	
2161	2	223	Coal
2162		222	
2171	9	213	Coal
2200		184	
2203	3	181	Coal
2284		100	
2288	4	96	Coal
2292		92	
2297	5	87	Coal
2311		73	
2316	5	68	Coal
2317		67	
2321	4	63	Coal
2343		41	
2345	2	39	Coal
2363		21	
2370	7	14	Coal
2374		10	
2384	10	0	Coal
2384		0	Top PC
2600		-216	T.D.
Total Coal	58		

NOTES: All measurements shown are in feet. Log depths in first column for each drill hole are measured from the Kelly bushi
PC = Pictured Cliffs Sandstone, T.D. = total depth, GL = ground level.

This page is blank.

Geologic mapping and fracture studies of the Upper Cretaceous Pictured Cliffs Sandstone and Fruitland Formation in selected parts of La Plata County, Colorado

By Steven M. Condon

With Contributions From E.A. Johnson, R.C. Milici, And J.E. Fassett

INTRODUCTION

In early 1995 a proposal was submitted by the U.S. Geological Survey to the Colorado Oil and Gas Commission to conduct a geologic study addressing the problem of coalbed methane gas seepage in La Plata County. Part of the original proposal was to map the entire outcrop of Fruitland Formation in the county, exclusive of land on the Southern Ute Indian Reservation, and to measure fractures in these same rocks. This proposal did not meet the budget requirements of the funding group, so a scaled-down proposal was submitted, and accepted, to study only selected parts of the county. Beginning in July, 1995, the USGS conducted studies at selected places in La Plata County that had been previously identified in a geochemical survey as having a potential for above-average amounts of methane and/or hydrogen sulfide gas seepage from coal beds in the Upper Cretaceous Fruitland Formation. These areas were at Basin Creek, southwest of Durango; Carbon Junction, at the south edge of Durango; Florida River, where the coal outcrops cross the river; the South Fork of Texas Creek, west of Columbus in northeastern La Plata County; and an extension of that area southeast to the Pine River, north of Bayfield (fig. 2-1).

The objective of this study was to provide detailed geologic maps of the various sites to establish the stratigraphic position of coal beds at the outcrop in the Fruitland Formation. This stratigraphic information could then be tied to subsurface stratigraphic studies on the same stratigraphic interval being conducted by J.E. Fassett (this report). Because methane is being extracted from Fruitland coal beds a short distance south of the outcrop, and because coal beds are known to be good conduits of gas and water (Gayer and Harris, 1996; Law and Rice, 1993; Schwochow, 1991), it is important to know the extent of coal beds in the subsurface and at surface exposures. An additional part of this study was to measure orientations of joints in sandstone and cleats in coal of the Fruitland Formation and Pictured Cliffs Sandstone at surface exposures. These data can be used to show the type of fracturing present and the regional trends of possible migration pathways for methane and/or hydrogen sulfide from the subsurface to surface outcrops.

Initial reconnaissance of the area was done in July, 1995 by S.M. Condon and E.A. Johnson; subsequent mapping and fracture studies were conducted by Condon and R.C. Milici in September and October, 1995; by Condon and J.E. Fassett in April, 1996; and by Condon in May, 1996. Techniques used were (1) to

measure sections of the Fruitland to gain an understanding of the rock types and the distribution of rock types in the formation, (2) to use topographic maps and aerial photographs to create geologic maps; and (3) to measure the orientations and characteristics of fractures in sandstone and coal in the Fruitland Formation and Pictured Cliffs Sandstone.

This report is divided into two parts. Part 1 describes the geologic framework of the Fruitland Formation as determined from geologic mapping and from measuring stratigraphic sections through all or part of the Fruitland in various places. Each of the five areas is first discussed separately, and then a synthesis follows that ties together the information gathered in all of the areas. Plates 1, 2, 3, and 5 are geologic maps of the separate areas. Plate 7 shows correlations of measured stratigraphic sections in each of the areas. Part 2 is a discussion of the fractures that were measured and described in each of the sub-areas. Plates 1, 2, 4, and 6 show the locations of where fractures were measured, plotted on a geologic base map. Note that the maps on plates 1 and 2 are at a scale of 1:6,000 and that the other maps are at a scale of 1:12,000. The small size of the mapped areas at Basin Creek (plate 1) and Carbon Junction (plate 2) allowed the use of the larger scale in those areas.

Thanks are extended to Jeff Olson, Bureau of Land Management in Durango, for his help with this project. Jeff had done preliminary geologic and geochemical studies and had contacted most of the landowners in the study areas prior to the involvement of the USGS in this project. He also provided valuable assistance in the field in collecting some of the data for this report. The manuscript benefited from the comments of Laura N.R. Roberts, Vito Nuccio, Tom Ann Casey, Debbie Baldwin, and Reed Scott.

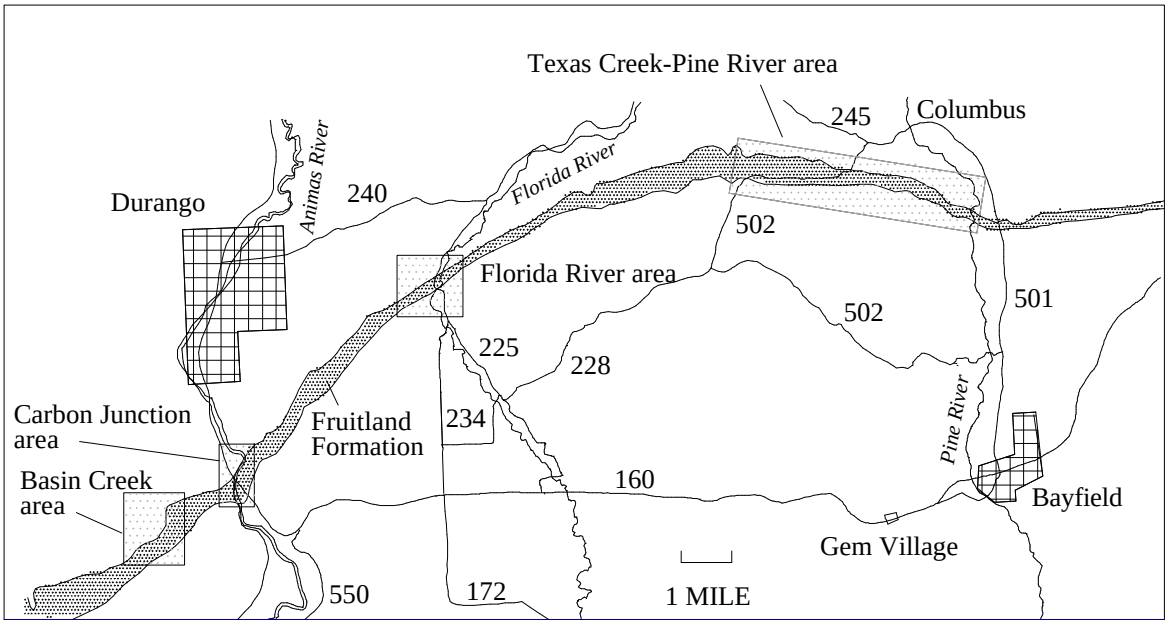

Figure 2-1. Map showing the location of the project area and individual sub-areas. Numbers indicate county and state roads and highways. (Modified from digital data provided by the Bureau of Land Management, Durango, Colo.)

PART 1—GEOLOGIC FRAMEWORK

Basin Creek

Mapping in the Basin Creek area was mainly in the southwest and northeast quarters of section 7 and a small part of the SE¼ of section 6, T. 34 N., R. 9 W. (plate 1). This area is characterized by fairly steep topography, with the Fruitland Formation outcrop ranging in elevation from less than 6700 ft along the creek to nearly 7500 ft in the northern part of the study area. The Upper Cretaceous Pictured Cliffs Sandstone and Fruitland Formation strike northeasterly in this area and dip to the southeast, forming part of the northwest side of the San Juan Basin. Dips range from 20 degrees to 42 degrees (Table 2-1), but average about 28 degrees.

A major obstacle to geologic mapping in the part of the area south of the creek is the presence of dense stands of brush that completely obscure much of the hillsides. In that area only scattered outcrops are exposed, mainly along ridge lines. The area north of the creek is covered by a piñon-juniper forest, typical for this area, with somewhat better exposures of the mapped rocks. A road is present along the north side of the creek, and several road cuts allow for examination of the Pictured Cliffs Sandstone, Fruitland Formation, and Kirtland Shale. The measured section in this area, shown on figure 2-2 and plate 7, was measured along the road. Plate 1 shows the geology of this area. The oldest geologic unit shown on the map is the Upper Cretaceous Lewis Shale, a gray marine shale unit. The contact of the Lewis with the overlying Pictured Cliffs Sandstone is not exposed south of the creek, but is visible high on the west and northwest-facing cliffs north of the creek. This contact was interpreted from aerial photographs, and was placed at the base of the massive sandstone beds of the Pictured Cliffs. The contact is gradational, with sandstone beds in the upper Lewis becoming thicker up-section. The Pictured Cliffs is light brown to light gray, very fine grained, well-sorted sandstone. Some intervals in the Pictured Cliffs are firmly cemented with calcite; other intervals are non-calcareous. Black accessory minerals and reddish-orange oxidized iron minerals are abundant in this area. Also abundant are burrows of the trace fossil *Ophiomorpha*, which can be observed on the large exposed dip slope just north of the road at station BC01[1]. The thickness of the Pictured Cliffs depends on where the contact is placed with the underlying Lewis Shale. Based on nearby drill holes, the thickness in this area is estimated to be between 125 and 200 ft.

Table 2-1. Strike and dip measurements in the Basin Creek area.
[Locations are shown on plate 1.]

Station No.	Strike and dip	Station No.	Strike and dip
BC01	N45ºE/29ºSE	BC14	N48ºE/28ºSE
BC03	N45ºE/32ºSE	BC16	N45ºE/25ºSE
BC04	N52ºE/24ºSE	BC17	N45ºE/37ºSE
BC05	N44ºE/24ºSE	BC18	N60ºE/42ºSE
BC07	N48ºE/26ºSE	BC21	N45ºE/26ºSE
BC08	N53ºE/20ºSE	BC26	N62ºE/31ºSE
BC09	N50ºE/20ºSE	BC28	N45ºE/31ºSE
BC13	N52ºE/24ºSE	BC44	N53ºE/23ºSE

[1] The numbering system for fracture stations is as follows: Basin Creek = BC__, Carbon Junction = CJ__, Florida River = FR__, Pine River = PR__. In these areas the prefix is not shown on the maps in order to make the maps easier to read. In the Texas Creek area a series of flatirons was lettered A through J and stations are designated TA__ through TJ__.

In the northern part of the area a tongue of Pictured Cliffs overlies the main body. From just north of the road to just west of station BC07 the tongue is separated from the main body by a thin coal bed. This coal bed pinches out to the north, but the tongue can still be differentiated on the basis of weathering characteristics. It forms an upper, more massive-weathering ledge that can be followed updip past the mapped area. The tongue is light gray, very fine grained, well sorted sandstone that has abundant dark accessory minerals that highlight crossbedding laminae in some places. No *Ophiomorpha* burrows were noted in the Pictured Cliffs tongue, but it does appear to be bioturbated in places. A rooted sandstone is at the top of the tongue, which is overlain by a coal bed of the Fruitland Formation. The tongue appears to thin and pinch out southward at about the position of the road through the area; it was not seen in the poor exposures south of the creek. In the northern part of the area, at station BC08, the tongue is about 50 ft thick, with the lower 35 ft being a mixture of sandstone and shale and the upper 15 ft a massive sandstone.

The Fruitland Formation is a heterogeneous unit consisting of interbedded sandstone, mudstone, carbonaceous shale, and coal beds (fig. 2-2). As mentioned above, in the central part of the mapped area a coal bed, which is a tongue of Fruitland, separates the main body and a tongue of the Pictured Cliffs Sandstone. This coal bed is only about 1 ft thick and is poorly exposed over most of its extent, so it was not mapped separately. The Fruitland measured along the road is just less than 400 ft thick (fig. 2-2, plate 7), which is slightly less than the thickness of the Fruitland in nearby wells. This discrepancy may be due to conservatively estimating a thick covered interval in the upper part of the formation along the road.

Sandstone beds of the Fruitland are very fine to fine grained, well sorted, and firmly cemented with calcite. Accessory minerals are abundant and are of a greater variety compared to Pictured Cliffs sandstones. Reddish-orange oxidized iron minerals are especially abundant in Fruitland sandstone beds. Clay rip-up clasts are abundant in one sandstone bed near the base of the formation. Sandstone beds in the Fruitland can generally be grouped into two types: channel sandstones and crevasse splay sandstones. The channel sandstones typically fine upward, have a lenticular geometry, and are crossbedded. Thicknesses of the channel sandstones in this area are as much as 25 ft. Crevasse splay sandstones are commonly thinner, on the order of 1-3 ft thick, and maintain a more constant thickness along strike than the channel sandstones. They are commonly bioturbated and don't display crossbedding. These thinner, more brittle sandstone beds fracture more readily and regularly than the channel sandstones though, and were used more than channels in measuring joints for this study.

Mudrock is a generic term for the clay- and silt-sized fraction of rocks in the Fruitland Formation. Two types of mudrock are recognized: mudstone and carbonaceous shale. Mudstone ranges from light to medium gray to greenish-gray. It commonly has a hackly, or blocky fracture pattern, but is fissile in some exposures. Carbonaceous shale is dark gray to black, moderately to highly carbonaceous, and commonly has a fissile or platy fracture. The two types of mudrock are normally interbedded and gradational into one another. Ironstone concretions are common in Fruitland mudrock of both lithologies. These concretions are a rusty orange color, and are very dense and hard.

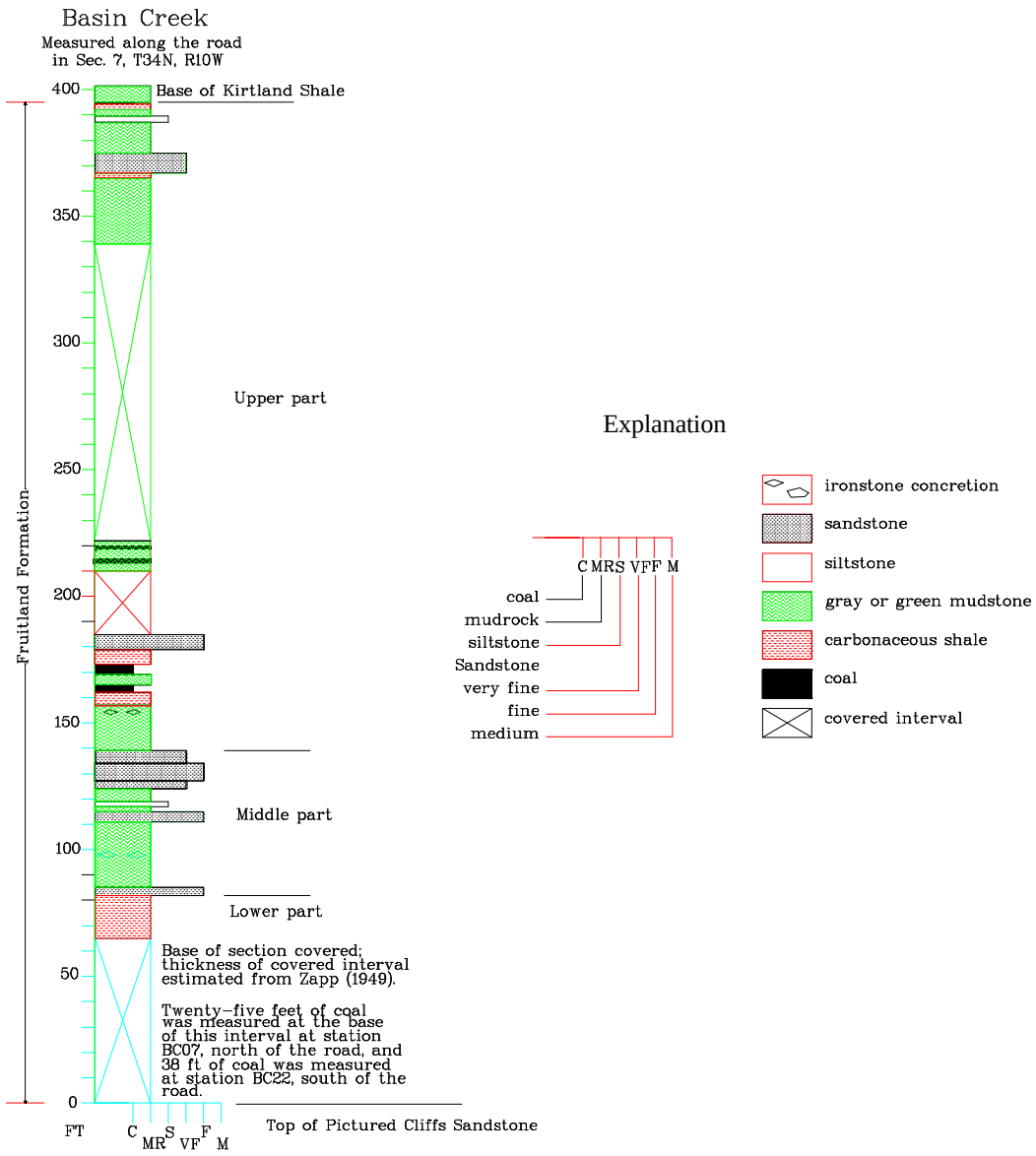

Figure 2-2. Stratigraphic section at Basin Creek. See plate 7 for correlation to other sections.

Coal in the Fruitland Formation in this area generally occurs in thin beds, except at the base of the formation, where thick beds are present. The occurrence of coal determined the division of the Fruitland into the units shown on the geologic map (plate 1) and the measured section (fig. 2-2, plate 7). Although at any given outcrop in this area several coal beds can be distinguished, these

beds cannot be traced very far laterally because of the poor exposures, especially south of the creek. Instead of tracing individual beds, the Fruitland was divided into lower, middle, and upper parts. The lower part consists of thick coal beds, with or without mudstone or sandstone partings. The middle part consists largely of sandstone and mudstone beds, with relatively minor amounts of carbonaceous shale and coal. The upper part consists of repeating cycles of carbonaceous shale, thin coal beds, and sandstone. South of the creek the lower and middle parts of the Fruitland could not be separated, due to cover, and so are mapped together.

The thickest coal beds in the Fruitland lie at the base of the formation, directly over the tongue of Pictured Cliffs, or over the main body where the tongue is not present. At station BC07 25 ft of coal was measured, overlain by an additional 5-10 ft of ash from burned coal. This basal coal thickens to the south of the creek where 38 ft was measured at station BC22. An additional 21 ft of coal above the basal coal was measured at station BC24. A small adit was dug into the basal coal just west of station BC07, north of the creek, and a collapsed mine entrance is at station BC18 on the south side of the creek. Kaolinite beds are present in the lower coal interval, but outcrops are so discontinuous that the clay beds couldn't be traced from one area to another.

One feature of the Basin Creek area that was not seen in any of the other studied areas is the presence of thick intervals of ash from burned coal beds in the lower part of the Fruitland. As much as 10 ft of ash is present above the coal at station BC07, and ash is common in the narrow gully north of station BC31. An associated feature is the presence of abundant amounts of reddish-orange, burned sandstone that has been shattered into small pieces by heat. This burned sandstone is known by the general term "clinker", and a large area of it was mapped in the north-central part of the area. Although this is the largest area of clinker, the whole area north of the road has scattered occurrences of it. The thick beds of coal at the base of the Fruitland burned, but the thin beds higher in the section did not.

The middle part of the Fruitland in this area is dominated by channel sandstone beds, but also includes mudrock and coal. In general, the middle part coarsens upward, with mudstone and carbonaceous shale being more abundant low in the middle part and sandstone being more abundant high in the middle part. The top of the middle part is marked by a thick sequence of stacked fluvial channels that can be seen both south and north of the creek. Coal is present in thin beds in the middle part of the Fruitland, but is not abundant.

The upper part of the Fruitland consists of thin coal beds interbedded with mudstone, carbonaceous shale, and sandstone. In this area there are three complete sequences of mudrock, coal, and sandstone and a partial fourth sequence. The sandstone beds are relatively thin, about 10 ft being a maximum thickness, but they can be traced laterally throughout the area north of the road. The sandstone beds serve as marker beds because they always overlie 1-3 ft thick coal beds in this area. Similar sequences of mudrock, coal, and sandstone are also present south of the creek, but the poor exposures make it impossible to trace the units laterally.

The uppermost part of the Fruitland is well-exposed at station BC17. This unit consists of interbedded mudstone, carbonaceous shale, thin streaks of coal, minor sandstone, and green siltstone. Characteristic features are light-orange septarian nodules that formed in siltstone intervals. A 1.5 inch pelecypod was found in gray mudstone in this upper unit. This unit appears to be transitional with the overlying Upper Cretaceous Kirtland Shale; the main difference being the presence of the carbonaceous beds in the Fruitland and their absence in the Kirtland. The lower part of the Kirtland also has relatively more sandstone than the upper part of the Fruitland, in this area and in the other areas studied.

A small fault is well-exposed in the outcrop described above at station BC17. Viewed from the south side of the road, the trace of the fault is U-shaped, with a broad, nearly horizontal trace along most of the outcrop. There is only about 1-2 ft of offset on the fault and it is down to the northwest. Since this fault is only seen in a vertical outcrop face, it couldn't be shown on the geologic map (plate 1). A second possible fault was noted just north of station BC34. This fault appears to cut the top sandstone in the middle part of the Fruitland. It trends N30ºW and dips steeply to the northeast. It is down to the southwest and there may be as much as 10 ft of offset. A third area of possible faulting or slumping is near station BC15 in a roadcut.

side of the gravel pit on Ewing Mesa, outside the mapped area (fig. 2-3). Both of these sections are shown on plate 7. The topography of Carbon Junction Canyon is steep, but the elevation is only between about 6500 and 6700 ft. The ridge line above the shooting range extends higher, up to about 6900 ft at the western end of the mapped area. As in the Basin Creek area, the Pictured Cliffs Sandstone and Fruitland Formation strike northeasterly and dip to the southeast. Dips range from 24 to 35 degrees and average 31 degrees (Table 2-2).

Table 2-2. Strike and dip measurements in the Carbon Junction area. [Locations are shown on plate 2.]

Station No.	Strike and dip	Station No.	Strike and dip
CJ01	N50ºE/33ºSE	CJ11	N53ºE/35ºSE
CJ02	N46ºE/24ºSE	CJ12	N53ºE/35ºSE
CJ04	N50ºE/33ºSE	CJ13	N45ºE/32ºSE
CJ06	N57ºE/31ºSE	CJ18	N48ºE/35ºSE
CJ07	N64ºE/29ºSE	CJ20	N58ºE/27ºSE
CJ08	N64ºE/29ºSE	CJ23	N47ºE/34ºSE
CJ09	N58ºE/34ºSE	CJ24	N50ºE/30ºSE
CJ10	N64ºE/24ºSE		

Although somewhat covered, it appears that there may have been faulting or slumping along bedding planes in carbonaceous shale low in the upper part of the Fruitland.

Carbon Junction

Mapping in the Carbon Junction area was in sections 4 and 5, T. 34 N., R. 9 W., east of the Animas River (plate 2). Reconnaissance was also done on the west side of the river above the shooting range. Two sections were measured in this area; one at the lower end of Carbon Junction Canyon, extending southward along the highway roadcut, and the other on the northeast

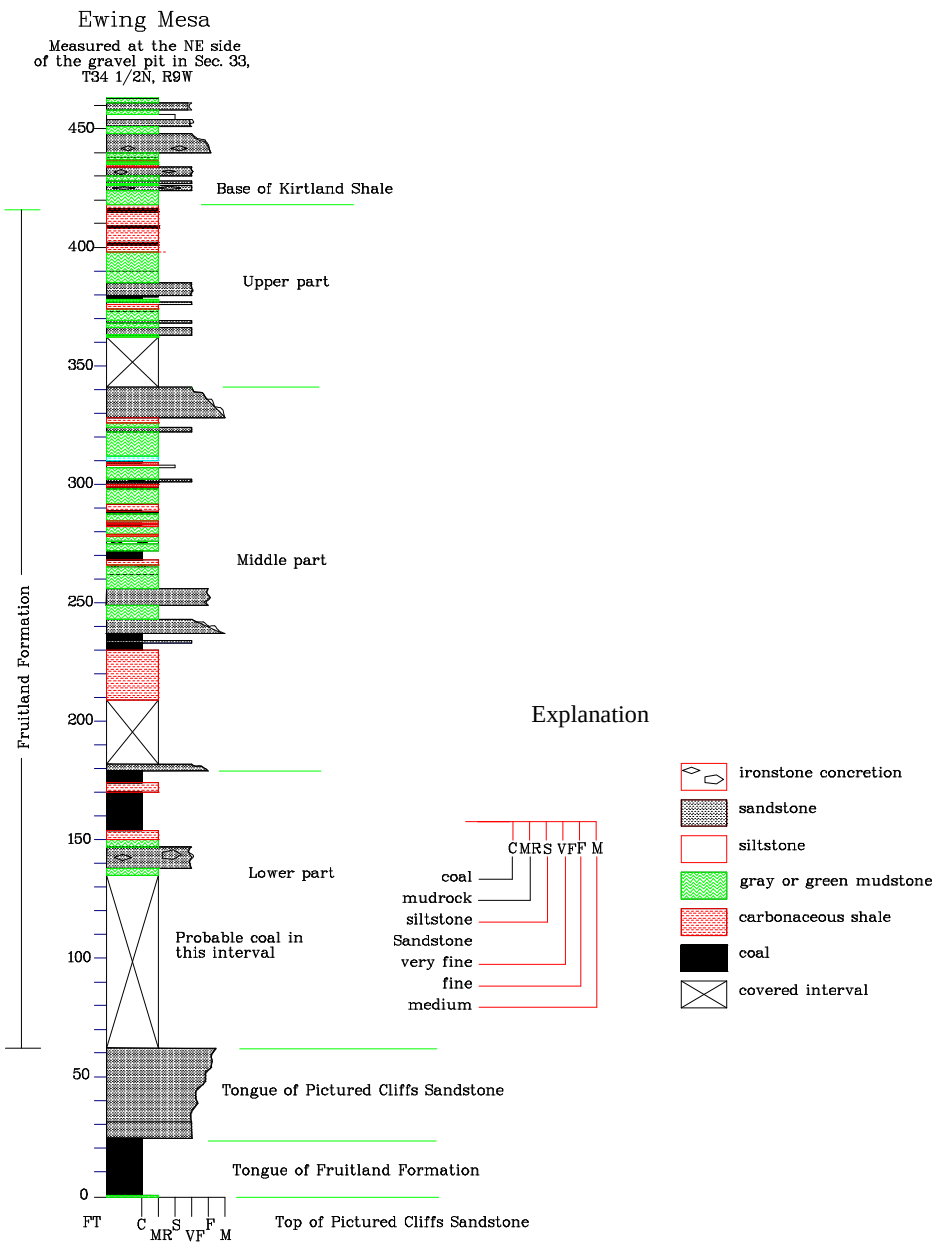

Figure 2-3. Stratigraphic section at Ewing Mesa. See plate 7 for correlation to other sections.

The vegetation in the Carbon Junction area is similar to that at Basin Creek—piñon-juniper forest. The underbrush is not quite as dense at Carbon Junction as at Basin Creek, but the steep southeast canyon wall made it somewhat difficult to accurately locate outcrops on the aerial photographs to make the geologic map. The best exposures of the Fruitland are at two places along the creek, in eroded gullies that cut the southeast canyon wall, and also along the old highway road cuts south of the canyon.

Plate 2 shows the geology of the Carbon Junction area. The oldest unit shown is the Lewis Shale, which underlies the Pictured Cliffs Sandstone. The contact of the Lewis with the

Pictured Cliffs was interpreted from aerial photographs in this area. The lithology of the Pictured Cliffs is the same here as at Basin Creek—light brown to light gray, very fine grained, well sorted sandstone. A dark gray to black sandstone is at the top of the Pictured Cliffs in some exposures. This sandstone is rooted, similar to the one found at the top of the tongue of Pictured Cliffs at Basin Creek. The Pictured Cliffs forms a narrow ridge line held up by massive sandstone beds in the upper part of the formation.

A tongue of Pictured Cliffs is present in Carbon Junction Canyon, but it is only well-exposed at the northeastern end of the mapped area (plate 2). At this outcrop the unit is about 30 ft thick, is light yellowish-gray, fine grained, and well sorted. It displays minor amounts of small-scale crossbedding, but mainly has horizontal, wavy bedding. The upper part of the sandstone contains abundant carbonaceous material. This bed thins abruptly southwestward and is replaced by thick coal at the base of the Fruitland Formation (plate 7).

Lithologies of the Fruitland Formation at Carbon Junction are the same as those in the Basin Creek area, which are sandstone, mudrock, and coal (fig. 2-3). The Fruitland was divided into the same lower, middle, and upper units that were mapped at Basin Creek. The section of Fruitland measured in and near Carbon Junction Canyon is only about 280 ft thick; the upper part of the unit is covered by terrace gravels. A complete section was measured at the Ewing Mesa gravel pit. There, the Fruitland is about 355 ft thick, not including a tongue of coal and mudstone 25 ft thick below the tongue of Pictured Cliffs Sandstone (fig 2-3, plate 7).

The lower part of the Fruitland is composed mainly of coal, with minor mudrock and siltstone partings. There are two good exposures of this unit at stations CJ01 and CJ25, and partial exposures at station CJ02. At station CJ25 a total of 80 ft of coal was measured, consisting of a lower bed 37 ft thick and an upper bed 43 ft thick, separated by 4 ft of mudrock and siltstone. At station CJ01 the lower contact of the coal is not exposed; 20 ft of coal is exposed above the stream bed and is overlain by 3-4 ft of partings that correlate with the same interval at station CJ25. An upper bed of coal 45 ft thick overlies the partings. At station CJ02 about 12 ft of coal is exposed above the stream and it is overlain by the tongue of Pictured Cliffs Sandstone. A kaolinite bed, 6”-7” thick, that occurs approximately 1 ft below the parting is present at both stations CJ01 and CJ02. The thick coal beds in the lower part of the Fruitland are partially replaced northeastward by the tongue of Pictured Cliffs, and partially overlie the tongue. A strong odor of hydrogen sulfide was noted in several places in Carbon Junction Canyon at the top of the basal coal of the Fruitland.

The middle part of the Fruitland is composed of interbedded carbonaceous shale and sandstone with relatively minor amounts of coal. Northeast of about station CJ15 a channel sandstone bed is at the base of the middle part; southwest of that locality carbonaceous shale is at the base. Otherwise, the amount of sandstone in the middle part increases upward in the section, similar to the middle part at Basin Creek. Sandstone beds are of channel and crevasse splay origin and reach a thickness of as much as 25 ft at the top of the middle part of the Fruitland. One or two 1 ft thick coal beds are present just below this upper sandstone; only carbonaceous shale was noted lower in the middle part.

The best exposures of the upper part of the Fruitland are at stations CJ7-10. As at Basin Creek, the upper part here consists of sequences of carbonaceous shale and coal intervals separated by sandstone beds. The carbonaceous shale beds are as thick as 40 ft; the coal beds are as thick as about 3 ft; the sandstone beds average about 6-10 ft thick. The contact with the Kirtland Shale occurs in the gravel-covered slopes just west of the water tank at the southeast corner of the mapped area (marked WT on the base map, plate 2). The contact was placed at a zone of septarian nodules that weathers out of the gravel-covered slope. I believe that this zone is at the same stratigraphic position as that noted at the top of the Fruitland at Basin Creek.

Exposures of the Fruitland Formation adjacent to the shooting range (plate 2) were examined and found to be essentially the same lithologies as those at Basin Creek and in Carbon

Junction Canyon. There is a thick coal sequence at the base of the Fruitland overlain by a sequence of carbonaceous shale, coal, and sandstone beds. Much of the Fruitland just west of the shooting range is obscured by landslide deposits, shown on the map as the Qls unit. I did climb up the rim of the Pictured Cliffs west of the range to examine what appeared to be a thick coal bed, but what is actually tailings from mining activity. The "coal" bed is a mixture of finely ground carbonaceous shale, mudstone, and coal that has been dumped on top of the Pictured Cliffs Sandstone.

No definite faulting was seen in Carbon Junction Canyon, but an area of disrupted bedding just northeast of station CJ15 was noted. It appears that there is some offset of a channel sandstone at the base of the middle part of the Fruitland Formation at that locality, but poor exposures made it difficult to determine if there was offset on a fault or just slumping of the outcrop.

Florida River

Mapping in the Florida River area was mainly in sec. 24, T. 35 N., R. 9 W., but extended southwestward into the SE¼ of section 23 and northeastward into sections 18 and 19, T. 35 N., R. 8 W. The area ranges in elevation from about 7100 ft along the Florida River to over 8100 ft where the Pictured Cliffs Sandstone forms the ridge in the southwest part of the study area. This outcrop area is a continuation of the exposures at Carbon Junction and the strike of the Pictured Cliffs Sandstone and Fruitland Formation remain northeasterly. Dip is southeast into the San Juan Basin. Dips in this area are the highest of any of the areas mapped, ranging from 27 degrees (which seems anomalously low) to 59 degrees, averaging 48 degrees (Table 2-3).

Much of this area is covered by piñon-juniper forest, but the increase in elevation is enough for Ponderosa pine and other larger conifer trees to grow in places. In the lower elevations, especially on the southwest side of the river and on slopes adjacent to the east side of the river, dense underbrush again obscures much of the surface geology. An old road traverses part of the area southwest of the river, providing limited access to some of the area. The best exposures in the area are along the Florida canal,

Table 2-3. Strike and dip measurements in the Florida River area.
[Locations are shown on plate 4.]

Station No.	Strike and dip	Station No.	Strike and dip
FR01	N63ºE/54ºSE	FR23	N62ºE/45ºSE
FR02	N50ºE/45ºSE	FR24	N51ºE/55ºSE
FR03	N58ºE/53ºSE	FR26	N64ºE/54ºSE
FR04	N58ºE/53ºSE	FR27	N66ºE/45ºSE
FR05	N62ºE/42ºSE	FR28	N60ºE/45ºSE
FR08	N57ºE/27ºSE	FR30	N74ºE/56ºSE
FR11	N65ºE/39ºSE	FR31	N54ºE/51ºSE
FR12	N59ºE/44ºSE	FR32	N65ºE/52ºSE
FR15	N60ºE/38ºSE	FR35	N65ºE/40ºSE
FR16	N64ºE/46ºSE	FR36	N55ºE/59ºSE
FR17	N68ºE/48ºSE	FR38	N70ºE/50ºSE
FR19	N68ºE/58ºSE	FR39	N66ºE/51ºSE
FR20	N64ºE55`SE	FR40	N61ºE/54ºSE

adjacent to the north-south paved road. A stratigraphic section was measured in the cuts along the canal (fig. 2-4, plate 7).

Plate 3 shows the geology of the Florida River area. The contact of the Lewis Shale with the Pictured Cliffs shown on the maps was interpreted by aerial photo analysis. The Pictured Cliffs Sandstone—Fruitland Formation contact is conformable and intertonging in this area. A tongue of Fruitland Formation is present below a tongue of Pictured Cliffs Sandstone at the Florida River area, but pinches out a short distance northeast of the river. The contact between the Fruitland Formation and Kirtland Shale is also conformable and gradational in this entire area.

In the mapped area the Pictured Cliffs Sandstone occurs as a lower main body and an upper tongue. The main body transitionally overlies the Lewis Shale and is composed of a lower and an upper part. The lower part consists of interbedded very fine-grained, argillaceous, thin, rippled sandstone and gray shale; sandstones in this interval become thicker-bedded higher in the section, and the percentage of gray shale decreases upward. *Ophiomorpha* burrows were noted at one outcrop in this interval. The top of this lower part is composed of massive, yellowish sandstones that form the dip slopes at stations FR02 and FR07 (plate 4). This lower part of the main body is not continuously exposed, but is estimated to be about 150-200 ft thick, depending on the placement of the lower contact with the Lewis Shale. The upper part of the main body is composed of a light-gray, fine-grained sandstone that forms a distinctive ridge along the outcrop. It is much less argillaceous than sandstones of the lower part of the main body of the Pictured Cliffs. This upper part is relatively thin, on the order of 15-25 ft thick. A dark gray to black rooted zone is present at the top of this unit. The main body, mapped as Kpc, is poorly exposed northeast of Florida River, but regional stratigraphic relations suggest that it pinches out depositionally into the Lewis Shale a short distance northeast of the river.

The tongue of Pictured Cliffs Sandstone is light gray to yellowish gray, very fine to fine-grained, well sorted sandstone. It is well-exposed near the highest point in the mapped area, downslope from station FR08. There it consists of a series of thick sandstone beds that have a combined thickness of at least 100 ft. Along the Florida canal, near County Road 225 (plate 3), the tongue was measured at 123 ft thick. The tongue forms a prominent outcropping ridge along the north side of Horse Gulch Road (County Road 237) and along the irrigation canal, but is poorly exposed northeast of Florida River. Northeast of the river it is hidden in the trees on the north-facing slope of the hogback. It gradually rises topographically northeastward and eventually forms the ridge line northeastward from section 17.

As shown on figure 2-4 and plate 3, the Fruitland Formation is divided into several mapped intervals on the basis of lithology. As measured along the Florida canal, the Fruitland is about 460 ft thick. Where the Fruitland Formation is well exposed it can be broadly divided into as many as three coal-bearing intervals, separated by sandstone and mudstone. Extensive cover in the Florida River area made it difficult to accurately trace out these intervals and some units were combined in some areas. In the Florida River area the tongue of Fruitland Formation (Kft), a lower coal-bearing interval (Kfab), and an upper coal-bearing interval (Kfu) are highlighted on the geologic map. The tongue of Fruitland contains a thin (1-3 ft thick) bed of coal at the base and another about 20 ft above the base, but otherwise is composed of mudstone, carbonaceous shale, and thin sandstone beds. At station FR09 a bed of carbonaceous shale underlies the tongue of Pictured Cliffs Sandstone. It is quite possible that this carbonaceous shale is replaced by coal in other areas nearby. In the Ewing Mesa area, southwest of Florida River (plate 7), a coal bed is present just below the tongue of Pictured Cliffs Sandstone. The tongue of Fruitland Formation was estimated to be approximately 30 ft thick at station FR09; it thins northeastward and pinches out in the alluvium-covered, north-facing slope northeast of Florida River.

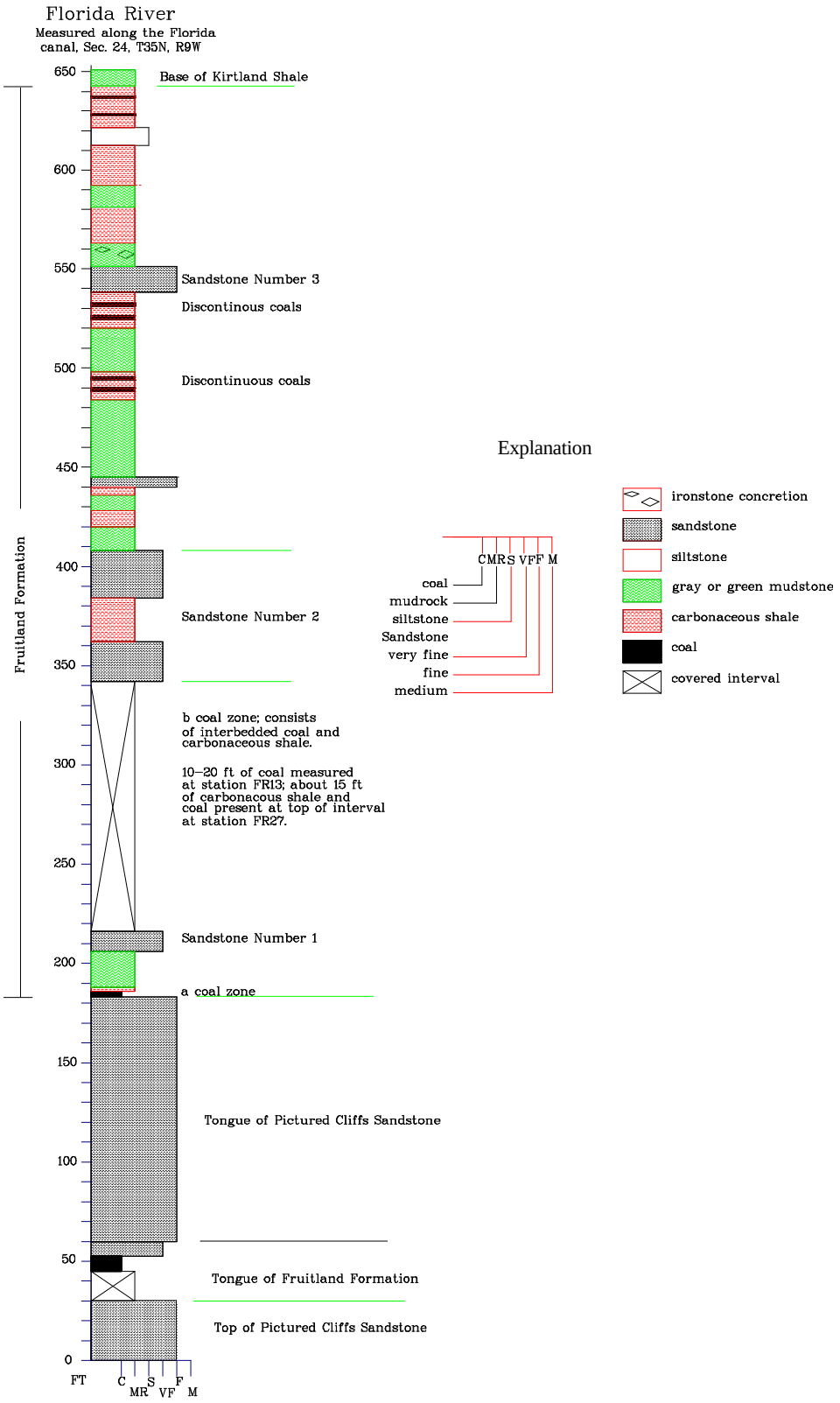

Figure 2-4. Stratigraphic section at Florida River. See plate 7 for correlation to other sections.

The unit labeled Kfab on the geologic map contains the thickest beds of coal in this area. The coal immediately overlying the upper tongue of Pictured Cliffs Sandstone is poorly exposed in most of the area, and is quite thin in comparison with coals in similar stratigraphic positions in the Carbon Junction and Texas Creek areas. The Kfab unit contains a thin sandstone above the lowest coal, and is overlain by another carbonaceous shale and coal interval. The lowest coal is 3 ft thick along the Florida canal (plate 7) and is overlain by about 20 ft of carbonaceous shale and brown mudstone. The first sandstone in the Fruitland, which was not mapped separately due to poor exposures, is a composite of about 3 ft of sandstone interbedded with 7 ft of mudstone along the canal. The interval between the first and second sandstones is about 125 ft thick along the canal (possibly overestimated in this covered interval). Coal just below Kf2 is the thickest in the area; a unit of interbedded coal and carbonaceous shale about 15 ft thick immediately underlies Kf2. A kaolinite bed was noted in this coal sequence at station FR18. An adit was discovered just off the old road in the SW¼ of section 24 within the Kfab interval (see plates 3 or 4 for the location of the adit). Northeast of the river a small area of the upper Kfab unit is covered with reddish-orange chips of sandstone typical of burned coal intervals. Heavy brush in this area made it difficult to trace the clinker very far to the northeast.

Kf2 is a sandstone that forms a steep hogback on the southwestern end of the study area and forms the low ridge that much of the old road in section 24 was built on. The upper part of Kf2 forms the ridgeline northeast of Florida River. Kf2 is very thick (50-75 ft) in the southwest part of the area, where it appears to be a fining-upward stacked channel complex. The unit thins somewhat to the northeast.

At the southwest end of the mapped area another sandstone, Kf3, overlies the Kf2 sandstone. In that part of the area no coal was seen separating the two sandstones; however, at the Florida canal (plate 7) and east of the river, coal is present below this third sandstone interval. Two to three feet of coal is present along the irrigation canal, and a similar amount is present east of the river.

The upper part of the Fruitland, mapped as Kfu, is a unit transitional with the Kirtland Shale. It consists of thin sandstone beds, greenish-gray mudstone, carbonaceous shale, and thin coal beds. Kfu generally weathers to a poorly exposed slope, but is well-exposed along the Florida canal. The top contact was mapped at the base of a greenish, argillaceous sandstone that forms a low ridge in many places. This upper unit of the Fruitland contains characteristic yellowish-orange septarian concretions that were also seen in the Basin Creek and Carbon Junction areas. A coal bed 1-2 ft thick was measured at stations FR21 and FR22 at the top of the Kfu unit (plate 4). Carbonaceous shale with thin streaks of coal are present lower in Kfu, but no other continuous coal beds were seen.

The Fruitland Formation is gradationally overlain by the Kirtland Shale throughout this area. As noted previously in other areas along the Fruitland outcrop, the basal Kirtland beds are similar to the upper beds of the Fruitland, but lack the carbonaceous shale and coal. One other difference in this area is that sandstone beds of the Kirtland have a greenish color or are iron-rich and are dark brown as opposed to the yellowish-brown sandstone beds characteristic of the Fruitland. The contact between the Fruitland and Kirtland could thus change laterally if coal beds occur higher or lower in the section.

Fairly large areas just southwest and northeast of Horse Gulch (plate 3), are obscured by terrace gravel and were mapped as Qg. These units, and a smaller, similar unit just east of the Florida River are composed of pebbles and cobbles of igneous and metamorphic rocks. Quaternary alluvium (Qal) is present in the valley of Florida River and in a drainage adjacent to the largest terrace gravel deposit. Exposures in Horse Gulch, especially on the south side of the stream, are quite poor. Contacts were drawn as dashes across the drainage to show the inferred distribution of units.

No faulting or other structural complications were noted in this mapped area. The main structural feature is the extreme dip of the beds;

however, the dip moderates abruptly just a short distance basinward from the Fruitland outcrop.

South Fork of Texas Creek to the Pine River

An extensive area was mapped along part of the South Fork of Texas Creek and southeastward to the Pine River in northeastern La Plata County. This area includes parts of sections 6, 7, 8, 9, 10, 14, and 15, T. 35 N., R. 7 W. and a small bit of sec. 12, T. 35 N., R. 8 W. (plate 5). The character of this area changes significantly from west to east. In the west the Pictured Cliffs Sandstone and Fruitland Formation form a series of isolated peaks (flatirons) separated by deep drainages. This topography produces a zig-zag pattern of units in the Fruitland as the units cross the gullies and hills. In contrast, in the eastern part of the area the Pictured Cliffs and units of the Fruitland form a long, linear outcrop. The elevations of the area gradually decrease from west to east, from nearly 8900 ft at Vosburg Pike in the west to about 7200 ft in the east at the Pine River. This area of outcrops lies at the northern rim of the San Juan Basin; this particular segment of the rim has a northwestward strike and the rocks dip southwestward. In the Texas Creek part of the area dips range from 12 to 35 degrees and average 22 degrees (table 2-4). In the Pine River part of the area the dips range from 23 to 52 degrees and average 35 degrees (table 2-5).

While mapping from Texas Creek to the Pine River it became apparent that significant errors exist on the topographic map in some places, especially at the boundary between the Rules Hill and Ludwig Mountain quadrangles along the Fruitland—Kirtland contact (plates 5 and 6).

Table 2-4. Strike and dip measurements in the South Fork of Texas Creek area. [Locations are shown on plate 6.]

Station No.	Strike and dip	Station No.	Strike and dip
TA01	N85ºW/13ºSW	TD03	N76ºW/28ºSW
TA03	N85ºW/25ºSW	TD04	N72ºW/25ºSW
TA04	N80ºW/19ºSW	TD05	N85ºW/25ºSW
TA05	N85ºW/16ºSW	TD06	N77ºW/23ºSW
TA08	N80ºE/34ºSE	TD07	N90ºE/28ºS
TA10	N88ºE/19ºSE	TE02	N81ºW/31ºSW
TA11	N90ºE/20ºS	TE03	N85ºW/23ºSW
TB01	N80ºE/35ºSE	TE04	N52ºW/15ºSE
TB02	N88ºW/17ºSW	TE05	N79ºW/31ºSW
TB03	N80ºE/21ºSE	TE06	N40ºW/20ºSW
TB04	N90ºE/17ºS	TE07	N75ºW/25ºSE
TB07	N89ºE/26ºSE	TF01	N80ºW/24ºSW
TC02	N80ºE/20ºSW	TF03	N80ºE/21ºSW
TC04	N84ºW/22ºSE	TF04	N44ºW/25ºSW
TC05	N84ºW/12ºSW	TG01	N70ºW/12ºSW
TC06	N77ºW/25ºSW	TG02	N67ºW/25ºSW
TC08	N85ºW/18ºSW	TH01	N44ºW/15ºSW
TD01	N79ºE/24ºSW	TI01	N50ºW/15ºSW
TD02	N73ºW/22ºSW	TJ01	N50ºW/24ºSW

For example, the wide, flat-topped hill just to the west of the Hoier property is not really as flat as the map shows. Also, the hills shown north and east of the unit shown as Qal, just east of Hoier's property, do not agree with the aerial photographs. The geologic contacts were adjusted to the topographic map, but be advised of the problems with the base map.

A wide range in vegetation corresponds to the change in elevation across the area. In the west, vegetation consists of Ponderosa pine forest with other mixed conifers. There is some brush in the western area, but in general the forest is open. The eastern part of the area has mixed vegetation of both tall conifer and piñon-juniper forest mixed with some stands of dense underbrush. The most covered area is in the central part of the eastern half of the area, just west of the Hoier property. A critical area in the NW¼ of sec. 14 is also very poorly exposed, which makes interpretation of faulting in that area difficult. A completely exposed section of Fruitland was not found anywhere in the mapped area, so the measured section for this area, shown in fig. 2-5 and on plate 7, is a composite of observations made at several places. Most of the descriptions were made in the western half of the mapped area; however, stratigraphic units can be traced through most of the mapped area. See appendix 2-1 for a composite stratigraphic section that was compiled for the western section along Texas Creek.

Plate 5 shows the geology from Texas Creek to the Pine River. The oldest unit shown is the Lewis Shale, which is overlain by the Pictured Cliffs Sandstone. In this area there is one main body of Pictured Cliffs overlain by one interval of Fruitland. The Pictured Cliffs Sandstone in this area is the same lithologic unit as the tongue of Pictured Cliffs Sandstone in the Florida River area (plate 7). A northeastward stratigraphic rise resulted in the lower part of the Pictured Cliffs at the Florida River pinching out depositionally into the Lewis Shale in a northeastward direction while the stratigraphically higher tongue extends into this area. The Pictured Cliffs here can also be generally divided into a lower, yellowish, argillaceous part that is transitional with the Lewis Shale and an upper part that is composed of clean, well sorted sandstone. A thin coal is present within the Pictured Cliffs in part of the northern San Juan Basin, such as in the AMOCO Gurr Federal Gas Unit No. 1 well. Although the coal was not seen at the outcrop in this study, the break between the lower and upper Pictured Cliffs would be a likely place for the coal to occur. The difference in lithology causes the two parts of the Pictured Cliffs to weather differently

Table 2-5. Strike and dip measurements in the Pine River area.
[Locations are shown on plate 6.]

Station No.	Strike and dip	Station No.	Strike and dip
PR01	N43ºE/23ºSE	PR20	N57ºW/35ºSW
PR02	N80ºW/36ºSW	PR22	N61ºW/28ºSW
PR04	N70ºW/30ºSW	PR23	N85ºW/35ºSW
PR05	N44ºW/32ºSW	PR27	N84ºW/39ºSW
PR08	N52ºW/31ºSW	PR28	N84ºW/39ºSW
PR10	N66ºW/39ºSW	PR29	N70ºW/45ºSW
PR11	N69ºW/35ºSW	PR31	N70ºW/40ºSW
PR12	N70ºW/31ºSW	PR33	N65ºW/52ºSW
PR13	N85ºW/31ºSW	PR36	N68ºW/25ºSW
PR16	N85ºW/32ºSW	PR38	N80ºW/34ºSW

and to form a double outcrop in places. On lobe H (plate 6), north of the Ragsdale property, it appears that the upper part of the Pictured Cliffs has been eroded, producing a stripped surface that is at a lower elevation than the top of the Pictured Cliffs on lobe G. This difference in elevation of the two outcrops could be mistaken for offset on a fault, but we checked this area for evidence of a fault and didn't see one.

The Fruitland in this area was again divided into several units of sandstone and coal-bearing intervals. The basal interval (Kfab) consists of mudstone, carbonaceous shale, and coal, with one, thin sandstone near the middle of the unit. This coal interval has the best exposure of any in this mapped area, particularly at the crests of the flatirons where the coal is being eroded. Reddish-orange burned sandstone chips, or clinker, are found in some areas in the basal interval, but are not abundant in this area. Altered volcanic ash beds (kaolinite) were also seen in some of the better-exposed outcrops, but are not abundant in the lower coal. The coal immediately on top of the Pictured Cliffs Sandstone thins irregularly to the southeast along this outcrop. The thickest coal was found at the base of the Fruitland at the western end of the mapped area (station TA04, plate 6). The section described below is of that outcrop.

Several small mines, with collapsed entrances, were found in the lower coal interval, at stations TB06, TJ02, and PR20 (plate 6). Poor exposures made it difficult to measure a thickness of the coal at TJ02, but about 3 to 5 ft is estimated. In contrast, the lowest coal thins to 1 foot or less in some areas toward the Pine River and thickens to 2-4 ft at the southeast end of the outcrop. A thicker interval of coal is present near the top of the Kfab unit, but it is also poorly exposed. The whole Kfab unit maintains a thickness of 40-50 ft from west to east across the whole area. I believe that this Kfab unit corresponds with the Ignacio coal seams as identified by AMOCO (1994) in the subsurface nearby.

An odor of hydrogen sulfide (H_2S) was noted in three places in the lower coal interval. A moderate odor was noted at station TI01, just east of the Ragsdale property on one occasion in May. Another was just down-slope to the west of station PR01, the third was on the crest of the hill east of station PR20. An extensive area of dead vegetation is associated with the H_2S area at PR20. A fourth area with H_2S is just downslope from station PR35, in the Kfcd coal interval.

Overlying Kfab is sandstone mapped as Kf2. This sandstone forms many of the long dip slopes at Texas Creek and toward the Pine River. It is a

FT	Description
~1	Soil; top of exposure
2.3	Coal, black, dull, poorly developed cleat and bedding. Breaks into blocky to irregular fragments up to 1" across; fractured
2.6	Claystone, weathered, yellowish orange to moderate yellowish brown with carbonaceous laminae in upper part
6.0	Coal, dark gray to black, generally dull, cleat poorly developed, poorly bedded. Includes 6" of impure (silty?) coal about 1.9' from top of bed
0.3	Claystone, yellowish gray to pale yellowish brown; kaolinitic(?)
1.0	Coal, black, dull, blocky, well cleated
0.3	Claystone, brownish gray
1.4	Coal, bright, black, weathered, well bedded, good cleat
0.9	Seat-earth, sandstone, medium gray, carbonaceous; very thin, irregular beds; rooted. Base of coal
--	Pictured Cliffs Sandstone. Sandstone, quartzose, very fine grained, very light gray, thickly bedded, wavy bedded with finely disseminated dark minerals.

composite channel sandstone that thickens to as much as 100 ft or more in some places. The lower part of this sandstone is silica-cemented in some areas and has a distinctive rose color.

A unit mapped as Kfcd overlies the second sandstone of the Fruitland Formation in this area. This unit consists of a coal bed at the base, a concretionary limestone interval in the middle, and another coal bed at the top. The coal beds are fairly thin, averaging about 2-4 ft thick. The zone of concretions between the coals is the informally named "skeleton bed" (appendix 2-1). This bed served as a marker in the west part of the study area because of the resistant nature of the concretions and their distinctive color. This coal zone was mined at the east end of the outcrop at the Pine River. According to Barnes (1953) this was the Schutz Mine. Based on thickness and stratigraphic position, I believe that this coal interval corresponds to that identified as the Lemon coal seams by AMOCO (1994). Two sandstone intervals overlie Kfcd, the Kf3 and Kf4 units. The Kf3 sandstone is continuous across the whole mapped area, but the Kf4 sandstone could not be traced all the way to the Pine River. Kf3 is as thick as 50 ft on the west end of the study area, but thins to about 15 ft near the Pine River. Kf4 appears to thin southeastward from about 35 ft and disappeared near the area just west of section 14 that is obscured by vegetation. Kf4 was not found in the better exposures of this part of the section just west of the Pine River.

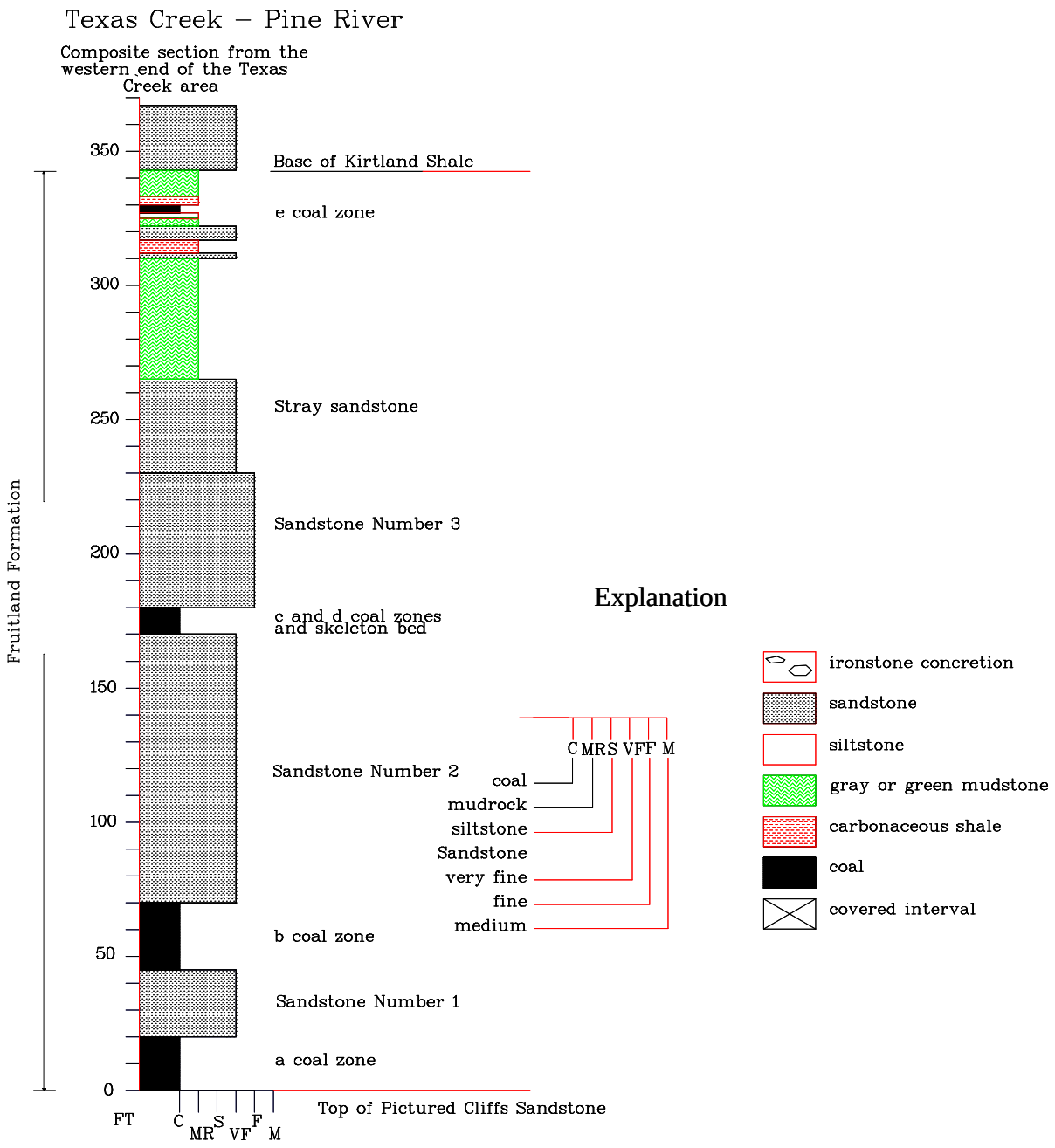

Figure 2-5. Stratigraphic section at Texas Creek-Pine River. See plate 7 for correlation to other areas.

As in the other areas discussed in this report, the top unit of the Fruitland Formation was mapped as Kfu. The lithology is similar to that at Basin Creek and at Florida River and consists of greenish mudstone, thin sandstone, carbonaceous shale, and thin coal beds. The thickness of this unit is approximately 80 ft. Here too, it has a lithology similar to the Kirtland Shale, except that the Kirtland lacks the coals. Fairly good exposures are present at stations

PR15, PR18, and PR36 (plate 6). There is not a good marker bed that can be used to separate the Fruitland Formation from the Kirtland Shale; the presence or absence of coal beds and carbonaceous shale was used to place the contact in an interval that was otherwise very similar lithologically. Based on stratigraphic position, this upper interval of the Fruitland most likely corresponds with the Pargin coal zone of AMOCO (1994).

Quaternary alluvium (Qal) is present primarily in the valley of Pine River, but was also mapped east of the Hoier property. An attempt was made to show the inferred position of Fruitland units under the alluvium in the valley of the South Fork of Texas Creek (plate 5).

One of the more interesting features of the Pictured Cliffs—Fruitland outcrop in this area is a fault at the extreme east end of the outcrop, just west of the Pine River (fig. 2-6). This fault was previously mapped by Barnes (1953) as a normal fault, down to the north. Some features lead me to speculate that it could be a moderate- to high-angle thrust fault, with thrusting directed

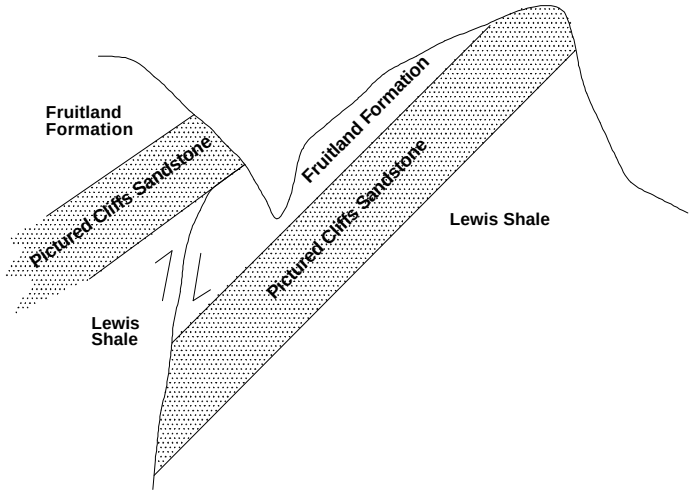

Figure 2-6. Schematic diagram of reverse fault just west of the Pine River.

northward. The fault trace is along a steep-walled gully that cuts the outcrop just behind the Field property adjacent to the outcrop. On the north side of the gully Pictured Cliffs Sandstone and the Kfab and Kf2 units of the Fruitland roll steeply into the gully at about 45 degrees. Boulders of Pictured Cliffs that were used to construct a retaining wall on the north side of the gully display slickenside striations, which is clear evidence that the Pictured Cliffs is faulted at this locality.

On the south side of the gully it appears that there is a complete repeated section of Pictured Cliffs Sandstone that is between 100 and 130 ft thick. Below the lowest identified Pictured Cliffs are a few feet of fissile, fossiliferous, gray shale, underlain by Fruitland coal, probably from the Kfab unit. Initially I speculated that the gray shale might be a sliver of Lewis Shale, but D. Baldwin (written commun., 1996) indicated that there is a similar gray shale associated with the basal coal in several monitoring wells in the Pine River Ranches area adjacent to the outcrop. It still appears that a repeated section of Pictured Cliffs overlies the Kfab unit of the Fruitland in the gully, however, suggesting that the Pictured Cliffs was pushed northward over the coal, causing the abrupt increase in dip of the underlying wedge of Pictured Cliffs—Fruitland on the north side of the fault. D. Baldwin (written commun., 1996) noted that no fault was encountered in the James No. 1 monitor well, which was drilled approximately .2 mi east of the gully in which the fault occurs. Unfortunately the well was not drilled all the way through the Pictured Cliffs Sandstone to test whether there is a repeated section of Pictured Cliffs in that area. The only way to know if there is a fault there would be to drill completely through the Pictured Cliffs into underlying rocks to see if there is either Lewis Shale or a repeated section of Pictured Cliffs. The fault in the gully could not be traced confidently very far west due to cover by vegetation, but perhaps the poor exposures can be explained, in part, by disruption of bedding due to the faulting. No other significant faulting was noted in this mapped area, although a few inches of offset was seen on sandstone beds at station TI02.

Synthesis

Following is a description of regional changes and correlations of stratigraphic units from Basin Creek to the Pine River, based on my outcrop studies. Fassett and Hinds (1971), Fassett (1988), Ambrose and Ayers (1991), Ayers and others (1991), and Roberts and McCabe (1992) have previously summarized the Pictured Cliffs, Fruitland, Kirtland, and associated strata, and their depositional environments.

The study area is located on what was the western shore of the Upper Cretaceous seaway that bisected North America (Fassett and Hinds, 1971; Fassett, 1988). Sedimentation rate and sea level rise and fall had marked effects on deposition of sediments that comprise the Pictured Cliffs Sandstone and Fruitland Formation in the study area. Seaward progradations and landward transgressions of the shoreline are part of a complex interplay between sea level, sediment influx, tectonic events, and other variables.

The effects of sea level changes are clearly expressed in the Pictured Cliffs Sandstone in La Plata County. The stratigraphic intertonguing of nearshore marine and coastal plain deposits indicates that there were a series of seaward progradations of the shoreline followed by shoreline buildups and transgressions back to the southwest across nearshore peat swamps. In the far southwestern end of the study area, on the south side of Basin Creek, there is only one main body of Pictured Cliffs, overlain by Fruitland coal. However, in the northern part of the Basin Creek area a tongue of Pictured Cliffs overlies the main body and is separated from the main body by a thin coal in places. This represents a progradation of the Pictured Cliffs shoreline sandstone to the northeast in a seaward direction, followed by a transgression back to the southwest over the swamp deposits of the Fruitland Formation. This was a relatively short-lived transgression, and the tongue merges with the main body of the Pictured Cliffs northeastward into the Carbon Junction area about 2 mi to the northeast.

At Carbon Junction there is another doublet of a main body of Pictured Cliffs and an overlying tongue. Near the landward extent of the tongue is a thick buildup of coal in the basal Fruitland Formation, indicating a period of shoreline stability just seaward of the coal. The doublet of Pictured Cliffs sandstones continues to the northeast slightly past the Florida River (Zapp, 1949), at which point the lower Pictured Cliffs sandstone grades out into the Lewis Shale and the tongue becomes the only Pictured Cliffs unit present. This represents a stratigraphic rise of the prograding shoreline sandstone to the northeast. In the Texas Creek to Pine River area there is only the one Pictured Cliffs sandstone unit.

The thickness of coal in the basal part of the Fruitland Formation is closely tied to the rate at which the shoreline changed. In the Basin Creek area there is a combined thickness of 50-60 ft of coal at the base of the formation; at Carbon Junction there is approximately 80 ft of coal at the base. This indicates a relatively long period of stability in which coal swamps developed. In contrast, in the Florida River area the coal at the base of the main body of Fruitland is only a few feet thick and much of the rest of the lower part of the Fruitland is carbonaceous shale or mudstone. This indicates a relatively quick seaward progradation of the shoreline; an environment in which the peat in swamps did not have time to accumulate. At the west end of the Texas Creek area the basal coal is fairly thick, but it thins toward the Pine River, indicating another period of stability, followed by more rapid progradation. This sequence of progradation and aggradation of the shoreline was shown diagrammatically by Fassett and Hinds (1971, p. 11) and is documented in the subsurface by Ayers and others (1991, p. 11) and Roberts and McCabe (1992, p. 121).

In the Basin Creek and Carbon Junction areas the rock interval just above the basal coals consists of mudstone and carbonaceous shale that gradually becomes more sandstone-dominated upward in the section and culminates in a stacked-channel complex that is approximately 25 ft thick. This sandstone complex is very well developed at the southwest end of the Florida

River area, where it approaches 75 ft of nearly all sandstone (mapped as the number 2 sandstone [Kf2]) and comprises most of the middle part of the Fruitland. The sandstone complex is also present in the Texas Creek to Pine River area, where it and associated mudrocks are as thick as 100 ft. This interval in the Fruitland is interpreted to represent a major influx of sediment from the source area to the southwest of the La Plata County area.

Strata in the upper part of the Fruitland in the Basin Creek and Carbon Junction areas consist of a series of interbedded mudrock, coal, and sandstone beds that repeat in several cycles. A similar series of rocks is present in the Florida River and Texas Creek—Pine River areas in the upper part of the Fruitland. Coal beds in this interval are relatively thin, usually only 3-4 ft thick maximum, and the sandstone channels are also relatively thin, commonly about 10 ft, but as much as 30 ft thick in places. Where coal beds are present they are commonly directly overlain by sandstone beds. This upper part of the Fruitland section is interpreted as representing meandering streams on a surface of low relief, such as a delta plain. Some of the sandstone beds are thin and tabular, and probably are of crevasse splay origin. The coal developed in swampy areas adjacent to the fluvial channels and this accounts for their relative thinness and lenticularity. Coal-bearing horizons do appear to be fairly persistent laterally, but the coal beds pinch and swell within those intervals.

The uppermost unit of the Fruitland is transitional with the overlying Kirtland Shale and is present in all the mapped areas. This unit has certain features characteristic of the Fruitland, such as carbonaceous shale and thin coal beds, but has other features characteristic of the Kirtland, such as dense, green siltstone and abundant yellowish-orange concretions. As a whole, the unit has very little sandstone and is commonly weathered and poorly exposed. The transitional unit is recognizable in all of the areas, however, and makes a good marker bed for the contact between the Fruitland and Kirtland. It was deposited farther up the depositional slope than the lower and middle parts of the Fruitland, and thus does not have a good development of coal beds.

PART 2--FRACTURE STUDIES

Joints in sandstone and cleats in coal were measured at 209 localities in the project area. By area, the totals are 47 localities, or stations, at Basin Creek, 27 stations at Carbon Junction, 40 stations at the Florida River, 57 stations along the south fork of Texas Creek, and 38 stations between Texas Creek and the Pine River. Each of the areas is summarized separately below; rose diagrams of the individual stations are shown in appendix 2-2. Tables 2-6 through 2-10 show in which geologic unit the stations were recorded; plates 1, 2, 4, and 6 show the locations of each station. The rose diagrams were constructed using a Macintosh program called Rosy. Rose diagrams in figures 2-8 through 2-12 and in appendix 2-2 show statistics for each area or station.

In each of the rose diagrams, N is the number of readings in each data set used to construct the diagram. The class interval indicates the number of degrees each wedge of the diagram shows. A class interval of 10 degrees was used for all the diagrams. The size of the wedge is a relative measure of the number of readings within each wedge. The statistics are intended to provide measures of central values and dispersion of the data. All the tests, such as maximum percentage, mean percentage, and standard deviation, are made on cells having values greater than 0. Other calculations are as follows. The vector mean is the combined azimuth of all the readings used to construct the diagram. The R magnitude is the magnitude of the vector mean. Data sets that exhibit large dispersion about the mean will have small resultants, and those sets that are tightly grouped have large resultants. R is standardized to range between 0 and 1; tightly clustered data sets have R values near 1. The confidence angle is another test of the reliability of the vector mean. The confidence angle forms an arc plus or minus either side of the calculated vector mean. A small confidence angle indicates tightly clustered data, a large angle indicates dispersed data. There is a 95% probability that the arc formed by the confidence angle contains the true population mean direction. The Rayleigh number is a test for uniformity in a data set. Values less than 0.05 (95% confidence level) indicate that the data are non-uniform and show a preferential orientation. These tests of uniformity only apply to figures 2-7 through 2-12 in this report, because these figures show single sets of joints or cleats.

In general, in each area there is one main joint set in each geologic unit, and a second set that is oriented at about right angles to the first. These joint sets were named the J1 and J2 sets. In some areas a third set, and even a fourth set, are also present. This discussion focuses on the J1 and J2 sets because they are the most common and pervasive in all the areas; individual localities where the other sets are important are pointed out below. All the joint sets are oriented perpendicular to bedding, even in areas of steep

Table 2-6. Average orientations of joints in sandstone and cleats in coal in the project area

	Kpc-J1	Kpc-J2	Face	Butt	Kf-J1	Kf-J2
Basin Creek	N. 28º W.	N. 59º E.	N. 2º W.	N. 88º E.	N. 2º W.	East-West
Carbon Junction	N. 77º E.	N. 50º W.	N. 20º W.	N. 69º E.	N. 9º W.	N. 85º E.
Florida River	N. 23º W.	N. 64º E.	N. 31º W.	N. 58º E.	N. 20º W.	N. 67º E.
Texas Creek	N. 9º W.	N. 79º E.	N. 22º W.	N. 68º E.	N. 1º E.	N. 89º W.
Pine River	N. 5º E.	N. 75º W.	N. 35º W.	N. 54º E.	N. 7º E.	N. 81º W.
Totals	**N. 14º W.**	**N. 74º E.**	**N. 21º W.**	**N. 69º E.**	**N. 3º W.**	**East-West**

Kpc - Pictured Cliffs Sandstone; Kf - Fruitland Formation

dip. In coal beds, fractures are known as 'cleats', and in coal too, there are two main sets, a face cleat and a butt cleat. The face cleat is the main fracture set in coal beds; butt cleats are oriented at about 90º to the face cleats.

For this study, four main characteristics of joints and cleats were emphasized—length, spacing, sinuosity, and mineral fillings. In addition, basic parameters of joints, such as terminations of one joint set against another (to determine relative age) and surface features (to determine mode of origin) were also noted. In general, joint surfaces in this area are weathered, obscuring surface ornamentation. Some joints of each set do display features such as plumose structures, arrest lines, and twist hackle, features characteristic of opening mode (mode I) fractures (Kulander and others, 1979). No evidence of shear movement, such as slickenside striations, was noted on any of the joint sets.

Figure 2-7 shows rose diagrams that summarize over 1850 readings taken of all J1 and J2 joints and of all face and butt cleats in coal in the entire study area. Figure 2-7 also shows that in a regional sense there is a good clustering of joint and cleat directions. For the Pictured Cliffs Sandstone the regional average of J1 joints is 346º, or N. 14º W., and the average of J2 joints is 74º, or N. 74º E. The regional average of all face cleats in all coal beds is 339º, or N. 21º W., and the average of all butt cleats is 69º, or N. 69º E. The average J1 orientation for all sandstone beds in the Fruitland Formation is 357º, or N. 3º W., and for J2 joints is 90º, or East-West. Table 2-6 tabulates the average orientations of each of the mapped areas in addition to the totals for the whole area.

.

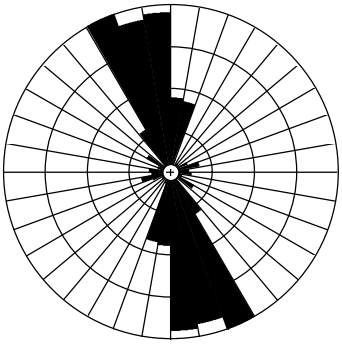

All J1 joints in project area in Pictured Cliffs		Statistics
N = 315		Vector Mean = 346.1
Class Interval = 10 degrees		Conf. Angle = 6.95
Maximum Percentage = 19.4		R Magnitude = 0.577
Mean Percentage = 5.56	Standard Deviation = 6.32	Rayleigh = 0.0000

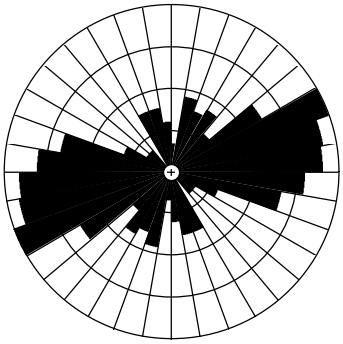

All J2 joints in project area in Pictured Cliffs		Statistics
N = 177		Vector Mean = 74.2
Class Interval = 10 degrees		Conf. Angle = 9.22
Maximum Percentage = 18.6		R Magnitude = 0.584
Mean Percentage = 5.88	Standard Deviation = 5.87	Rayleigh = 0.0000

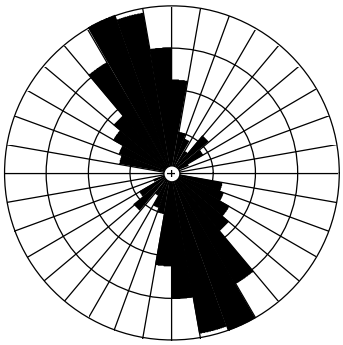

All face cleats in project area, all coals		Statistics
N = 342		Vector Mean = 338.8
Class Interval = 10 degrees		Conf. Angle = 4.65
Maximum Percentage = 23.4		R Magnitude = 0.745
Mean Percentage = 6.67	Standard Deviation = 7.65	Rayleigh = 0.0000

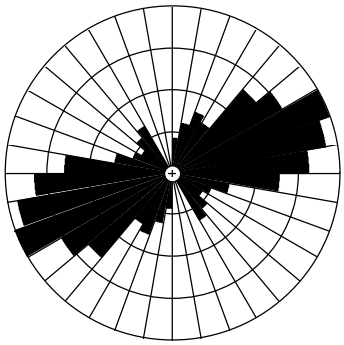

All butt cleats in project area, all coals		Statistics
N = 313		Vector Mean = 68.8
Class Interval = 10 degrees		Conf. Angle = 5.36
Maximum Percentage = 20.8		R Magnitude = 0.696
Mean Percentage = 6.67	Standard Deviation = 6.61	Rayleigh = 0.0000

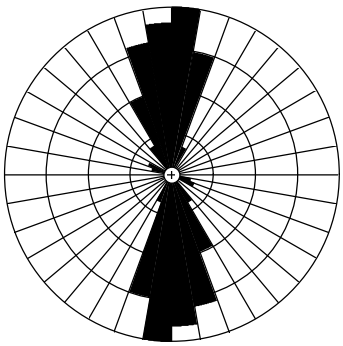

All J1 joints in project area, Fruitland sands		Statistics
N = 434		Vector Mean = 357.2
Class Interval = 10 degrees		Conf. Angle = 2.47
Maximum Percentage = 29.7		R Magnitude = 0.897
Mean Percentage = 11.11	Standard Deviation = 11.15	Rayleigh = 0.0000

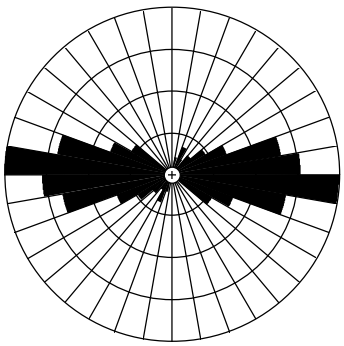

All J2 joints in project area, Fruitland sands		Statistics
N = 273		Vector Mean = 90.0
Class Interval = 10 degrees		Conf. Angle = 3.84
Maximum Percentage = 33.3		R Magnitude = 0.852
Mean Percentage = 8.33	Standard Deviation = 10.21	Rayleigh = 0.0000

Figure 2-7. Summary rose diagrams of all J1 and J2 joints in Pictured Cliffs and Fruitland sandstones and all face and butt cleats of coal in the project area.

Basin Creek

Figure 2-8 shows summary rose diagrams of joint and cleat orientations in the Pictured Cliffs Sandstone, Fruitland Formation coals, and Fruitland sandstone beds. In the Pictured Cliffs (including both the main body and tongue) the average orientation of the J1 joint set is 332º, or N. 28º W. The average orientation of the J2 set is 59º, or N. 59º E. There were only scattered occurrences of J3 or J4 sets in the Pictured Cliffs in this area. In general, the main body of the Pictured Cliffs has few joints at Basin Creek. However, the outcrop just north of the road, at station BC01, has some of the largest J1 joints in the area. The J1 joints there exceed 100 ft in length and are irregularly spaced, from as close as 6 inches to as wide as about 20 ft. The length of the J2 set also varies from 6 inches to 20 ft, depending on the spacing of the J1 set. J2 joints are spaced 6-10 ft apart here. The joints are somewhat sinuous, but extend across the entire outcrop. No mineralization of either set was noted. This locality is good for examining joints because it is a large, stripped dip slope at the top of the Pictured Cliffs.

In the entire Basin Creek area, the exposed lengths of J1 joints in the Pictured Cliffs vary from 1 ft to over 100 ft; spacing between joints is from 6 inches to 20 ft, and there is a wide range of sinuous to linear traces of joints across the outcrops. No calcite fillings were seen in the Pictured Cliffs, but iron-rich bands, or halos, are present along some joints. Exposed lengths of J2 joints range from 6 inches to 20 ft, spacing varies from 2-10 ft, and the joints are fairly planar. No mineralization was noted in the J2 set either.

Face cleat orientations in all coal beds at Basin Creek average 358º, or N. 2º W. and butt cleats average 89º, or N. 88º E (fig. 2-8). Lengths of cleats could not be readily seen in this area because most of the coal beds are weathered and have to be dug out to see the cleat pattern. Spacing of face cleats ranges from about ¼ inch to 6 inches, spacing of butt cleats is from ¼ inch to a maximum of about 2 inches. Most outcrops of coal have no mineral fillings in the cleats, but traces of iron were seen at several locations, and there is abundant iron mineralization of cleats at station BC33.

For all sandstone beds of the Fruitland Formation at Basin Creek the average orientation of the J1 set is 358º, or N. 2º W. The average orientation of the J2 set is 270º (fig. 2-8). Exposed lengths of J1 joints in Fruitland sandstone beds are 1-20 ft, although the top surfaces of these sandstone beds are rarely exposed. Spacing is from 2 inches to about 24 inches, and many joints in these sandstones are planar and well-formed. Calcite fillings are common in joints in Fruitland sandstone beds, as are coatings of iron oxide. In general, well-cemented, relatively thin sandstones display a greater abundance and better-formed joints than thick, poorly cemented sandstone beds. J2 joints in these sandstones have exposed lengths of 1-6 ft, are spaced 1-8 ft apart, and are also fairly linear and planar. The J2 joints also display fillings of calcite.

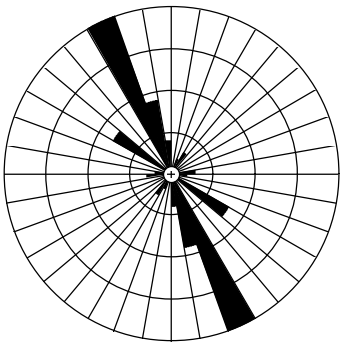

Basin Creek, Kpc, J1 set		Statistics
N = 53		Vector Mean = 331.8
Class Interval = 10 degrees		Conf. Angle = 16.47
Maximum Percentage = 37.7		R Magnitude = 0.595
Mean Percentage = 10.00	Standard Deviation = 10.75	Rayleigh = 0.0000

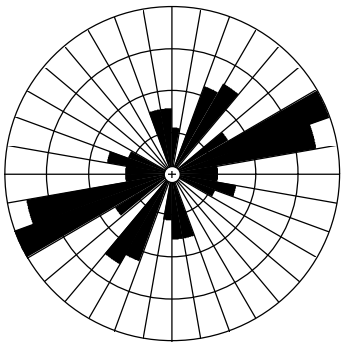

Basin Creek, Kpc, J2 set		Statistics
N = 44		Vector Mean = 59.2
Class Interval = 10 degrees		Conf. Angle = 18.50
Maximum Percentage = 29.5		R Magnitude = 0.583
Mean Percentage = 8.33	Standard Deviation = 8.70	Rayleigh = 0.0000

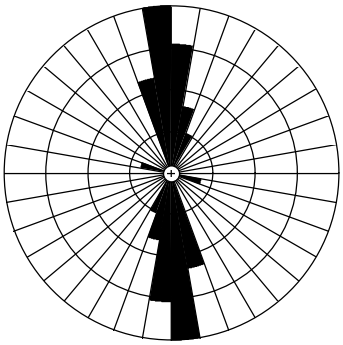

Basin Creek, all coals, face cleat		Statistics
N = 66		Vector Mean = 357.6
Class Interval = 10 degrees		Conf. Angle = 5.27
Maximum Percentage = 45.5		R Magnitude = 0.927
Mean Percentage = 16.67	Standard Deviation = 16.19	Rayleigh = 0.0000

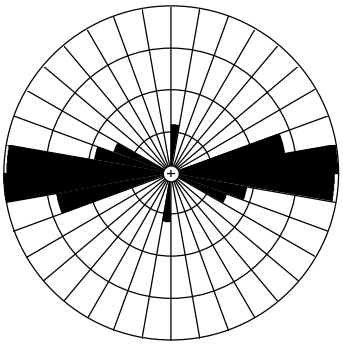

Basin Creek, all coals, butt cleats		Statistics
N = 66		Vector Mean = 88.8
Class Interval = 10 degrees		Conf. Angle = 6.94
Maximum Percentage = 34.8		R Magnitude = 0.884
Mean Percentage = 16.67	Standard Deviation = 13.64	Rayleigh = 0.0000

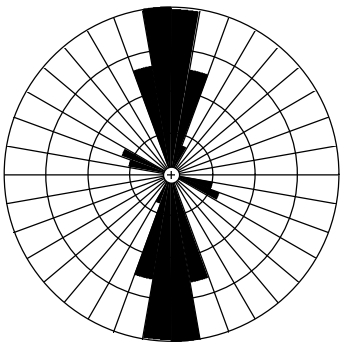

Basin Creek, Fruitland sandstones, J1 set		Statistics
N = 90		Vector Mean = 358.5
Class Interval = 10 degrees		Conf. Angle = 6.46
Maximum Percentage = 33.3		R Magnitude = 0.859
Mean Percentage = 14.29	Standard Deviation = 13.15	Rayleigh = 0.0000

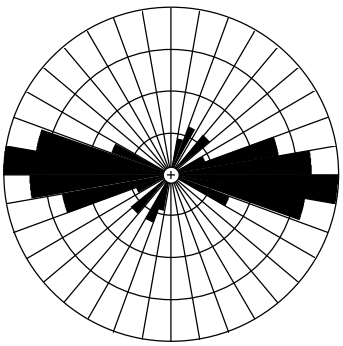

Basin Creek, Fruitland sandstones, J2 set		Statistics
N = 68		Vector Mean = 270.2
Class Interval = 10 degrees		Conf. Angle = 8.47
Maximum Percentage = 30.9		R Magnitude = 0.822
Mean Percentage = 11.11	Standard Deviation = 10.68	Rayleigh = 0.0000

Figure 2-8. Summary rose diagrams of joints and cleats in the Basin Creek area.

Carbon Junction

Figure 2-9 shows summary rose diagrams of joint and cleat orientations in the Pictured Cliffs Sandstone, Fruitland Formation coal beds, and Fruitland sandstone beds.

In the Pictured Cliffs (including readings from the tongue of Pictured Cliffs) the average orientation of the J1 set is 77º, or N. 77º E. The average orientation of the J2 set is 310º, or N. 50º W, although there is quite a bit of scatter in the readings obtained from the Pictured Cliffs in this area. The scatter in these diagrams is a result of combining the orientations measured at the individual stations (CJ11, CJ13, CJ 24, CJ27, CJ03, and CJ19, appendix 2-2). Joints of the J1 set in the main body of the Pictured Cliffs, measured in Carbon Junction Canyon, are clustered between N. 70º-80º E., whereas those measured southwest of the canyon are oriented strongly northwest, and those northeast of the canyon are just a little east of north. J1 joints in the tongue of Pictured Cliffs are also oriented strongly northwest to east-west. These divergent directions all are displayed on the summary rose plot (fig. 2-9). J2 joints are oriented nearly at right angles to those of the J1 set, and their divergent directions also are apparent in figure 2-9.

In this area the Pictured Cliffs main body and tongue generally lack good jointing, resulting in a small number of readings. Laubach and others (1991) noted that the outcrop at Carbon Junction Canyon has few fractures, and that many of those are surficial. Station CJ11 is at a locality described by Laubach and others (1991) as a fracture "swarm", where the joints are tightly clustered. Station CJ27 is another area where the joints are tightly clustered. Elsewhere, joints may be more a result of stress release or of weathering.

The J1 joints range in length from 2 to about 30 ft, except at station CJ27, where they are as long as 60 ft or more. Spacing is from less than 1 inch in the "swarms" to as much as 10 ft. Most of the J1 joints in this area in the Pictured Cliffs are somewhat sinuous, not linear. Most joints had either no mineralization or slight amounts of iron coatings, except at station CJ24, where there are abundant iron coatings on joint surfaces. The J2 joints are somewhat poorly developed and range in length from 6 inches to about 30 inches. They are spaced from 6 inches to 15 ft apart. Most of them are also relatively sinuous and unmineralized.

More consistent results were obtained from measurements of coal cleats in the Carbon Junction area. The face cleats are tightly clustered at an orientation of 340º, or N. 20º W., and the butt cleats are oriented at 69º, or N. 69º E. (fig. 2-9). In this area, as at the other areas, the total length of the cleats could not be observed, due to cover. The spacing of face cleats ranges from ¼ inch to 3 inches; the spacing of butt cleats ranges from ¼ inch to about 2½ inches. Many of the outcrops have films of iron oxide coating the cleat surfaces.

Joint orientations of sandstone beds in the Fruitland Formation are also fairly tightly clustered in this area. The average orientation of J1 joints is 351º, or N. 9º W.; that of the J2 set is 85º, or N. 85º E. (fig. 2-9). A J3 set was observed at station CJ20, and the orientation of this set is about 296º, or N. 64º W. The J1 set ranges from an exposed length of about 1 ft to 8 ft and has spacing of from 2 to 36 inches. They are relatively well-formed and are planar and linear in many outcrops. Mineral fillings of iron and calcite are present in many J1 joints in Fruitland sandstone beds. The J2 set length is from 2 inches to 4 ft, spacing is from 6 inches to 4 ft, and they are relatively abundant and well-formed in several outcrops. They also displayed fillings of iron and calcite.

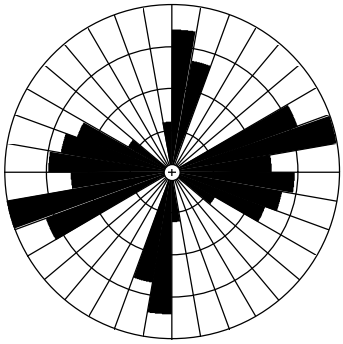

Carbon Junction, Kpc, J1 set	Statistics
N = 52	Vector Mean = 77.7
Class Interval = 10 degrees	Conf. Angle = 27.78
Maximum Percentage = 21.2	R Magnitude = 0.382
Mean Percentage = 10.00 Standard Deviation = 5.70	Rayleigh = 0.0005

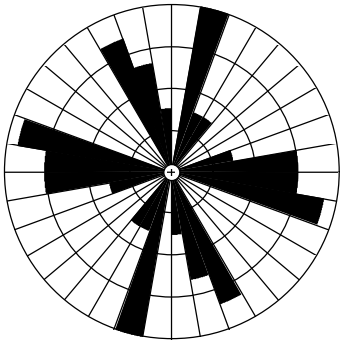

Carbon Junction, Kpc, J2 set	Statistics
N = 33	Vector Mean = 309.5
Class Interval = 10 degrees	Conf. Angle = 192.62
Maximum Percentage = 21.2	R Magnitude = 0.073
Mean Percentage = 10.00 Standard Deviation = 6.68	Rayleigh = 0.8371

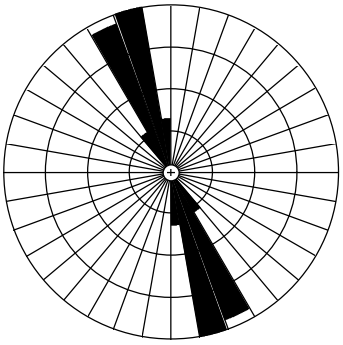

Carbon Junction, all coals, face cleats	Statistics
N = 79	Vector Mean = 339.6
Class Interval = 10 degrees	Conf. Angle = 2.54
Maximum Percentage = 48.1	R Magnitude = 0.982
Mean Percentage = 25.00 Standard Deviation = 22.08	Rayleigh = 0.0000

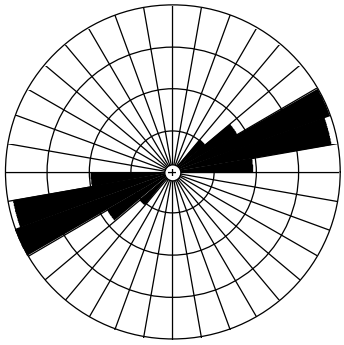

Carbon Junction, all coals, butt cleats	Statistics
N = 73	Vector Mean = 68.5
Class Interval = 10 degrees	Conf. Angle = 3.75
Maximum Percentage = 41.1	R Magnitude = 0.961
Mean Percentage = 20.00 Standard Deviation = 17.17	Rayleigh = 0.0000

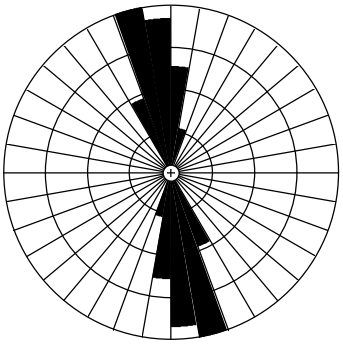

Carbon Juncton, Fruitland sandstones, J1 set	Statistics
N = 69	Vector Mean = 351.0
Class Interval = 10 degrees	Conf. Angle = 3.86
Maximum Percentage = 39.1	R Magnitude = 0.959
Mean Percentage = 20.00 Standard Deviation = 14.76	Rayleigh = 0.0000

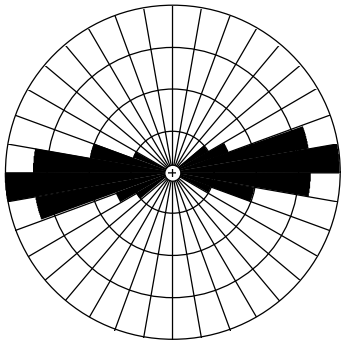

Carbon Junction, Fruitland sandstones, J2 set	Statistics
N = 46	Vector Mean = 85.0
Class Interval = 10 degrees	Conf. Angle = 6.74
Maximum Percentage = 34.8	R Magnitude = 0.924
Mean Percentage = 14.29 Standard Deviation = 12.58	Rayleigh = 0.0000

Figure 2-9. Summary rose diagrams of joints and cleats in the Carbon Junction area.

Florida River

Summary rose diagrams of Pictured Cliffs Sandstone, Fruitland Formation coal, and Fruitland sandstone beds in the Florida River area are shown in figure 2-10. Joint and cleat orientations are fairly tightly clustered for all units in this area. The average orientation for the J1 set for the Pictured Cliffs is 337º, or N. 23º W.; that for the J2 set is 64º, or N. 64º E. The observed lengths of J1 joints ranges from 1 to 10 ft; spacing ranges from 2 inches to 15 ft. The J1 joint set is linear and planar in many outcrops, but somewhat sinuous in others. Except for one outcrop at station FR38, which displays calcite coatings, none of the J1 joint stations were observed to have mineral fillings.

The J2 joint set in the Pictured Cliffs is poorly developed in this area; many of the stations had no J2 joint set. Of those observed, the length varies from about 2 ft to over 5 ft; spacing ranges from 2 inches to 3 ft. Bands of iron, in a halo effect, are present adjacent to J2 joints at station FR03, but no other associated mineralization was noted.

Face cleats in coal in the Florida River area have an average orientation of 329º, or N. 31º W.; butt cleats have an average orientation of 58º, or N. 58º E. Spacing of face cleats ranges from one-eighth inch to one inch; that of butt cleats ranges from one-eighth inch to one-half inch. No mineral coatings are present on cleats in most of the area; iron oxide is present at stations FR37 and FR40, near the Florida canal.

The average orientation of J1 joints in Fruitland sandstone beds is 340º, or N. 20º W.; that of J2 joints is 67º, or N. 67º E. J1 joints are from 18 inches to in excess of 10 ft long; spacing ranges from 2 inches to 10 ft. Most of the J1 joints in Fruitland sandstone beds are well-developed, linear and planar. Many of the joints cut multiple beds of Fruitland sands. Iron coatings were noted at a few stations, and calcite at one station, but many J1 joints do not have mineral coatings.

In contrast, the J2 joint set is poorly developed in Fruitland sands in this area, similar to the situation with the Pictured Cliffs Sandstone. Where they do occur the J2 set is from 1 to 4 ft long, but are so scattered that a reliable range of spacing could not be determined. Mineral fillings or coatings are also rare, consisting of minor iron oxide or calcite.

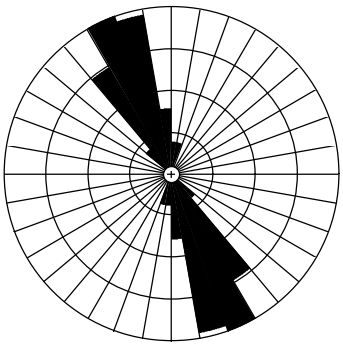

Florida River, Kpc, J1 set		Statistics
N = 71		Vector Mean = 337.4
Class Interval = 10 degrees		Conf. Angle = 5.06
Maximum Percentage = 36.6		R Magnitude = 0.934
Mean Percentage = 14.29	Standard Deviation = 15.10	Rayleigh = 0.0000

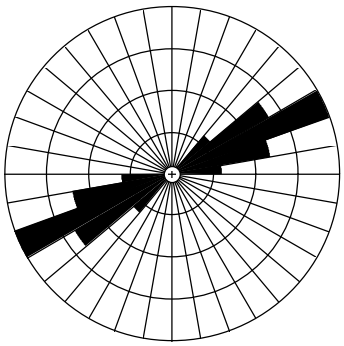

Florida River, Kpc, J2 set		Statistics
N = 22		Vector Mean = 63.6
Class Interval = 10 degrees		Conf. Angle = 7.68
Maximum Percentage = 50.0		R Magnitude = 0.947
Mean Percentage = 20.00	Standard Deviation = 17.57	Rayleigh = 0.0000

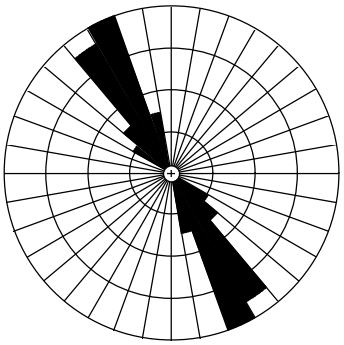

Florida River, all coals, face cleats		Statistics
N = 62		Vector Mean = 329.3
Class Interval = 10 degrees		Conf. Angle = 4.08
Maximum Percentage = 46.8		R Magnitude = 0.957
Mean Percentage = 20.00	Standard Deviation = 19.19	Rayleigh = 0.0000

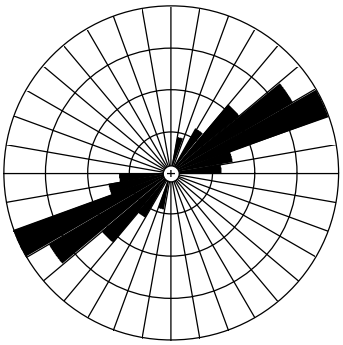

Florida River, all coals, butt cleats		Statistics
N = 50		Vector Mean = 58.2
Class Interval = 10 degrees		Conf. Angle = 6.87
Maximum Percentage = 42.0		R Magnitude = 0.914
Mean Percentage = 14.29	Standard Deviation = 14.94	Rayleigh = 0.0000

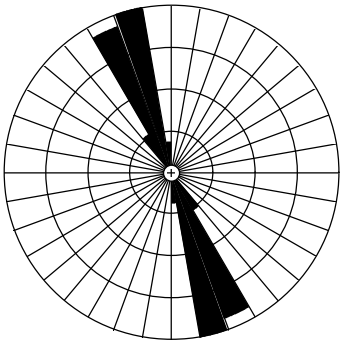

Florida River, Fruitland sandstones, J1 set		Statistics
N = 55		Vector Mean = 339.9
Class Interval = 10 degrees		Conf. Angle = 3.04
Maximum Percentage = 50.9		R Magnitude = 0.984
Mean Percentage = 25.00	Standard Deviation = 23.98	Rayleigh = 0.0000

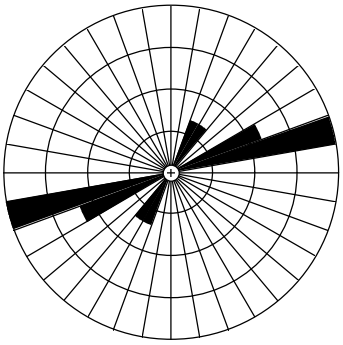

Florida River, Fruitland sandstones, J2 set		Statistics
N = 14		Vector Mean = 66.6
Class Interval = 10 degrees		Conf. Angle = 16.37
Maximum Percentage = 64.3		R Magnitude = 0.860
Mean Percentage = 25.00	Standard Deviation = 25.04	Rayleigh = 0.0000

Figure 2-10. Summary rose diagrams of joints and cleats in the Florida River area.

South Fork of Texas Creek

Figure 2-11 shows summary rose diagrams of joint and cleat orientations of the mapped units at the South Fork of Texas Creek. In that area the average orientation of J1 joints in the Pictured Cliffs is 351º, or N. 9º W.; the average orientation of J2 joints is 79º, or N. 79º E. Several areas exist at Texas Creek where a stripped dip slope exposes large areas of the top of the Pictured Cliffs, allowing for a more accurate assessment of the lengths of joints. Observed lengths of J1 joints range from 20 ft to over 100 ft. J1 joints occur in closely spaced zones in some areas, but are more evenly spaced in other areas. Where tightly clustered, the spacing is less than 2 inches to 1 ft. Otherwise, spacing ranges up to 8 ft. In the good exposures in this area the pattern of J1 joints is somewhat anastomosing, where one joint will die out into rock or hook into an adjacent joint. A cluster of joints will form a long, linear zone that consists of curvilinear joints. In this area only iron oxide coatings were seen on the J1 joints.

In this area, too, J2 joints are relatively poorly expressed in the Pictured Cliffs Sandstone. Their length depends on the spacing of J1 joints, and is therefore quite variable. Spacing of J2 joints is 6 inches to over 5 ft, but averages about 3-4 ft. In a few places J2 joints are relatively well-formed, but in general they are difficult to find. The only mineralization noted on J2 joints is iron oxide.

An interesting feature of the Texas Creek area is the presence of a third joint set in the Pictured Cliffs at some of the stations. Stations where this set was observed are TC04, TD01, TD02, TE01, AND TF01 (appendix 2-2). Except for TF01, the stations are concentrated in the central part of the mapped area. The orientation of the J3 set is about 325º, or N. 35º W. These joints terminate against the J1 and J2 sets, and are therefore believed to be younger than either of those sets. A fourth set is also rarely present that is at about right angles to the J3 set. All four sets are well-expressed at station TF01, just upslope from the Hobbs property, toward the eastern end of the mapped area. This site has an old road leading to it and is easily accessible.

Coal cleats in the Texas Creek area have mixed orientations, possibly due to slumping at some outcrops. The face cleats average 338º, or N. 22º W., and the butt cleats average 68º, or N. 68º E., with quite a bit of scatter. The majority of face cleats are sub-parallel with J1 joints in the Pictured Cliffs, and the butt cleats are sub-parallel to J2 joints of the Pictured Cliffs. Spacing of both face and butt cleats is one-eighth inch to one inch. No significant mineralization was noted on cleats in this area.

In sandstone beds of the Fruitland Formation, the average orientation of J1 joints is 1º, or N. 1º E.; the average orientation of J2 joints is 271º, or N. 89º W. Length of J1 joints is from 1 ft to 15 ft; spacing is about 2 inches to 2 ft. As with other mapped areas, the joints in Fruitland sandstone beds are well-formed, linear, and planar. Only minor iron oxide mineralization was noted on these joints. The J2 joint set varies from poorly expressed to common at different localities at Texas Creek. They are commonly short, less than 2 ft, and have a spacing of about 1-3 ft. Only minor iron oxide coatings were noted on this set.

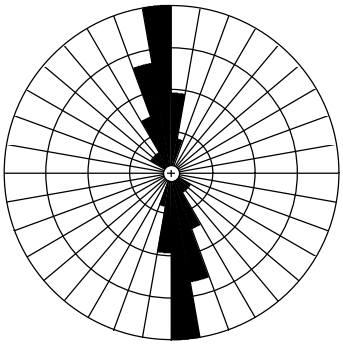

Texas Creek, Kpc, J1 set		Statistics
N = 91		Vector Mean = 351.2
Class Interval = 10 degrees		Conf. Angle = 4.47
Maximum Percentage = 52.7		R Magnitude = 0.933
Mean Percentage = 12.50	Standard Deviation = 17.37	Rayleigh = 0.0000

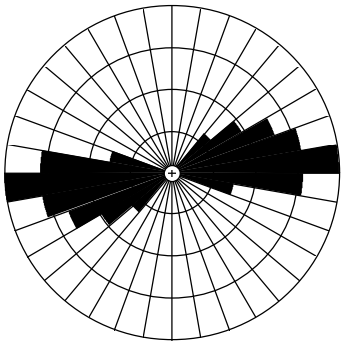

Texas Creek, Kpc, J2 set		Statistics
N = 66		Vector Mean = 78.9
Class Interval = 10 degrees		Conf. Angle = 6.65
Maximum Percentage = 31.8		R Magnitude = 0.890
Mean Percentage = 14.29	Standard Deviation = 9.87	Rayleigh = 0.0000

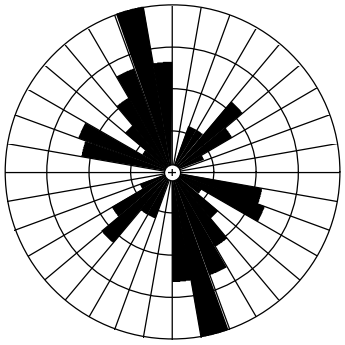

Texas Creek, all coals, face cleats		Statistics
N = 84		Vector Mean = 338.2
Class Interval = 10 degrees		Conf. Angle = 19.11
Maximum Percentage = 27.4		R Magnitude = 0.431
Mean Percentage = 7.69	Standard Deviation = 6.89	Rayleigh = 0.0000

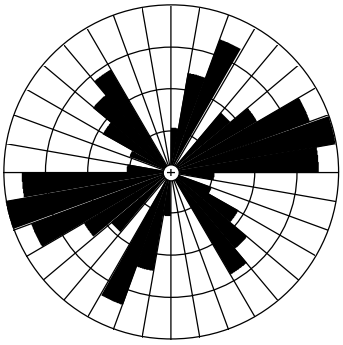

Texas Creek, all coals, butt cleats		Statistics
N = 77		Vector Mean = 67.6
Class Interval = 10 degrees		Conf. Angle = 23.41
Maximum Percentage = 18.2		R Magnitude = 0.375
Mean Percentage = 7.69	Standard Deviation = 5.53	Rayleigh = 0.0000

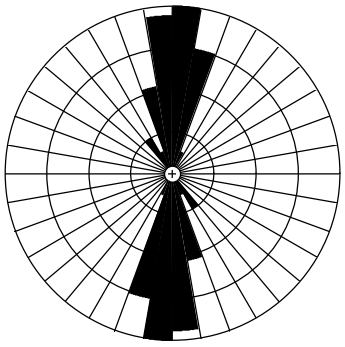

Texas Creek, Fruitland sandstones, J1 set		Statistics
N = 134		Vector Mean = 0.6
Class Interval = 10 degrees		Conf. Angle = 3.68
Maximum Percentage = 35.1		R Magnitude = 0.934
Mean Percentage = 14.29	Standard Deviation = 14.09	Rayleigh = 0.0000

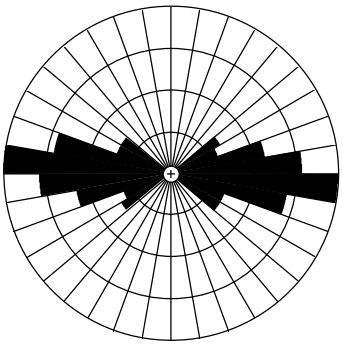

Texas Creek, Fruitland sandstones, J2 set		Statistics
N = 98		Vector Mean = 270.7
Class Interval = 10 degrees		Conf. Angle = 5.72
Maximum Percentage = 34.7		R Magnitude = 0.876
Mean Percentage = 12.50	Standard Deviation = 10.95	Rayleigh = 0.0000

Figure 2-11. Summary rose diagrams of joints and cleats in the Texas Creek area.

Pine River

Figure 2-12 shows the average orientations of joints and cleats in the area between the South Fork of Texas Creek and the Pine River. There is a bit of scatter in average orientations of the Pictured Cliffs Sandstone, but J1 joints average 5º, or N. 5º E.; J2 joints average 285º, or N. 75º W. In this area the Pictured Cliffs is characterized by relatively few systematic joints. In many outcrops there is abundant surficial jointing, or spalling of blocks of sandstone. J1 joints range in length from 10 to 20 ft. Spacing averages from 6 inches to 10 ft, although there is clustering of joints in some areas where spacing is as close as 2 inches. The J1 set consists of long, linear, and planar joints. Minor calcite and iron oxide was noted on some joint surfaces.

J2 joints in the Pictured Cliffs are poorly developed. They range in length from 8 inches to 5 ft and have spacing of 1-4 ft. Like the J1 joints, mineralization is not a significant feature.

The average orientation of face cleats in coal here is 325º, or N. 35º W.; butt cleat orientations are 54º, or N. 54º E. Face cleats are spaced one-eighth inch to 2 inches; butt cleats are spaced one-eighth inch to one inch. Iron oxide was noted at several localities coating both sets of cleats.

There is a good development of J1 joints in Fruitland Formation sandstone beds in this area. The average orientation is 7º, or N. 7º E.; the average orientation of J2 joints is 279º, or N. 81º W. The length of J1 joints ranges from less than 1 ft to greater than 60 ft. An especially well-exposed dip slope of the number 2 sandstone is present at station PR12, where the longest joints are present. This outcrop is probably typical of surface jointing in the Fruitland sandstone beds in this and other areas. In most places these sandstones are poorly exposed, making it likely to underestimate the extent of jointing. Spacing of J1 joints in this area ranges from 1 to 18 inches; iron oxide was noted at several localities coating the joint surfaces.

J2 joints are also fairly abundant in this area and range from less than 1 ft to about 3 ft in length. Spacing is 1 to 3 ft in most localities. Only minor iron oxide was noted on some J2 joints; no calcite was seen on this or the J1 set.

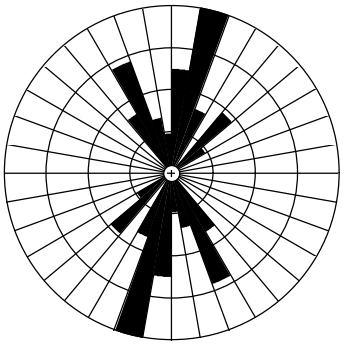

Pine River, Kpc, J1 set		Statistics
N = 48		Vector Mean = 4.8
Class Interval = 10 degrees		Conf. Angle = 13.35
Maximum Percentage = 37.5		R Magnitude = 0.710
Mean Percentage = 11.11	Standard Deviation = 11.02	Rayleigh = 0.0000

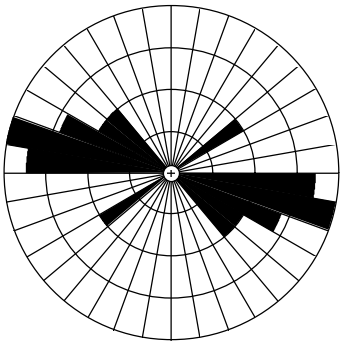

Pine River, Kpc, J2 set		Statistics
N = 12		Vector Mean = 284.9
Class Interval = 10 degrees		Conf. Angle = 21.36
Maximum Percentage = 33.3		R Magnitude = 0.803
Mean Percentage = 16.67	Standard Deviation = 10.05	Rayleigh = 0.0004

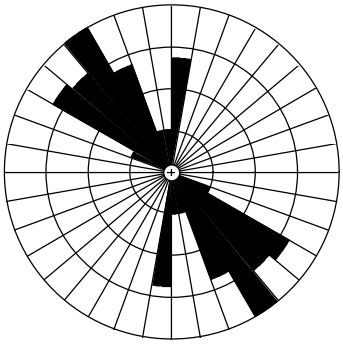

Pine River, all coals, face cleats		Statistics
N = 51		Vector Mean = 324.6
Class Interval = 10 degrees		Conf. Angle = 10.07
Maximum Percentage = 29.4		R Magnitude = 0.812
Mean Percentage = 12.50	Standard Deviation = 9.66	Rayleigh = 0.0000

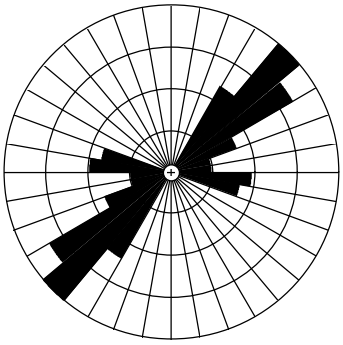

Pine River, all coals, butt cleats		Statistics
N = 47		Vector Mean = 53.5
Class Interval = 10 degrees		Conf. Angle = 11.40
Maximum Percentage = 36.2		R Magnitude = 0.780
Mean Percentage = 12.50	Standard Deviation = 11.75	Rayleigh = 0.0000

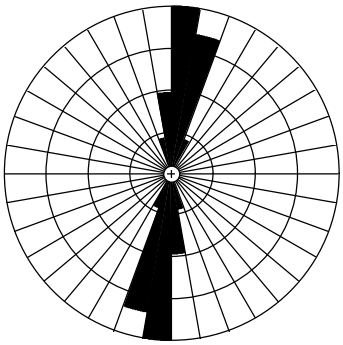

Pine River, Fruitland sandstones, J1 set		Statistics
N = 86		Vector Mean = 6.7
Class Interval = 10 degrees		Conf. Angle = 3.45
Maximum Percentage = 48.8		R Magnitude = 0.964
Mean Percentage = 20.00	Standard Deviation = 19.71	Rayleigh = 0.0000

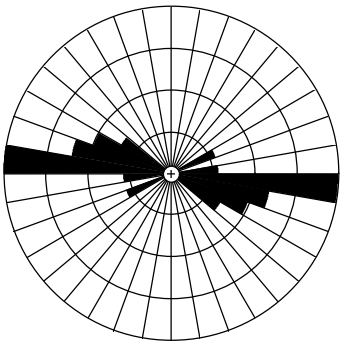

Pine River, Fruitland sandstones, J2 set		Statistics
N = 47		Vector Mean = 279.2
Class Interval = 10 degrees		Conf. Angle = 6.69
Maximum Percentage = 53.2		R Magnitude = 0.916
Mean Percentage = 16.67	Standard Deviation = 17.94	Rayleigh = 0.0000

Figure 2-12. Summary rose diagrams of joints and cleats in the Pine River area.

Discussion of fractures

Orientations of joints and cleats vary somewhat over the entire study area, but these variations are less evident when the area as a whole is considered. Figure 2-7 shows that there are regional similarities of joint orientations in the various geologic units studied. However, each individual mapped area has its own identity, as shown in figures 2-8 through 2-12. More specific information about individual localities is shown in appendix 2-2.

In each area one main joint or cleat set can be identified in each geologic unit. This set is composed of relatively long, commonly linear joints, and in some instances joints of this set occur in narrowly clustered zones. Joint fillings or coatings consist of iron oxide or calcite, with iron and calcite being abundant at Basin Creek, moderately abundant at Carbon Junction, rare at the Florida River, and relatively rare at Texas Creek and at the Pine River. No slickenside striations were noted on any of the J1 or other joint sets in the study area. The joints are oriented perpendicular to bedding surfaces in most instances, which may indicate that the jointing occurred prior to the rocks being uplifted into their present configuration.

The lithology of the rock unit has an important impact on the degree of fracturing that occurs. Coal is relatively brittle and breaks easily, resulting in the closely spaced face and butt cleats. Sandstone beds of the Fruitland Formation are relatively thin and firmly cemented, which also promotes the development of joints. Thick, weakly cemented rocks, characteristic of the upper part of the Pictured Cliffs Sandstone, are the least prone to develop good, systematic joint sets.

In some outcrops, a second joint set is also present. This joint set is commonly at nearly right angles to and terminates against the main joint set. This set is clearly secondary to the main set. This secondary set is also oriented perpendicular to bedding surfaces.

In a few outcrops a third or a fourth joint set were also observed. These joints terminate against both the J1 and J2 joints, indicating that they are younger than the other two sets. Although a cluster of these joints was found in the Texas Creek area, they are generally rare in the entire project area.

The joints and cleats in the study area share characteristics of those in this and nearby areas previously described by myself (Condon, 1988, 1989, 1995) and by others Close (1993), Close and Mavor (1991), Laubach and others (1991), Tremain and Whitehead (1990), Tremain and others (1991a, b).

Fundamental questions in fracture studies involve the cause of fracturing, time of fracturing, and predictions of fracture trends in the subsurface. These topic are briefly discussed below.

Joints. Based on surface features and the lack of shear displacement, the joints along the northern rim of the basin were interpreted as mode I fractures (Laubach and others, 1991), otherwise known as opening mode or extension fractures. In sandstones, this type of fracture is thought to initiate at inhomogeneities in the rock, such as fossils, clasts, voids, microcracks, or other features, which concentrate local tensile stresses in an overall compressive stress field (Pollard and Aydin, 1988). Opening mode fractures form parallel to the maximum compressive stress direction and perpendicular to the least compressive stress direction (Lorenz and others, 1991). Pore pressure also has been recognized as an important component in the formation of natural fractures by decreasing the effective confining pressure of rocks in the subsurface (Secor, 1965; Lorenz and others, 1991).

The timing of fracture development in sandstones of the Fruitland and Pictured Cliffs is not very well constrained. Before fracturing can occur the sediments must have been lithified to some degree. The Pictured Cliffs and Fruitland Formation are Campanian to Maastrichtian in age (roughly 75 to 72 Ma) (Molenaar and Baird, 1991). Lorenz (1995) suggested that the Frontier Formation in the Green River basin was lithified at a depth of approximately 3,000 ft. In the San Juan Basin the Pictured Cliffs and Fruitland first reached that depth of burial at about 60 million years ago in the Paleocene and reached a depth of

nearly 7,000 ft in the Miocene (Law, 1992). A complicating factor in the San Juan Basin is elevated thermal maturity caused by a thermal event 40 to 20 m.y. ago, extending from the late Eocene to the early Miocene (Law, 1992).

Law and others (1989) suggested an endogenetic mechanism whereby thermogenic gas generation causes overpressuring that eventually leads to the creation of fractures in the enclosing rocks. Lorenz and others (1991), however, maintained that pore pressure cannot exceed the least compressive stress and therefore cannot alone cause tensile fracturing. Differential stress is needed for the development of systematic joint sets.

The tectonic fabric of this part of the southwestern USA was established at about 1,790 to 1,700 Ma in the Proterozoic during accretion of a series of crustal provinces (Condie, 1992). Baars and Stevenson (1982) attributed the orientation of major northwest- and northeast-oriented basement faults and lineaments to north-south compression that formed conjugate shear zones. Given that opening mode fractures form parallel to the maximum compressive stress direction (Lorenz and others, 1991), it is not unreasonable to expect north-south-oriented fractures in basement rocks of the San Juan Basin. The northwest-northeast pattern of basement faults has also been interpreted from seismic lines (Huffman and Taylor, 1989), and the pattern of faulting was shown in Huffman and Condon (1993). Although probably not propagated upward through the geologic section as distinct features, the north-south-oriented fractures may have formed zones of weakness or anisotropy that affected fracture orientations in rocks deposited at later times.

The main compressional tectonic events that occurred during and after deposition of the Pictured Cliffs Sandstone and Fruitland Formation were the Sevier and Laramide orogenies (Armstrong, 1968; Dickinson, 1978; Hamilton, 1987; Heller and others, 1986; Tweto, 1975). Lorenz (1985) provided a concise history of tectonic events in the nearby Piceance Creek basin, on the other side of the Uncomphagre uplift, north of the San Juan Basin.

The Sevier thrust belt developed in response to general east-west compression and crustal shortening along an Andean-type continental margin (Coney, 1978). Although much of the compression was east-west, the configuration of the orogenic belt and adjacent foreland basin suggests a significant southeastward component to the compressive stress (Heller and others, 1986). The effects of the Sevier orogeny are thought to have largely dissipated by about 72 Ma, however (Lorenz, 1985), so the sandy sediments of the Pictured Cliffs and Fruitland would not have been buried deeply enough to lithify and form fractures as a result of Sevier-related stress.

There has been much discussion regarding the cause of the change in tectonic style between the Sevier and Laramide orogenies and the mechanisms for Laramide deformation, topics which are beyond the scope of this report. Whatever the causes, Laramide tectonism is characterized by basement-cored anticlinal uplifts that are bounded by deep structural basins. East-west crustal shortening occurred from Montana to New Mexico in Late Cretaceous to late Eocene time (roughly 75 to 40 Ma) (Coney, 1978; Hamilton, 1987; Lorenz, 1985). This structural event would seem to be the most likely to have caused fracturing in the Pictured Cliffs and Fruitland because (1) the units would have been buried deep enough to have lithified and (2) initial gas generation could have increased the pore pressure to a point favorable for initiation of fracturing. The problem with this scenario is that the orientations of the main joints in the units are not parallel to the east-west-oriented stress, and are in fact, nearly perpendicular to it.

The generally north-south orientation of the main joints may be explained by the stress generated by the clockwise rotation of the Colorado Plateau at this time (Hamilton, 1987) or by late Laramide north-south-oriented compression (Gries, 1983). The rotation or compression of the San Juan Basin resulted in convergence of the basin with the Uncompahgre uplift to the north. The uplift may have acted as a buttress and the stress would have been roughly north-south, parallel to the fractures generated in Proterozoic time (these directions refer to current

orientations). This collision of the basin with the Uncompahgre uplift may also have led to the development of the reverse fault just west of the Pine River (plate 5) and to thrust faults discussed by Huffman and Taylor (this report).

The time between the Laramide and the present has been characterized by extension, along with one period of intense volcanism in the Oligocene and several periods of regional uplift and erosion (Coney, 1978; Lorenz, 1985). Transform movement along the western continental boundary led to the relaxation of the east-west Laramide stress, allowing for the present extensional mode of the Basin and Range province (Hamilton, 1987). This time period seems to lack the necessary compression event or events that could have caused initial fracturing in the Pictured Cliffs and Fruitland Formation. The J2 and younger sets could possibly have formed during this time as a result of unloading of the overburden.

Cleats. Tremain and Whitehead (1990), Tremain and others (1991a, b), and Laubach and others (1991) summarized the characteristics and origin of coal cleats in the northern San Juan Basin, and my studies generally support their conclusions. Important facts to note are that coal cleats are also mode I fractures that formed parallel to the principle compressive stress and perpendicular to the least compressive stress. Close (1993) emphasized that two mechanisms, or a combination of the two, have been proposed for the formation of cleats. Endogenetic processes include dewatering and compaction, while exogenetic processes include paleotectonic or neotectonic responses to stress.

Law and others (1983) noted that peat contains 80 to 90% water by volume, which decreases to about 7% in high-volatile B bituminous and higher-rank coals. Much of the water is expelled early in coalification, decreasing to about 20% by volume at the subbituminous B rank. The mechanisms for dewatering are mainly physical compaction and thermal destruction of functional groups (Law and others, 1983). Many coal beds in the Fruitland are immediately overlain by channel sandstones which contributed to compaction.

The coals of the Fruitland were subjected to the same stresses that produced joints in sandstones, but cleat formation may have occurred earlier than the development of joints. Close and Mavor (1993) thought that lithification of Fruitland coals may have occurred in as little as 3.4 million years after deposition. Early formation of cleats has also been reported in Pennsylvanian-age strata in Wales (Gayer and others, 1996), where coal clasts were eroded from coals belonging to the same stage as sediments in which the clasts were redeposited. Some of these clasts had already developed cleat as a result of extensional fracturing of overpressured coal in response to compression. Another example of early formation of cleats was reported by Pattison and others (1996). Based on age dates from mineral fillings in cleats, Pattison and others (1996) interpreted the cleats to have formed less than 10 Ma after peat accumulation. Cleats were interpreted to have formed parallel to the maximum horizontal stress.

On the basis of these other studies, it seems likely that cleats in the Fruitland formed relatively soon after deposition, possibly as a result of southeastward-directed compression from the Sevier thrust belt to the west. As with the joints in sandstone, the possibility exists that basement fractures or faults had some influence on the orientation of stress in the coals of the Fruitland.

Fracture trends in the subsurface. Determining joint and cleat trends in the subsurface is complex and involves many uncertainties (Grout and Verbeek, 1985; Lorenz, 1995; Verbeek and Grout, 1984). Techniques such as drilling oriented core and pressure tests between nearby wells are of use in limited areas, but cannot usually be extended over a large area. Well log analysis (Johnston and Scholes, 1991; Mullen, 1991) may also be of use in some areas.

Advances in understanding the origin of joints and cleats (Lorenz and others, 1991), however, suggest that joint orientations may be consistent over fairly large areas, so surface studies of joints can be of use in predicting subsurface orientations (Lorenz and Finley, 1991). Cleat domain studies (Kulander and

Dean, 1993; Tremain and others, 1991b) indicated that large areas having similar cleat orientations exist, but that there may be overlap of domains and that domains can change abruptly, depending on local structure.

Even given the uncertainties, it seems likely to me that the largest, oldest joints in sandstones of the Pictured Cliffs and Fruitland in the subsurface of the northern San Juan Basin are oriented north-south and north-northwest to south-southeast. I would expect that face cleats in coal would have a dominantly north-northwest to south-southeast orientation in the subsurface. Within that context, there seem to be a slight clockwise rotation of the joints in sandstone in the Texas Creek and Pine River areas (figs. 2-6 and 2-7).

Summary

1. Joints and cleats in the Pictured Cliffs Sandstone and Fruitland Formation are opening mode fractures.

2. The main joints in the Pictured Cliffs Sandstone are oriented N. 14º W. over the whole project area, and an orthogonal set trends N. 74º E. There appears to be clockwise rotation of the sets from west to east across the study area.

3. The main joints in sandstones of the Fruitland Formation are oriented N. 3º W. on average, and an orthogonal set trends East-West. There is also clockwise rotation of these sets from west to east across the area.

4. Face cleats in all coals of the Fruitland Formation are at an average orientation of N. 21º W.; butt cleats are oriented N. 69º E.

5. The most likely time of jointing of Pictured Cliffs and Fruitland sandstones was during north-south-oriented Laramide deformation when the San Juan Basin rotated clockwise into the Uncompahgre uplift. Joint trends may have been influenced by previously formed zones of weakness in basement rocks.

6. The most likely time of cleat formation was in the Late Cretaceous, probably during or shortly after coalification, and in response to deformation in the Sevier thrust belt.

7. Joint and cleat orientations measured at the outcrop probably extend some distance south into the subsurface. Differences do exist between different studied areas of the outcrop, however, so each area must be considered individually.

REFERENCES CITED

AMOCO, 1994, Pine River Fruitland coal outcrop investigation: Southern Rockies Business Unit, Amoco Production Company, Denver, Colorado, September 15, 1994.

Armstrong, R.L., 1968, Sevier orogenic belt in Nevada and Utah: Geological Society of America Bulletin, v. 79, p. 429-458.

Ayers, W.B., Jr., Ambrose, W.A., and Yeh, Joseph, 1991, Depositional and structural controls on coalbed methane occurrence and resources in the Fruitland Formation, San Juan Basin, *in* Ayers, W. B, Jr., and others, Geologic and hydrologic controls on the occurrence and producibility of coalbed methane, Fruitland Formation, San Juan Basin: Chicago, Gas Research Institute, GRI-91/0072, p. 9-46.

Baars, D.L., and Stevenson, G.M., 1982, Subtle stratigraphic traps in Paleozoic rocks of Paradox Basin, *in* Halbouty, M.T., ed., The deliberate search for the subtle trap: American Association of Petroleum Geologists Memoir 32, p. 131-158.

Barnes, Harley, 1953, Geology of the Ignacio area, Ignacio and Pagosa Springs quadrangles, La Plata and Archuleta Counties, Colorado: U.S. Geological Survey Oil and Gas Investigations Map OM 138, scale 1:63,360.

Close, J.C., 1993, Natural fractures in coal, *in* Law, B.E., and Rice, D.D., eds., Hydrocarbons from coal: American Association of Petroleum Geologists, Studies in Geology No. 38, p. 119-132.

Close, J.C., and Mavor, M.J., 1991, Influence of coal composition and rank on fracture development in Fruitland coal gas reservoirs of San Juan Basin, *in* Schwochow, S.D., ed., Coalbed methane of western North America: Rocky Mountain Association of Geologists, 1991 guidebook, p. 109-121.

Condie, K.C., 1992, Proterozoic terranes and continental accretion in southwestern North America, *in* Condie, K.C., ed., Proterozoic Crustal Evolution: Amsterdam, Elsevier Science Publishers, p. 447-480.

Condon, S.M., 1988, Joint patterns on the northwest side of the San Juan Basin (Southern Ute Reservation), southwest Colorado, *in* Fassett, J.E., ed., Geology and coal-bed methane resources of the northern San Juan Basin, Colorado and New Mexico: Rocky Mountain Association of Geologists Field Conference, 1988, p. 61-68.

Condon, S.M., 1989, Fracture studies on the eastern side of the Southern Ute Reservation, 1988: U.S. Geological Survey Administrative Report BIA-190-II-E, 34 p.

Condon, S.M., 1995, Surface and subsurface geologic studies of the Mormon Seep and adjacent areas, Valencia Canyon, Southern Ute Indian Reservation: U.S. Geological Survey Administrative Report to the Southern Ute Indian Tribe, 31 p.

Coney, P.J., 1978, Mesozoic-Cenozoic Cordilleran plate tectonics, *in* Smith, R.B., and Eaton, G.P., eds., Cenozoic tectonics and regional geophysics of the western Cordillera: Geological Society of America Memoir 152, p. 33-50.

Dickinson, W.R., and Snyder, W.L., 1978, Plate tectonics of the Laramide orogeny: Geological Society of America Memoir 151, p. 355-366.

Fassett, J.E., 1988, Geometry and depositional environment of Fruitland Formation coal beds, San Juan Basin, New Mexico and Colorado, Anatomy of a giant coal-bed methane deposit, *in* Fassett, J.E., ed., Geology and coal-bed methane resources of the northern San Juan Basin, Colorado: Rocky Mountain Association of Geologists Field Conference, 1988, p. 23-38.

Fassett, J.E., and Hinds, J.S., 1971, Geology and fuel resources of the Fruitland Formation and Kirtland Shale of the San Juan Basin, New Mexico and Colorado: U.S.

Geological Survey Professional Paper 676, 76 p.

Gayer, R.A., and Harris, I., eds., 1996, Coalbed methane and coal geology: London, The Geological Society, 344 p.

Gayer, R.A., Pesek, J. Sýkorová, I., and Valterová, P., 1996, Coal clasts in the upper Westphalian sequence of the South Wales coal basin—implications for the timing of maturation and fracture permeability, *in* Gayer, R.A., and Harris, I., eds., Coalbed methane and coal geology: London, The Geological Society, Special Publication No. 109, p. 103-120.

Gries, Robbie, 1983, North-south compression of Rocky Mountain foreland structures, *in* Lowell, J.D., ed., Rocky Mountain foreland basins and uplifts: Rocky Mountain Association of Geologists, 1983 guidebook, p. 9-32.

Grout, M.A., and Verbeek, E.R., 1985, Fracture history of the Plateau Creek and adjacent Colorado River valleys, southern Piceance Basin: Implications for predicting joint patterns at depth: U.S. Geological Survey Open-File Report 85-744, 17 p.

Hamilton, Warren, 1987, Plate-tectonic evolution of the western U.S.A.: Episodes, v. 10, no. 4, p. 271-276.

Heller, P.L., Bowdler, S.S., Chambers, H.P., Coogan, J.C., Hagen, E.S., Shuster, M.W., and Winslow, N.S., 1986, Time of initial thrusting in the Sevier orogenic belt, Idaho-Wyoming and Utah: Geology, v. 14, p. 388-391.

Huffman, A.C., Jr., and Condon, S.M., 1993, Stratigraphy, structure, and paleogeography of Pennsylvanian and Permian rocks, San Juan Basin and adjacent areas, Utah, Colorado, Arizona, and New Mexico: U.S. Geological Survey Bulletin 1808-O, 44 p.

Huffman, A.C., Jr., and Taylor, D.F., 1989, San Juan Basin faulting-more than meets the eye [abs.]: American Association of Petroleum Geologists Bulletin, v. 73, no. 9, p. 1161.

Johnston, D.J. and Scholes, P.L., 1991, Predicting cleats in coal seams from mineral and maceral composition with wireline logs, *in* Schwochow, S.D., ed., Coalbed methane of western North America: Rocky Mountain Association of Geologists, 1991 guidebook, p. 123-136.

Kulander, B.R., Barton, C.C., and Dean, S.L., 1979, The application of fractography to core and outcrop fracture investigations: U.S. Department of Energy, METC/SP-79/3, 174 p.

Kulander, B.R., and Dean, S.L., 1993, Coal-cleat domains and domain boundaries in the Allegheny Plateau of West Virginia: American Association of Petroleum Geologists Bulletin, v. 77, no. 8, p. 1374-1388.

Laubach, S.E., Tremain, C.M., and Baumgardner, R.W., Jr., 1991, Fracture swarms in Upper Cretaceous sandstone and coal, northern San Juan Basin, Colorado: Potential targets for methane exploration, *in* Ayers, W.B., Jr., and others, Geologic and hydrologic controls on the occurrence and producibility of coalbed methane, Fruitland Formation, San Juan Basin: Chicago, Gas Research Institute, GRI-91-0072, p. 119-140.

Law, B.E., 1992, Thermal maturity patterns of Cretaceous and Tertiary rocks, San Juan Basin, Colorado and New Mexico: Geological Society of America Bulletin, v. 104, p. 192-207.

Law, B.E., Hatch, J.R., Kukal, G.C., and Keighin, C.W., 1983, Geologic implications of coal dewatering: American Association of Petroleum Geologists Bulletin, v. 67, no. 12., p. 2255-2260.

Law, B.E., Nuccio, V.F., and Barker, C.E., 1989, Kinky vitrinite reflectance well profiles: evidence of paleopore pressure in low-permeability, gas-bearing sequences in Rocky Mountain foreland basins: American Association of Petroleum Geologists Bulletin, v. 73, no. 8, p. 999-1010.

Law, B.E., and Rice, D.D., eds., 1993, Hydrocarbons from coal: American Association of Petroleum Geologists, Studies in Geology No. 38, 400 p.

Lorenz, J.C., 1985, Tectonic and stress histories of the Piceance Creek Basin and the MWX Site, from 75 million years ago to the present--Preliminary report: Sandia National Laboratories, SAND84-2603; UC-92, 48 p.

Lorenz, J.C., 1995, Predictions of fracture and stress orientations: subsurface Frontier Formation, Green River Basin: Chicago, Gas Research Institute, GRI-95-0151, 96 p.

Lorenz, J.C., and Finley, S.J., 1991, Regional fractures II: fracturing of Mesaverde reservoirs in the Piceance Basin, Colorado: American Association of Petroleum Geologists Bulletin, v. 75, no. 11, p. 1738-1757.

Lorenz, J.C., Teufel, L.W., and Warpinski, N.R., 1991, Regional fractures I: a mechanism for the formation of regional fractures at depth in flat-lying reservoirs: American Association of Petroleum Geologists Bulletin, v. 75, no. 11, p. 1714-1737.

Molenaar, C.M., and Baird, J.K., 1991, Stratigraphic cross sections of Upper Cretaceous rocks in the northern San Juan Basin, Southern Ute Indian Reservation, southwestern Colorado: U.S. Geological Survey Professional Paper 1505-C, p. C1-C12.

Mullen, M.J., 1991, Cleat detection in coalbeds using the microlog, *in* Schwochow, S.D., ed., Coalbed methane of western North America: Rocky Mountain Association of Geologists, 1991 guidebook, p. 137-147.

Pattison, C.I., Fielding, C.R., McWatters, R.H., and Hamilton, L.H., 1996, Nature and origin of fractures in Permian coals from the Bowen Basin, Queensland, Australia, *in* Gayer, R.A., and Harris, I., eds., Coalbed methane and coal geology: London, The Geological Society, Special Publication No. 109, p. 133-150.

Pollard, D.D., and Aydin, Atilla, 1988, Progress in understanding jointing over the past century: Geological Society of America Bulletin, v. 100, p. 1181-1204.

Roberts, L.N.R., and McCabe, P.J., 1992, Peat accumulation in coastal-plain mires: a model for coals of the Fruitland Formation (Upper Cretaceous) of southern Colorado, USA: International Journal of Coal Geology, v. 21, p. 115-138.

Schwochow, S.D., ed., 1991, Coalbed methane of western North America: Rocky Mountain Association of Geologists, guidebook, 1991, 336 p.

Secor, D.T., Jr., 1965, Role of fluid pressure in jointing: American Journal of Science, v. 263, p. 633-646.

Tremain, C.M. and Whitehead, N.H., III, 1990, Natural fracture (cleat and joint) characteristics and patterns in Upper Cretaceous and Tertiary rocks of the San Juan Basin, New Mexico and Colorado, *in* Ayers, W.B., Jr., and others, Geologic evaluation of critical production parameters for coalbed methane resources, part 1, San Juan Basin: Chicago, Gas Research Institute, GRI-90/0014.1, p. 73-98.

Tremain, C.M., Laubach, S.E., and N.H. Whitehead III, 1991a, Coal fracture (cleat) patterns in Upper Cretaceous Fruitland Formation, San Juan Basin, Colorado and New Mexico: Implications for coalbed methane exploration and development, *in* Ayers, W.B., Jr., and others, Geologic and hydrologic controls on the occurrence and producibility of coalbed methane, Fruitland Formation, San Juan Basin: Chicago, Gas Research Institute, GRI-91/0072, p. 97-117.

Tremain, C.M., Laubach, S.E., and N.H. Whitehead III, 1991b, Coal fracture (cleat) patterns in Upper Cretaceous Fruitland Formation, San Juan Basin, Colorado and New Mexico—implications for coalbed methane exploration and development, *in* Schwochow, S.D., ed., Coalbed methane

of western North America: Rocky Mountain Association of Geologists, 1991 guidebook, p. 49-59.

Tweto, O.L., 1975, Laramide (Late Cretaceous-Early Tertiary) orogeny in the Southern Rocky Mountains, *in* Curtis, B.F., ed., Cenozoic history of the Southern Rocky Mountains: Geological Society of America Memoir 144, p. 1-44.

Verbeek, E.R., and Grout, M.A., 1984, Prediction of subsurface fracture patterns from surface studies of joints—an example from the Piceance Creek Basin, Colorado, *in* Spencer, C.W., and Keighin, C.W., eds., Geologic studies in support of the U.S. Department of Energy's Multiwell Experiment: U.S. Geological Survey Open-File Report 84-757, p. 75-86.

Zapp, A.D., 1949, Geology and coal resources of the Durango area, La Plata and Montezuma Counties, Colorado: U.S. Geological Survey Oil and Gas Investigations Preliminary Map 109.

APPENDIX 2-1.

Composite Stratigraphic Section of the Fruitland Formation in the Texas Creek Area (Described by S.M. Condon and R.C. Milici)

Kirtland Shale	**Kk**	**Sandstone and mudstone**	thickness not measured
Leaf beds		**Mudstone**, some slightly silty, carbonaceous, light olive gray to olive gray; with abundant impressions of leaves and other plant fossils, slightly rooted, with muscovite flakes; some beds massive, jointed; with interbeds of silty, yellowish gray to dusky yellow sandstone; irregularly bedded, hackly weathering, with abundant muscovite flakes and finely disseminated carbonaceous material, rooted; 10 feet exposed	
Sandstone		**Sandstone**, very fine grained, clay rich, with interstitial kaolinite(?), limonite, grayish orange to yellowish gray, with rip-up clasts of olive-gray mudstone, impressions of plants; bedding is massive to tabular; three feet measured; minimum thickness estimated to be about 25 feet	
Fruitland Formation			total thickness about 350 feet
Upper part	**Kfu**	**Mudstone,** slightly silty, pale yellowish brown, with finely disseminated carbonaceous material; 8-10 feet thick **Shale**, carbonaceous, medium-dark gray; 2-3 feet thick **Coal,** weathered; 2-3 feet thick **Shale,** carbonaceous, medium dark to dark gray; 1-2 feet thick **Mudstone,** olive gray; 3 feet thick **Sandstone,** very fine grained, and very slightly calcareous siltstone, with finely disseminated carbonaceous material and muscovite flakes; irregularly bedded, beds 6 to 8 inches thick; with septaria of dolomitic limestone up to 2 feet across in upper part; with plant fossils; 5 feet thick **Mudstone,** olive gray, and dark-gray carbonaceous shale, with leaf impressions; 5 feet thick **Sandstone**, very fine grained, argillaceous, very slightly calcareous, with muscovite flakes, finely disseminated carbonaceous material; irregularly bedded, weathers grayish orange; 2 feet thick **Mudstone,** light gray to olive gray; 45 feet thick	
No. 4 sandstone	**Kf4**	**Sandstone,** very fine to fine grained, well sorted, with white interstitial minerals, black accessory minerals, carbonaceous material on bedding surfaces; weathers yellowish gray, grayish yellow; beds generally range from 1 to 10 inches thick; basal bed is about 5 feet thick; some beds with abundant leaf impressions, twigs, sticks; few beds with abundant invertebrate fossils, including gastropods and pelecypods; estimated thickness about 35 feet	

No. 3 sandstone	**Kf3**	**Sandstone**, fine grained, light olive gray, weathers grayish red to dark reddish brown; well sorted, subangular to subrounded; moderately calcareous, argillaceous, with black accessory minerals, feldspathic, with abundant interstitial limonite; contains yellowish-orange septarian concretions; bedding up to 18 inches thick, massive and cross-bedded near base, ripple bedded at top, with some slumped, contorted bedding; minimum thickness about 50 feet
d coal zone	**Kcd**	Occurs at top of No. 2 sandstone; 2-4 feet thick
Skeleton bed		Not mapped separately; occurs between c and d coal zones; outcrops consist of lenticular masses of septarian limestone up to 10 feet long, 2 to 3 feet across, and one or two feet thick; exhibits radial and concentric fracture patterns; septae are filled with white calcite crystals and another dark brown carbonate minerals; limestone consists of light-olive gray dolomitic micrite; weathers dark yellowish orange
c coal zone	**Kcd**	Overlies No. 2 sandstone; 3-4 feet thick
No. 2 sandstone	**Kf2**	**Sandstone,** very fine grained, well sorted, grayish red, with finely disseminated hematite, very slightly calcareous; basal unit cross bedded, with scour base; tightly cemented, with quartz overgrowths; overlain by fine-grained, light-to medium-gray, irregularly bedded sandstone, rippled at base, horizontally laminated at top; bedding up to one foot thick; with woody debris, plant fragments, fossil pelecypods; thickness estimated to be up to 100 feet
ab coal zone	**Kfab**	**Coal**; occurs where No. 1 sandstone thins to a parting and the two coal zones combine into one; thickness, including partings, about 50 feet
b coal zone	**b**	**Coal;** thickness about 20-25 feet
No. 1 sandstone	**Kf1**	**Sandstone,** upper beds are very fine grained, very well sorted, slightly calcareous, well cemented with quartz overgrowths; light brownish gray to light olive gray; bedding about 1 inch to 1 foot thick, some rippled, some burrowed, with clay chips; basal unit consists of 6 inches of irregularly bedded, carbonaceous, argillaceous to silty, fine- to medium-grained sandstone that is overlain by 3 feet of medium-gray mudrock; No. 1 sandstone thins to east; estimated thickness up to 25 feet
a coal zone	**a**	**Coal;** estimated thickness 15-20 feet, including partings
Pictured Cliffs Sandstone	**Kpc**	**Sandstone,** fine grained, very light to light gray, medium to thick bedded, irregularly bedded, with abundant *Ophiomorpha* in upper part; divided into two main units; the lower is massively bedded, the upper is thinner bedded; in general, bedding is uneven and wavy, some is massive or cross bedded; top is marked by grayish-black rooted sandstone; sandstone dikes that are locally several inches thick occur in places in the upper beds of the unit; thickness not measured.

APPENDIX 2-2. ROSE DIAGRAMS AT INDIVIDUAL FRACTURE STATIONS.

Tables 2-7 through 2-11 show a breakdown of which geologic unit each joint or cleat station was recorded in. Rose diagrams of the individual stations are also grouped by geologic unit.

Table 2-7. Joint and cleat stations established in the Basin Creek study area, grouped by geologic unit. Station locations are shown on plate 1.

Kpc	Kft	Kpct	Kflc	Kfls	Kfmc	Kfms	Kfuc	Kfus
BC01	BC03	BC05	BC02	BC11	BC33	BC10	BC15	BC16
BC04		BC08	BC06	BC18		BC12	BC17	BC25
BC21		BC09	BC07	BC23		BC14	BC28	BC26
		BC31	BC13	BC45		BC27	BC30	BC29
		BC46	BC19			BC32	BC35	BC36
			BC20			BC34	BC37	BC38
			BC22			BC44	BC39	BC40
			BC24				BC42	BC41
							BC47	BC43

Kpc - Pictured Cliffs Sandstone, main body; Kft - coal below tongue of Pictured Cliffs; Kpct - tongue of Pictured Cliffs Sandstone; Kflc - coal in lower part of Fruitland Formation; Kfls - sandstone in lower part of Fruitland; Kfmc - coal in middle part of Fruitland Formation; Kfms - sandstone in middle part of Fruitland; Kfuc - coal in upper part of Fruitland; Kfus - sandstone in upper part of Fruitland.

Pictured Cliffs Sandstone, main body:

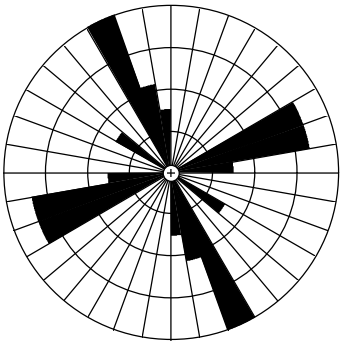

BC01	Statistics
N = 22	Vector Mean = 284.4
Class Interval = 10 degrees	Conf. Angle = 209.12
Maximum Percentage = 31.8	R Magnitude = 0.082
Mean Percentage = 14.29 Standard Deviation = 10.82	Rayleigh = 0.8635

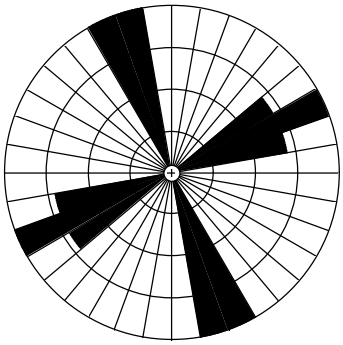

BC04	Statistics
N = 8	Vector Mean = 20.1
Class Interval = 10 degrees	Conf. Angle = 467.20
Maximum Percentage = 25.0	R Magnitude = 0.060
Mean Percentage = 20.00 Standard Deviation = 6.45	Rayleigh = 0.9715

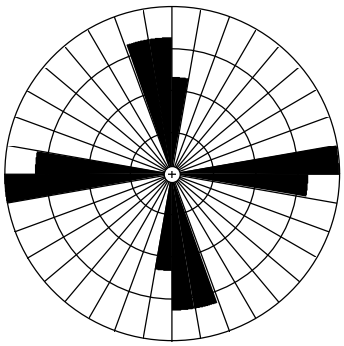

BC21	Statistics
N = 10	Vector Mean = 305.9
Class Interval = 10 degrees	Conf. Angle = 204.93
Maximum Percentage = 30.0	R Magnitude = 0.124
Mean Percentage = 20.00 Standard Deviation = 6.67	Rayleigh = 0.8570

Coal below tongue of Pictured Cliffs Sandstone:

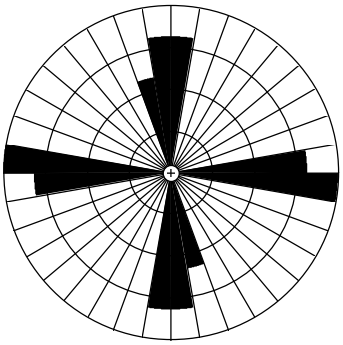

BC03	Statistics
N = 10	Vector Mean = 310.8
Class Interval = 10 degrees	Conf. Angle = 245.84
Maximum Percentage = 30.0	R Magnitude = 0.104
Mean Percentage = 20.00 Standard Deviation = 6.67	Rayleigh = 0.8978

Pictured Cliffs Sandstone, tongue:

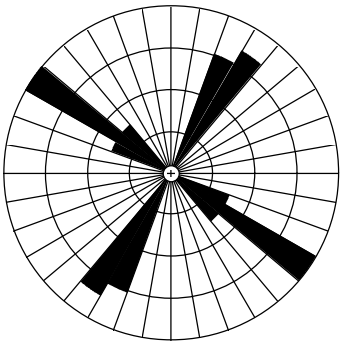

BC05	Statistics
N = 18	Vector Mean = 347.7
Class Interval = 10 degrees	Conf. Angle = 190.38
Maximum Percentage = 38.9	R Magnitude = 0.096
Mean Percentage = 20.00 Standard Deviation = 13.66	Rayleigh = 0.8467

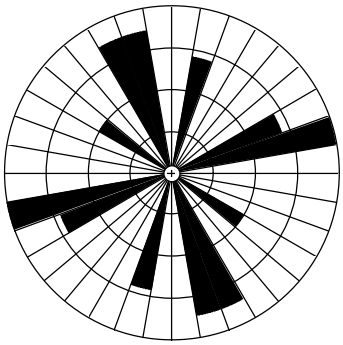

BC08	Statistics
N = 15	Vector Mean = 356.8
Class Interval = 10 degrees	Conf. Angle = 249.31
Maximum Percentage = 26.7	R Magnitude = 0.084
Mean Percentage = 16.67 Standard Deviation = 6.67	Rayleigh = 0.8990

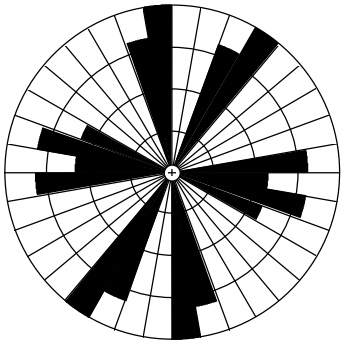

BC09	Statistics
N = 16	Vector Mean = 17.6
Class Interval = 10 degrees	Conf. Angle = 163.84
Maximum Percentage = 18.8	R Magnitude = 0.121
Mean Percentage = 12.50 Standard Deviation = 4.56	Rayleigh = 0.7898

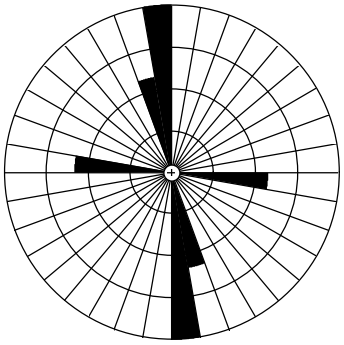

BC31	Statistics
N = 5	Vector Mean = 350.4
Class Interval = 10 degrees	Conf. Angle = 52.68
Maximum Percentage = 60.0	R Magnitude = 0.600
Mean Percentage = 33.33 Standard Deviation = 20.66	Rayleigh = 0.1657

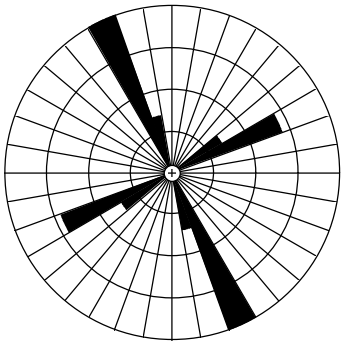

BC46	Statistics
N = 14	Vector Mean = 337.2
Class Interval = 10 degrees	Conf. Angle = 71.98
Maximum Percentage = 57.1	R Magnitude = 0.287
Mean Percentage = 25.00 Standard Deviation = 21.93	Rayleigh = 0.3162

Fruitland Formation, coal in lower part:

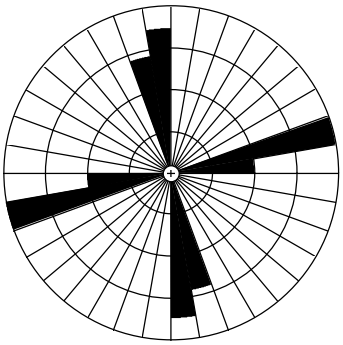

BC02	Statistics
N = 10	Vector Mean = 29.3
Class Interval = 10 degrees	Conf. Angle = 408.19
Maximum Percentage = 40.0	R Magnitude = 0.063
Mean Percentage = 25.00 Standard Deviation = 11.95	Rayleigh = 0.9611

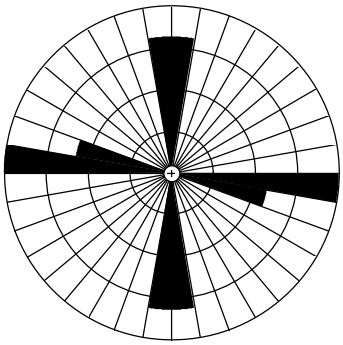

BC06	Statistics
N = 8	Vector Mean = 318.7
Class Interval = 10 degrees	Conf. Angle = 274.82
Maximum Percentage = 37.5	R Magnitude = 0.104
Mean Percentage = 25.00 Standard Deviation = 9.45	Rayleigh = 0.9174

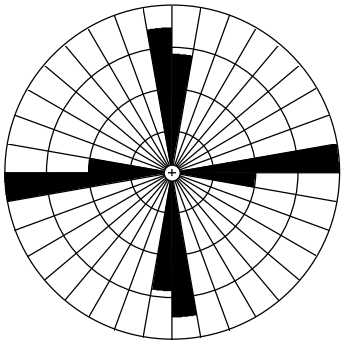

BC07	Statistics
N = 10	Vector Mean = 320.8
Class Interval = 10 degrees	Conf. Angle = INF
Maximum Percentage = 40.0	R Magnitude = 0.004
Mean Percentage = 25.00 Standard Deviation = 11.95	Rayleigh = 0.9999

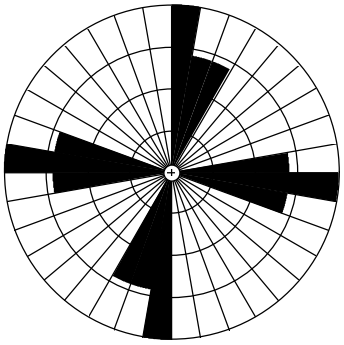

BC13	Statistics
N = 8	Vector Mean = 55.5
Class Interval = 10 degrees	Conf. Angle = 238.12
Maximum Percentage = 25.0	R Magnitude = 0.115
Mean Percentage = 16.67 Standard Deviation = 6.15	Rayleigh = 0.8996

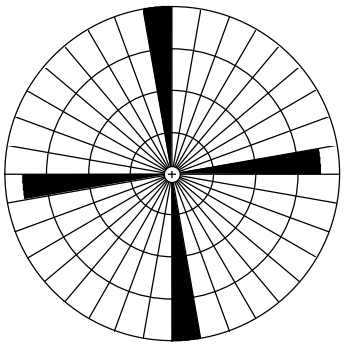

BC19	Statistics
N = 9	Vector Mean = 348.3
Class Interval = 10 degrees	Conf. Angle = 223.28
Maximum Percentage = 55.6	R Magnitude = 0.116
Mean Percentage = 50.00 Standard Deviation = 6.42	Rayleigh = 0.8855

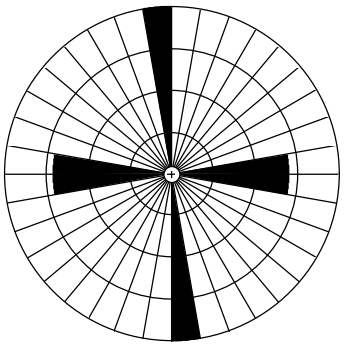

BC20	Statistics
N = 8	Vector Mean = 311.9
Class Interval = 10 degrees	Conf. Angle = 164.73
Maximum Percentage = 50.0	R Magnitude = 0.168
Mean Percentage = 33.33 Standard Deviation = 12.91	Rayleigh = 0.7971

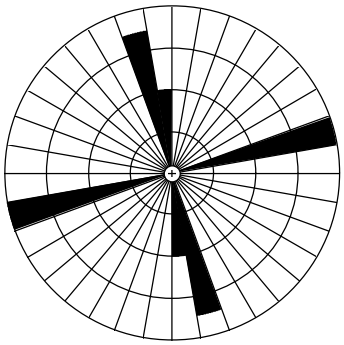

BC22	Statistics
N = 8	Vector Mean = 31.9
Class Interval = 10 degrees	Conf. Angle = 869.10
Maximum Percentage = 50.0	R Magnitude = 0.035
Mean Percentage = 33.33 Standard Deviation = 17.08	Rayleigh = 0.9904

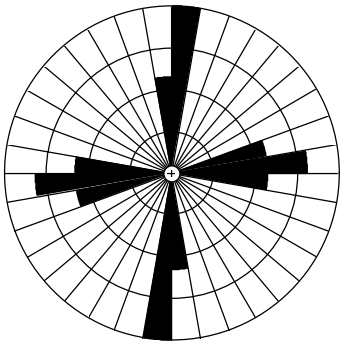

BC24	Statistics
N = 8	Vector Mean = 40.4
Class Interval = 10 degrees	Conf. Angle = 211.97
Maximum Percentage = 37.5	R Magnitude = 0.134
Mean Percentage = 20.00 Standard Deviation = 10.54	Rayleigh = 0.8666

Fruitland Formation, sandstone in lower part:

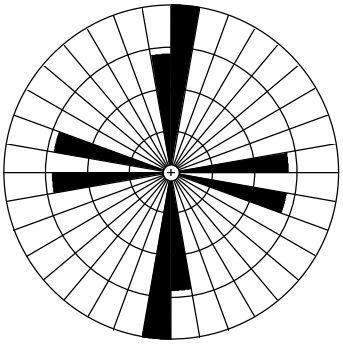

BC11	Statistics
N = 5	Vector Mean = 1.1
Class Interval = 10 degrees	Conf. Angle = 152.70
Maximum Percentage = 40.0	R Magnitude = 0.229
Mean Percentage = 25.00 Standard Deviation = 9.26	Rayleigh = 0.7697

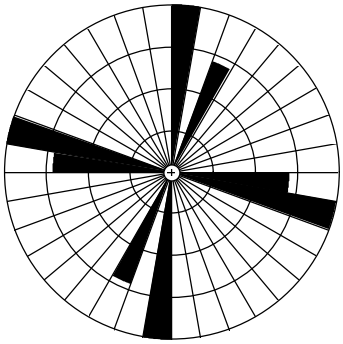

BC18	Statistics
N = 6	Vector Mean = 324.6
Class Interval = 10 degrees	Conf. Angle = 1704.76
Maximum Percentage = 33.3	R Magnitude = 0.018
Mean Percentage = 25.00 Standard Deviation = 8.91	Rayleigh = 0.9980

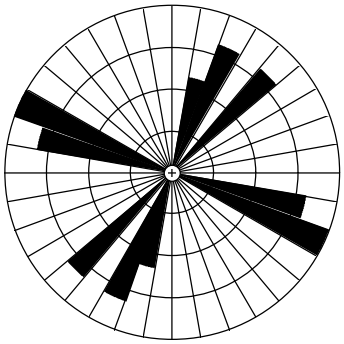

BC23	Statistics
N = 10	Vector Mean = 75.3
Class Interval = 10 degrees	Conf. Angle = 176.46
Maximum Percentage = 30.0	R Magnitude = 0.143
Mean Percentage = 20.00 Standard Deviation = 6.67	Rayleigh = 0.8145

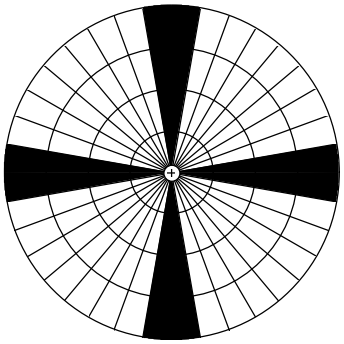

BC45	Statistics
N = 4	Vector Mean = 46.5
Class Interval = 10 degrees	Conf. Angle = 2135.33
Maximum Percentage = 25.0	R Magnitude = 0.017
Mean Percentage = 25.00 Standard Deviation = 0.00	Rayleigh = 0.9988

Fruitland Formation, coal in middle part:

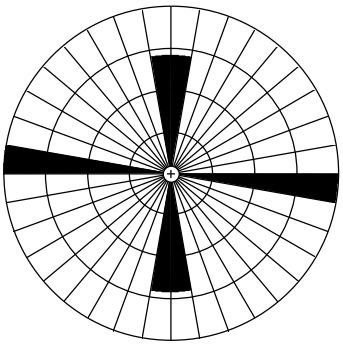

BC33	Statistics
N = 4	Vector Mean = 316.5
Class Interval = 10 degrees	Conf. Angle = 656.04
Maximum Percentage = 50.0	R Magnitude = 0.061
Mean Percentage = 33.33 Standard Deviation = 12.91	Rayleigh = 0.9853

Fruitland Formation , sandstone in middle part:

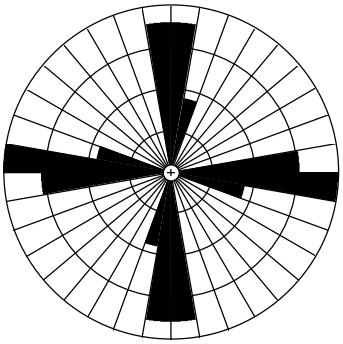

BC10	Statistics
N = 18	Vector Mean = 322.9
Class Interval = 10 degrees	Conf. Angle = 677.61
Maximum Percentage = 27.8	R Magnitude = 0.025
Mean Percentage = 16.67 Standard Deviation = 8.86	Rayleigh = 0.9884

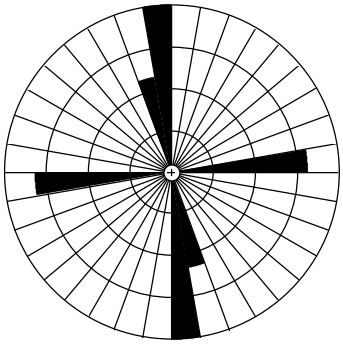

BC12	Statistics
N = 6	Vector Mean = 353.0
Class Interval = 10 degrees	Conf. Angle = 95.99
Maximum Percentage = 50.0	R Magnitude = 0.326
Mean Percentage = 33.33 Standard Deviation = 14.91	Rayleigh = 0.5284

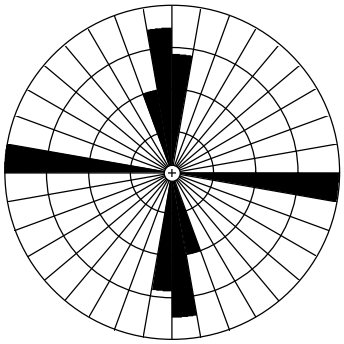

BC14	Statistics
N = 10	Vector Mean = 341.5
Class Interval = 10 degrees	Conf. Angle = 106.76
Maximum Percentage = 40.0	R Magnitude = 0.234
Mean Percentage = 25.00 Standard Deviation = 11.95	Rayleigh = 0.5782

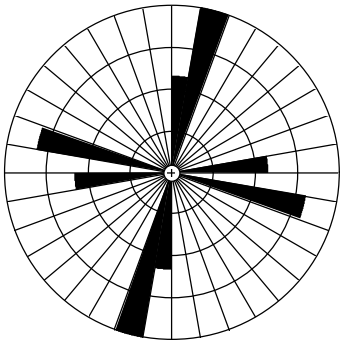

BC27	Statistics
N = 7	Vector Mean = 13.9
Class Interval = 10 degrees	Conf. Angle = 183.79
Maximum Percentage = 42.9	R Magnitude = 0.165
Mean Percentage = 25.00 Standard Deviation = 12.66	Rayleigh = 0.8274

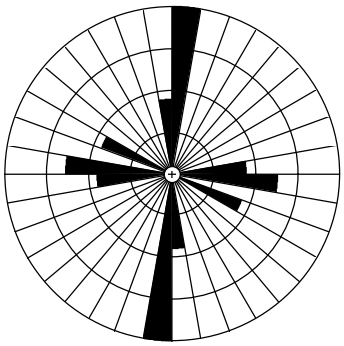

BC32	Statistics
N = 10	Vector Mean = 357.1
Class Interval = 10 degrees	Conf. Angle = 112.90
Maximum Percentage = 50.0	R Magnitude = 0.219
Mean Percentage = 20.00 Standard Deviation = 16.33	Rayleigh = 0.6181

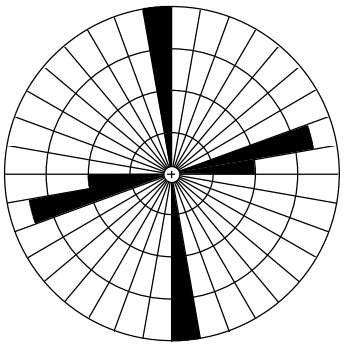

BC34	Statistics
N = 8	Vector Mean = 34.7
Class Interval = 10 degrees	Conf. Angle = 133.24
Maximum Percentage = 50.0	R Magnitude = 0.207
Mean Percentage = 33.33 Standard Deviation = 17.08	Rayleigh = 0.7105

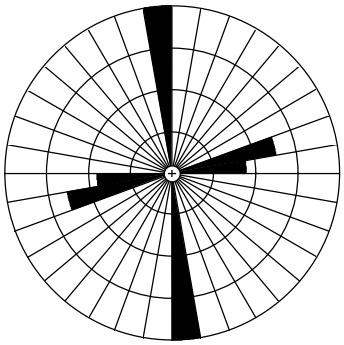

BC44	Statistics
N = 8	Vector Mean = 358.9
Class Interval = 10 degrees	Conf. Angle = 106.78
Maximum Percentage = 62.5	R Magnitude = 0.257
Mean Percentage = 33.33 Standard Deviation = 23.27	Rayleigh = 0.5903

Fruitland Formation, coal in upper part:

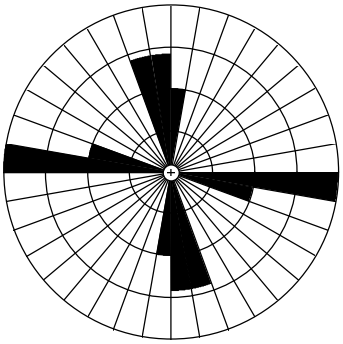

BC15	Statistics
N = 10	Vector Mean = 314.0
Class Interval = 10 degrees	Conf. Angle = 116.93
Maximum Percentage = 40.0	R Magnitude = 0.215
Mean Percentage = 20.00 Standard Deviation = 11.55	Rayleigh = 0.6307

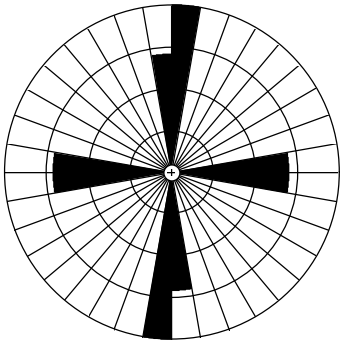

BC17	Statistics
N = 5	Vector Mean = 11.0
Class Interval = 10 degrees	Conf. Angle = 174.47
Maximum Percentage = 40.0	R Magnitude = 0.203
Mean Percentage = 25.00 Standard Deviation = 9.26	Rayleigh = 0.8139

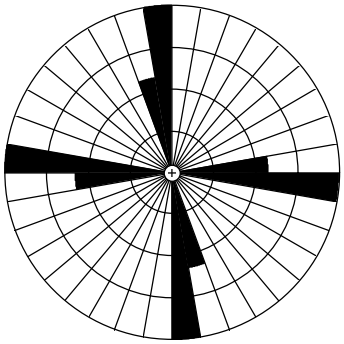

BC28	Statistics
N = 8	Vector Mean = 312.6
Class Interval = 10 degrees	Conf. Angle = 156.24
Maximum Percentage = 37.5	R Magnitude = 0.176
Mean Percentage = 25.00 Standard Deviation = 13.36	Rayleigh = 0.7795

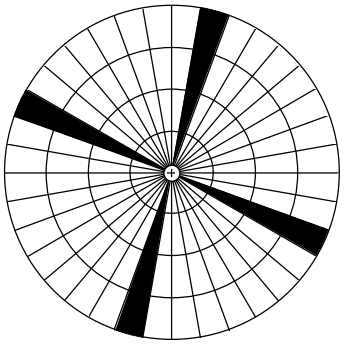

BC30	Statistics
N = 4	Vector Mean = 333.0
Class Interval = 10 degrees	Conf. Angle = 197.02
Maximum Percentage = 50.0	R Magnitude = 0.199
Mean Percentage = 50.00 Standard Deviation = 0.00	Rayleigh = 0.8536

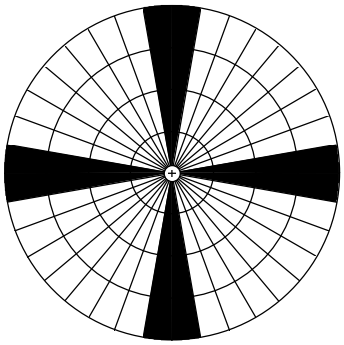

BC35	Statistics
N = 4	Vector Mean = 45.3
Class Interval = 10 degrees	Conf. Angle = 777.03
Maximum Percentage = 25.0	R Magnitude = 0.052
Mean Percentage = 25.00 Standard Deviation = 0.00	Rayleigh = 0.9892

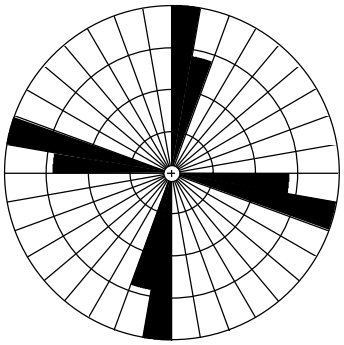

BC37	Statistics
N = 6	Vector Mean = 328.5
Class Interval = 10 degrees	Conf. Angle = 1724.95
Maximum Percentage = 33.3	R Magnitude = 0.018
Mean Percentage = 25.00 Standard Deviation = 8.91	Rayleigh = 0.9981

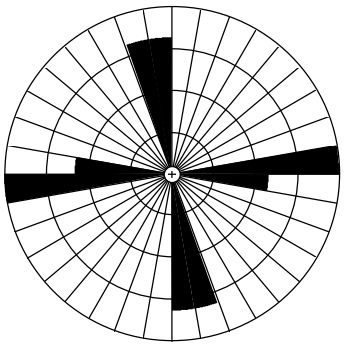

BC39	Statistics
N = 8	Vector Mean = 308.8
Class Interval = 10 degrees	Conf. Angle = 449.98
Maximum Percentage = 37.5	R Magnitude = 0.065
Mean Percentage = 25.00 Standard Deviation = 9.45	Rayleigh = 0.9670

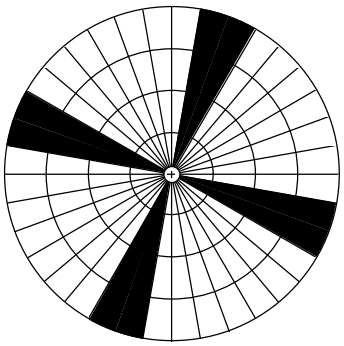

BC42	Statistics
N = 4	Vector Mean = 65.5
Class Interval = 10 degrees	Conf. Angle = 4250.26
Maximum Percentage = 25.0	R Magnitude = 0.009
Mean Percentage = 25.00 Standard Deviation = 0.00	Rayleigh = 0.9997

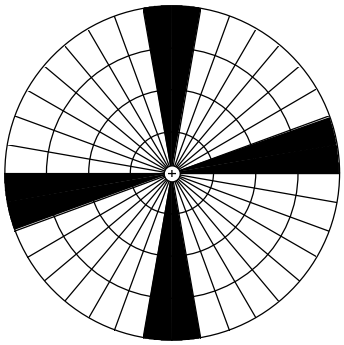

BC47	Statistics
N = 8	Vector Mean = 38.2
Class Interval = 10 degrees	Conf. Angle = 172.30
Maximum Percentage = 25.0	R Magnitude = 0.164
Mean Percentage = 25.00 Standard Deviation = 0.00	Rayleigh = 0.8068

Fruitland Formation, sandstone in upper part:

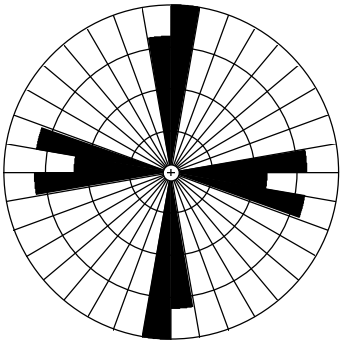

BC16	Statistics
N = 10	Vector Mean = 324.3
Class Interval = 10 degrees	Conf. Angle = 282.51
Maximum Percentage = 30.0	R Magnitude = 0.087
Mean Percentage = 20.00 Standard Deviation = 6.67	Rayleigh = 0.9264

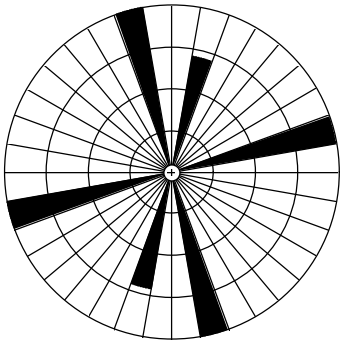

BC25	Statistics
N = 5	Vector Mean = 11.2
Class Interval = 10 degrees	Conf. Angle = 177.79
Maximum Percentage = 40.0	R Magnitude = 0.195
Mean Percentage = 33.33 Standard Deviation = 10.33	Rayleigh = 0.8261

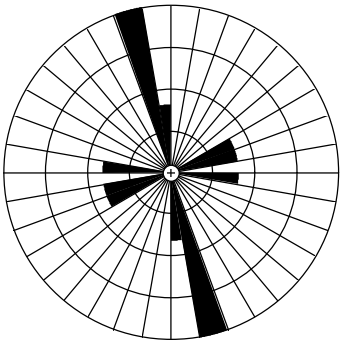

BC26	Statistics
N = 10	Vector Mean = 345.6
Class Interval = 10 degrees	Conf. Angle = 56.95
Maximum Percentage = 60.0	R Magnitude = 0.419
Mean Percentage = 20.00 Standard Deviation = 21.08	Rayleigh = 0.1722

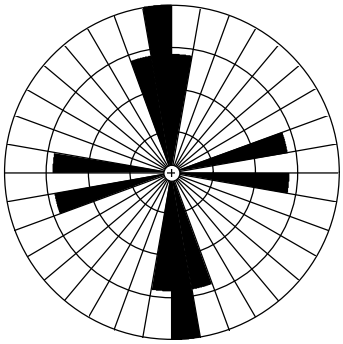

BC29	Statistics
N = 6	Vector Mean = 354.0
Class Interval = 10 degrees	Conf. Angle = 97.85
Maximum Percentage = 33.3	R Magnitude = 0.325
Mean Percentage = 20.00 Standard Deviation = 7.03	Rayleigh = 0.5310

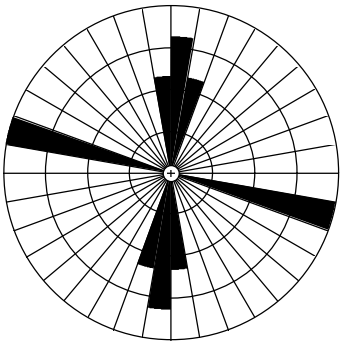

BC36	Statistics
N = 7	Vector Mean = 340.8
Class Interval = 10 degrees	Conf. Angle = 136.03
Maximum Percentage = 42.9	R Magnitude = 0.216
Mean Percentage = 25.00 Standard Deviation = 12.66	Rayleigh = 0.7217

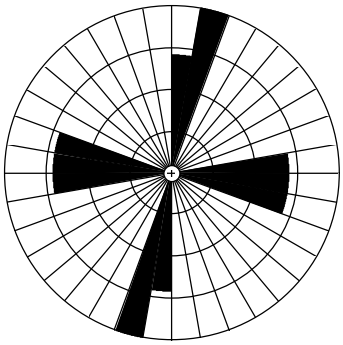

BC38	Statistics
N = 6	Vector Mean = 51.6
Class Interval = 10 degrees	Conf. Angle = 247.96
Maximum Percentage = 33.3	R Magnitude = 0.130
Mean Percentage = 20.00 Standard Deviation = 7.03	Rayleigh = 0.9031

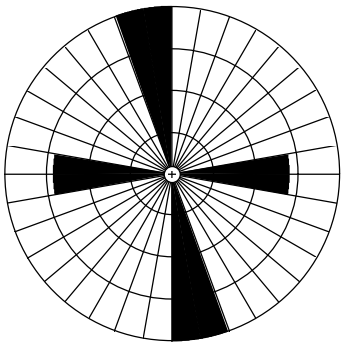

BC40	Statistics
N = 6	Vector Mean = 338.5
Class Interval = 10 degrees	Conf. Angle = 83.97
Maximum Percentage = 33.3	R Magnitude = 0.374
Mean Percentage = 25.00 Standard Deviation = 8.91	Rayleigh = 0.4323

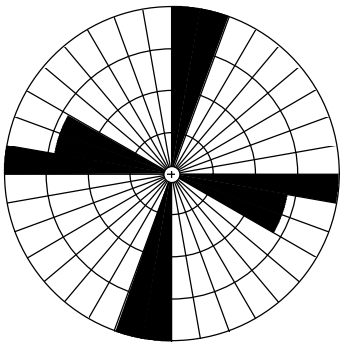

BC41	Statistics
N = 8	Vector Mean = 348.6
Class Interval = 10 degrees	Conf. Angle = 3555.69
Maximum Percentage = 25.0	R Magnitude = 0.006
Mean Percentage = 20.00 Standard Deviation = 6.45	Rayleigh = 0.9997

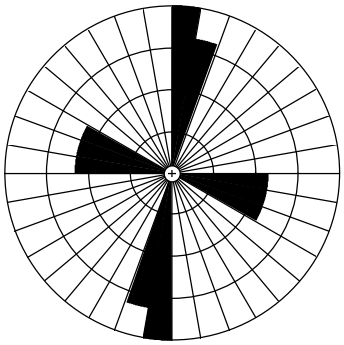

BC43	Statistics
N = 8	Vector Mean = 1.1
Class Interval = 10 degrees	Conf. Angle = 98.55
Maximum Percentage = 37.5	R Magnitude = 0.278
Mean Percentage = 20.00 Standard Deviation = 10.54	Rayleigh = 0.5385

Table 2-8. Joint and cleat stations established in the Carbon Junction study area, grouped by geologic unit. Station locations are shown on plate 2.

Kpc	Kft	Kpct	Kflc	Kfls	Kfmc	Kfms	Kfuc	Kfus
CJ11	CJ02	CJ03	CJ01	CJ14	CJ06	CJ05	CJ07	CJ08
CJ13	CJ26	CJ19	CJ04	CJ20	CJ22	CJ15	CJ09	CJ10
CJ24			CJ12			CJ16	CJ17	CJ23
CJ27			CJ25			CJ18		
						CJ21		

Kpc - Pictured Cliffs Sandstone, main body; Kft - coal below tongue of Pictured Cliffs; Kpct - tongue of Pictured Cliffs Sandstone; Kfcl - coal in lower part of Fruitland Formation; Kfls - sandstone in lower part of Fruitland; Kfmc - coal in middle part of Fruitland Formation; Kfms - sandstone in middle part of Fruitland; Kfuc - coal in upper part of Fruitland; Kfus - sandstone in upper part of Fruitland. Note that stations CJ26 and CJ27 are not shown on the map because they are located in or near the Ewing Mesa gravel pit, outside the map boundary.

Pictured Cliffs Sandstone, main body:

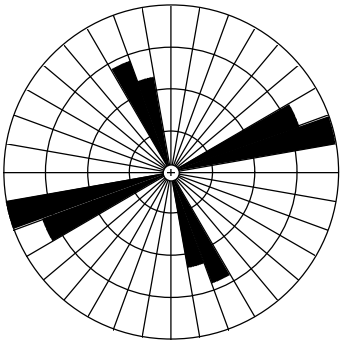

CJ11	Statistics
N = 15	Vector Mean = 72.8
Class Interval = 10 degrees	Conf. Angle = 58.82
Maximum Percentage = 40.0	R Magnitude = 0.336
Mean Percentage = 25.00 Standard Deviation = 10.54	Rayleigh = 0.1842

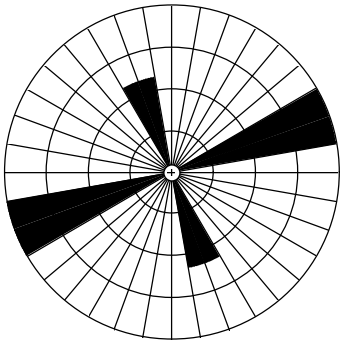

CJ13	Statistics
N = 8	Vector Mean = 72.5
Class Interval = 10 degrees	Conf. Angle = 53.14
Maximum Percentage = 37.5	R Magnitude = 0.495
Mean Percentage = 25.00 Standard Deviation = 13.36	Rayleigh = 0.1411

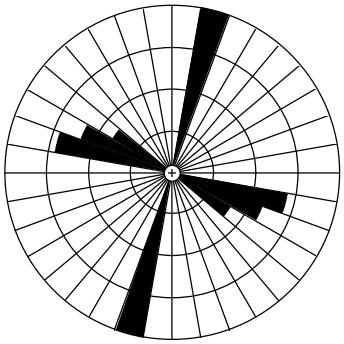

CJ24	Statistics
N = 12	Vector Mean = 337.0
Class Interval = 10 degrees	Conf. Angle = 289.57
Maximum Percentage = 50.0	R Magnitude = 0.078
Mean Percentage = 25.00 Standard Deviation = 16.67	Rayleigh = 0.9294

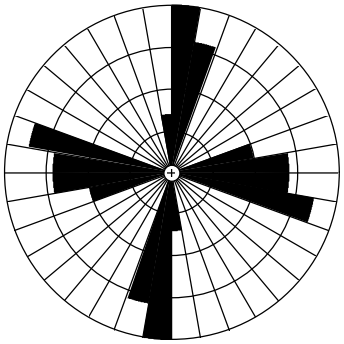

AF11	Statistics
N = 30	Vector Mean = 65.9
Class Interval = 10 degrees	Conf. Angle = 163.20
Maximum Percentage = 26.7	R Magnitude = 0.087
Mean Percentage = 14.29 Standard Deviation = 7.56	Rayleigh = 0.7955

Note: Station AF11 renamed CJ27.

Coal below tongue of Pictured Cliffs Sandstone:

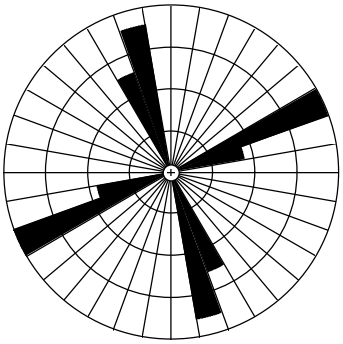

CJ02	Statistics
N = 12	Vector Mean = 24.6
Class Interval = 10 degrees	Conf. Angle = 568.50
Maximum Percentage = 41.7	R Magnitude = 0.041
Mean Percentage = 25.00 Standard Deviation = 14.09	Rayleigh = 0.9804

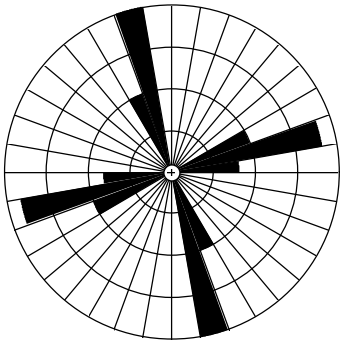

AF09	Statistics
N = 30	Vector Mean = 304.4
Class Interval = 10 degrees	Conf. Angle = 361.60
Maximum Percentage = 40.0	R Magnitude = 0.040
Mean Percentage = 20.00 Standard Deviation = 14.57	Rayleigh = 0.9528

Note: Station AF09 renamed CJ26.

Pictured Cliffs Sandstone, tongue:

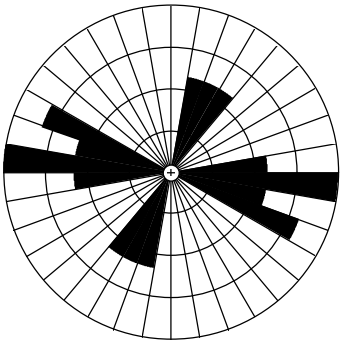

CJ03	Statistics
N = 10	Vector Mean = 89.3
Class Interval = 10 degrees	Conf. Angle = 59.76
Maximum Percentage = 30.0	R Magnitude = 0.404
Mean Percentage = 14.29 Standard Deviation = 7.56	Rayleigh = 0.1955

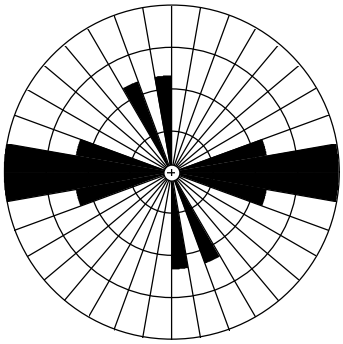

CJ19	Statistics
N = 10	Vector Mean = 272.9
Class Interval = 10 degrees	Conf. Angle = 37.13
Maximum Percentage = 30.0	R Magnitude = 0.604
Mean Percentage = 16.67 Standard Deviation = 9.85	Rayleigh = 0.0261

Fruitland Formation, coal in lower part:

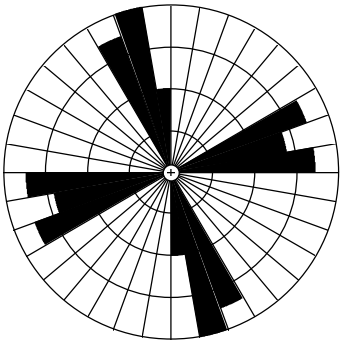

CJ01	Statistics
N = 16	Vector Mean = 316.5
Class Interval = 10 degrees	Conf. Angle = 640.77
Maximum Percentage = 25.0	R Magnitude = 0.032
Mean Percentage = 16.67 Standard Deviation = 6.15	Rayleigh = 0.9838

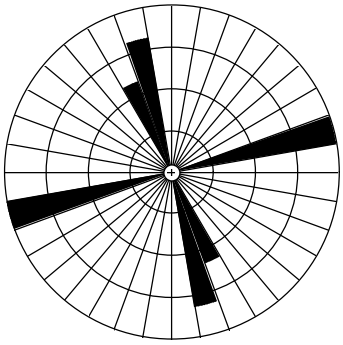

CJ04	Statistics
N = 6	Vector Mean = 284.6
Class Interval = 10 degrees	Conf. Angle = 4013.76
Maximum Percentage = 50.0	R Magnitude = 0.007
Mean Percentage = 33.33 Standard Deviation = 14.91	Rayleigh = 0.9997

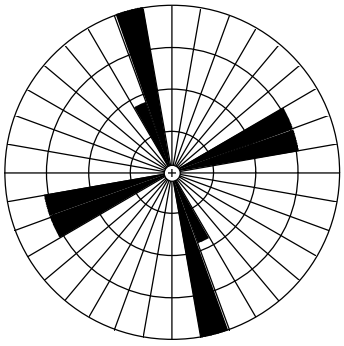

CJ12	Statistics
N = 12	Vector Mean = 23.7
Class Interval = 10 degrees	Conf. Angle = 549.39
Maximum Percentage = 41.7	R Magnitude = 0.043
Mean Percentage = 25.00 Standard Deviation = 12.60	Rayleigh = 0.9776

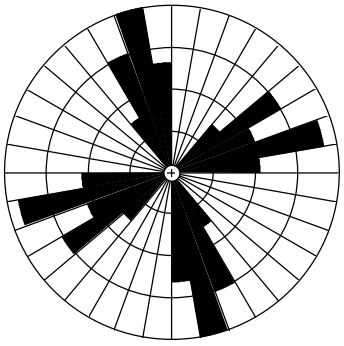

AF07	Statistics
N = 30	Vector Mean = 19.8
Class Interval = 10 degrees	Conf. Angle = 145.95
Maximum Percentage = 23.3	R Magnitude = 0.098
Mean Percentage = 11.11 Standard Deviation = 6.86	Rayleigh = 0.7489

Note: Station AF07 renamed CJ25.

Fruitland Formation, sandstone in lower part:

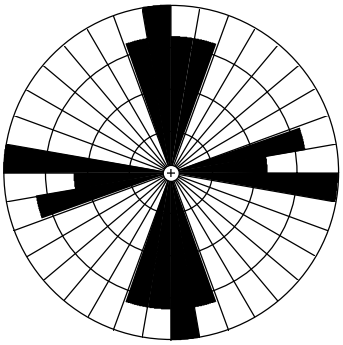

CJ14	Statistics
N = 15	Vector Mean = 3.5
Class Interval = 10 degrees	Conf. Angle = 100.53
Maximum Percentage = 20.0	R Magnitude = 0.204
Mean Percentage = 14.29 Standard Deviation = 4.42	Rayleigh = 0.5365

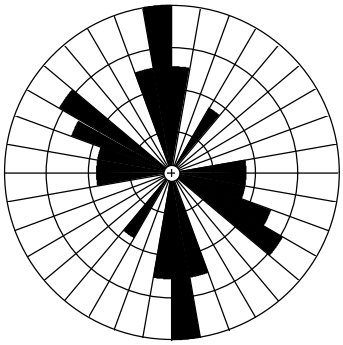

CJ20	Statistics
N = 18	Vector Mean = 332.2
Class Interval = 10 degrees	Conf. Angle = 48.99
Maximum Percentage = 27.8	R Magnitude = 0.366
Mean Percentage = 11.11 Standard Deviation = 7.13	Rayleigh = 0.0895

Fruitland Formation, coal in middle part:

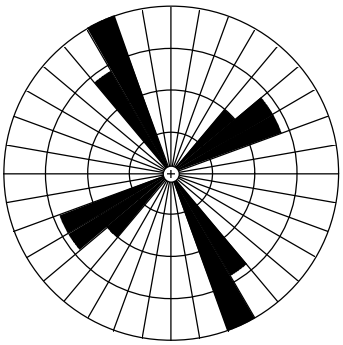

CJ06	Statistics
N = 11	Vector Mean = 341.8
Class Interval = 10 degrees	Conf. Angle = 218.30
Maximum Percentage = 36.4	R Magnitude = 0.109
Mean Percentage = 20.00 Standard Deviation = 9.39	Rayleigh = 0.8781

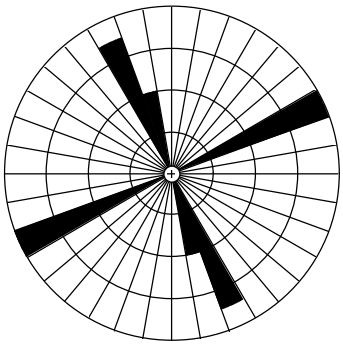

CJ22	Statistics
N = 8	Vector Mean = 21.9
Class Interval = 10 degrees	Conf. Angle = 708.52
Maximum Percentage = 50.0	R Magnitude = 0.039
Mean Percentage = 33.33 Standard Deviation = 17.08	Rayleigh = 0.9878

Fruitland Formation, sandstone in middle part:

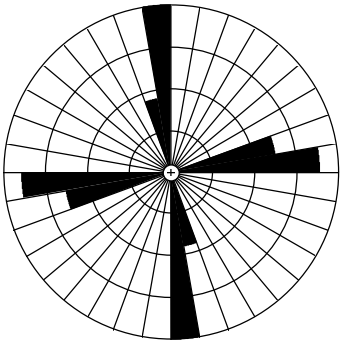

CJ05	Statistics
N = 12	Vector Mean = 29.8
Class Interval = 10 degrees	Conf. Angle = 708.24
Maximum Percentage = 41.7	R Magnitude = 0.035
Mean Percentage = 25.00 Standard Deviation = 14.09	Rayleigh = 0.9855

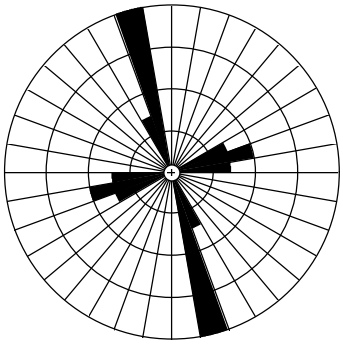

CJ15	Statistics
N = 13	Vector Mean = 343.6
Class Interval = 10 degrees	Conf. Angle = 54.46
Maximum Percentage = 61.5	R Magnitude = 0.386
Mean Percentage = 20.00 Standard Deviation = 22.12	Rayleigh = 0.1446

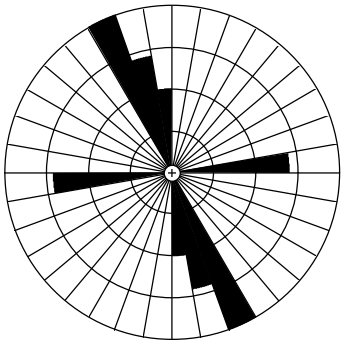

CJ16	Statistics
N = 9	Vector Mean = 335.8
Class Interval = 10 degrees	Conf. Angle = 40.19
Maximum Percentage = 44.4	R Magnitude = 0.588
Mean Percentage = 25.00 Standard Deviation = 12.94	Rayleigh = 0.0445

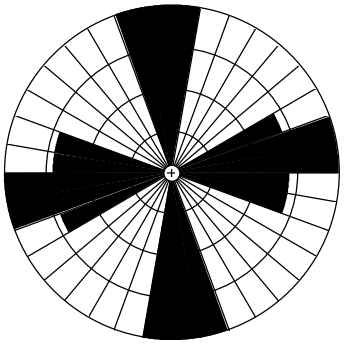

CJ18	Statistics
N = 13	Vector Mean = 77.1
Class Interval = 10 degrees	Conf. Angle = 423.86
Maximum Percentage = 15.4	R Magnitude = 0.054
Mean Percentage = 12.50 Standard Deviation = 3.85	Rayleigh = 0.9629

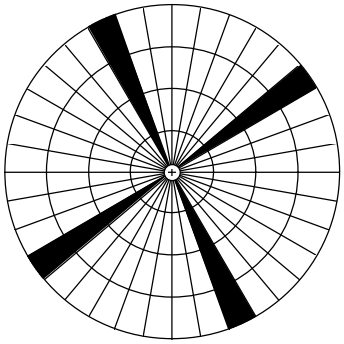

CJ21	Statistics
N = 2	Vector Mean = 16.0
Class Interval = 10 degrees	Conf. Angle = 265.69
Maximum Percentage = 50.0	R Magnitude = 0.208
Mean Percentage = 50.00 Standard Deviation = 0.00	Rayleigh = 0.9172

Fruitland Formation, coal in upper part:

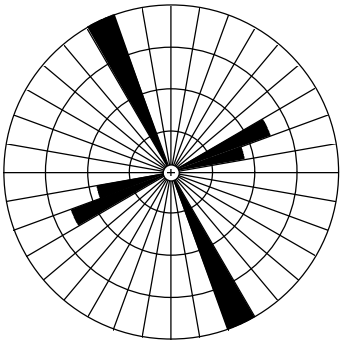

CJ07	Statistics
N = 8	Vector Mean = 333.5
Class Interval = 10 degrees	Conf. Angle = 110.17
Maximum Percentage = 62.5	R Magnitude = 0.251
Mean Percentage = 33.33 Standard Deviation = 23.27	Rayleigh = 0.6030

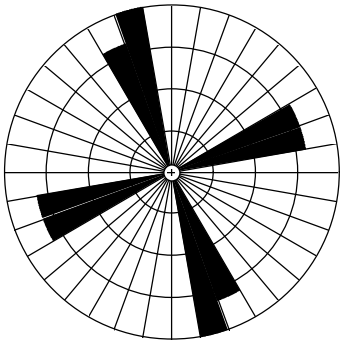

CJ09	Statistics
N = 9	Vector Mean = 343.0
Class Interval = 10 degrees	Conf. Angle = 238.99
Maximum Percentage = 33.3	R Magnitude = 0.111
Mean Percentage = 25.00 Standard Deviation = 5.14	Rayleigh = 0.8953

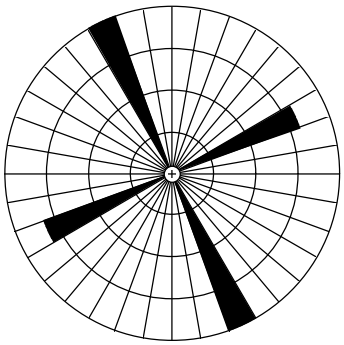

CJ17	Statistics
N = 10	Vector Mean = 342.7
Class Interval = 10 degrees	Conf. Angle = 118.71
Maximum Percentage = 60.0	R Magnitude = 0.208
Mean Percentage = 50.00 Standard Deviation = 11.55	Rayleigh = 0.6480

Fruitland Formation, sandstone in upper part:

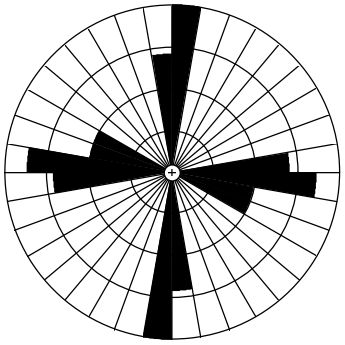

CJ08	Statistics
N = 13	Vector Mean = 295.4
Class Interval = 10 degrees	Conf. Angle = 244.26
Maximum Percentage = 30.8	R Magnitude = 0.090
Mean Percentage = 16.67 Standard Deviation = 8.57	Rayleigh = 0.9001

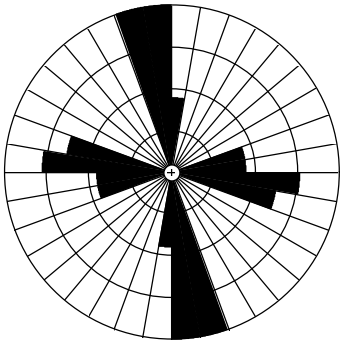

CJ10	Statistics
N = 18	Vector Mean = 335.5
Class Interval = 10 degrees	Conf. Angle = 60.58
Maximum Percentage = 27.8	R Magnitude = 0.303
Mean Percentage = 14.29 Standard Deviation = 9.68	Rayleigh = 0.1907

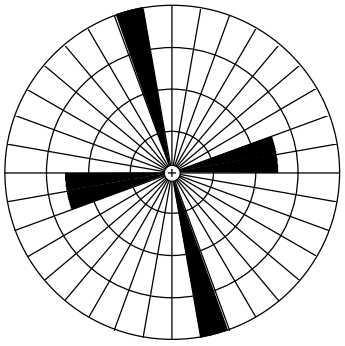

CJ23	Statistics
N = 9	Vector Mean = 334.6
Class Interval = 10 degrees	Conf. Angle = 190.88
Maximum Percentage = 55.6	R Magnitude = 0.136
Mean Percentage = 33.33 Standard Deviation = 17.21	Rayleigh = 0.8467

Table 2-9. Joint and cleat stations established in the Florida River area, grouped by geologic unit. Station locations are shown on plate 4.

Kpc	Kftc	Kfts	Kpct	Kfab	Kf1	Kf2	Kf3c	Kf3s	Kfuc
FR01	FR04	FR30	FR11	FR12	FR10	FR19	FR37	FR20	FR21
FR02	FR06		FR14	FR13	FR17	FR31	FR40	FR23	FR22
FR03	FR09		FR15	FR16		FR35		FR24	
FR05	FR25		FR26	FR18		FR36		FR32	
FR07	FR29		FR33	FR27					
FR08			FR39	FR34					
FR28									
FR38									

Kpc - Pictured Cliffs Sandstone, main body; Kftc - Fruitland Formation, tongue, coal; Kfts - Fruitland Formation, tongue, sandstone; Kpct - Pictured Cliffs Sandstone, tongue; Kfab - Fruitland Formation, lower coal interval; Kf1 - Fruitland Formation sandstone number 1; Kf2 - Fruitland Formation sandstone number 2; Kf3c - Fruitland Formation, coal below sandstone number 3; Kf3s - Fruitland Formation sandstone number 3; Kfuc - Fruitland Formation, upper interval coal.

Pictured Cliffs Sandstone, main body:

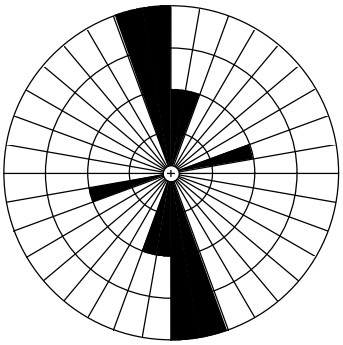

FR01	Statistics
N = 7	Vector Mean = 358.6
Class Interval = 10 degrees	Conf. Angle = 38.29
Maximum Percentage = 28.6	R Magnitude = 0.667
Mean Percentage = 20.00 Standard Deviation = 7.38	Rayleigh = 0.0443

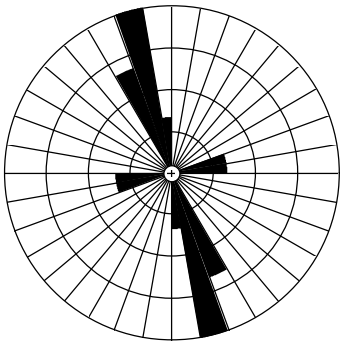

FR02	Statistics
N = 8	Vector Mean = 339.5
Class Interval = 10 degrees	Conf. Angle = 52.12
Maximum Percentage = 37.5	R Magnitude = 0.501
Mean Percentage = 20.00 Standard Deviation = 10.54	Rayleigh = 0.1347

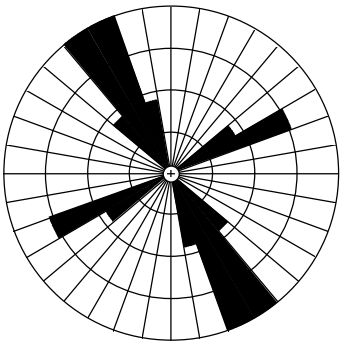

FR03	Statistics
N = 16	Vector Mean = 327.1
Class Interval = 10 degrees	Conf. Angle = 37.92
Maximum Percentage = 31.2	R Magnitude = 0.486
Mean Percentage = 16.67 Standard Deviation = 11.72	Rayleigh = 0.0229

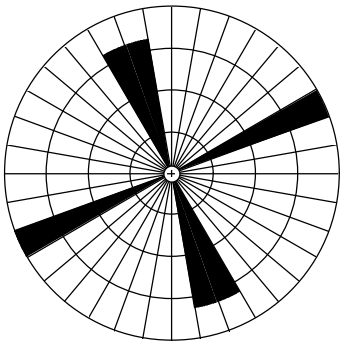

FR05	Statistics
N = 7	Vector Mean = 356.0
Class Interval = 10 degrees	Conf. Angle = 176.14
Maximum Percentage = 42.9	R Magnitude = 0.168
Mean Percentage = 33.33 Standard Deviation = 7.38	Rayleigh = 0.8201

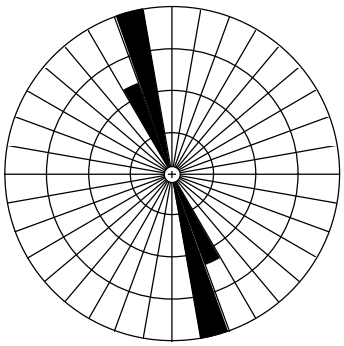

FR07	Statistics
N = 4	Vector Mean = 342.3
Class Interval = 10 degrees	Conf. Angle = 7.97
Maximum Percentage = 75.0	R Magnitude = 0.989
Mean Percentage = 50.00 Standard Deviation = 28.87	Rayleigh = 0.0200

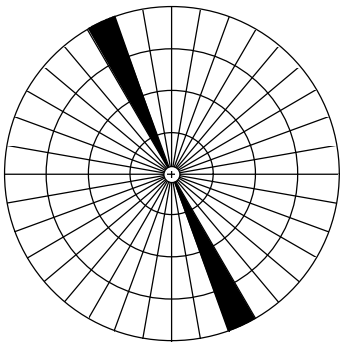

FR08	Statistics
N = 7	Vector Mean = 334.6
Class Interval = 10 degrees	Conf. Angle = 6.00
Maximum Percentage = 100.0	R Magnitude = 0.995
Mean Percentage = 100.00 Standard Deviation = 0.00	Rayleigh = 0.0010

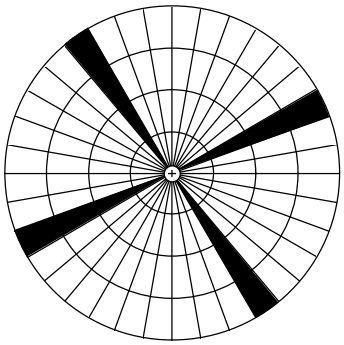

FR28	Statistics
N = 4	Vector Mean = 283.1
Class Interval = 10 degrees	Conf. Angle = 250.28
Maximum Percentage = 50.0	R Magnitude = 0.155
Mean Percentage = 50.00 Standard Deviation = 0.00	Rayleigh = 0.9081

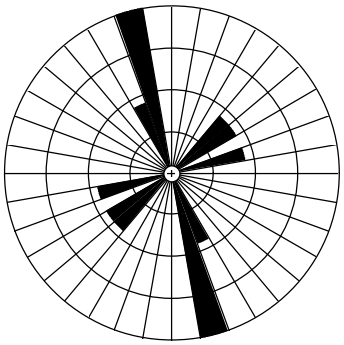

FR38	Statistics
N = 9	Vector Mean = 352.8
Class Interval = 10 degrees	Conf. Angle = 55.56
Maximum Percentage = 55.6	R Magnitude = 0.449
Mean Percentage = 20.00 Standard Deviation = 18.74	Rayleigh = 0.1624

Coal in tongue of Fruitland Formation:

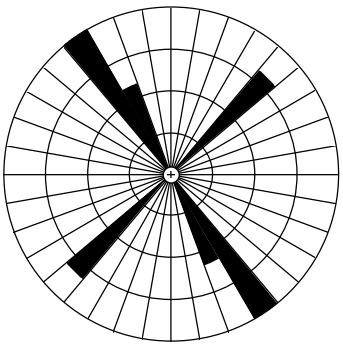

FR04	Statistics
N = 6	Vector Mean = 335.2
Class Interval = 10 degrees	Conf. Angle = 86.59
Maximum Percentage = 50.0	R Magnitude = 0.363
Mean Percentage = 33.33 Standard Deviation = 14.91	Rayleigh = 0.4536

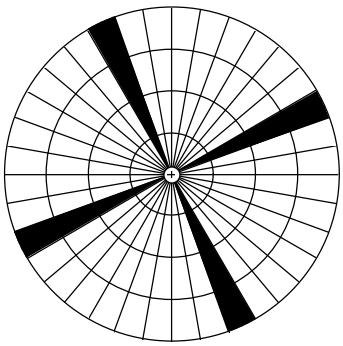

FR06	Statistics
N = 8	Vector Mean = 20.0
Class Interval = 10 degrees	Conf. Angle = 672.25
Maximum Percentage = 50.0	R Magnitude = 0.044
Mean Percentage = 50.00 Standard Deviation = 0.00	Rayleigh = 0.9849

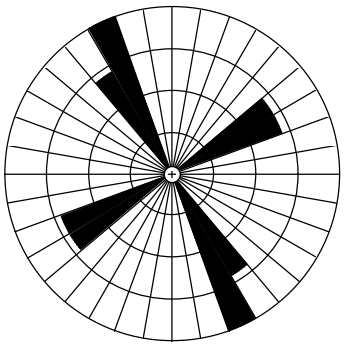

FR09	Statistics
N = 5	Vector Mean = 333.1
Class Interval = 10 degrees	Conf. Angle = 177.59
Maximum Percentage = 40.0	R Magnitude = 0.196
Mean Percentage = 25.00 Standard Deviation = 9.26	Rayleigh = 0.8254

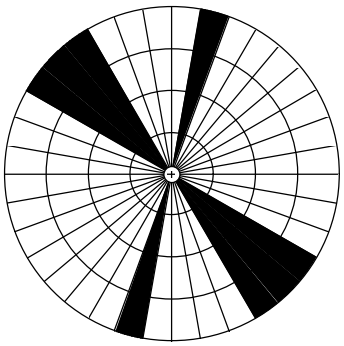

FR25	Statistics
N = 4	Vector Mean = 323.0
Class Interval = 10 degrees	Conf. Angle = 55.12
Maximum Percentage = 25.0	R Magnitude = 0.631
Mean Percentage = 25.00 Standard Deviation = 0.00	Rayleigh = 0.2037

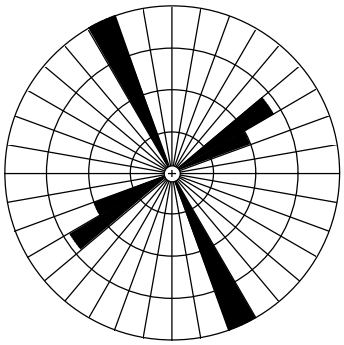

FR29	Statistics
N = 7	Vector Mean = 354.8
Class Interval = 10 degrees	Conf. Angle = 128.27
Maximum Percentage = 57.1	R Magnitude = 0.232
Mean Percentage = 33.33 Standard Deviation = 19.52	Rayleigh = 0.6869

Sandstone in tongue of Fruitland Formation:

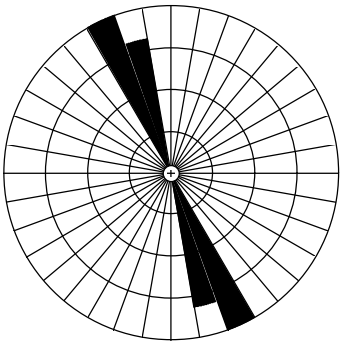

FR30	Statistics
N = 5	Vector Mean = 339.6
Class Interval = 10 degrees	Conf. Angle = 7.13
Maximum Percentage = 60.0	R Magnitude = 0.987
Mean Percentage = 50.00 Standard Deviation = 11.55	Rayleigh = 0.0076

Pictured Cliffs Sandstone, tongue:

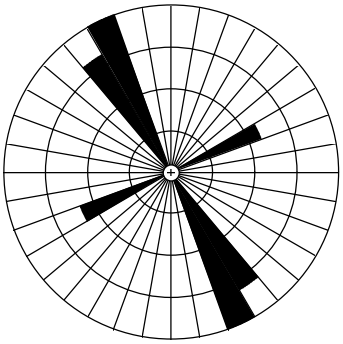

FR11	Statistics
N = 6	Vector Mean = 328.3
Class Interval = 10 degrees	Conf. Angle = 42.21
Maximum Percentage = 50.0	R Magnitude = 0.659
Mean Percentage = 33.33 Standard Deviation = 14.91	Rayleigh = 0.0737

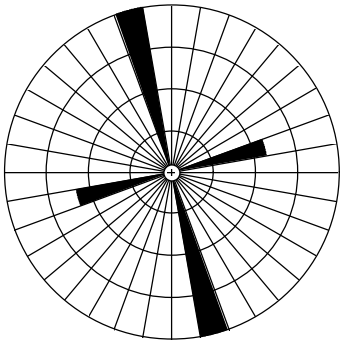

FR14	Statistics
N = 4	Vector Mean = 343.5
Class Interval = 10 degrees	Conf. Angle = 73.80
Maximum Percentage = 75.0	R Magnitude = 0.499
Mean Percentage = 50.00 Standard Deviation = 28.87	Rayleigh = 0.3689

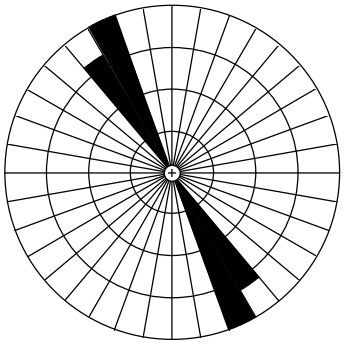

FR15	Statistics
N = 5	Vector Mean = 331.2
Class Interval = 10 degrees	Conf. Angle = 10.12
Maximum Percentage = 60.0	R Magnitude = 0.975
Mean Percentage = 50.00 Standard Deviation = 11.55	Rayleigh = 0.0086

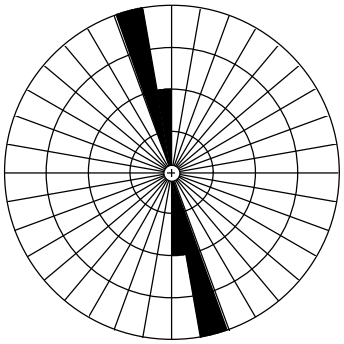

FR26	Statistics
N = 5	Vector Mean = 348.4
Class Interval = 10 degrees	Conf. Angle = 10.08
Maximum Percentage = 80.0	R Magnitude = 0.983
Mean Percentage = 50.00 Standard Deviation = 34.64	Rayleigh = 0.0080

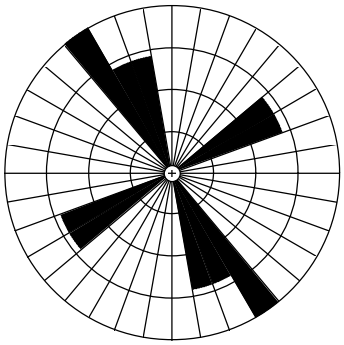

FR33	Statistics
N = 6	Vector Mean = 332.8
Class Interval = 10 degrees	Conf. Angle = 102.02
Maximum Percentage = 33.3	R Magnitude = 0.310
Mean Percentage = 20.00 Standard Deviation = 7.03	Rayleigh = 0.5628

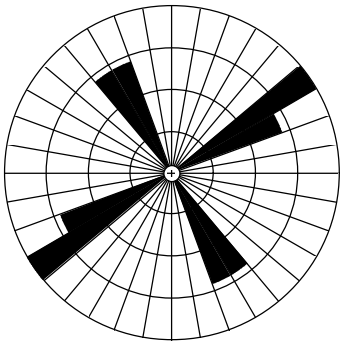

FR39	Statistics
N = 5	Vector Mean = 63.9
Class Interval = 10 degrees	Conf. Angle = 177.29
Maximum Percentage = 40.0	R Magnitude = 0.197
Mean Percentage = 25.00 Standard Deviation = 9.26	Rayleigh = 0.8244

Fruitland Formation, lower coal interval:

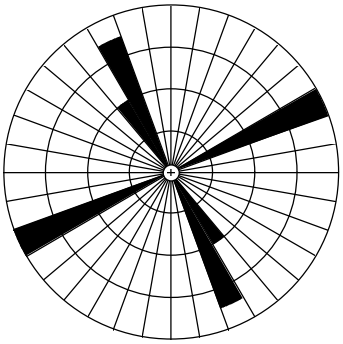

FR12	Statistics
N = 8	Vector Mean = 285.8
Class Interval = 10 degrees	Conf. Angle = 2459.00
Maximum Percentage = 50.0	R Magnitude = 0.013
Mean Percentage = 33.33 Standard Deviation = 17.08	Rayleigh = 0.9986

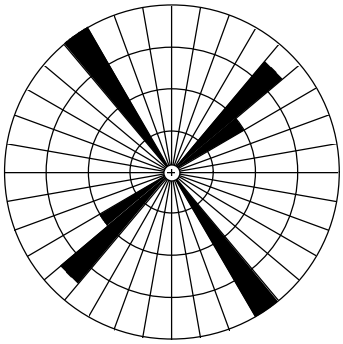

FR13	Statistics
N = 8	Vector Mean = 5.4
Class Interval = 10 degrees	Conf. Angle = 280.71
Maximum Percentage = 50.0	R Magnitude = 0.100
Mean Percentage = 33.33 Standard Deviation = 17.08	Rayleigh = 0.9238

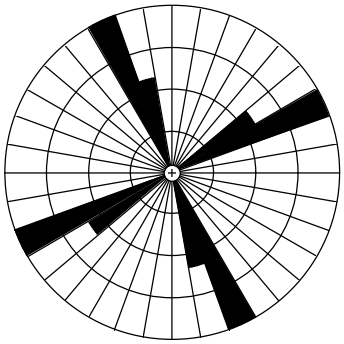

FR16	Statistics
N = 8	Vector Mean = 19.9
Class Interval = 10 degrees	Conf. Angle = 280.16
Maximum Percentage = 37.5	R Magnitude = 0.100
Mean Percentage = 25.00 Standard Deviation = 13.36	Rayleigh = 0.9232

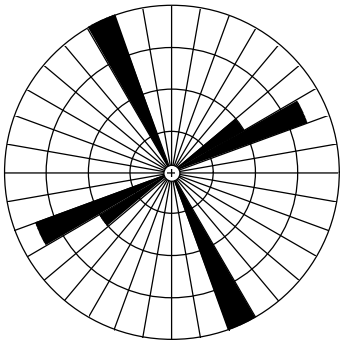

FR18	Statistics
N = 8	Vector Mean = 18.0
Class Interval = 10 degrees	Conf. Angle = 672.99
Maximum Percentage = 50.0	R Magnitude = 0.043
Mean Percentage = 33.33 Standard Deviation = 17.08	Rayleigh = 0.9850

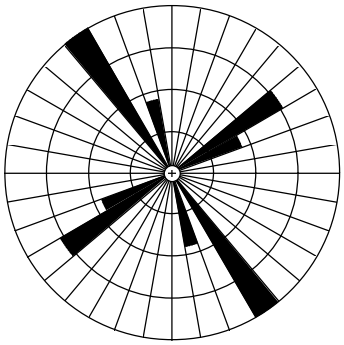

FR27	Statistics
N = 10	Vector Mean = 329.9
Class Interval = 10 degrees	Conf. Angle = 129.48
Maximum Percentage = 50.0	R Magnitude = 0.194
Mean Percentage = 25.00 Standard Deviation = 17.73	Rayleigh = 0.6855

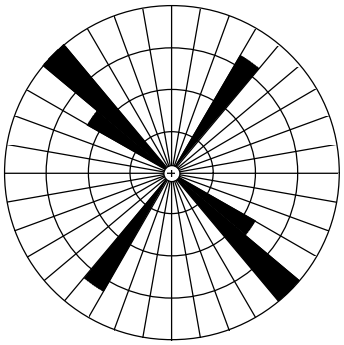

FR34	Statistics
N = 6	Vector Mean = 317.1
Class Interval = 10 degrees	Conf. Angle = 89.42
Maximum Percentage = 50.0	R Magnitude = 0.352
Mean Percentage = 33.33 Standard Deviation = 14.91	Rayleigh = 0.4764

Fruitland Formation, sandstone No. 1:

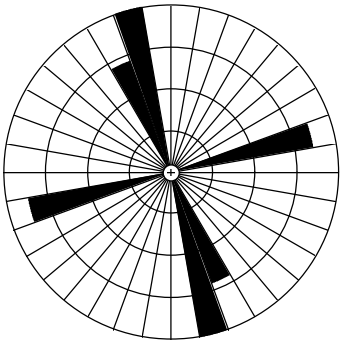

FR10		Statistics
N = 9		Vector Mean = 340.7
Class Interval = 10 degrees		Conf. Angle = 77.85
Maximum Percentage = 44.4		R Magnitude = 0.330
Mean Percentage = 33.33	Standard Deviation = 9.94	Rayleigh = 0.3743

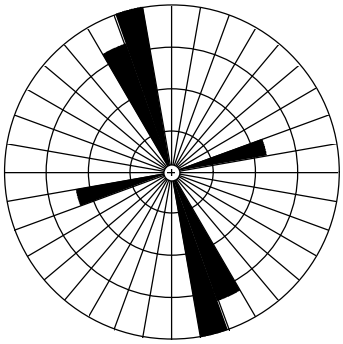

FR17		Statistics
N = 6		Vector Mean = 338.8
Class Interval = 10 degrees		Conf. Angle = 41.31
Maximum Percentage = 50.0		R Magnitude = 0.669
Mean Percentage = 33.33	Standard Deviation = 14.91	Rayleigh = 0.0683

Fruitland Formation, sandstone No. 2:

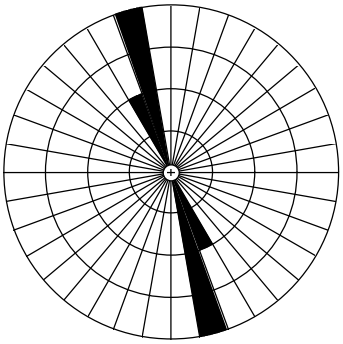

FR19		Statistics
N = 5		Vector Mean = 342.6
Class Interval = 10 degrees		Conf. Angle = 7.11
Maximum Percentage = 80.0		R Magnitude = 0.993
Mean Percentage = 50.00	Standard Deviation = 34.64	Rayleigh = 0.0072

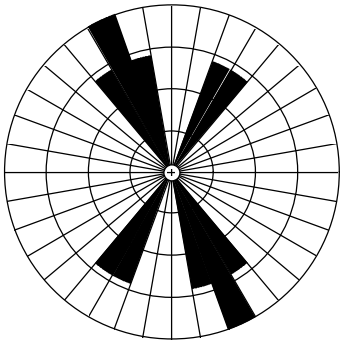

FR31		Statistics
N = 6		Vector Mean = 350.1
Class Interval = 10 degrees		Conf. Angle = 42.17
Maximum Percentage = 33.3		R Magnitude = 0.660
Mean Percentage = 20.00	Standard Deviation = 7.03	Rayleigh = 0.0730

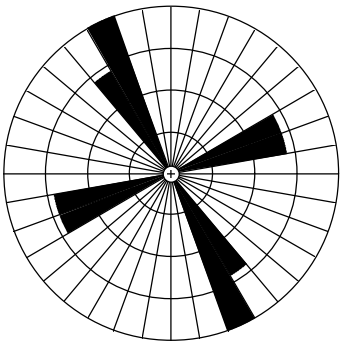

FR35		Statistics
N = 5		Vector Mean = 323.0
Class Interval = 10 degrees		Conf. Angle = 159.51
Maximum Percentage = 40.0		R Magnitude = 0.220
Mean Percentage = 25.00	Standard Deviation = 9.26	Rayleigh = 0.7855

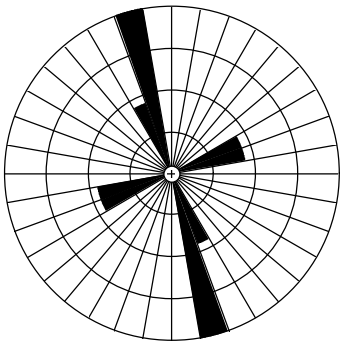

FR36		Statistics
N = 8		Vector Mean = 344.9
Class Interval = 10 degrees		Conf. Angle = 51.14
Maximum Percentage = 62.5		R Magnitude = 0.506
Mean Percentage = 25.00	Standard Deviation = 23.15	Rayleigh = 0.1288

Fruitland Formation, coal below sandstone No. 3:

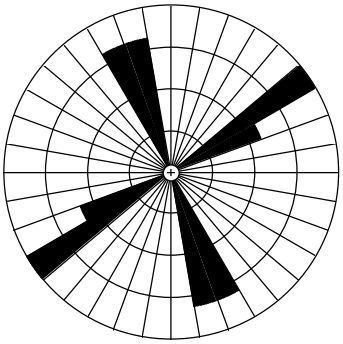

FR37	Statistics
N = 8	Vector Mean = 15.2
Class Interval = 10 degrees	Conf. Angle = 116.20
Maximum Percentage = 37.5	R Magnitude = 0.236
Mean Percentage = 25.00 Standard Deviation = 9.45	Rayleigh = 0.6402

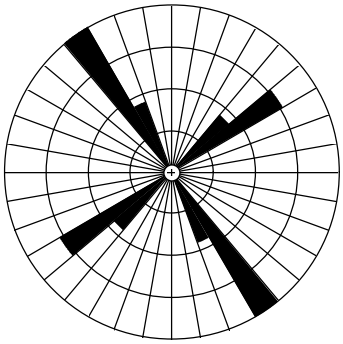

FR40	Statistics
N = 10	Vector Mean = 337.6
Class Interval = 10 degrees	Conf. Angle = 112.62
Maximum Percentage = 50.0	R Magnitude = 0.220
Mean Percentage = 25.00 Standard Deviation = 17.73	Rayleigh = 0.6152

Fruitland Formation, sandstone No. 3:

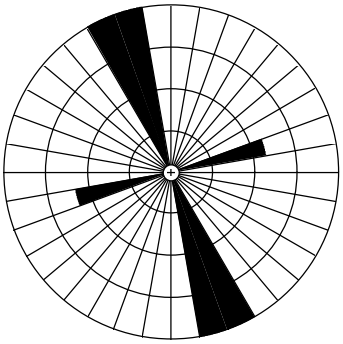

FR20	Statistics
N = 7	Vector Mean = 340.4
Class Interval = 10 degrees	Conf. Angle = 34.92
Maximum Percentage = 42.9	R Magnitude = 0.711
Mean Percentage = 33.33 Standard Deviation = 14.75	Rayleigh = 0.0289

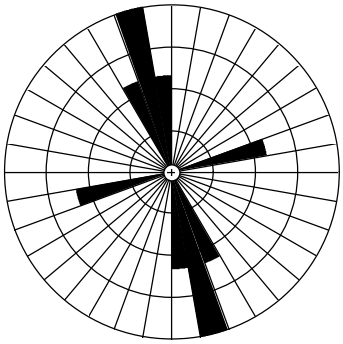

FR23	Statistics
N = 6	Vector Mean = 343.5
Class Interval = 10 degrees	Conf. Angle = 42.97
Maximum Percentage = 50.0	R Magnitude = 0.654
Mean Percentage = 25.00 Standard Deviation = 15.43	Rayleigh = 0.0765

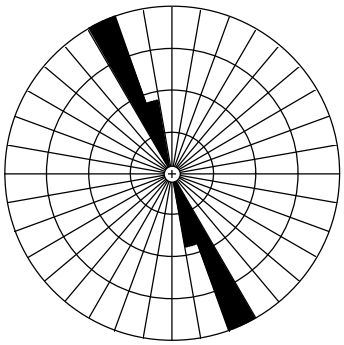

FR24	Statistics
N = 6	Vector Mean = 335.3
Class Interval = 10 degrees	Conf. Angle = 6.51
Maximum Percentage = 83.3	R Magnitude = 0.988
Mean Percentage = 50.00 Standard Deviation = 38.49	Rayleigh = 0.0029

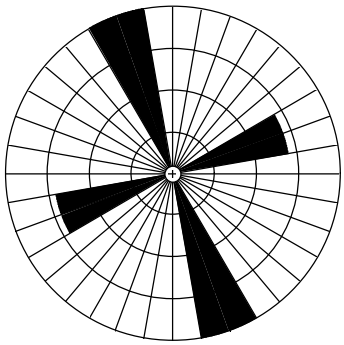

FR32	Statistics
N = 6	Vector Mean = 338.5
Class Interval = 10 degrees	Conf. Angle = 95.29
Maximum Percentage = 33.3	R Magnitude = 0.331
Mean Percentage = 25.00 Standard Deviation = 8.91	Rayleigh = 0.5185

Fruitland Formation, upper interval coal:

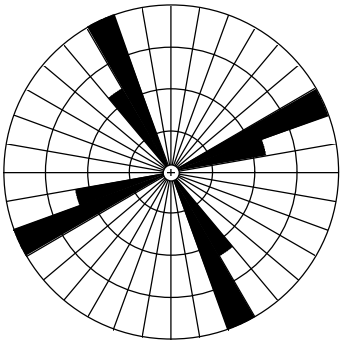

FR21	Statistics
N = 8	Vector Mean = 291.1
Class Interval = 10 degrees	Conf. Angle = 465.11
Maximum Percentage = 37.5	R Magnitude = 0.061
Mean Percentage = 25.00 Standard Deviation = 13.36	Rayleigh = 0.9710

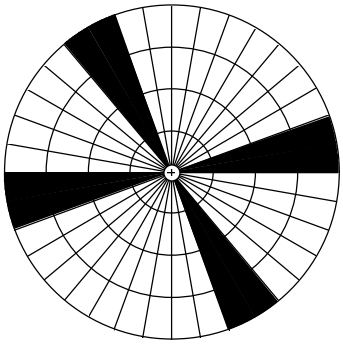

FR22	Statistics
N = 8	Vector Mean = 294.9
Class Interval = 10 degrees	Conf. Angle = 73.10
Maximum Percentage = 25.0	R Magnitude = 0.370
Mean Percentage = 25.00 Standard Deviation = 0.00	Rayleigh = 0.3344

Table 2-10. Joint and cleat stations established in the South Fork of Texas Creek area, grouped by geologic unit. Stations marked with an asterisk (*) provided data from more than one geologic unit. No orientations were recorded at stations TA06, TA07, TA09, and TB06. Station locations are shown on plate 6.

Kpc	a coal	Kf1	b coal	Kf2	c coal	Kf3	Kf4	Kfu	Kirtland Shale
TA04*	TA01	TC03*	TA11	TA03	TC06*	TA08	TC07	TB07	TB03
TA05	TA02		TC03*	TD02*	TD04	TB01	TD05	TB08	TC08
TA10	TA04*			TF03	TE04	TC05	TE05	TE07	TD07
TB02	TB04*			TG02	TE06	TC06*			
TB04*	TB05*			TI01	TF04	TD06			
TB05*	TC01			TJ01	TJ03	TI02			
TC02	TD02*								
TC03*	TD03								
TC04	TE02								
TD01	TF02								
TD02*	TG01								
TE01	TJ02								
TE03									
TF01									
TH01									

Kpc - Pictured Cliffs Sandstone; Kf1 - Fruitland Formation sandstone number 1; Kf2 - Fruitland Formation sandstone number 2; Kf3 - Fruitland Formation sandstone number 3; Kf4 - Fruitland Formation sandstone number 4; Kfu - Fruitland Formation, upper part; Kk - Kirtland Shale

Pictured Cliffs Sandstone:

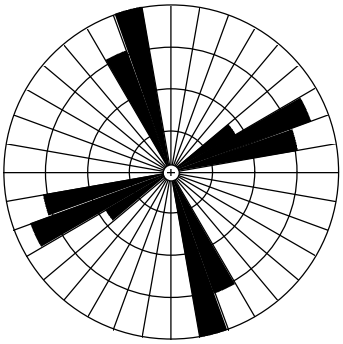

TA04 JOINTS		Statistics
N = 16		Vector Mean = 14.0
Class Interval = 10 degrees		Conf. Angle = 669.37
Maximum Percentage = 31.2		R Magnitude = 0.029
Mean Percentage = 20.00	Standard Deviation = 8.74	Rayleigh = 0.9864

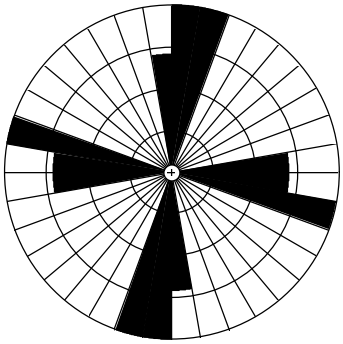

TA05 JOINTS		Statistics
N = 9		Vector Mean = 17.2
Class Interval = 10 degrees		Conf. Angle = 238.44
Maximum Percentage = 22.2		R Magnitude = 0.111
Mean Percentage = 16.67	Standard Deviation = 5.80	Rayleigh = 0.8944

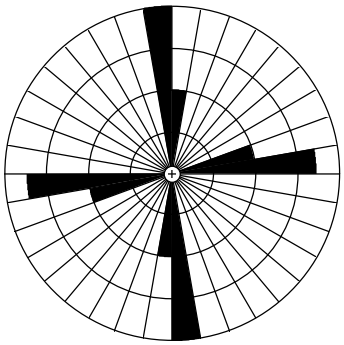

TA10 JOINTS		Statistics
N = 9		Vector Mean = 17.2
Class Interval = 10 degrees		Conf. Angle = 155.33
Maximum Percentage = 44.4		R Magnitude = 0.168
Mean Percentage = 25.00	Standard Deviation = 15.43	Rayleigh = 0.7749

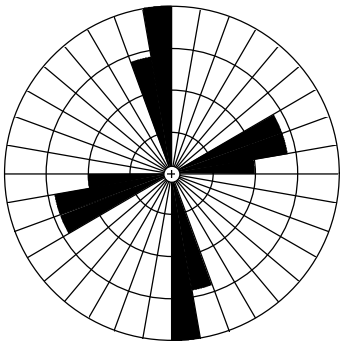

TB02 JOINTS		Statistics
N = 11		Vector Mean = 14.7
Class Interval = 10 degrees		Conf. Angle = 131.59
Maximum Percentage = 36.4		R Magnitude = 0.181
Mean Percentage = 20.00	Standard Deviation = 9.39	Rayleigh = 0.6977

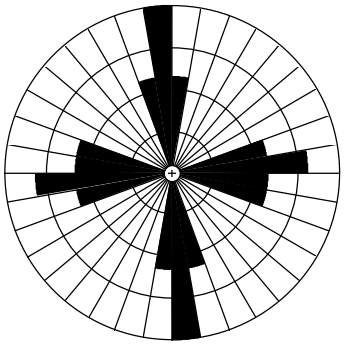

TB04 JOINTS		Statistics
N = 10		Vector Mean = 322.0
Class Interval = 10 degrees		Conf. Angle = 485.95
Maximum Percentage = 30.0		R Magnitude = 0.053
Mean Percentage = 14.29	Standard Deviation = 7.56	Rayleigh = 0.9720

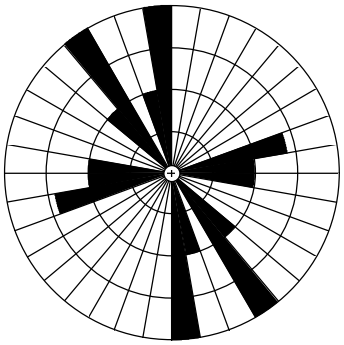

TB05 JOINTS		Statistics
N = 14		Vector Mean = 329.4
Class Interval = 10 degrees		Conf. Angle = 54.95
Maximum Percentage = 28.6		R Magnitude = 0.374
Mean Percentage = 14.29	Standard Deviation = 9.71	Rayleigh = 0.1408

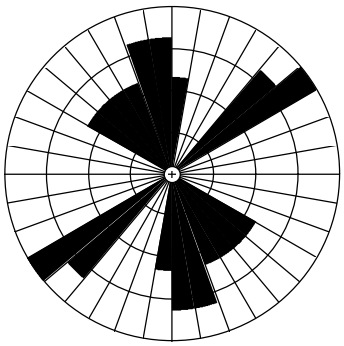

TC02 JOINTS		Statistics
N = 14		Vector Mean = 356.9
Class Interval = 10 degrees		Conf. Angle = 66.47
Maximum Percentage = 21.4		R Magnitude = 0.312
Mean Percentage = 11.11	Standard Deviation = 5.03	Rayleigh = 0.2549

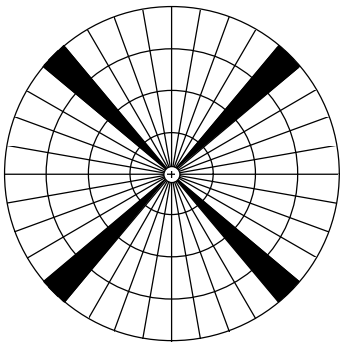

TC03 JOINTS (Kpc)		Statistics
N = 2		Vector Mean = 357.5
Class Interval = 10 degrees		Conf. Angle = 632.71
Maximum Percentage = 50.0		R Magnitude = 0.087
Mean Percentage = 50.00	Standard Deviation = 0.00	Rayleigh = 0.9849

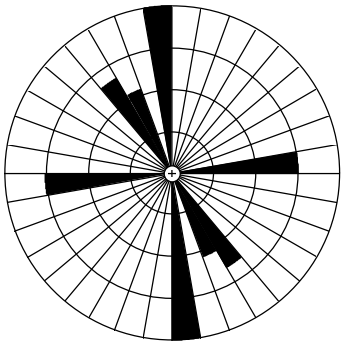

TC04 JOINTS		Statistics
N = 16		Vector Mean = 337.8
Class Interval = 10 degrees		Conf. Angle = 42.63
Maximum Percentage = 43.8		R Magnitude = 0.442
Mean Percentage = 25.00	Standard Deviation = 12.50	Rayleigh = 0.0441

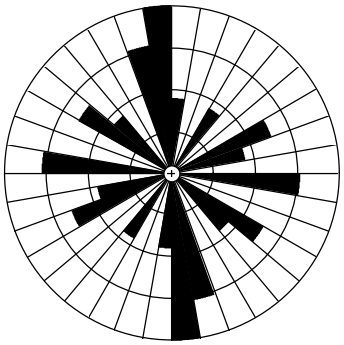

TD01 JOINTS		Statistics
N = 19		Vector Mean = 336.4
Class Interval = 10 degrees		Conf. Angle = 81.26
Maximum Percentage = 26.3		R Magnitude = 0.223
Mean Percentage = 11.11	Standard Deviation = 6.97	Rayleigh = 0.3892

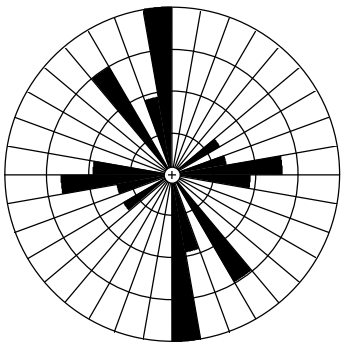

TD02 JOINTS (Kpc)		Statistics
N = 24		Vector Mean = 336.2
Class Interval = 10 degrees		Conf. Angle = 52.98
Maximum Percentage = 37.5		R Magnitude = 0.298
Mean Percentage = 14.29	Standard Deviation = 11.52	Rayleigh = 0.1195

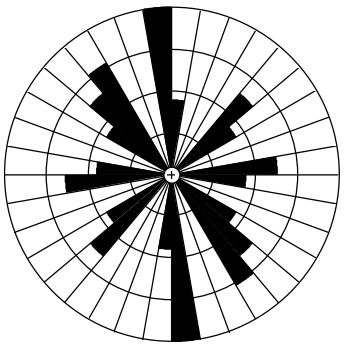

TE01 JOINTS		Statistics
N = 18		Vector Mean = 336.6
Class Interval = 10 degrees		Conf. Angle = 65.94
Maximum Percentage = 27.8		R Magnitude = 0.276
Mean Percentage = 11.11	Standard Deviation = 7.13	Rayleigh = 0.2534

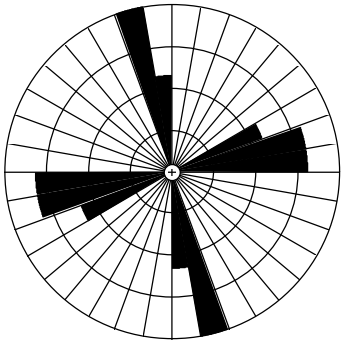

TE03 JOINTS		Statistics
N = 9		Vector Mean = 78.2
Class Interval = 10 degrees		Conf. Angle = 264.21
Maximum Percentage = 33.3		R Magnitude = 0.100
Mean Percentage = 20.00	Standard Deviation = 8.76	Rayleigh = 0.9142

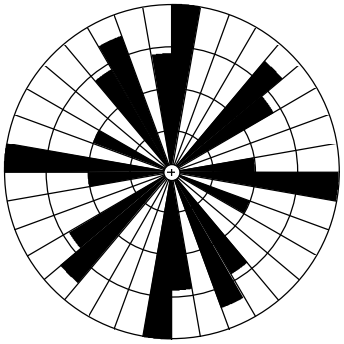

TF01 JOINTS		Statistics
N = 22		Vector Mean = 356.8
Class Interval = 10 degrees		Conf. Angle = 140.77
Maximum Percentage = 18.2		R Magnitude = 0.120
Mean Percentage = 11.11	Standard Deviation = 4.98	Rayleigh = 0.7298

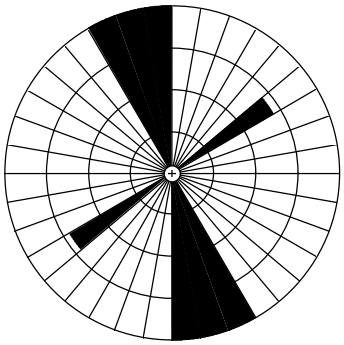

TH01 JOINTS		Statistics
N = 7		Vector Mean = 350.3
Class Interval = 10 degrees		Conf. Angle = 34.84
Maximum Percentage = 28.6		R Magnitude = 0.715
Mean Percentage = 25.00	Standard Deviation = 6.61	Rayleigh = 0.0280

Fruitland Formation, a coal:

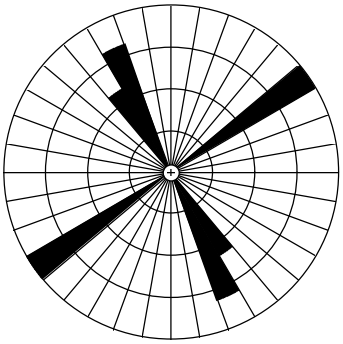

TA01 CLEATS		Statistics
N = 6		Vector Mean = 11.5
Class Interval = 10 degrees		Conf. Angle = 463.87
Maximum Percentage = 50.0		R Magnitude = 0.070
Mean Percentage = 33.33	Standard Deviation = 14.91	Rayleigh = 0.9714

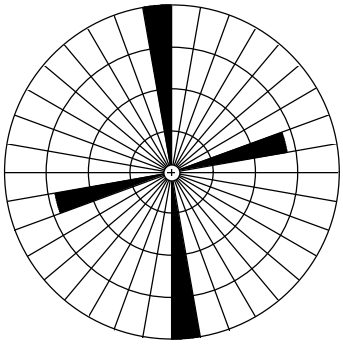

TA02 CLEATS		Statistics
N = 3		Vector Mean = 356.9
Class Interval = 10 degrees		Conf. Angle = 130.16
Maximum Percentage = 66.7		R Magnitude = 0.343
Mean Percentage = 50.00	Standard Deviation = 19.25	Rayleigh = 0.7027

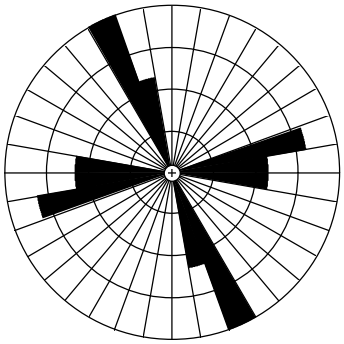

TA04 CLEATS		Statistics
N = 8		Vector Mean = 299.9
Class Interval = 10 degrees		Conf. Angle = 101.37
Maximum Percentage = 37.5		R Magnitude = 0.273
Mean Percentage = 20.00	Standard Deviation = 10.54	Rayleigh = 0.5497

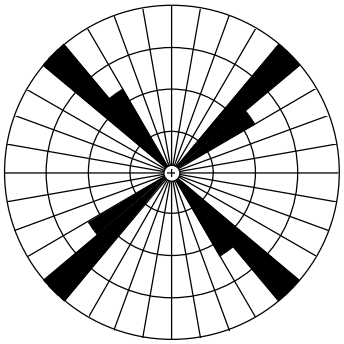

TB04 CLEATS		Statistics
N = 8		Vector Mean = 357.6
Class Interval = 10 degrees		Conf. Angle = 1332.74
Maximum Percentage = 37.5		R Magnitude = 0.022
Mean Percentage = 25.00	Standard Deviation = 13.36	Rayleigh = 0.9961

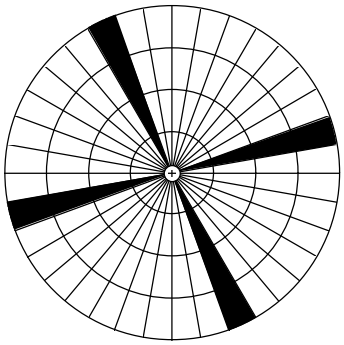

TB05 CLEATS		Statistics
N = 2		Vector Mean = 291.0
Class Interval = 10 degrees		Conf. Angle = 400.27
Maximum Percentage = 50.0		R Magnitude = 0.139
Mean Percentage = 50.00	Standard Deviation = 0.00	Rayleigh = 0.9620

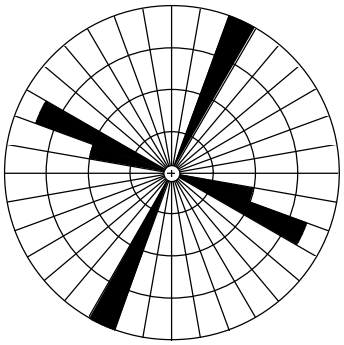

TC01 CLEATS		Statistics
N = 8		Vector Mean = 66.5
Class Interval = 10 degrees		Conf. Angle = 1505.50
Maximum Percentage = 50.0		R Magnitude = 0.017
Mean Percentage = 33.33	Standard Deviation = 17.08	Rayleigh = 0.9976

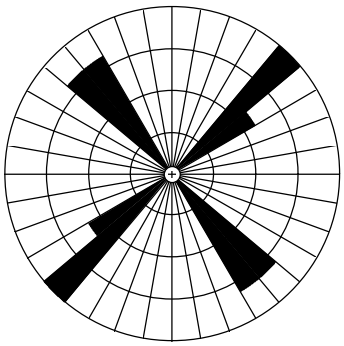

TD02 CLEATS		Statistics
N = 8		Vector Mean = 5.0
Class Interval = 10 degrees		Conf. Angle = 1503.11
Maximum Percentage = 37.5		R Magnitude = 0.017
Mean Percentage = 25.00	Standard Deviation = 9.45	Rayleigh = 0.9976

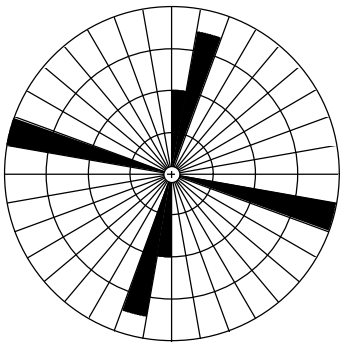

TD03 CLEATS		Statistics
N = 8		Vector Mean = 325.0
Class Interval = 10 degrees		Conf. Angle = 3016.64
Maximum Percentage = 50.0		R Magnitude = 0.009
Mean Percentage = 33.33	Standard Deviation = 17.08	Rayleigh = 0.9994

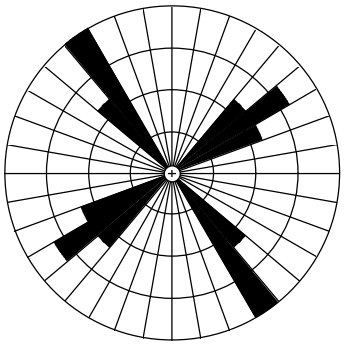

TE02 CLEATS		Statistics
N = 8		Vector Mean = 283.7
Class Interval = 10 degrees		Conf. Angle = 747.60
Maximum Percentage = 37.5		R Magnitude = 0.035
Mean Percentage = 20.00	Standard Deviation = 10.54	Rayleigh = 0.9901

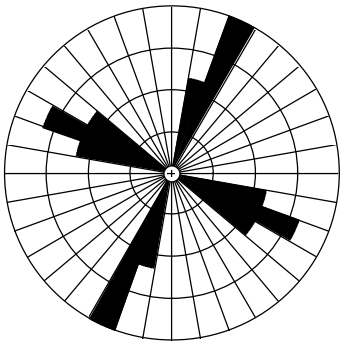

TF02 CLEATS		Statistics
N = 8		Vector Mean = 2.9
Class Interval = 10 degrees		Conf. Angle = 3494.49
Maximum Percentage = 37.5		R Magnitude = 0.006
Mean Percentage = 20.00	Standard Deviation = 10.54	Rayleigh = 0.9997

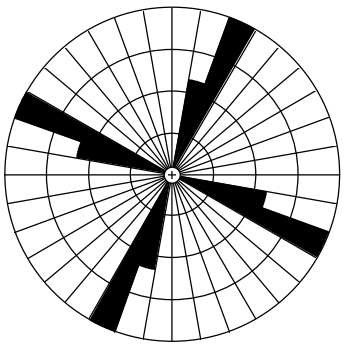

TG01 CLEATS		Statistics
N = 8		Vector Mean = 335.8
Class Interval = 10 degrees		Conf. Angle = 1004.29
Maximum Percentage = 37.5		R Magnitude = 0.026
Mean Percentage = 25.00	Standard Deviation = 13.36	Rayleigh = 0.9946

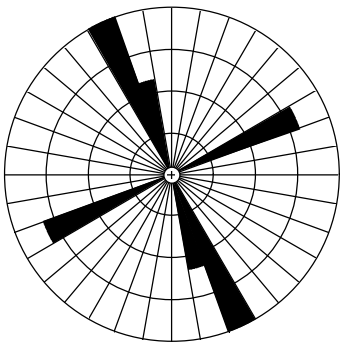

TJ02		Statistics
N = 6		Vector Mean = 338.0
Class Interval = 10 degrees		Conf. Angle = 95.00
Maximum Percentage = 50.0		R Magnitude = 0.333
Mean Percentage = 33.33	Standard Deviation = 14.91	Rayleigh = 0.5143

Fruitland Formation, sandstone No. 1:

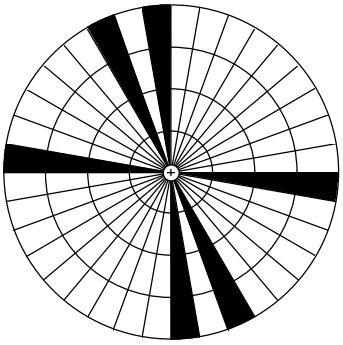

TC03 JOINTS (Kf)		Statistics
N = 3		Vector Mean = 326.5
Class Interval = 10 degrees		Conf. Angle = 98.93
Maximum Percentage = 33.3		R Magnitude = 0.437
Mean Percentage = 33.33	Standard Deviation = 0.01	Rayleigh = 0.5633

Fruitland Formation, b coal:

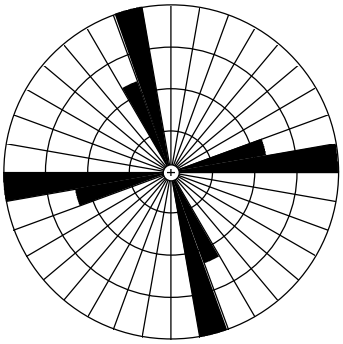

TA11 CLEATS		Statistics
N = 8		Vector Mean = 300.9
Class Interval = 10 degrees		Conf. Angle = 345.72
Maximum Percentage = 37.5		R Magnitude = 0.082
Mean Percentage = 25.00	Standard Deviation = 13.36	Rayleigh = 0.9474

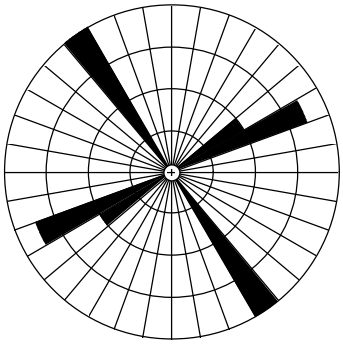

TC03 CLEATS		Statistics
N = 8		Vector Mean = 282.5
Class Interval = 10 degrees		Conf. Angle = 308.89
Maximum Percentage = 50.0		R Magnitude = 0.091
Mean Percentage = 33.33	Standard Deviation = 17.08	Rayleigh = 0.9353

Fruitland Formation, sandstone No. 2:

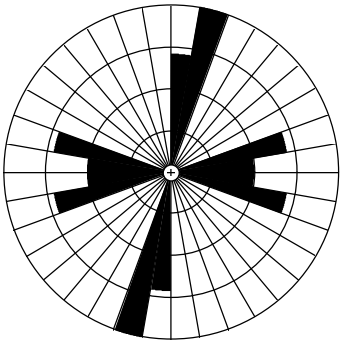

TA03 JOINTS		Statistics
N = 12		Vector Mean = 41.5
Class Interval = 10 degrees		Conf. Angle = 120.82
Maximum Percentage = 33.3		R Magnitude = 0.186
Mean Percentage = 16.67	Standard Deviation = 8.70	Rayleigh = 0.6602

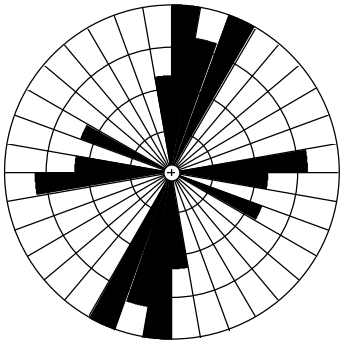

TD02 JOINTS (Kf)		Statistics
N = 13		Vector Mean = 16.3
Class Interval = 10 degrees		Conf. Angle = 55.57
Maximum Percentage = 23.1		R Magnitude = 0.382
Mean Percentage = 14.29	Standard Deviation = 6.65	Rayleigh = 0.1502

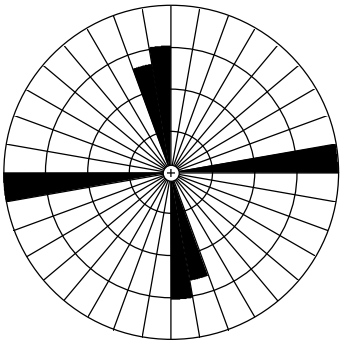

TF03 JOINTS		Statistics
N = 14		Vector Mean = 304.2
Class Interval = 10 degrees		Conf. Angle = 426.05
Maximum Percentage = 50.0		R Magnitude = 0.050
Mean Percentage = 33.33	Standard Deviation = 13.30	Rayleigh = 0.9662

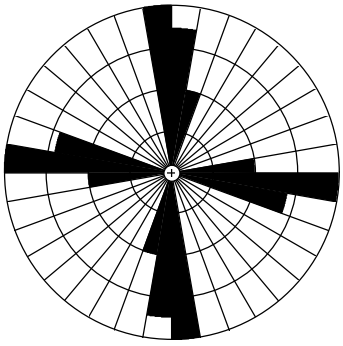

TG02 JOINTS		Statistics
N = 15		Vector Mean = 346.5
Class Interval = 10 degrees		Conf. Angle = 288.49
Maximum Percentage = 26.7		R Magnitude = 0.072
Mean Percentage = 16.67	Standard Deviation = 8.76	Rayleigh = 0.9252

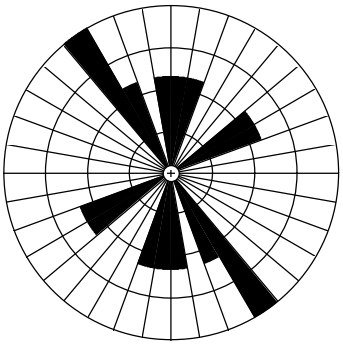

TI01		Statistics
N = 9		Vector Mean = 349.3
Class Interval = 10 degrees		Conf. Angle = 58.14
Maximum Percentage = 33.3		R Magnitude = 0.434
Mean Percentage = 14.29	Standard Deviation = 8.07	Rayleigh = 0.1830

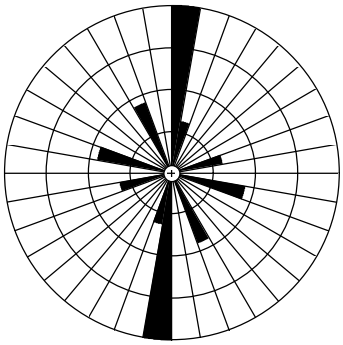

TJ01 JOINTS		Statistics
N = 16		Vector Mean = 2.4
Class Interval = 10 degrees		Conf. Angle = 30.11
Maximum Percentage = 62.5		R Magnitude = 0.589
Mean Percentage = 20.00	Standard Deviation = 22.59	Rayleigh = 0.0039

Fruitland Formation, c coal:

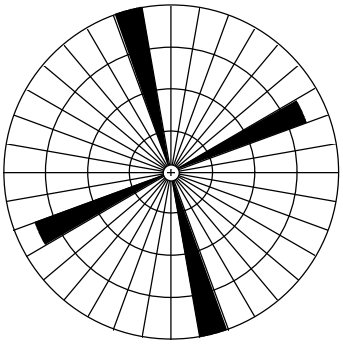

TC06 CLEATS		Statistics
N = 7		Vector Mean = 9.4
Class Interval = 10 degrees		Conf. Angle = 128.72
Maximum Percentage = 57.1		R Magnitude = 0.230
Mean Percentage = 50.00	Standard Deviation = 8.25	Rayleigh = 0.6905

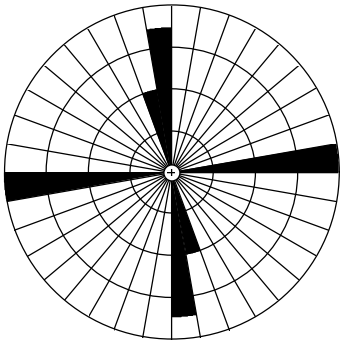

TD04 CLEATS		Statistics
N = 8		Vector Mean = 307.6
Class Interval = 10 degrees		Conf. Angle = 463.90
Maximum Percentage = 50.0		R Magnitude = 0.061
Mean Percentage = 33.33	Standard Deviation = 17.08	Rayleigh = 0.9707

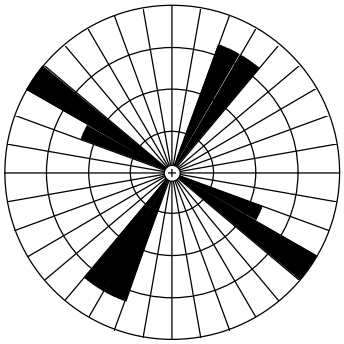

TE04 CLEATS		Statistics
N = 8		Vector Mean = 60.6
Class Interval = 10 degrees		Conf. Angle = INF
Maximum Percentage = 37.5		R Magnitude = 0.005
Mean Percentage = 25.00	Standard Deviation = 9.45	Rayleigh = 0.9998

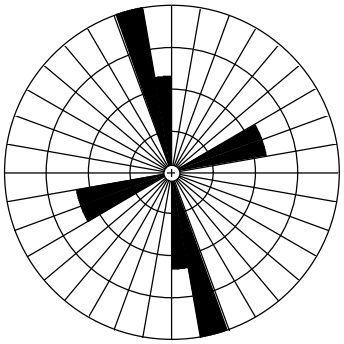

TE06 CLEATS		Statistics
N = 6		Vector Mean = 354.6
Class Interval = 10 degrees		Conf. Angle = 89.96
Maximum Percentage = 50.0		R Magnitude = 0.347
Mean Percentage = 25.00	Standard Deviation = 15.43	Rayleigh = 0.4850

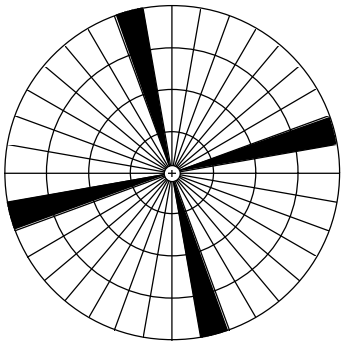

TF04 CLEATS		Statistics
N = 8		Vector Mean = 300.1
Class Interval = 10 degrees		Conf. Angle = 414.73
Maximum Percentage = 50.0		R Magnitude = 0.065
Mean Percentage = 50.00	Standard Deviation = 0.00	Rayleigh = 0.9665

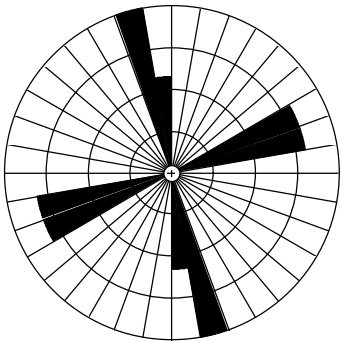

TJ03		Statistics
N = 8		Vector Mean = 28.2
Class Interval = 10 degrees		Conf. Angle = 156.08
Maximum Percentage = 37.5		R Magnitude = 0.177
Mean Percentage = 25.00	Standard Deviation = 9.45	Rayleigh = 0.7787

Fruitland Formation, sandstone No. 3:

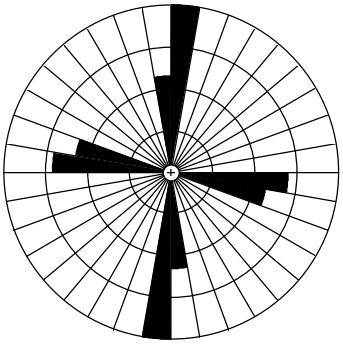

TA08 JOINTS		Statistics
N = 13		Vector Mean = 354.6
Class Interval = 10 degrees		Conf. Angle = 90.59
Maximum Percentage = 46.2		R Magnitude = 0.239
Mean Percentage = 25.00	Standard Deviation = 13.48	Rayleigh = 0.4758

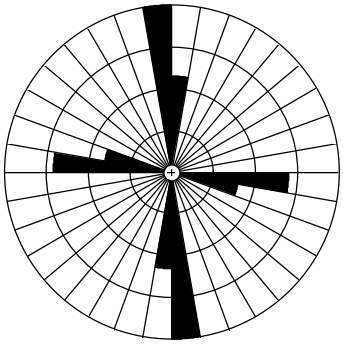

TB01 JOINTS		Statistics
N = 12		Vector Mean = 347.0
Class Interval = 10 degrees		Conf. Angle = 59.88
Maximum Percentage = 50.0		R Magnitude = 0.368
Mean Percentage = 25.00	Standard Deviation = 16.67	Rayleigh = 0.1975

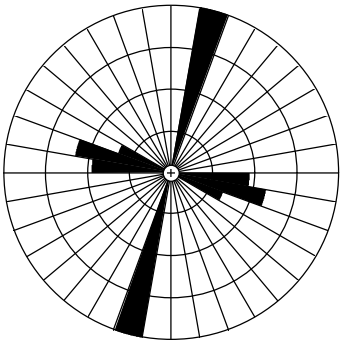

TC05 JOINTS		Statistics
N = 15		Vector Mean = 16.0
Class Interval = 10 degrees		Conf. Angle = 96.72
Maximum Percentage = 60.0		R Magnitude = 0.209
Mean Percentage = 25.00	Standard Deviation = 22.18	Rayleigh = 0.5188

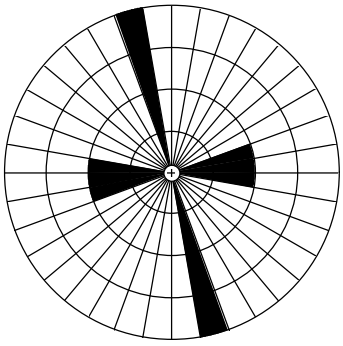

TC06 JOINTS		Statistics
N = 7		Vector Mean = 325.5
Class Interval = 10 degrees		Conf. Angle = 127.94
Maximum Percentage = 57.1		R Magnitude = 0.233
Mean Percentage = 25.00	Standard Deviation = 19.84	Rayleigh = 0.6842

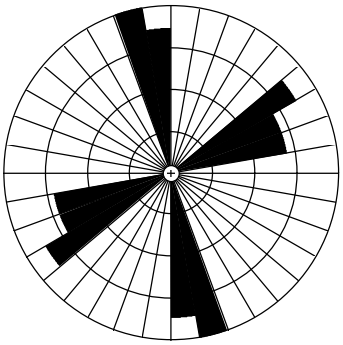

TD06 JOINTS		Statistics
N = 14		Vector Mean = 24.4
Class Interval = 10 degrees		Conf. Angle = 86.33
Maximum Percentage = 28.6		R Magnitude = 0.244
Mean Percentage = 20.00	Standard Deviation = 5.63	Rayleigh = 0.4334

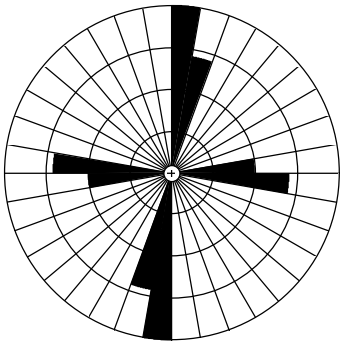

TI02		Statistics
N = 9		Vector Mean = 14.5
Class Interval = 10 degrees		Conf. Angle = 75.98
Maximum Percentage = 44.4		R Magnitude = 0.335
Mean Percentage = 25.00	Standard Deviation = 12.94	Rayleigh = 0.3632

Fruitland Formation, sandstone No. 4:

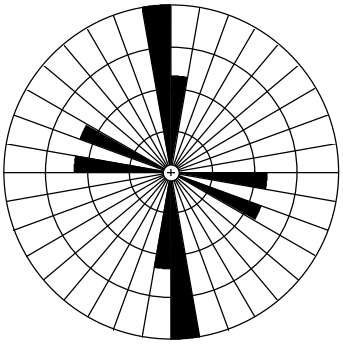

TC07 JOINTS		Statistics
N = 6		Vector Mean = 345.4
Class Interval = 10 degrees		Conf. Angle = 69.89
Maximum Percentage = 50.0		R Magnitude = 0.438
Mean Percentage = 25.00	Standard Deviation = 15.43	Rayleigh = 0.3160

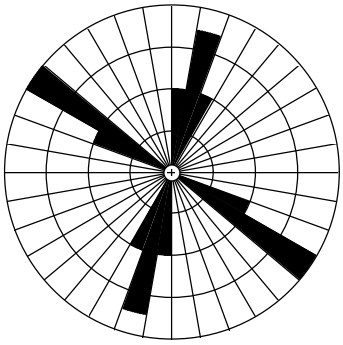

TD05 JOINTS		Statistics
N = 10		Vector Mean = 336.2
Class Interval = 10 degrees		Conf. Angle = 75.93
Maximum Percentage = 40.0		R Magnitude = 0.324
Mean Percentage = 20.00	Standard Deviation = 13.33	Rayleigh = 0.3509

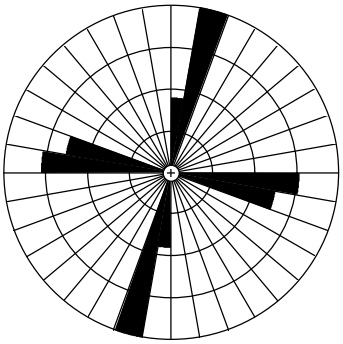

TE05 JOINTS		Statistics
N = 11		Vector Mean = 19.1
Class Interval = 10 degrees		Conf. Angle = 237.65
Maximum Percentage = 45.5		R Magnitude = 0.101
Mean Percentage = 25.00	Standard Deviation = 14.37	Rayleigh = 0.8939

Fruitland Formation, upper part:

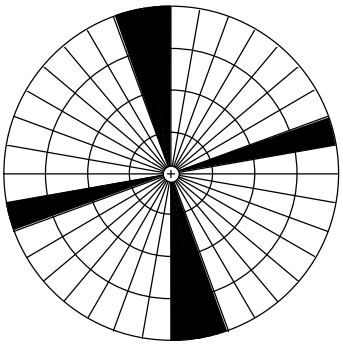

TB07 CLEATS		Statistics
N = 3		Vector Mean = 355.0
Class Interval = 10 degrees		Conf. Angle = 134.92
Maximum Percentage = 33.3		R Magnitude = 0.330
Mean Percentage = 33.33	Standard Deviation = 0.01	Rayleigh = 0.7211

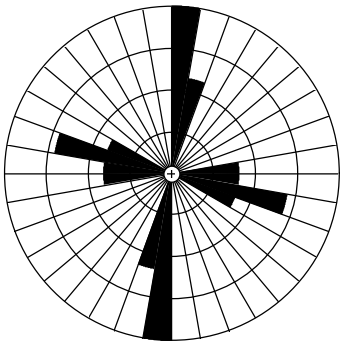

TB08 JOINTS		Statistics
N = 14		Vector Mean = 0.5
Class Interval = 10 degrees		Conf. Angle = 125.50
Maximum Percentage = 42.9		R Magnitude = 0.166
Mean Percentage = 16.67	Standard Deviation = 13.39	Rayleigh = 0.6807

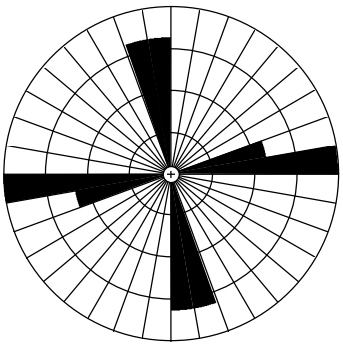

TE07 CLEATS	Statistics
N = 8	Vector Mean = 306.1
Class Interval = 10 degrees	Conf. Angle = 573.63
Maximum Percentage = 37.5	R Magnitude = 0.048
Mean Percentage = 25.00 Standard Deviation = 9.45	Rayleigh = 0.9819

Kirtland Formation sandstones:

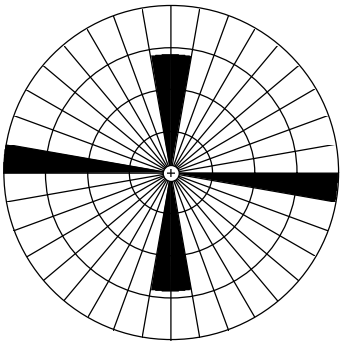

TB03 JOINTS	Statistics
N = 12	Vector Mean = 314.3
Class Interval = 10 degrees	Conf. Angle = 316.28
Maximum Percentage = 50.0	R Magnitude = 0.075
Mean Percentage = 33.33 Standard Deviation = 12.91	Rayleigh = 0.9350

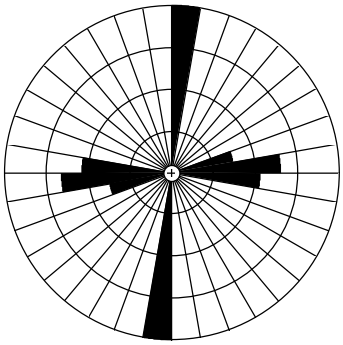

TC08 JOINTS	Statistics
N = 13	Vector Mean = 27.3
Class Interval = 10 degrees	Conf. Angle = 127.78
Maximum Percentage = 53.8	R Magnitude = 0.172
Mean Percentage = 25.00 Standard Deviation = 18.73	Rayleigh = 0.6801

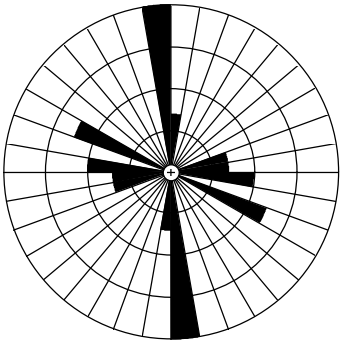

TD07 JOINTS	Statistics
N = 16	Vector Mean = 339.8
Class Interval = 10 degrees	Conf. Angle = 80.85
Maximum Percentage = 50.0	R Magnitude = 0.244
Mean Percentage = 16.67 Standard Deviation = 16.28	Rayleigh = 0.3862

Table 2-11. Joint and cleat stations established in the Pine River area, grouped by geologic unit. Station locations are shown on plate 6.

Kpc	Kfab	Kf1	Kf2	Kfcd	Kf3	Kf4
PR01	PR03	PR07	PR02	PR13	PR15	PR18
PR04	PR06	PR11	PR12	PR16	PR17	
PR05	PR08	PR23	PR19	PR31	PR32	
PR09	PR14		PR21	PR34	PR33	
PR10	PR20		PR26	PR37	PR35	
PR22	PR25		PR30		PR36	
PR24	PR28					
PR27	PR29					
PR38						

Kpc - Pictured Cliffs Sandstone; Kfab - Fruitland Formation, lower coal interval; Kf1 - Fruitland Formation sandstone number 1; Kf2 - Fruitland Formation sandstone number 2; Kfcd - Fruitland Formation, middle coal interval; Kf3 - Fruitland Formation sandstone number 3; Kf4 - Fruitland Formation sandstone number 4

Pictured Cliffs Sandstone:

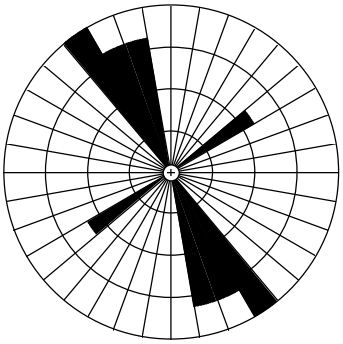

PR01	Statistics
N = 8	Vector Mean = 334.6
Class Interval = 10 degrees	Conf. Angle = 30.47
Maximum Percentage = 37.5	R Magnitude = 0.742
Mean Percentage = 25.00 Standard Deviation = 9.45	Rayleigh = 0.0123

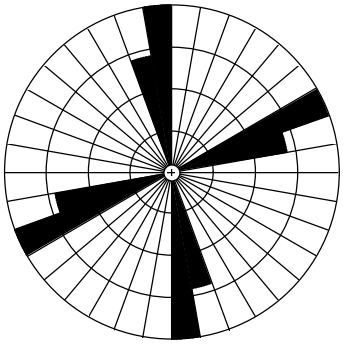

PR04	Statistics
N = 6	Vector Mean = 26.9
Class Interval = 10 degrees	Conf. Angle = 106.25
Maximum Percentage = 33.3	R Magnitude = 0.296
Mean Percentage = 25.00 Standard Deviation = 8.91	Rayleigh = 0.5914

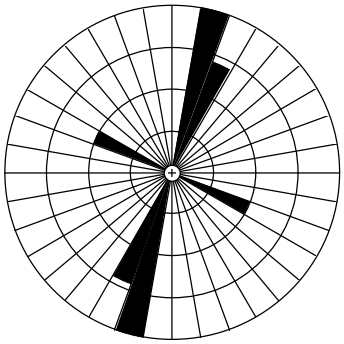

PR05	Statistics
N = 7	Vector Mean = 18.0
Class Interval = 10 degrees	Conf. Angle = 34.93
Maximum Percentage = 57.1	R Magnitude = 0.711
Mean Percentage = 33.33 Standard Deviation = 19.52	Rayleigh = 0.0290

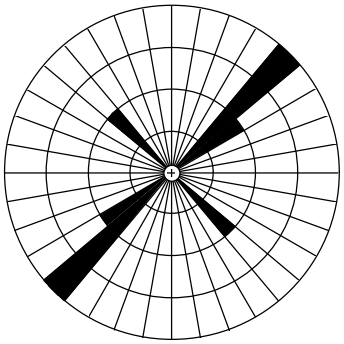

PR09	Statistics
N = 6	Vector Mean = 47.7
Class Interval = 10 degrees	Conf. Angle = 42.09
Maximum Percentage = 66.7	R Magnitude = 0.663
Mean Percentage = 33.33 Standard Deviation = 25.82	Rayleigh = 0.0716

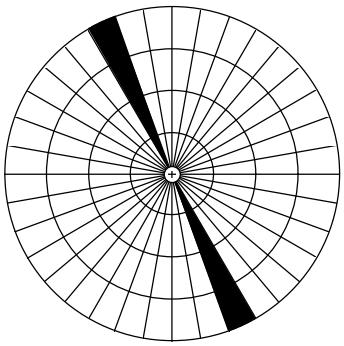

PR10	Statistics
N = 7	Vector Mean = 334.0
Class Interval = 10 degrees	Conf. Angle = 6.00
Maximum Percentage = 100.0	R Magnitude = 0.996
Mean Percentage = 100.00 Standard Deviation = 0.00	Rayleigh = 0.0010

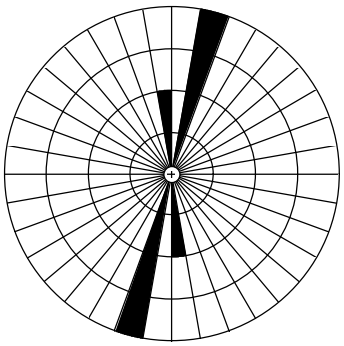

PR22	Statistics
N = 5	Vector Mean = 10.4
Class Interval = 10 degrees	Conf. Angle = 16.05
Maximum Percentage = 80.0	R Magnitude = 0.954
Mean Percentage = 50.00 Standard Deviation = 34.64	Rayleigh = 0.0106

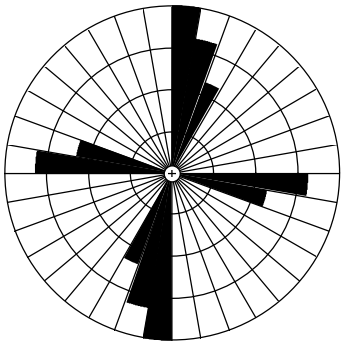

PR24	Statistics
N = 9	Vector Mean = 15.2
Class Interval = 10 degrees	Conf. Angle = 77.65
Maximum Percentage = 33.3	R Magnitude = 0.332
Mean Percentage = 20.00 Standard Deviation = 8.76	Rayleigh = 0.3705

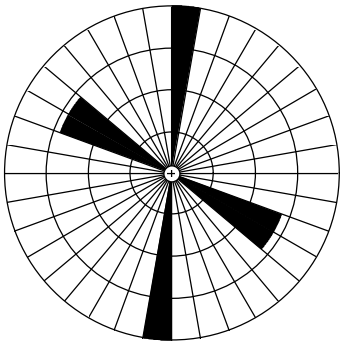

PR27	Statistics
N = 4	Vector Mean = 333.8
Class Interval = 10 degrees	Conf. Angle = 77.15
Maximum Percentage = 50.0	R Magnitude = 0.482
Mean Percentage = 33.33 Standard Deviation = 12.91	Rayleigh = 0.3941

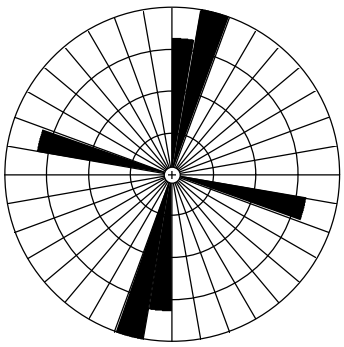

PR38	Statistics
N = 7	Vector Mean = 8.0
Class Interval = 10 degrees	Conf. Angle = 68.32
Maximum Percentage = 42.9	R Magnitude = 0.416
Mean Percentage = 33.33 Standard Deviation = 7.38	Rayleigh = 0.2972

Fruitland Formation, lower coal interval:

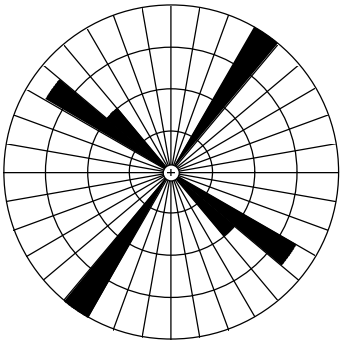

PR03	Statistics
N = 8	Vector Mean = 350.5
Class Interval = 10 degrees	Conf. Angle = 235.64
Maximum Percentage = 50.0	R Magnitude = 0.117
Mean Percentage = 33.33 Standard Deviation = 17.08	Rayleigh = 0.8955

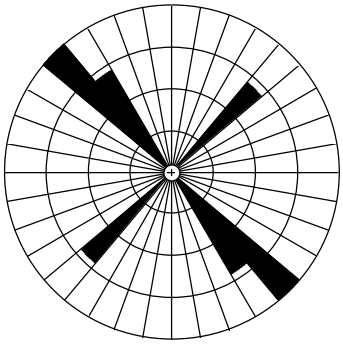

PR06	Statistics
N = 4	Vector Mean = 319.5
Class Interval = 10 degrees	Conf. Angle = 75.73
Maximum Percentage = 50.0	R Magnitude = 0.487
Mean Percentage = 33.33 Standard Deviation = 12.91	Rayleigh = 0.3870

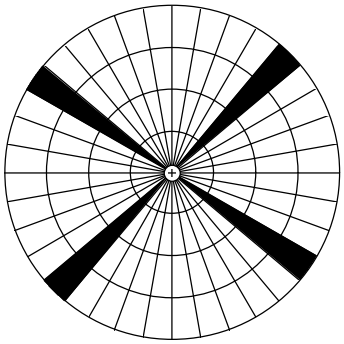

PR08	Statistics
N = 8	Vector Mean = 84.6
Class Interval = 10 degrees	Conf. Angle = 214.90
Maximum Percentage = 50.0	R Magnitude = 0.130
Mean Percentage = 50.00 Standard Deviation = 0.00	Rayleigh = 0.8732

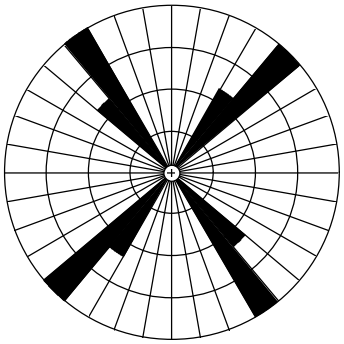

PR14	Statistics
N = 8	Vector Mean = 359.2
Class Interval = 10 degrees	Conf. Angle = 303.27
Maximum Percentage = 37.5	R Magnitude = 0.095
Mean Percentage = 25.00 Standard Deviation = 13.36	Rayleigh = 0.9306

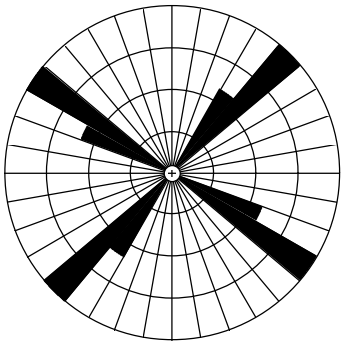

PR20	Statistics
N = 8	Vector Mean = 81.4
Class Interval = 10 degrees	Conf. Angle = 233.35
Maximum Percentage = 37.5	R Magnitude = 0.120
Mean Percentage = 25.00 Standard Deviation = 13.36	Rayleigh = 0.8916

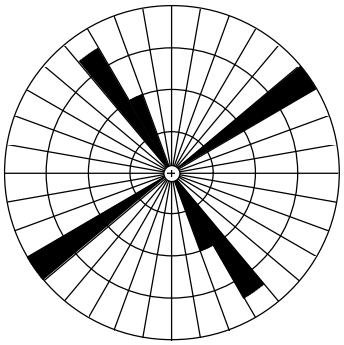

PR25	Statistics
N = 8	Vector Mean = 11.4
Class Interval = 10 degrees	Conf. Angle = 573.23
Maximum Percentage = 50.0	R Magnitude = 0.048
Mean Percentage = 33.33 Standard Deviation = 17.08	Rayleigh = 0.9818

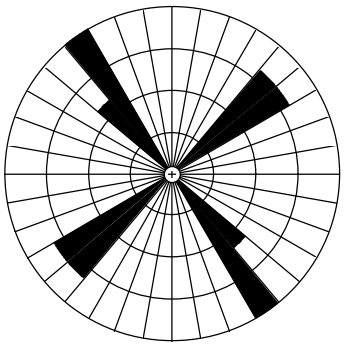

PR28	Statistics
N = 8	Vector Mean = 6.3
Class Interval = 10 degrees	Conf. Angle = 345.71
Maximum Percentage = 37.5	R Magnitude = 0.082
Mean Percentage = 25.00 Standard Deviation = 9.45	Rayleigh = 0.9474

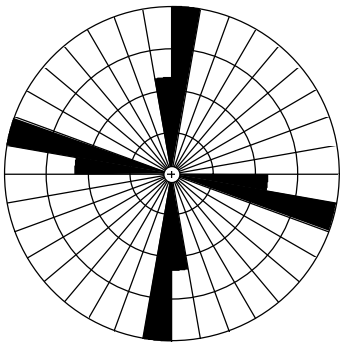

PR29	Statistics
N = 8	Vector Mean = 322.6
Class Interval = 10 degrees	Conf. Angle = 174.80
Maximum Percentage = 37.5	R Magnitude = 0.159
Mean Percentage = 25.00 Standard Deviation = 13.36	Rayleigh = 0.8166

Fruitland Formation, sandstone No. 1:

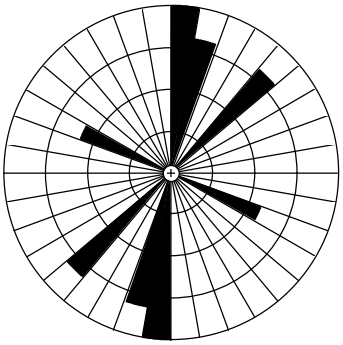

PR07	Statistics
N = 8	Vector Mean = 17.7
Class Interval = 10 degrees	Conf. Angle = 44.31
Maximum Percentage = 37.5	R Magnitude = 0.574
Mean Percentage = 25.00 Standard Deviation = 9.45	Rayleigh = 0.0715

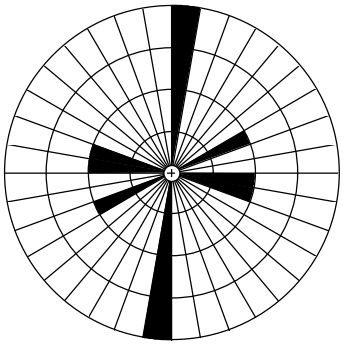

PR11	Statistics
N = 7	Vector Mean = 12.3
Class Interval = 10 degrees	Conf. Angle = 136.12
Maximum Percentage = 57.1	R Magnitude = 0.216
Mean Percentage = 25.00 Standard Deviation = 19.84	Rayleigh = 0.7224

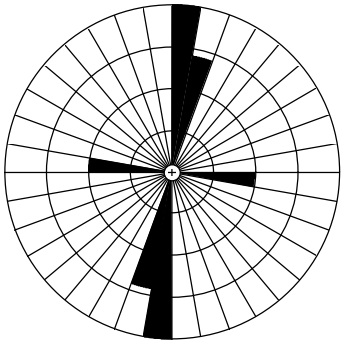

PR23	Statistics
N = 7	Vector Mean = 7.4
Class Interval = 10 degrees	Conf. Angle = 35.00
Maximum Percentage = 57.1	R Magnitude = 0.708
Mean Percentage = 33.33 Standard Deviation = 19.52	Rayleigh = 0.0299

Fruitland Formation, sandstone No. 2:

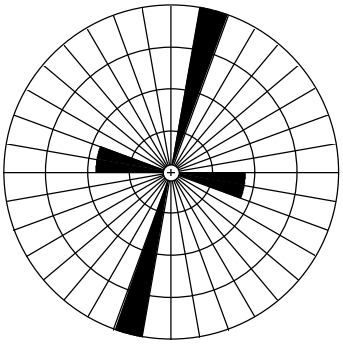

PR02	Statistics
N = 7	Vector Mean = 16.3
Class Interval = 10 degrees	Conf. Angle = 66.07
Maximum Percentage = 71.4	R Magnitude = 0.432
Mean Percentage = 33.33 Standard Deviation = 29.51	Rayleigh = 0.2700

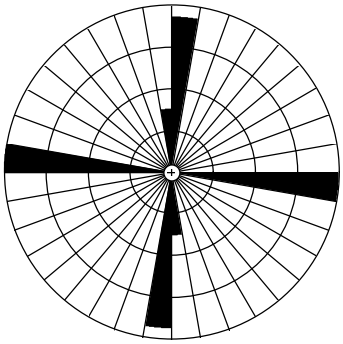

PR12	Statistics
N = 14	Vector Mean = 54.8
Class Interval = 10 degrees	Conf. Angle = 1115.29
Maximum Percentage = 50.0	R Magnitude = 0.018
Mean Percentage = 33.33 Standard Deviation = 20.54	Rayleigh = 0.9954

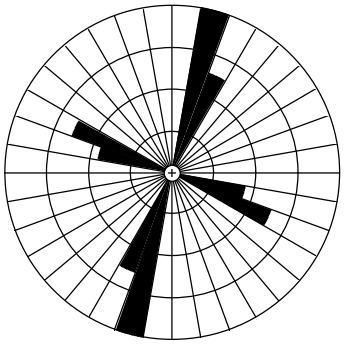

PR19	Statistics
N = 10	Vector Mean = 13.7
Class Interval = 10 degrees	Conf. Angle = 58.40
Maximum Percentage = 50.0	R Magnitude = 0.411
Mean Percentage = 25.00 Standard Deviation = 16.04	Rayleigh = 0.1851

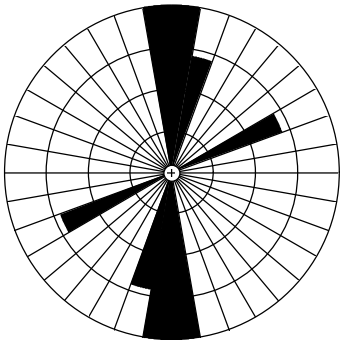

PR21	Statistics
N = 6	Vector Mean = 5.7
Class Interval = 10 degrees	Conf. Angle = 36.13
Maximum Percentage = 33.3	R Magnitude = 0.727
Mean Percentage = 25.00 Standard Deviation = 8.91	Rayleigh = 0.0419

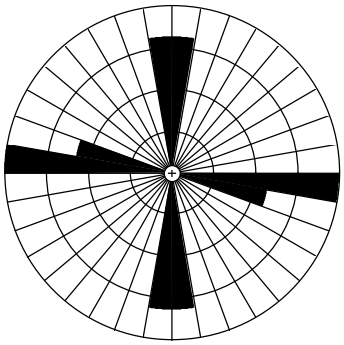

PR26	Statistics
N = 8	Vector Mean = 319.4
Class Interval = 10 degrees	Conf. Angle = 162.82
Maximum Percentage = 37.5	R Magnitude = 0.172
Mean Percentage = 25.00 Standard Deviation = 9.45	Rayleigh = 0.7885

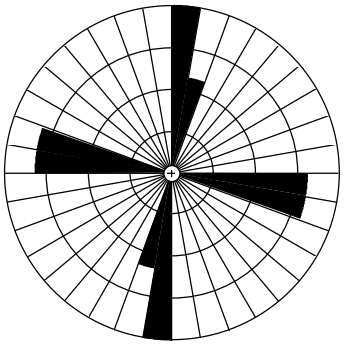

PR30	Statistics
N = 8	Vector Mean = 325.7
Class Interval = 10 degrees	Conf. Angle = 317.85
Maximum Percentage = 37.5	R Magnitude = 0.086
Mean Percentage = 25.00 Standard Deviation = 9.45	Rayleigh = 0.9421

Fruitland Formation, middle coal interval:

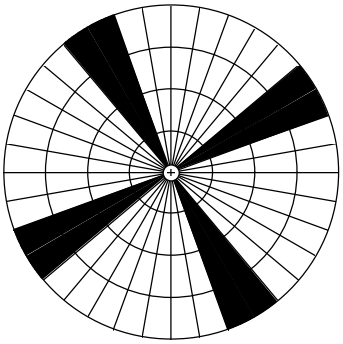

PR13	Statistics
N = 8	Vector Mean = 14.8
Class Interval = 10 degrees	Conf. Angle = 932.93
Maximum Percentage = 25.0	R Magnitude = 0.030
Mean Percentage = 25.00 Standard Deviation = 0.00	Rayleigh = 0.9927

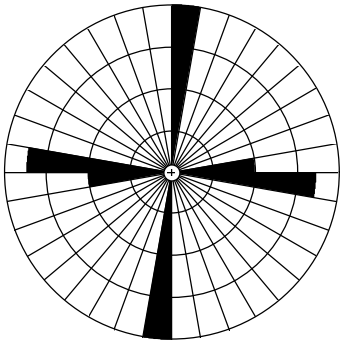

PR16	Statistics
N = 8	Vector Mean = 28.7
Class Interval = 10 degrees	Conf. Angle = 1575.86
Maximum Percentage = 50.0	R Magnitude = 0.016
Mean Percentage = 33.33 Standard Deviation = 17.08	Rayleigh = 0.9980

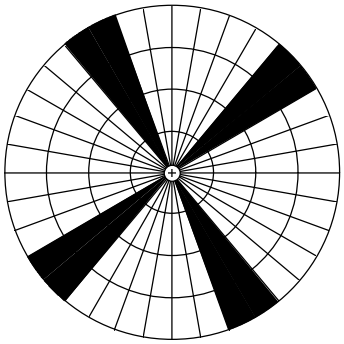

PR31	Statistics
N = 8	Vector Mean = 9.3
Class Interval = 10 degrees	Conf. Angle = 197.98
Maximum Percentage = 25.0	R Magnitude = 0.142
Mean Percentage = 25.00 Standard Deviation = 0.00	Rayleigh = 0.8506

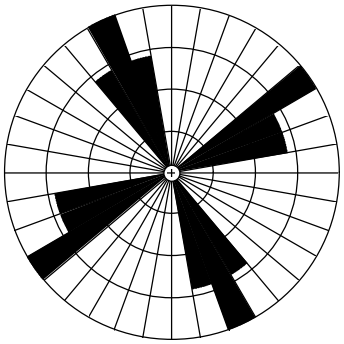

PR34	Statistics
N = 8	Vector Mean = 3.6
Class Interval = 10 degrees	Conf. Angle = 868.68
Maximum Percentage = 25.0	R Magnitude = 0.035
Mean Percentage = 16.67 Standard Deviation = 6.15	Rayleigh = 0.9904

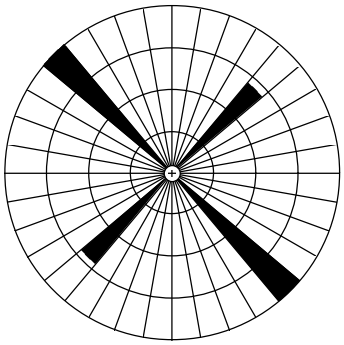

PR37	Statistics
N = 6	Vector Mean = 314.0
Class Interval = 10 degrees	Conf. Angle = 95.64
Maximum Percentage = 66.7	R Magnitude = 0.328
Mean Percentage = 50.00 Standard Deviation = 19.25	Rayleigh = 0.5234

Fruitland Formation, sandstone No. 3:

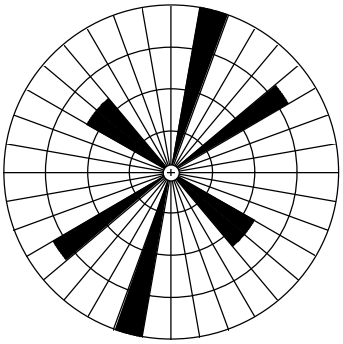

PR15	Statistics
N = 7	Vector Mean = 19.7
Class Interval = 10 degrees	Conf. Angle = 86.07
Maximum Percentage = 42.9	R Magnitude = 0.336
Mean Percentage = 25.00 Standard Deviation = 12.66	Rayleigh = 0.4535

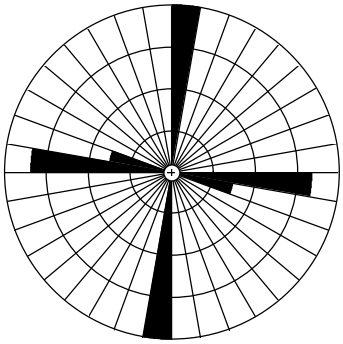

PR17	Statistics
N = 13	Vector Mean = 356.5
Class Interval = 10 degrees	Conf. Angle = 271.21
Maximum Percentage = 53.8	R Magnitude = 0.082
Mean Percentage = 33.33 Standard Deviation = 21.02	Rayleigh = 0.9160

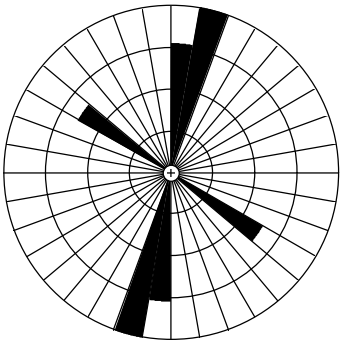

PR32	Statistics
N = 10	Vector Mean = 4.5
Class Interval = 10 degrees	Conf. Angle = 32.69
Maximum Percentage = 50.0	R Magnitude = 0.660
Mean Percentage = 33.33 Standard Deviation = 13.66	Rayleigh = 0.0129

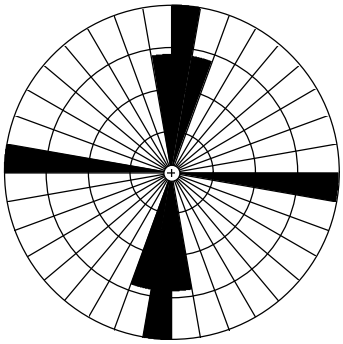

PR33	Statistics
N = 6	Vector Mean = 2.4
Class Interval = 10 degrees	Conf. Angle = 99.05
Maximum Percentage = 33.3	R Magnitude = 0.317
Mean Percentage = 25.00 Standard Deviation = 8.91	Rayleigh = 0.5472

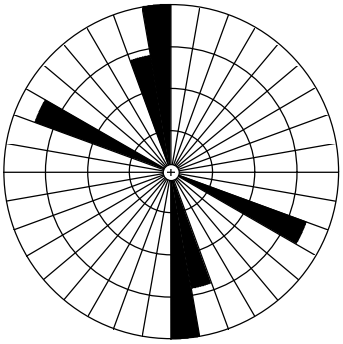

PR35	Statistics
N = 9	Vector Mean = 336.3
Class Interval = 10 degrees	Conf. Angle = 40.01
Maximum Percentage = 44.4	R Magnitude = 0.593
Mean Percentage = 33.33 Standard Deviation = 9.94	Rayleigh = 0.0422

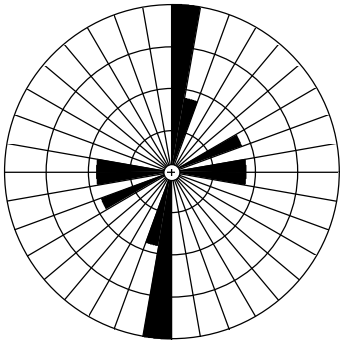

PR36	Statistics
N = 9	Vector Mean = 15.8
Class Interval = 10 degrees	Conf. Angle = 60.23
Maximum Percentage = 55.6	R Magnitude = 0.417
Mean Percentage = 20.00 Standard Deviation = 18.74	Rayleigh = 0.2097

Fruitland Formation, sandstone No. 4:

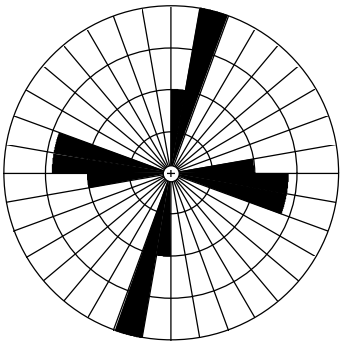

PR18	Statistics
N = 10	Vector Mean = 53.6
Class Interval = 10 degrees	Conf. Angle = 166.06
Maximum Percentage = 40.0	R Magnitude = 0.151
Mean Percentage = 20.00 Standard Deviation = 11.55	Rayleigh = 0.7968

Seismic Structure Studies of the Pine River Gas Seep Area, La Plata County, Colorado

By A. Curtis Huffman, Jr. and David J. Taylor

INTRODUCTION

The objective of this part of the study was to determine what influence deep-seated controls might have exerted on fracturing and faulting in the Fruitland Formation and related rocks in La Plata County. In order to hold down costs, the investigation was limited to existing seismic and drill hole data in the vicinity of the Los Pinos River. The USGS had a seismic reflection line owned by Maxus Exploration Company (Natomas line AAC-1, 2,and 3) from a previous study and Amoco Production Company contributed three shallow high-resolution seismic reflection lines (HXS-1,-2,-3). The recording parameters of the Maxus line were designed to best resolve reflectors at depth (Pennsylvanian) while the Amoco lines were designed to resolve the shallow (Cretaceous) reflectors best. Fortunately, one of the Amoco lines (HXS-3) was recorded coincident with part of Maxus line 1 which enabled us to superimpose the two, thus recovering detail from the entire section, not possible using either of the lines separately. However, due to the lack of detail and accuracy on the shot-point map we received from Amoco, we are unable to precisely correlate the two lines nor are we able to accurately describe or locate any interpreted features. Also, because we had no east-west seismic lines in the area, we are unable to fully describe the geometry of the interpreted features.

In addition to the seismic lines, Amoco also made available an unpublished 1994 report, "Pine River Fruitland Coal Outcrop Investigation", put together by the Southern Rockies Business Unit of Amoco Production Company. K.N. Energy Inc. contributed three seismic lines acquired by Fuelco. These lines were too far away from the area of study to be directly applicable but were of considerable use in obtaining a regional perspective because they were also designed to resolve the shallow part of the section and were far enough removed from the basin margin faulting that we could use them for comparative purposes. Also useful were previous studies performed by the authors in various parts of the San Juan Basin.

Thrust faulting underlying the Hogback Monocline along the northwestern rim of the San Juan Basin was first described by Taylor and Huffman (1988) and this interpretation was later expanded to include the monoclines along the northern and northeastern rims (Huffman and Taylor, 1989). Huffman and Taylor (1989) also reported an orthogonal pattern of basement faulting throughout the San Juan Basin. This pattern is reflected in the overlying sedimentary section and has influenced the occurrence and production of energy resources throughout the basin (Huffman and Taylor, 1991). Huffman and Condon (1993) used these faults to help explain Pennsylvanian and Permian depositional patterns. Analysis of effects on Cretaceous deposition and structure, however, has been largely conjecture primarily due to the lack of good seismic data in the shallower part of the section. The lines supplied by Amoco are the first high resolution seismic data we have been able to work with and although the data have serious shortcomings, they have provided new insights into the structure and tectonic style along the margins of the basin.

SEISMIC AND BOREHOLE DATA

As part of the La Plata County study, the U.S. Geological Survey received three shallow high resolution seismic lines from Amoco. A coarse location map, paper copies of the lines, and digital SEG-Y tapes of the processed data were also included. The USGS asked for, and did receive, copies of the side labels for the seismic lines.

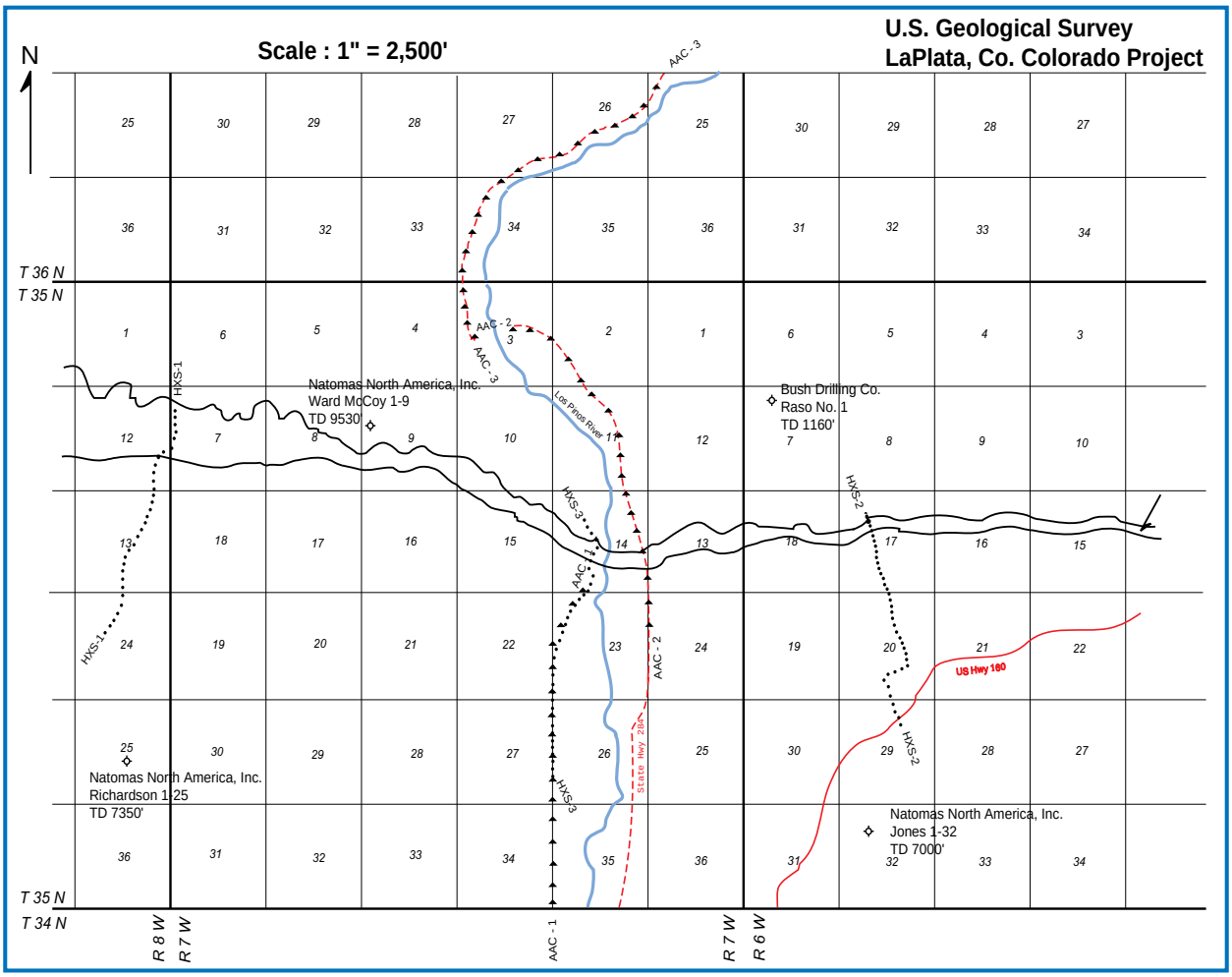

Figure 3-1. Map showing location of well and seismic data used in the study.

This provided us with acquisition information needed in order to perform additional processing on the seismic data.

Using the Landmark/Advance ProMAX seismic data processing system we re-displayed all three lines at a common scale. Unfortunately, we could not correlate the CDP numbers from the SEG-Y headers on tape with the shot numbers on both the location map and the original paper copies of the data. Therefore, we were forced to estimate the correlation between the shot locations from the map and the seismic data. The resulting configuration is shown in figure 3-1 and, although we recognize that the positions are not exact, we feel confident that they allow a reasonably accurate representation of the data.

Synthetic seismograms generated from logs for the following four wells were used to correlate subsurface horizons with seismic reflectors. Locations of the wells are shown in figure 3-1.

Natomas North America Inc.
Ward McCoy 1-9
SW of the NW: T35N, R7W, Section 9
TD 9,350'

Natomas North America Inc.
Richardson 1-25
NW of the SE: T35N, R8W, Section 25
TD 7,350'

Natomas North America Inc.
Jones 1-32
SE of the NW: T35N, R6W, Section 32
TD 7,000'

Bush Drilling Company
Raso 1
NE of the NW: T35N, R6W, Section 7
TD 1,160'

The McCoy well is located about 2 miles east of the north end of seismic line HXS-1 and 2.3 miles west-northwest of the north end of seismic line HXS-3. The Richardson well is located approximately 1.2 miles south of the southern end of seismic line HXS-1 and 4.5 miles west of the southern end of seismic line HXS-3. The Jones well is located about 1 mile south of the southern end of seismic line HXS-2 and 3.3 miles east-southeast of the southern end of seismic line HXS-3. The Raso well is located 1.5 miles northwest of the northern end of seismic line HXS-2.

SYNTHETIC SEISMOGRAMS

A synthetic seismogram is generated by calculating a reflection coefficient series from an acoustic velocity log (and optionally, a density log) measured in a borehole. The reflection coefficient series is then convolved with an estimate of the seismic source waveform to produce the final synthetic seismic response. The object is to create a close match between the synthetic seismogram and the surface seismic section. Once the match is made identification of reflecting interfaces observed on the surface seismic section can be made.

A reflection coefficient is defined as the ratio of the amplitude of a reflected wave to that of the incident wave. For normal incidence on an interface which separates media of densities (gm/cc) p_n and p_{n+1} and velocities (ft./sec.) V_n and V_{n+1}, the reflection coefficient can be calculated by:

$$(p_{n+1} V_{n+1} - p_n V_n) / (p_{n+1} V_{n+1} + p_n V_n)$$

where n is the sample number of the density or acoustic velocity log.

In the absence of a measured density log, we can use a constant value for the density, or density can be estimated using a number of empirical relationships between velocity and density. Similarly in the absence of a measured acoustic velocity log a sonic log can be estimated using one of several empirical relationships between resistivity measurements and acoustic velocity.

Sonic and density logs were digitized for the Jones well. A sonic log was digitized for the Raso well, but no density log was available. No sonic logs were available for the McCoy and Richardson wells, so the dual induction - SFL logs were digitized for these wells instead. Sonic logs were generated from these resistivity logs using Faust's equation (Faust, 1951 and Faust, 1953) as described below.

$$10^6 / \text{SONIC} = 1948 (Z^{1/6}) (R^{1/6})$$

or

$$\text{SONIC} = 1948 (Z^{1/6}) (R^{1/6}) / 10^6$$

where "Z" is the depth in feet "R" is the resistivity value in ohms at that depth, and "SONIC" is the resultant acoustic velocity value in μs/ft.

The Raso well did not have a density log available so a conversion was used to create one from the sonic log. Using Lindseth's equation (Lindseth, 1979), described below, a pseudo density log in gm/cc was generated.

$$p = (V-3460) / (V(.308))$$

where *"p"* is the density value in gm/cc and "V" is the compressional wave velocity in ft/sec which is derived using the equation:

$$V \text{ (ft/sec)} = 10^6/\text{SONIC } (\mu s/ft)$$

Sonic and density values were used to produce the impedance and reflection coefficient logs. Figures 3-2 through 3-5 are plots of the various logs used to create the reflectivity series with geologic tops annotated. Sonic logs were also used to create depth, and velocity logs.

Figure 3-6 is a plot of the wavelet used to generate the synthetic seismograms. It is a zero phase bandpass wavelet with a frequency content of 12 to 55 hertz. This wavelet matches the primary frequency content of the seismic data. Because the seismic data has been deconvolved, a zero phase wavelet is appropriate. Figure 3-7 is a plot showing all of the final synthetic seismograms for the four wells used in the study.

SEISMIC DATA—PROCESSING

As mentioned previously, the U.S. Geological Survey received three shallow high-resolution multichannel seismic lines from Amoco. Initial examination of the data showed that these lines were processed through CDP stack with no

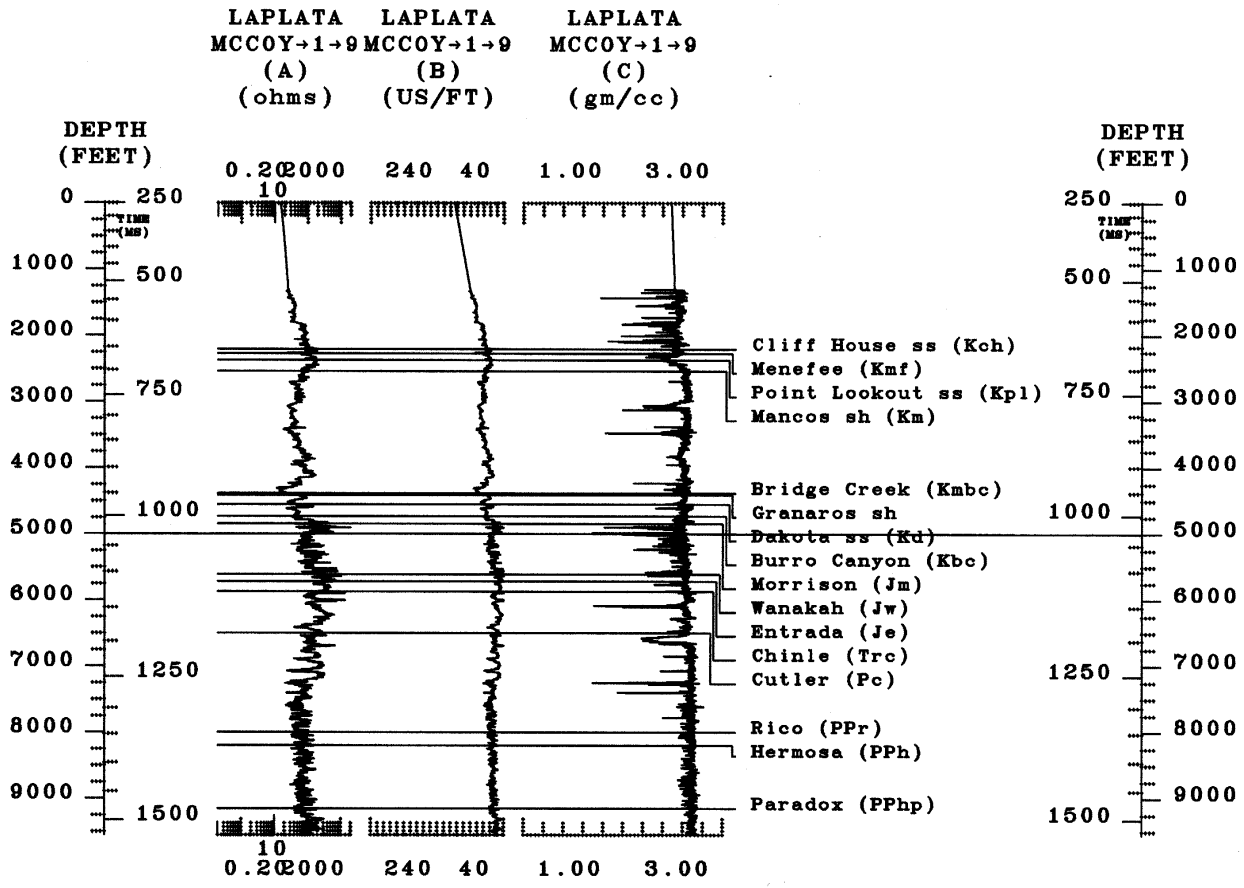

Figure 3-2. Display of the (A) measured resistivity log, (B) sonic log generated using Faust's equation, and (C) density log generated from the sonic log utilizing Lindseth's equation used to generate a synthetic seismogram for the Ward McCoy No. 1-9 well.

migration applied. There was also a significant amount of noise in the section and what we interpreted to be interbed multiples below the strong reflectors of the Dakota Formation.

We used several post-stack processing techniques in an effort to decrease the noise content of the data without degrading the signal. These included spike and noise burst reduction, F-X deconvolution, and bandpass filtering. All of these processes attacked a specific noise problem and produced a section that was easier to interpret after they were applied. The post-stack processing sequence included:

*SEG-Y Tape Input
*Disk Data Input
*Spike Burst Edit
*Noise Burst Edit
*F-X Deconvolution
*Bandpass Filter (8-12-55-60 Hz.)
*Automatic Gain Control
*Disk Data Output

Once a satisfactory stacked section was produced, the data were migrated to collapse the diffractions and move the reflectors to their true subsurface location using a Kirchoff time migration algorithm.

Because the original field data were not available to us we could not determine migration velocities directly from the seismic data, therefore, we converted the sonic and velocity information from the wells to RMS velocities and used the results for the migration. Key reflecting horizons were picked and the RMS velocities within those horizons were averaged. The averaged RMS velocities were then held constant across the section but the application time window was varied according to the dip of the key reflecting horizons. This procedure produced a satisfactory result as the section did not seem to be severely under or over migrated. The horizons and the averaged RMS velocities used were:

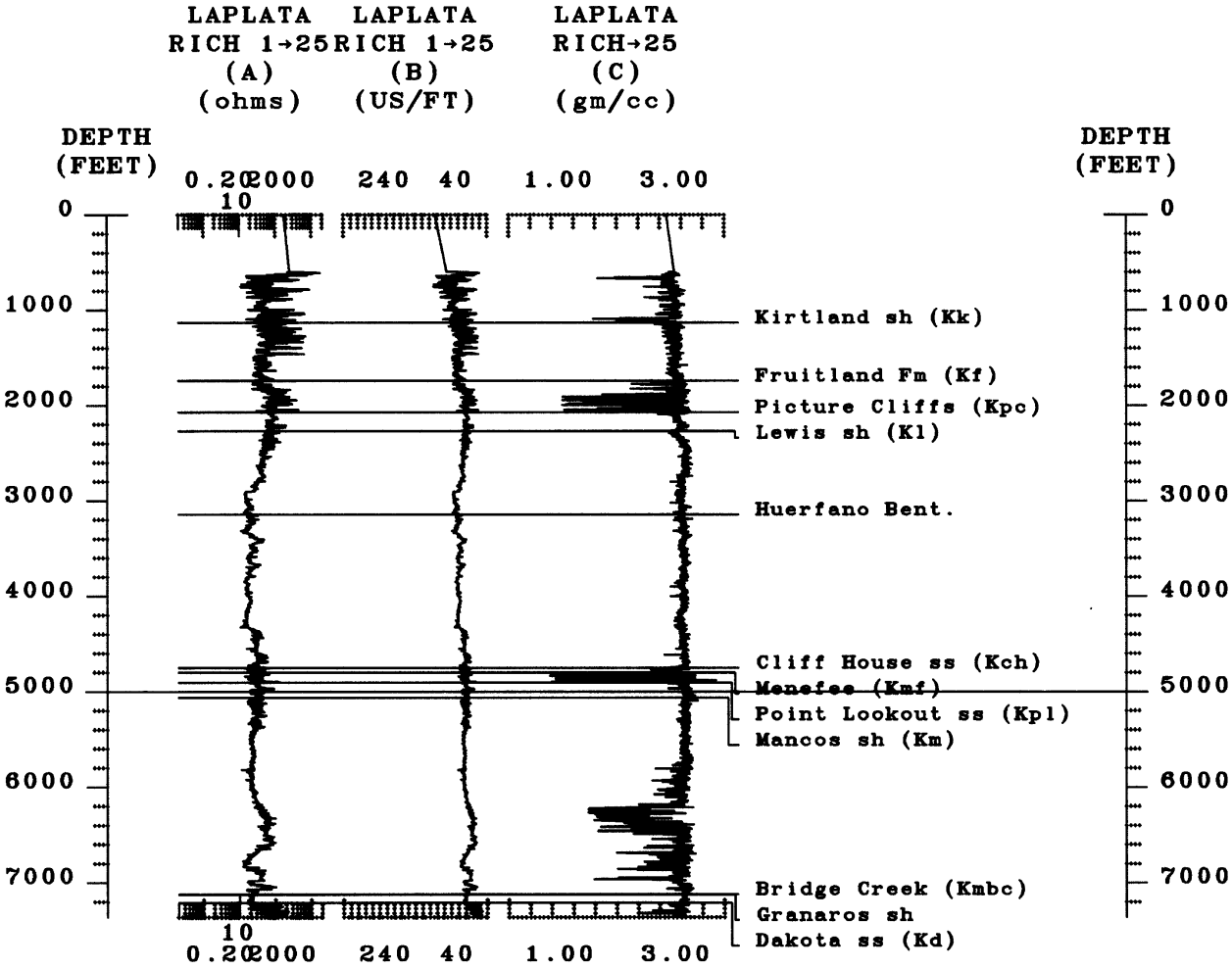

Figure 3-3. Display of the (A) measured resistivity log, (B) sonic log generated using Faust's equation, and (C) density log generated from the sonic log utilizing Lindseth's equation used to generate a synthetic seismogram for the Ward McCoy No. 1-9 well.

Top of Data	8860 ft/sec. (2700 m/sec.)
Top of Lewis Shale	10700 ft/sec. (3261 m/sec.)
Base of Lewis Shale	11400 ft/sec. (3475 m/sec.)
Dakota Formation	13000 ft/sec. (3962 m/sec.)
Cutler Formation	14650 ft/sec. (4465 m/sec.)
Paradox Formation	15420 ft/sec. (4700 m/sec.)
Base of Data	18500 ft/sec. (5639 m/sec.)

The following post migration processing was performed.

*Disk Data Input
*Trace Muting (mute pattern duplicated from Amoco processed sections)
*Bandpass Filter (8-12-60-64 Hz.)
*Automatic Gain Control

Final results were displayed at various scales. A scale of 10 inches per second two-way travel time in the vertical direction and 20 traces per inch in the horizontal direction proved to be the best for the interpretation.

SEISMIC DATA—INTERPRETATION

Line figure interpretations of the Amoco lines are shown in figures 3-8, 3-9, and 3-10. Several features are common to all of the Amoco lines: (1) the Dakota sandstone is a strong continuous reflector with few discontinuities; (2) the Fruitland Formation is a strong continuous reflector with few discontinuities; (3) there is little thickness change between the Dakota and the Fruitland except at the northern end of each line; (4) the Mancos and Lewis shales are highly deformed in the northern and central portions of each line and; (5) the Mesaverde Group is broken

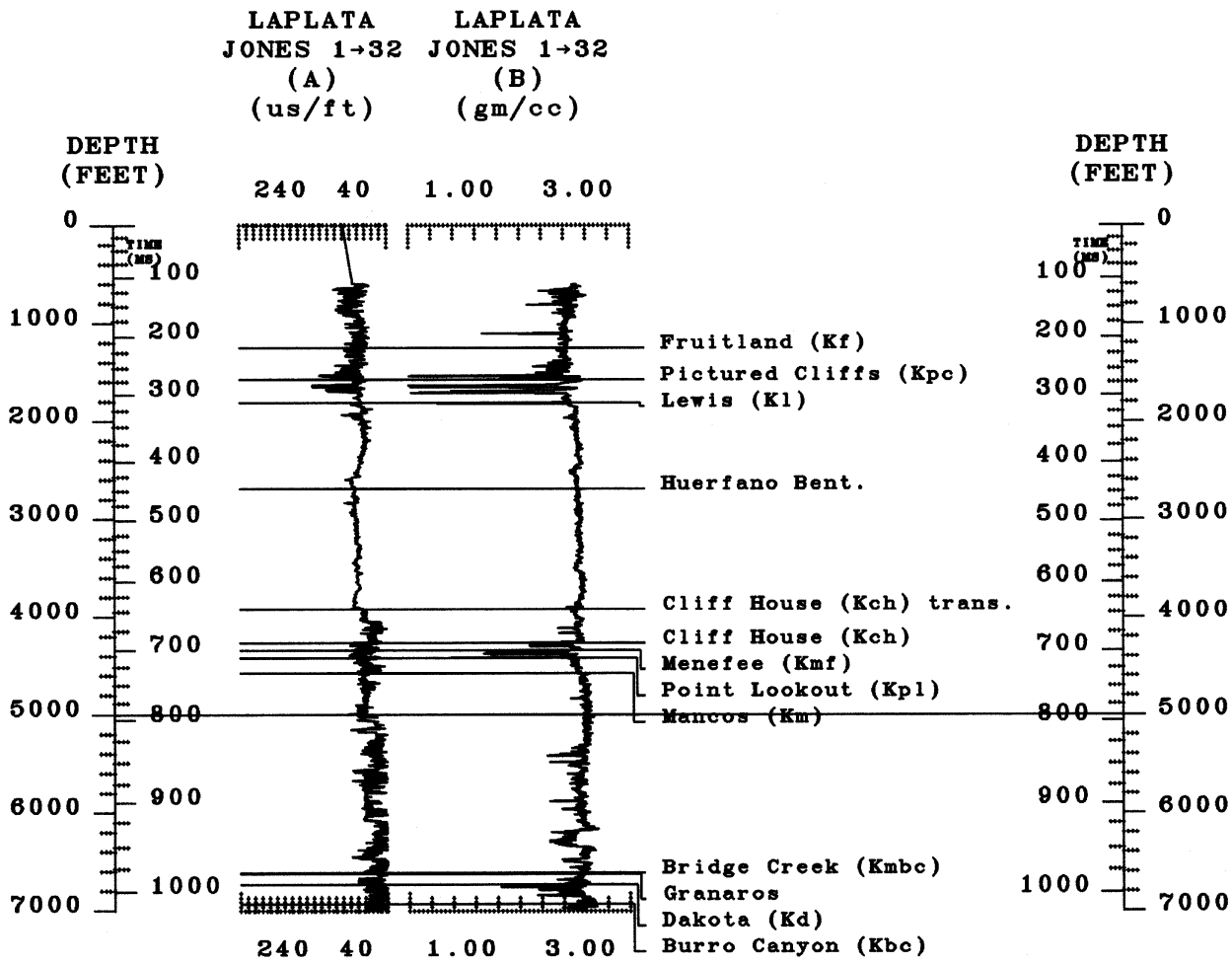

Figure 3-4. Display of the (A) measured sonic log and (C) density log generated from the sonic log utilizing Lindseth's equation used to generate a synthetic seismogram for the Jones No. 1-32 well.

and offset in a number of places on all lines. We interpret these features to indicate a certain amount of into-the-basin movement along glide planes in the shales with associated thrust faulting and back thrusting related to thrust faulting underlying the basin margin monocline.

Some of the apparently uplifted or downdropped (but not actually faulted) portions of certain reflectors, such as that in the Fruitland in the central part of line HXS-3, (fig. 3-10) could be attributed to: (1) a parallel fault underlying the line such that the line passes back and forth across the fault or; (2) to two separate faults at depth crossing the line at some angle. Such ambiguities cannot be totally resolved without a line at right angles to HXS-3. In this particular case, we prefer the underlying parallel fault interpretation because the apparent lithologic character of the Fruitland is the same on either side of the uplifted block but different from that within the block which would be more likely if the two downfaulted sides were actually part of a continuous section rather than two separate fault blocks. The Maxus line was of no help in this case because of data degradation at the ends of two of the line segments (AAC 1 and 2) immediately beneath the structure. In what may be a similar situation, the Dakota is offset by either a single underlying parallel fault or two cross-cutting faults in the southern part of line HXS-2 (fig. 3-9).

The northernmost end of line HXS-3 intercepts the basin margin thrust fault as well as a rather complicated set of thrusts and back thrusts associated with it. These associated faults also suggest that the apparent north verging reverse fault noted by Condon in this report could be a

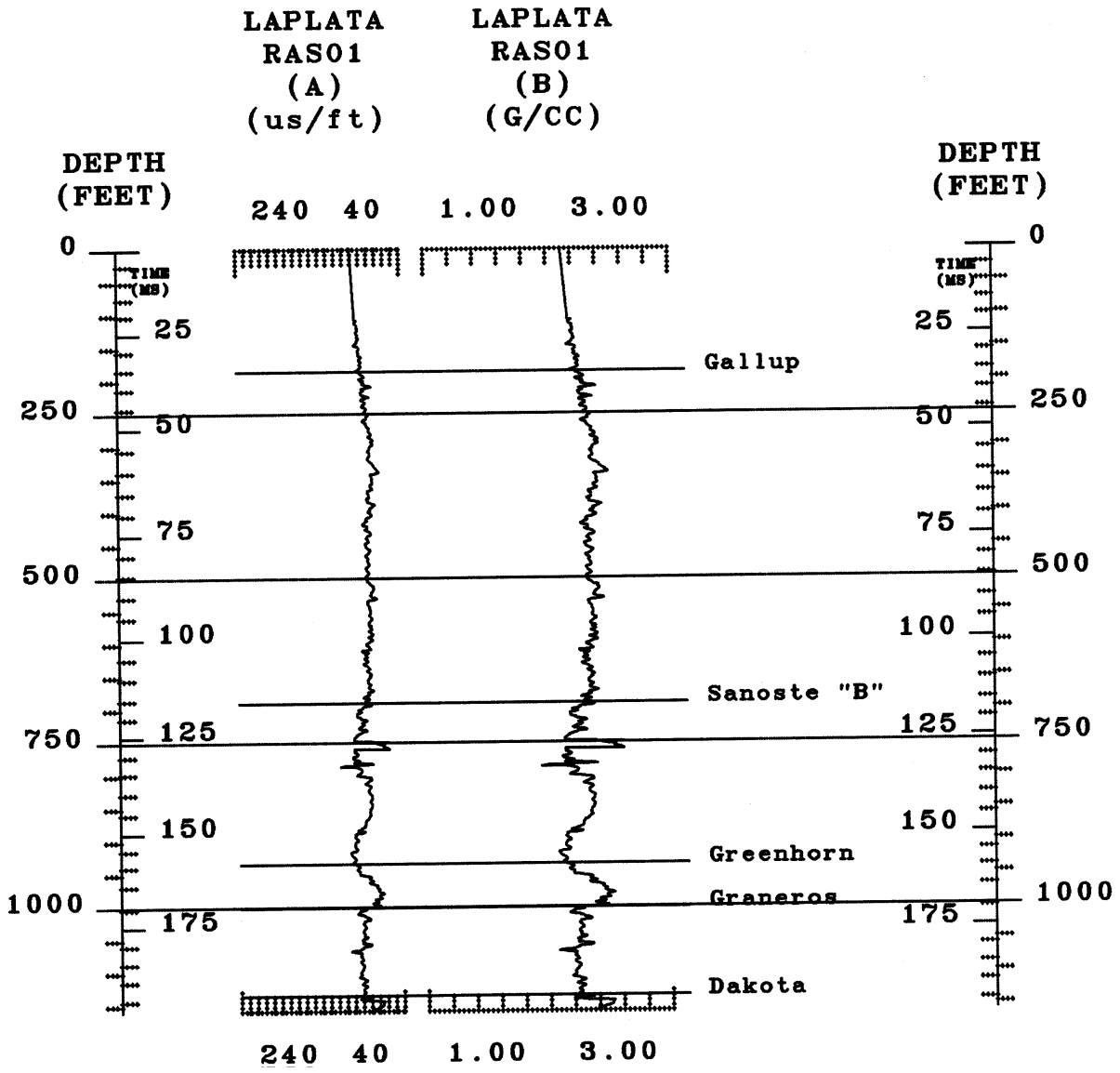

Figure 3-5. Display of the (A) measured sonic log and (C) density log generated from the sonic log utilizing Lindseth's equation used to generate a synthetic seismogram for the Raso No. 1 well.

back thrust (it should be noted that these interpretations are first approximations and only serve to illustrate the style and complexity of the structure).

Many lithologic variations can be seen, particularly in the Fruitland and Mesaverde of line HXS-3, as well as in the Mancos and Lewis shales of all the lines. Tongues of sand and shale enter the northern end of the marine units in all of the lines, particularly in the Lewis Shale, and we have interpreted a number of channels or delta lobes in the continental and marginal marine parts of the section. Some of the lithologic changes may have been localized by faulting at depth but most are probably the result of the position of the area within the Cretaceous seaway.

We interpret the apparent thickening between the Dakota and the Fruitland seen in the northern portion of the lines, particularly line HXS-2 (fig. 3-9), to be primarily tectonic in origin. South verging thrust faults related to the basin margin thrust are most prominent in HXS-2 but are present in the other lines as well. The overall effect of thrust faulting is to thicken the section; the basin margin thrusts interpreted in HXS-2 have caused a dramatic thickening in the Upper Cretaceous part of the section.

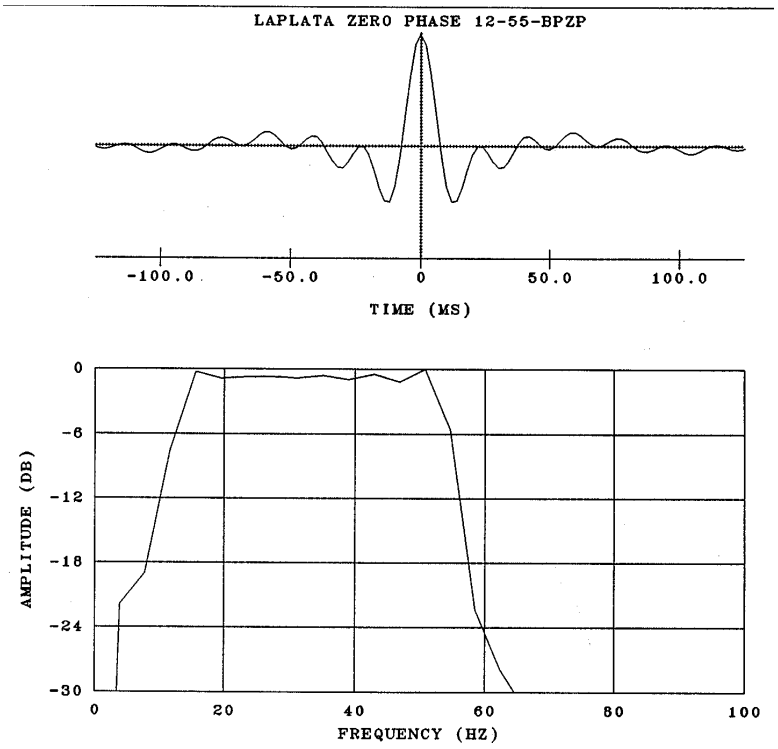

Figure 3-6. Plot showing the shape and frequency spectrum of the wavelet utilized to generate the synthetic seismograms for all of the wells used in the study area.

Line HXS-1 (fig. 3-8) contains the best evidence for a glide plane in the basal Mancos Shale. Thrust faults coming off this detachment surface, as well as associated back thrusts, break the Mesaverde into a number of blocks and significantly disrupt the Lewis Shale.

The only large though-going faults seen on any of the seismic lines available to this study are associated with the basin margin thrusting that underlies the monoclinal folding on three sides of the San Juan Basin. These thrust faults are typically multiple faults as they approach the surface (Taylor and Huffman,1988) and one or more of the branches may be seen to offset the Fruitland near the outcrop (figs. 3-8 and 3-9). We would expect a greater degree of fracturing in the vicinity of these faults than might otherwise be present. We can not comment on the probability of any north-south striking faults because of the absence of any east-west oriented data. The vicinity of the wind and water gaps and areas of changes in direction of the hogback would be likely places to look for such faults.

CONCLUSIONS

Little information specific to fracturing was gathered during the course of this study. The original intent was to compare faulting at depth to fracturing at the Fruitland Formation level and above. For the reasons cited previously, we were unable to map the faulting in the area so we were unable to compare the fracture patterns determined in other parts of this study with underlying fault patterns. Based on our experiences elsewhere in the basin, we would expect there to be an orthogonal fault system offsetting the basement through the Permian part of the section and for that pattern to be reflected in the depositional patterns and fracture patterns of the overlying units. We are unable to demonstrate such a relationship based on the findings of this investigation.

With the notable exception of the basin margin thrust fault, we have found no relationship of faulting in the Fruitland Formation with structure at depth in the study area but the data we had to work with are somewhat limited and do not allow for unambiguous interpretations. Several critical structures , such as the problematic north-south oriented faulting, could be easily resolved with a tie line or two and a small 3-D survey in the area of interest would undoubtedly resolve a number of the questions. We do not have enough

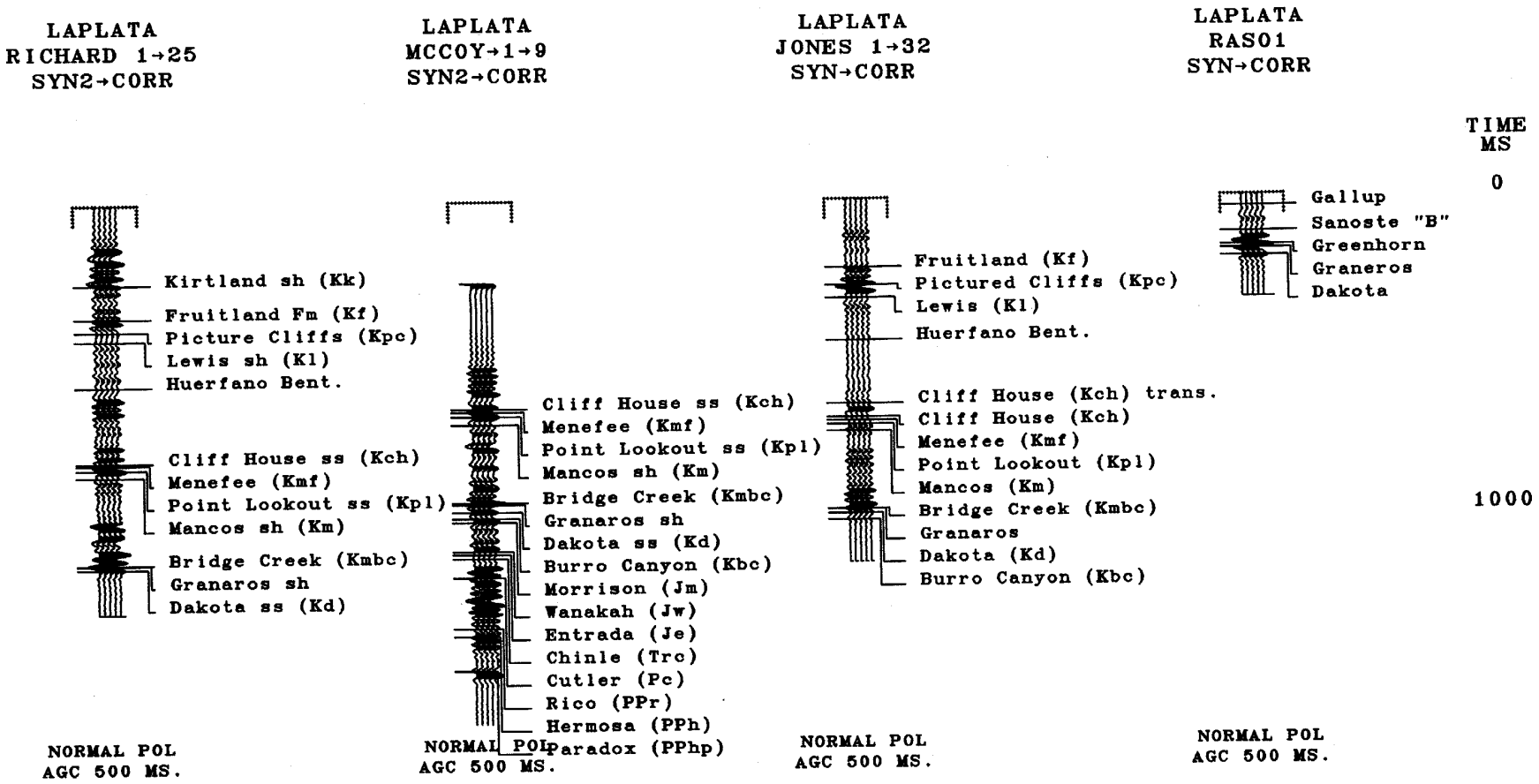

Figure 3-7. Display of the synthetic seismograms and the picked geologic horizons interpreted from the well information for each of the wells used in the study.

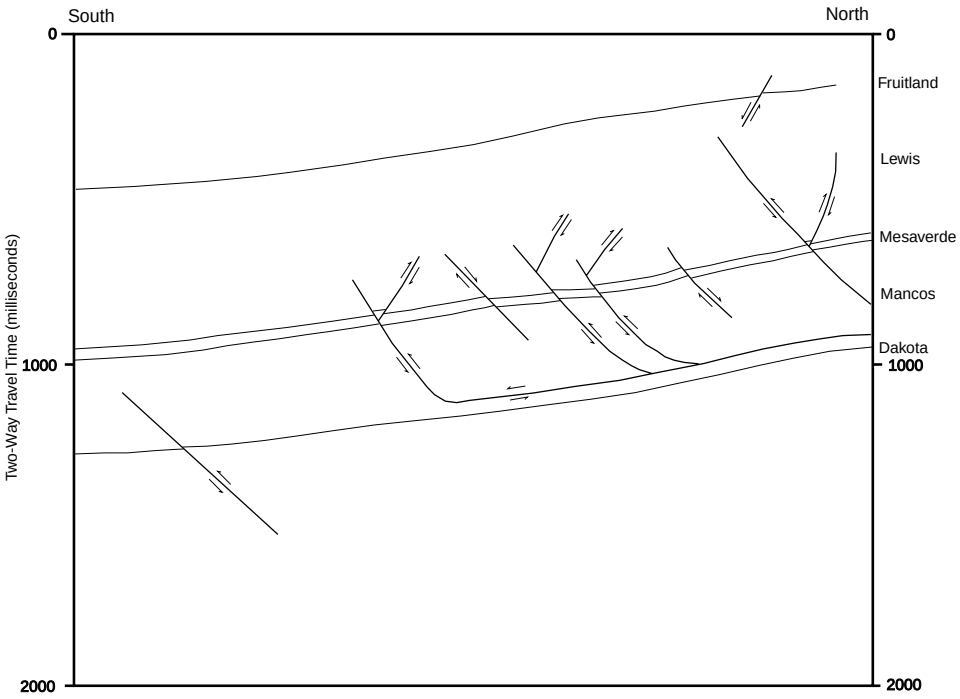

Figure 3-8. Line Drawing Interpretation of Amoco line HSX-1.

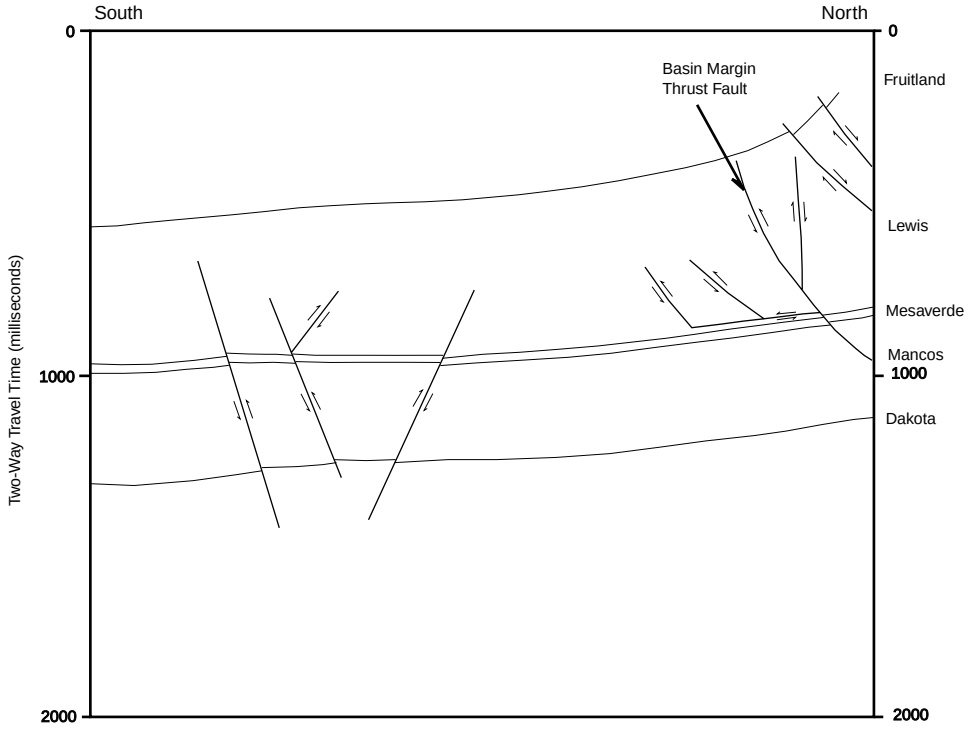

Figure 3-9. Line Drawing Interpretation of Amoco line HSX-2.

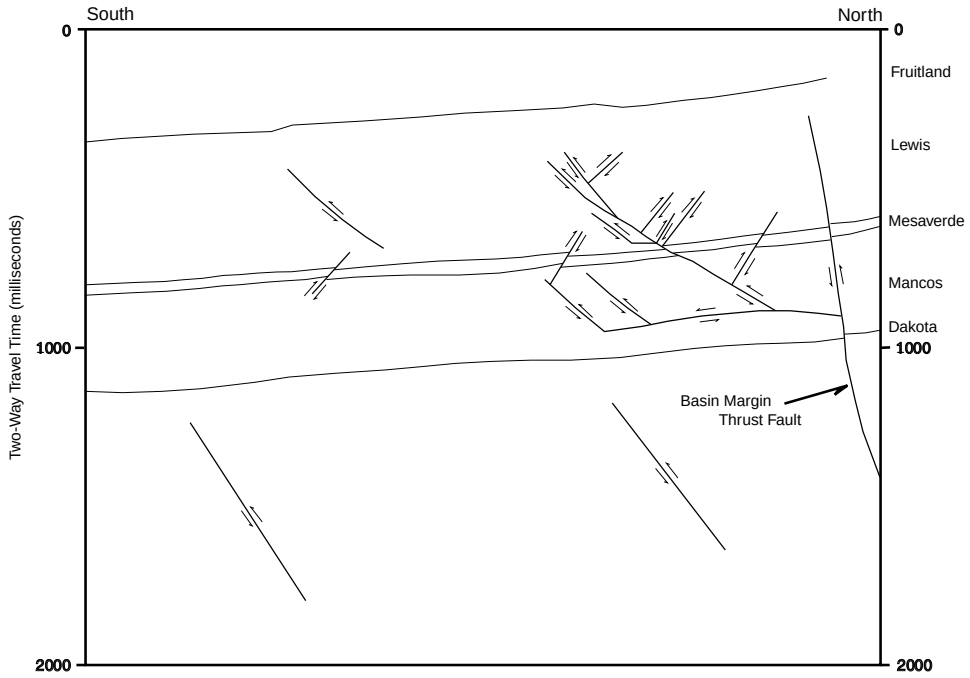

Figure 3-10. Line Drawing Interpretation of Amoco line HSX-3.

data in the right location to say there is or is not a pattern of faulting in the Fruitland that reflects the orthogonal basement pattern we have seen elsewhere in the basin.

The following is a summary of our principal conclusions:

1. The Dakota Sandstone is a strong continuous reflector with few offsets at a scale resolvable by the Amoco seismic data provided for this study.
2. The Fruitland Formation is a strong continuous reflector with few offsets at a scale resolvable by the Amoco seismic data.
3. In this area, the entire Cretaceous section, including the Fruitland, is offset by the basin margin thrust faults.
4. Much of the movement on the basin margin thrust is apparently taken up along a detachment surface in the lower Mancos and along related thrusts and back thrusts in the Mancos and Lewis Shales.
5. The Mesaverde is extensively broken and offset by the thrusts and back thrusts.
6. It is impossible to determine the pattern of faulting and its relationship to fracturing in the Cretaceous without more data, particularly some lines at right angles to the existing data.

ACKNOWLEDGMENTS

We are grateful to Amoco Production Company, Maxus Exploration Company, and K.N. Energy, Inc. for providing the data necessary for this study. We also benefited from discussions with a number of people, particularly Harry TerBest, Tom Ann Casey, and Curt Johnson, as well as from review comments by Chris Potter and John Miller. The interpretations and conclusions expressed, however, are ours alone.

REFERENCES CITED

Faust, L.Y., 1951, Seismic velocity as a function of depth and geologic time: Geophysics, v. 16, no. 2, p. 192-206.

Faust, L.Y., 1953, A velocity function including lithologic variation: Geophysics, v. 18, no. 2, p. 271-288.

Huffman, A.C., Jr., and Condon, S.M., 1993, Stratigraphy, structure, and paleogeography of Pennsylvanian and Permian rocks, San Juan Basin and adjacent areas, Arizona, Colorado, New Mexico, and Utah: U.S. Geological Survey Bulletin 1808-O, 44 p., 18 pl.

Huffman, A.C., Jr., and Taylor, D.J., 1989, San Juan Basin faulting—more than meets the eye

(abs): American Association of Petroleum Geologists Bulletin, v.73, no. 9, p. 1161.
Huffman, A.C., Jr., and Taylor, D.J., 1991, Basement fault control on the occurrence and development of San Juan Basin energy resources (abs): Geological Society of America Abstracts with Programs: v. 23, no. 4, p. 34.
Lindseth, R.O., 1979, Synthetic sonic logs—a process for stratigraphic interpretation: Geophysics, v. 44, no. 1, p. 1-26.
Taylor, D.J., and Huffman, A.C., Jr., 1988, Overthrusting in the northwestern San Juan Basin, New Mexico—A new interpretation of the Hogback Monocline, in Programs and Abstracts, 1988 McKelvey Forum: U.S. Geological Survey Circular 1025, p. 60-61.